

Université Louis Pasteur

THESE

Présentée à l'UFR de Chimie
pour obtenir le grade de

Docteur de l'Université Louis Pasteur de Strasbourg

par

Stéphane STEYER

*Utilisation de la plateforme calix[4]arène pour la
formation de phosphites et phosphinates fonctionnels.
Application en hydroformylation d'oléfines.*

Soutenue le 25 février 2005 devant la commission d'examen :

Françoise COLOBERT	Professeur à l'ECPM (Université Louis Pasteur, Strasbourg)	
Jean-Claude BÜNZLI	Professeur à l'Ecole Polytechnique de Lausanne (Suisse)	
Michael KNORR	Professeur à l'Université de Franche-Comté (Besançon)	
Dominique MATT	Directeur de Recherche au CNRS (ULP, Strasbourg)	Directeur de thèse

A mes parents

REMERCIEMENTS

Le travail présenté dans ce mémoire a été réalisé au sein du Laboratoire de Chimie Inorganique Moléculaire de l'Université Louis Pasteur.

Je tiens à remercier tout d'abord Dominique Matt de m'avoir accueilli au sein de son équipe et de m'avoir encadré durant ces années de thèse, ainsi que pour les discussions scientifiques et extra-professionnelles, toujours enrichissantes, que nous avons eues.

Un grand merci également à Catherine Jeunesse, qui en secondant Dominique m'a permis de surmonter des moments parfois difficiles, mais souvent constructifs.

Je suis très sensible à l'honneur que m'ont fait Madame Françoise Colobert et Messieurs Jean-Claude Bünzli et Michael Knorr en acceptant de juger le présent travail et en participant au jury de cette thèse.

Les travaux décrits dans ce mémoire n'auraient pu être menés à bien sans les contributions des différents services de la Faculté de Chimie. A ce titre, je voudrais remercier toute l'équipe de RMN et en particulier Monsieur Roland Graff. Je remercie également les cristallographes Messieurs Richard Welter et André De Cian de Strasbourg qui se sont investis dans la résolution des structures moléculaires.

Je ne saurais oublier les membres, stagiaires et invités qui par leurs discussions et leur aide ont également contribué à ce travail: Dominique Armspach, David Semeril, Cédric Dieleman, Manuel Lejeune, Pierre Kuhn, Laurent Poorters, Luc Eberhardt, Antony Meredith.

Finalement, un merci tout particulier à mes parents pour leur soutien matériel et financier ainsi que pour m'avoir encouragé à prendre cette voie.

RESUME

Ce mémoire décrit la synthèse ainsi que les propriétés complexes et catalytiques de divers phosphites et phosphinites construits sur le bord inférieur de *p-tert*-butyl-calix[4]arènes régiosélectivement préfonctionnalisés. Les calix[4]arènes sont des composés macrocycliques résultant de la condensation de phénols *p*-substitués avec du formaldéhyde. Ils constituent d'excellentes plateformes de préorganisation pour la confection de ligands polytopiques.

La première partie de ce mémoire est consacrée à la synthèse de calixarènes dans lesquels trois atomes d'oxygène "phenoxy" sont pontés par un atome de phosphore, le quatrième étant substitué par une fonctionnalité à atome d'oxygène donneur (éther, ester, oxyde de phosphine, amide). Ces phosphites, qui sont particulièrement robustes en milieu basique, présentent vis-à-vis de métaux de transition soit un comportement *P*-monodentate, soit *P,O*-chélatant. Associés à du rhodium, ils fournissent des catalyseurs très actifs en hydroformylation de l'octène. Une influence nette du pouvoir donneur de la fonction auxiliaire oxygénée a été mise en évidence, et ce tant au niveau de l'activité que de la sélectivité en aldéhyde.

La seconde partie de ce travail décrit des calixarènes porteurs de deux groupes PX₂ (X = OPh ou Ph) greffés sur des atomes d'oxygène occupant des positions distales de la matrice, les deux autres phenoxy ayant été substitués soit par une chaîne alkyle soit par un groupement porteur d'une fonction carbonyle. Ces ligands ont tendance à former facilement avec des ions transitionnels des complexes chélatés. Les complexes du type [Rh(diphos)(acac)] présentent une bonne activité en hydroformylation de l'octène. Ce sont les ligands phosphites qui conduisent aux meilleures sélectivités en nonanal, probablement en raison de leur aptitude à former autour du métal une poche étroite qui favorise la formation de l'intermédiaire "Rh(*n*-alkyle)" au détriment de l'intermédiaire "Rh(*iso*-alkyle)".

La dernière partie de ce mémoire est consacrée à la diquinone formée lors de l'oxydation chimique ou électrochimique du *p-tert*-butyl-calix[4]-{OCH₂P(O)Ph₂}₂-(OH)₂. Une étude par diffraction des rayons X établit la conformation *cône partiel* du composé à l'état solide. Des études par RMN montrent que les noyaux quinoniques basculent rapidement à travers la cavité macrocyclique.

Mots clés : Calixarène, Métaux de transition, Phosphite, Phosphinite, Hydroformylation, Calix-quinone

SUMMARY

This thesis describes the synthesis, characterisation and properties of phosphorus containing ligands built on a calix[4]arene scaffold.

The first chapter describes the synthesis of bulky, monodentate phosphites. Reaction of $\text{PCl}_3/\text{NEt}_3$ with *p*-*tert*-butyl-calix[4]-(OH)₃-OR, in which R contains an auxillary *O*-donor (R = -CH₂P(O)Ph₂, -CH₂CO₂Et, -CH₂C(O)NET₂, -CH₂CH₂OMe) afforded the expected conical calixarenes in which the P atom bridges three of the phenolic oxygen atoms. The thus formed phosphites which have cone angles larger than 180° are remarkably stable towards aqueous NaOH. When reacted with transition metal ions, they form either P-monodentate complexes or large *P,O*-chelate complexes involving the oxygen atom of the R group. The four ligands were assessed in the rhodium-catalysed hydroformylation of octene. Their activity is typically that of a bulky phosphite, but the reaction rate decreases as the donor strength of the side group increases. The L/B ratios lie in the range 1.4–3.6, the highest linear aldehyde selectivity being observed when the side group is CH₂CO₂Et.

The second chapter deals with 6 calixarenes distally-substituted at the lower rim by two PX₂ groups (X = OPh, Ph), the other two oxygen atoms of the calixarene platform being equipped with various substituents, R¹ = propyl, R² = CH₂CO₂Et, R³ = CO₂cholesteryl. Reaction of the di-P ligands with transition metals readily results in the formation of chelate complexes, provided the reaction is carried out at high dilution. All ligands, when mixed with [Rh(acac)CO]₂, effectively catalyse the hydroformylation of octene and styrene. In the hydroformylation of octene, the linear aldehyde selectivities observed with the phosphites which contain R² (**L**²) or R³ (**L**³) are significantly higher (linear/branched = ca. 10) than those obtained with the other 4 ligands of this study and also with respect to PPh₃. Molecular modelling shows that the lower rim substituents of **L**² and **L**³ form tighter pockets about the metal centre than do the other ligands and so sterically favour the formation of Rh(*n*-alkyl) intermediates over that of Rh(*i*-alkyl) ones. In styrene hydroformylation, all ligands result in the formation of unusually high amounts of the linear aldehyde, the b/l ratios being close to 65:35. The highest activities were found when using an L/Rh ratio of 1:1.

The final chapter describes the preparation of the diquinone obtained by chemical or electrochemical oxidation of the proximally phosphorylated calixarene 1,2-(Ph₂P(O)CH₂)₂-calix[4]arene-(OH)₂. As shown by an X-ray diffraction study, this calixarene adopts a *partial-cone* conformation with one quinone ring being anti-oriented. In solution the two quinone rings flip rapidly through the calixarene annulus.

Keywords: Calixarene, Transition metals, Phosphite, Phosphinite, Hydroformylation, Calix-quinone

ABREVIATIONS

Ac	-C(O)CH ₃
acac	acétyle acetonate
Ar	Aryle
COD	Cycloocta-1,5-diène
coll.	collaborateurs
COSY	CORrelation SpectroscopY
δ	déplacement chimique (ppm)
DMBA	diméthylbenzylamine
ESI MS	Electro-Spray Ionisation Mass Spectrometry
Et	éthyle
FAB MS	Fast Atom Bombardment Mass Spectrometry
IR	Spectroscopie Infra-Rouge
<i>n</i> -BuLi	<i>n</i> -butyle-lithium
ⁿ <i>J</i> _{AB}	constante de couplage (Hz) entre les noyaux A et B à travers n liaisons
NMR	Résonance Magnétique Nucléaire
NOESY	Nuclear Overhauser Effect SpectroscopY
<i>R</i> _f	rétention frontale
ROESY	Rotating frame Overhauser Effect SpectroscopY
THF	tétrahydrofurane
TOF	Turnover Frequency (mol(substrat).mol(catalyseur) ⁻¹ .h ⁻¹)

**CALIXARENE-DERIVATIVES IN TRANSITION METAL
CHEMISTRY. COORDINATION CHEMISTRY AND
CATALYSIS.**

1	Introduction	2
2	Complexes with O-bound metals derived from <i>p</i> -R-calix[n]arenes	2
2.1	Complexes having the metal centre bound to phenolic oxygen atoms	2
2.2	Complexes having a metal centre bound to oxygen or sulfur atoms belonging to pendent functional groups	7
3	Calixarene complexes with metals bound to N donor atoms	9
3.1	Attempts to prepare metallo-enzyme models	9
3.2	Complexes formed from resorcinarenes containing pendant nitrogen ligands	13
3.3	Other complexes obtained from calix[n]arenes substituted by nitrogen-containing ligands	14
4	Calixarene complexes obtained from phosphorus ligands	17
4.1	Complexes from calixarenes with phosphorus atoms tethered to the lower rim	17
4.2	Complexes of calixarenes with upper rim P substituents	29
5	Metallocalixarenes with metal centres bonded to π -donor units	31
6	Special uses of calixarenes in catalysis	33
7	Conclusion	33
8	References	35

METALLOCALIXARENES. MISE AU POINT COUVRANT

LA PERIODE 2000-2003.

1	Métallocalixarènes comportant des centres métalliques directement liés à des atomes d'oxygène phénoliques	40
1.1	Complexes obtenus avec des métaux du groupe IV	40
1.2	Complexes contenant des métaux du groupe V	43
1.3	Complexes contenant des métaux du groupe VI	44
1.4	Complexes contenant des métaux du groupe VII	51
1.5	Complexes contenant des métaux du groupe VIII	52
1.6	Complexes construits à partir de thiocalixarènes	53
2	Complexation par des calixarènes substitués au niveau du bord supérieur par des groupes fonctionnels contenant des atomes d'oxygène	54
3	Complexes formés à partir de calixarènes à fonctionnalités hybrides (N, O) ou (N, S)	54
4	Complexation par des calixarènes substitués par des groupes fonctionnels azotés	58
5	Complexes d'intérêt biomimétique	64
6	Complexes métalliques formés à partir d'isocyanocalixarènes	66
7	Complexes formés à partir de calixarènes substitués par des bras phosphorés	67
7.1	Calixarènes substitués au niveau du bord inférieur	67
7.2	Formation de liaisons P-M au niveau du bord supérieur	73
8	Calixarènes substitués par des unités ferrocéniques	79
9	Complexes π mettant en jeu un noyau aromatique du calixarène	79
10	Calixarènes en catalyse homogène	80
11	Références	82

***HETEROFUNCTIONALISED PHOSPHITES BUILT ON A
CALIX[4]ARENÉ SCAFFOLD AND THEIR USE IN
1-OCTENE HYDROFORMYLATION. FORMATION OF
12-MEMBERED P,O-CHELATE RINGS.***

Résumé	2
1 Introduction	4
2 Results and discussion	5
2.1 Synthesis and stability of the ligands	5
2.2 Complexes obtained from phosphites L ¹ -L ³	11
2.3 Hydroformylation with heterodifunctional calix phosphites	19
3 Conclusion	22
4 References	23
5 Experimental	26
5.1 General procedures	26
5.2 Syntheses	27
5.3 Hydroformylation experiments	49
5.4 X-Ray crystallography	49

***BIS-PHOSPHITES AND BIS-PHOSPHINITES BASED ON
DISTALLY-FUNCTIONALIZED CALIX[4]ARENES:
COORDINATION CHEMISTRY AND USE IN RHODIUM-
CATALYSED, LOW-PRESSURE OLEFIN
HYDROFORMYLATION.***

Résumé	2
1 Introduction	3
2 Results and discussion	5
2.1 Ligand syntheses	5
2.2 Catalytic studies	10
2.2.1 Hydroformylation of octene	11
2.2.2 Hydroformylation of styrene	15
3 Conclusion	16
4 References	18
5 Experimental	19

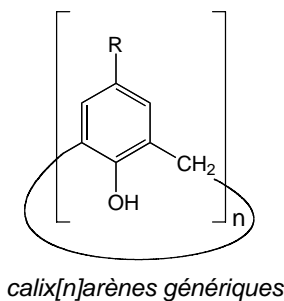
CONFORMATIONAL INSTABILITY OF A PROXIMALLY-DIFUNCTIONALIZED CALIX[4]-DIQUINONE.

Résumé	2
1 Introduction	2
2 Experimental	4
2.1 General	4
2.2 Alternative preparation of C	4
2.3 Important spectroscopic data for C	5
2.4 X-ray analysis	5
3 NMR and X-ray studies	7
4 Conclusion	11
5 References	12

INTRODUCTION GENERALE.

Cette thèse s'inscrit dans le cadre des recherches sur les cavitands actuellement développées au Laboratoire de Chimie Inorganique Moléculaire. Elle est consacrée à la synthèse et à la caractérisation de nouveaux dérivés de calix[4]arènes et, pour certains d'entre eux, à l'évaluation de leurs propriétés complexantes et catalytiques.

Les calix[n]arènes sont des molécules macrocycliques constituées de n entités phénoliques liées entre elles par des ponts méthyléniques.¹ Bien que ces polyphénols soient connus depuis les années 1940, il a fallu attendre les travaux fondamentaux de l'américain Gutsche, à la fin des années 1970, pour disposer de synthèses rationnelles permettant leur préparation en grandes quantités. Gutsche a démontré que la meilleure façon d'aboutir à un tel composé consistait à réaliser la condensation d'un phénol porteur d'un substituant en *para* avec du formaldéhyde, en présence de quantités catalytiques de base. C'est le contrôle de plusieurs paramètres, notamment le rapport base/phénol et la nature du cation associé à la base qui déterminent le nombre de noyaux aromatiques, n , constituant le calix[n]arène formé.

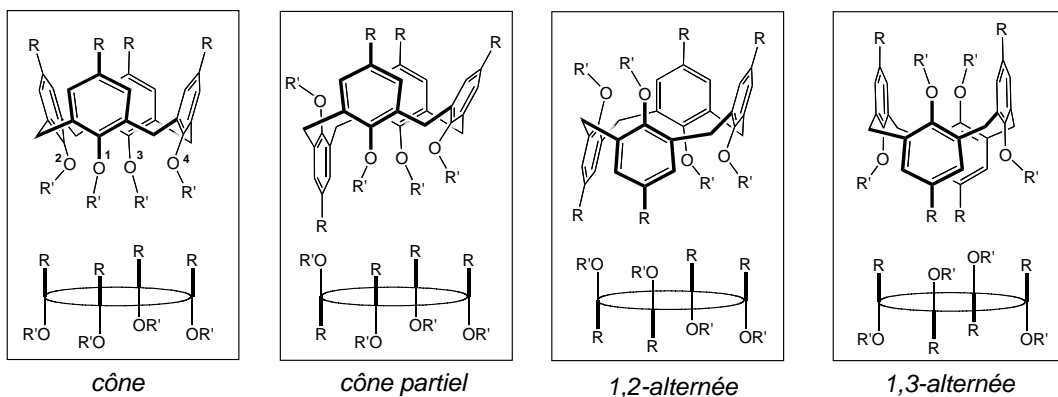


calix[n]arènes génériques

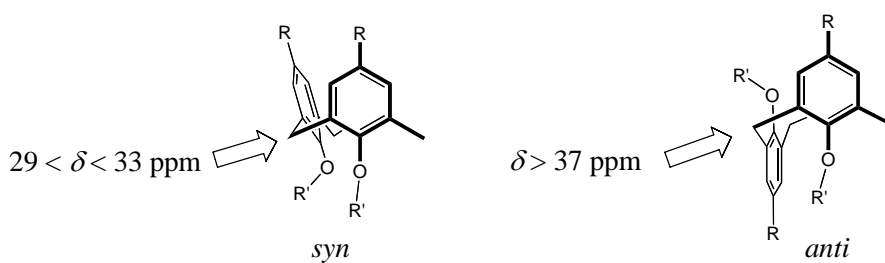
Deux raisons essentielles ont contribué au développement spectaculaire de cette classe de composés macrocycliques: a) les propriétés réceptrices de certains conformères qui forment avec de nombreux substrats des complexes d'inclusion; b) la possibilité d'utiliser les calixarènes comme plateformes pour l'ancrage de plusieurs ligands convergents, permettant ainsi de créer des sphères de coordinations très élaborées. C'est ce second aspect qui sera développé dans le présent travail plus

spécifiquement consacré à la synthèse de coordinats phosphorés à partir d'un calix[4]arène parent. Une des motivations particulières de ce travail était d'utiliser la matrice calix[4]arène pour la synthèse de nouveaux dérivés du P(III) présentant un encombrement élevé, notamment des phosphites et phosphinites, et ce, en vue d'une utilisation en hydroformylation d'oléfines.

Afin de faciliter la lecture de ce document, nous souhaitons rappeler au lecteur quelques caractéristiques structurales importantes des calix[4]arènes auxquelles il sera fréquemment fait référence dans ce travail. Ainsi, les calix[4]arènes peuvent exister dans quatre conformations extrêmes, dites *cône*, *cône partiel*, *1,2-alternée*, et *1,3-alternée*. Ce sont généralement les calix[4]arènes dans la conformation *cône* qui donnent lieu à des complexes d'inclusion. Précisons aussi que la plupart des conformères coniques présentent, en solution, un comportement dynamique caractérisé par une oscillation rapide coordonnée des noyaux aromatiques autour d'une position d'équilibre: ainsi, pendant que deux noyaux se rapprochent de l'axe du calixarène, les deux autres s'en éloignent.

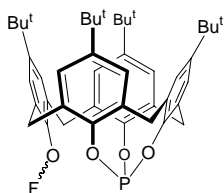


Pour ce qui est de l'identification des diverses conformations, le chimiste fait en général appel à des règles empiriques basées sur les déplacements chimiques des atomes de carbone des groupements CH₂ pontants.² Ainsi, pour un CH₂ pontant deux noyaux aromatiques orienté dans le même sens (*syn*), le déplacement du ¹³C est situé entre env. 29 et 33 ppm. Lorsque l'orientation relative est *anti*, le déplacement chimique du CH₂ est supérieur à 37 ppm. La différence, $\Delta\delta$ entre les déplacements chimiques de l'hydrogène H_{axial} et du H_{équatorial} du même groupement CH₂ fournit elle aussi des renseignements très utiles. Pour deux aromatiques *syn*-orientés, on a en général $\Delta\delta > 0.7$ ppm, alors que pour des aromatiques *anti*-orientés $\Delta\delta < 0.6$ ppm.

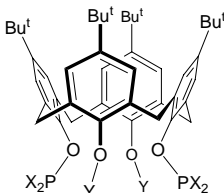


Ce manuscrit est divisé en quatre parties:

- Le premier chapitre est une mise au point sur les développements récents (1997-2003) dans la chimie des métallocalixarènes.
- Le second décrit la synthèse de phosphites fonctionnels basés sur une matrice calix[4]arène et évalue leur potentiel en hydroformylation d'octène.



- Le chapitre III décrit la synthèse de nouveaux calixarènes P-substitués au niveau de deux oxygènes phénoliques distaux (positions 1 et 3) et leur application en hydroformylation d'oléfines.



- Le dernier chapitre est consacré à l'étude structurale d'une diquinone obtenue par oxydation d'un calixarène difonctionnalisé.

Nous rappelons au lecteur un schéma simplifié de l'hydroformylation d'oléfine avec des phosphines monodentates.³

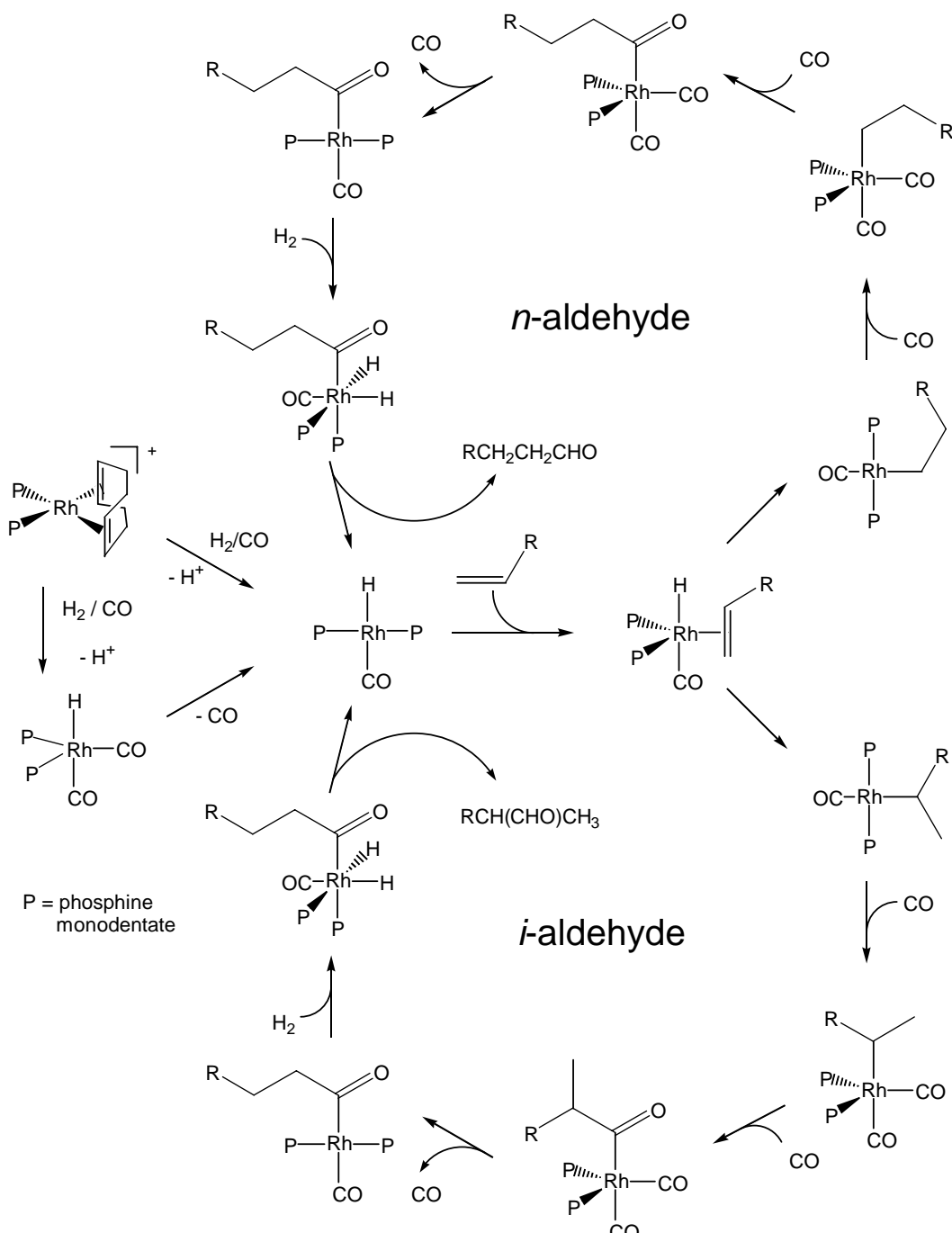


Schéma simplifié de l'hydroformylation d'oléfine

1. *Calixarenes 2001*, Asfari Z., Böhmer V., Harrowfield J., and Vicens J. (eds.), Kluwer, Dordrecht, **2001**.
2. D. C. Gutsche, *Calixarenes*, in *Monographs in Supramolecular Chemistry*, vol. 1, J. F. Stoddart (ed.), Royal Society of Chemistry, Cambridge, **1989**.
3. F. Plourde, K. Gilbert, J. Gagnon and P. D. Harvey, *Organometallics*, 2003, **22**, 2862-2875.

***CALIXARENE-DERIVATIVES IN TRANSITION METAL
CHEMISTRY. COORDINATION CHEMISTRY AND
CATALYSIS.***

1	Introduction	2
2	Complexes with O-bound metals derived from <i>p</i> -R-calix[n]arenes	2
2.1	Complexes having the metal centre bound to phenolic oxygen atoms	2
2.2	Complexes having a metal centre bound to oxygen or sulfur atoms belonging to pendent functional groups	7
3	Calixarene complexes with metals bound to N donor atoms	9
3.1	Attempts to prepare metallo-enzyme models	9
3.2	Complexes formed from resorcinarenes containing pendant nitrogen ligands	13
3.3	Other complexes obtained from calix[n]arenes substituted by nitrogen- containing ligands	14
4	Calixarene complexes obtained from phosphorus ligands	17
4.1	Complexes from calixarenes with phosphorus atoms tethered to the lower rim	17
4.2	Complexes of calixarenes with upper rim P substituents	29
5	Metalocalixarenes with metal centres bonded to π -donor units	31
6	Special uses of calixarenes in catalysis	33
7	Conclusion	33
8	References	35

1 Introduction

Calixarenes¹ provide unique platforms for the assembly not only of selective multidentate, monotopic ligands for transition metal ions but also of polytopic ligands capable of maintaining several discrete metal centres in close proximity. Such homo- or hetero-polymetallic systems offer important opportunities for studying reactions based on metal-metal cooperativity or metal transport along an organic backbone. Much recent work has focussed on the use of calixarenes in homogeneous catalysis and it has been recognized that cone-shaped calixarenes are ideal for the construction of new chelating ligands with non-conventional bite angles, a property relevant to selectivity in catalysis. The use of a calixarene cavity to house a catalytic centre is another promising application. Such metallo-cavatands provide the ability to select substrates according to their size and are likely to behave as catalysts displaying shape-selectivity. They are further discussed in "Calixarenes 2001".² Other potential applications in catalysis include the use of chiral chelators prepared from inherently chiral calixarenes.³ An already established application is the use of calixarenes as analogues of an oxide catalyst surface. Applications of transition metal complexes of functionalised calixarenes in areas other than catalysis are also discussed elsewhere.²

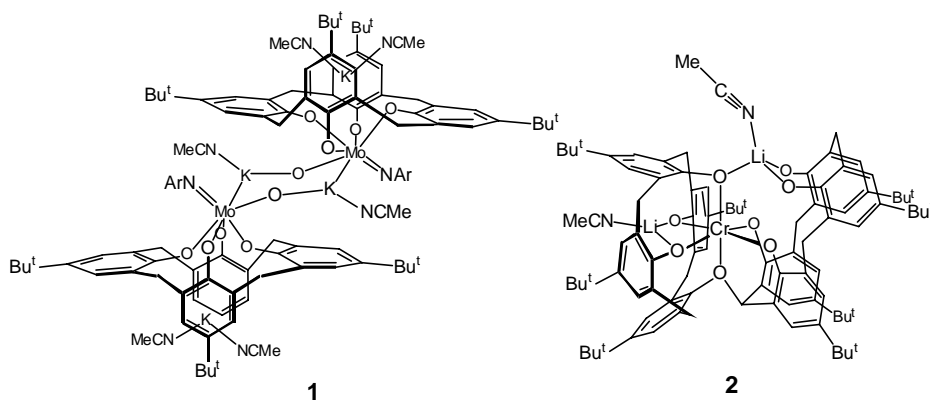
A background to the content of this chapter is provided in an earlier revue.⁴

2 Complexes with O-bound metals derived from *p*-R-calix[n]arenes

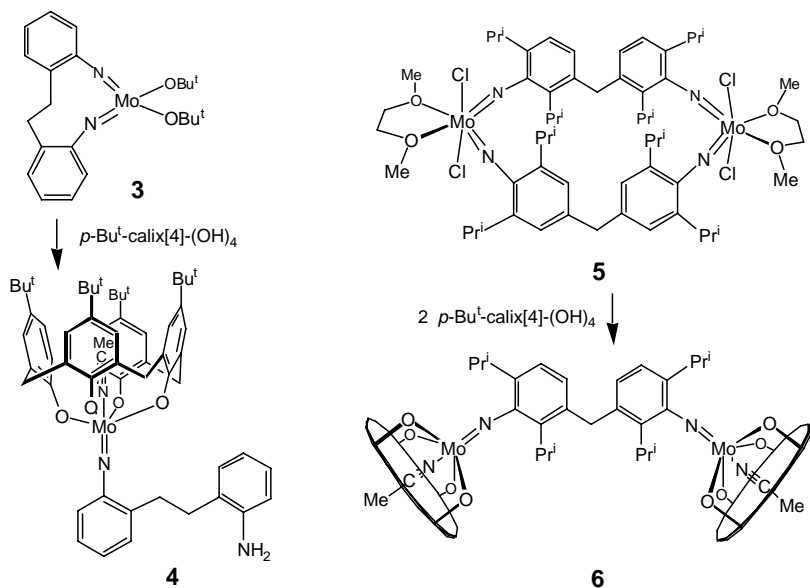
2.1 Complexes having the metal centre bound to phenolic oxygen atoms

Remarkable chemistry, such as the stepwise reduction of dinitrogen to nitride assisted by a niobium complex,^{5,6} has been observed through the use of calix[4]arene tetra-anions as ligands for early transition metals. It falls within a broader context of studies of the *p*-*tert*-butyl-calix-tetraanion as a terminal ligating group. Thus, treatment

of $[\text{Mo}(\text{NAr})(\text{CHCMe}_2\text{Ph})(\text{O}_3\text{SCF}_3)_2(\text{dme})]$ with *p*-But^t-calix[4]-(OK)₄ in tetrahydrofuran gave the dimeric complex $[\text{Mo}(\text{NAr})(\text{L})(\text{K})_2(\text{NCMe})_3\text{O}]_2$ **1** after crystallisation from acetonitrile.⁷ The presence of two oxygen atoms, presumably solvent-derived, results in the formation of a ladder motif. The rather flattened *cone* calixarenes contain a potassium ion which is π -bonded to two opposite phenoxy rings. Similarly, the reaction of $[\text{Cr}(\text{NBu}^t)_2(\text{OBu}^t)_2]$ with *p*-But^t-calix[4]arene gave complex **2** in which two oxidatively coupled calixarenes are coordinated to the chromium atom. One calixarene unit entraps a lithium ion.

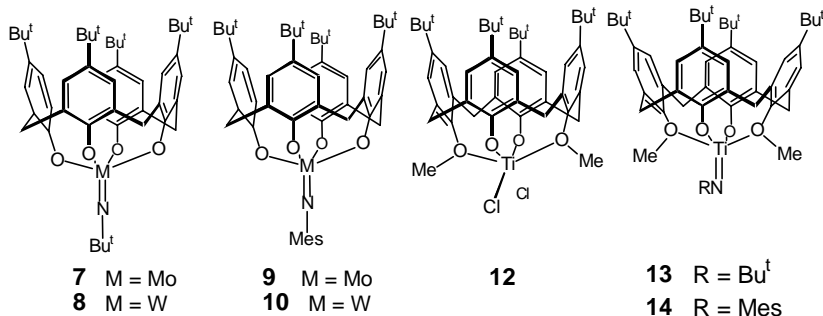


Reacting the diimido complex **3** with *p*-But^t-calix[4]-(OH)₄ resulted in ring-opening of the metallacycle and deprotonation of the four phenol units (Scheme 1)⁸ to give the imido complex **4**. Use of a bridging diimide in a similar reaction led to the binuclear complex **6**.



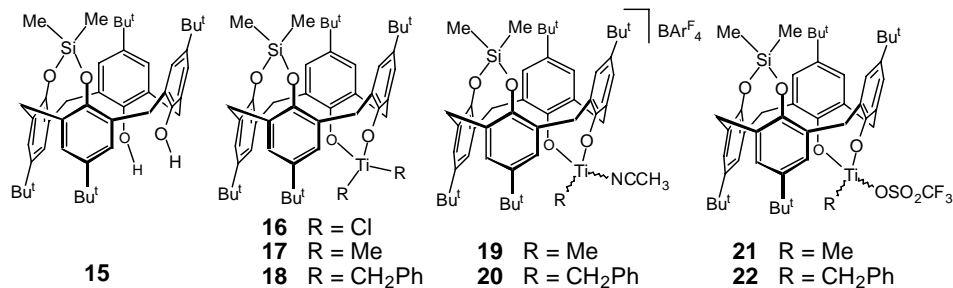
Scheme 1.

Reaction of *p*-Bu^t-calix[4]-(OH)₄ with the mixed imido/amino complexes [M(NBu^t)₂(NHBu^t)₂] (M = Mo, W) gave respectively complexes **7** and **8**,⁹ while performing the reaction with [M(NMes)₂Cl₂(dme)] (Mes = 2,4,6-Me₃-C₆H₂) afforded the related calixarenes **9** and **10**, respectively. Calixarenes **7-10** are able to include molecules such as CH₃CN, CNBu^t or H₂O. Coordination of acetonitrile causes the methyl signal to undergo an upfield shift of ca. 2 ppm, reflecting the shielding effects of the cavity. Significant upfield shifts were also observed for CNBu^t upon coordination.

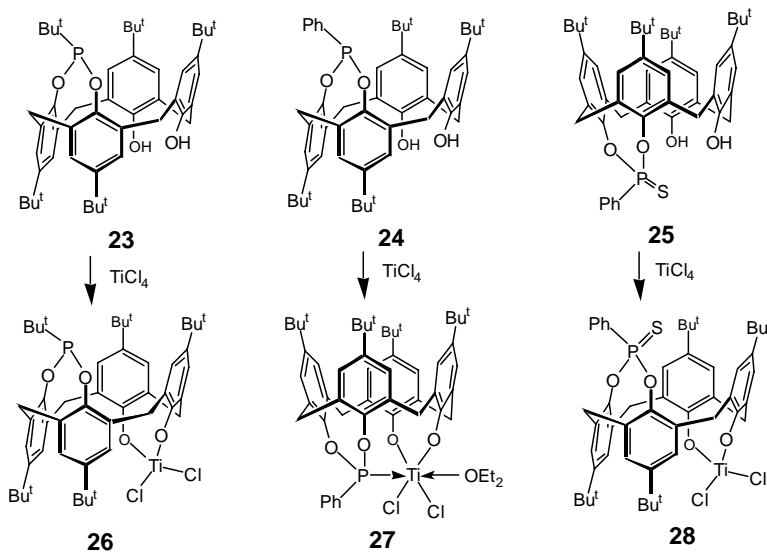


Mononuclear titanium imido complexes stabilized by the *p*-Bu^t-calix[4]-(OMe)₂(O)₂ dianion¹⁰ were obtained by reaction of **12**, formed from *p*-Bu^t-calix[4]-(OMe)₂(OH)₂ **11** and TiCl₄(THF)₂, with 2 equiv. of LiNHBu^t or LiNHMes (Mes = 2,4,6-trimethylphenyl) to give the *C*₂_V-symmetrical Ti(IV) species **13** and **14**, respectively. The Ti atom in **14** is distorted trigonal bipyramidal with the ether oxygen atoms in axial positions and the two phenoxide oxygen atoms and the imido N atom in the equatorial plane.

Reaction of TiCl₄ with 1,2-*alternate* calixarene **15** afforded the 1,2-TiCl₂-bridged complex **16** in which a single Ti centre is bound to two calixarene oxygen atoms.¹¹ The conformation imposes different stereochemical environments in the two TiCl bonds. At 80 °C, in C₆D₆, in the presence of excess Na, **16** catalyses the cyclotrimerization of terminal acetylenes to 1,2,4-trisubstituted benzenes in excellent yield with regioselectivities ≥ 95 %. Alkylation of **16** with MgR₂ (R = Me; CH₂Ph) afforded complexes **17** and **18**, respectively, the former decomposing readily.¹² Treatment of these complexes with [Ph₃C][B{3,5-(CF₃)₂C₆H₃}₄] in the presence of CH₃CN gave the cationic complexes **19** and **20**, respectively, which are relatively stable in solution. The use of [Ph₃C]CF₃SO₃ for chloride abstraction resulted in the formation of **21** and **22**. Reaction of **22** with Na[B{3,5-(CF₃)₂C₆H₃}₄] in the presence of CH₃CN gave **20**, whereas decomposition was observed with **21**.

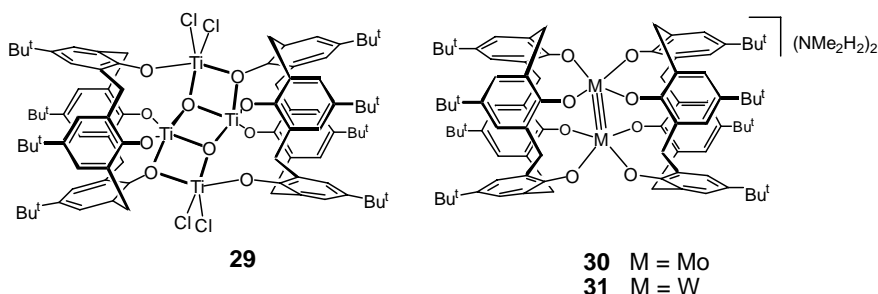


Mono-Ti calixarene complexes in which the metal bridges proximal positions, were also obtained by reacting $TiCl_4$ with **23**, **24** and **25** (Scheme 2), affording **26-28**, respectively.¹² In **26** the 1,2-alternate conformation is maintained, while formation of **27** is accompanied by a conformational change. The ^{31}P chemical shift of **27** shows that the phosphorus lone pair interacts with the Ti centre. Complex **28** exists in solution as an equilibrium mixture of cone and 1,2-alternate conformers. Over the range 298-348 K the equilibrium lies on the side of the 1,2-alternate isomer. With methylaluminoxane as activator, complexes **16-22** and **23-28** showed modest ethylene polymerization activities.

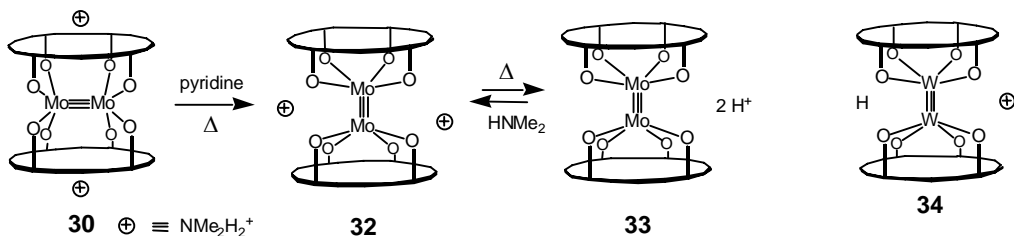


Scheme 2.

The dimeric complex $[\{Ti_2(\mu_3-O)Cl_2(p-Bu^t\text{-calix}[4]\text{-O}_4)\}_2]$ **29**,¹³ obtained by reacting an excess of $TiCl_4$ with *p*-Bu^t-calix[4]-(OH)₄, is centrosymmetric and possesses four Ti^{IV} atoms and two triply bridging O atoms forming a central planar ladder structure like that found in a calix[6]arene Ti-complex.¹⁴



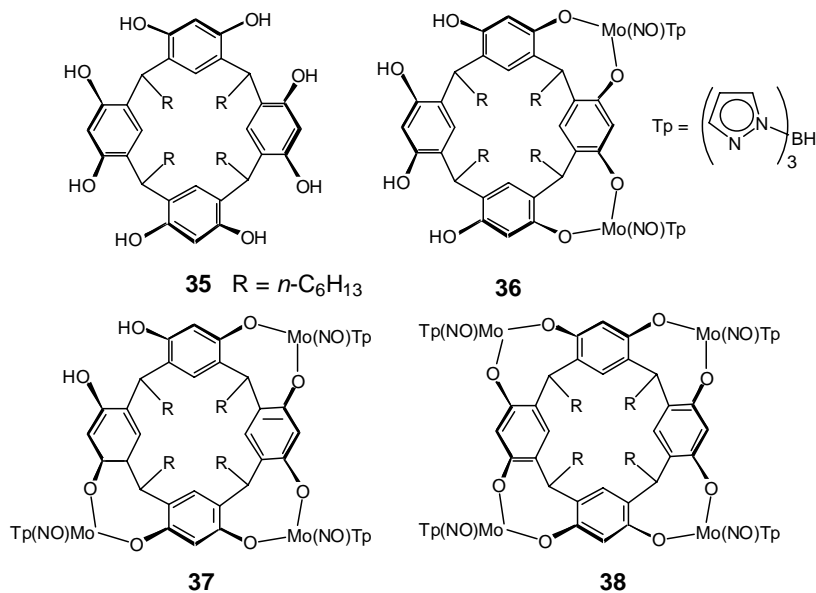
Reaction of *p*-Bu^t-calix[4]-OH₄ with [M₂(NMe₂)₆] (M = Mo, W) in hydrocarbon solvents gave dianionic complexes **30** and **31**, in which the metal-metal multiple bonds are supported by two bridging calixarenes both acting as tetraanionic species.^{15,16} The calixarenes have an elliptical cone section, and the metal-metal bond distances typically correspond to triple bonds. In the reaction of **30** with hot pyridine, complex **32** was formed (Scheme 3), both calixarene units encapsulating a pyridine molecule.¹⁷ This reaction is accompanied by a major structural change, since in this complex each calixarene acts as a terminal ligand. One oxygen atom of each calixarene ligand is hydrogen bonded to a H₂NMe₂ cation, and heating the pyridine solvate under dynamic vacuum for 3 days produced complex **33** containing only triply-deprotonated calixarene units. Reaction of the latter with HNMe₂ regenerated **32**. Complex **33** is also directly formed upon treatment of *p*-Bu^t-calix[4]-OH with [Mo(OBu^t)₆]. Similar reactions were found with tungsten. The tungsten analogues of **32** and **33** react in benzene to give complex **34** in which the metal-metal bond is spanned by one H₂NMe₂ cation that is hydrogen-bonded to a pair of phenolic oxygen atoms and also by a proton, attached to two other O atoms. Sandwich structures similar to those of **29-34** have been found in transition metal complexes of *p*-Bu^t-tetrathiocalixarene.¹⁸



Scheme 3.

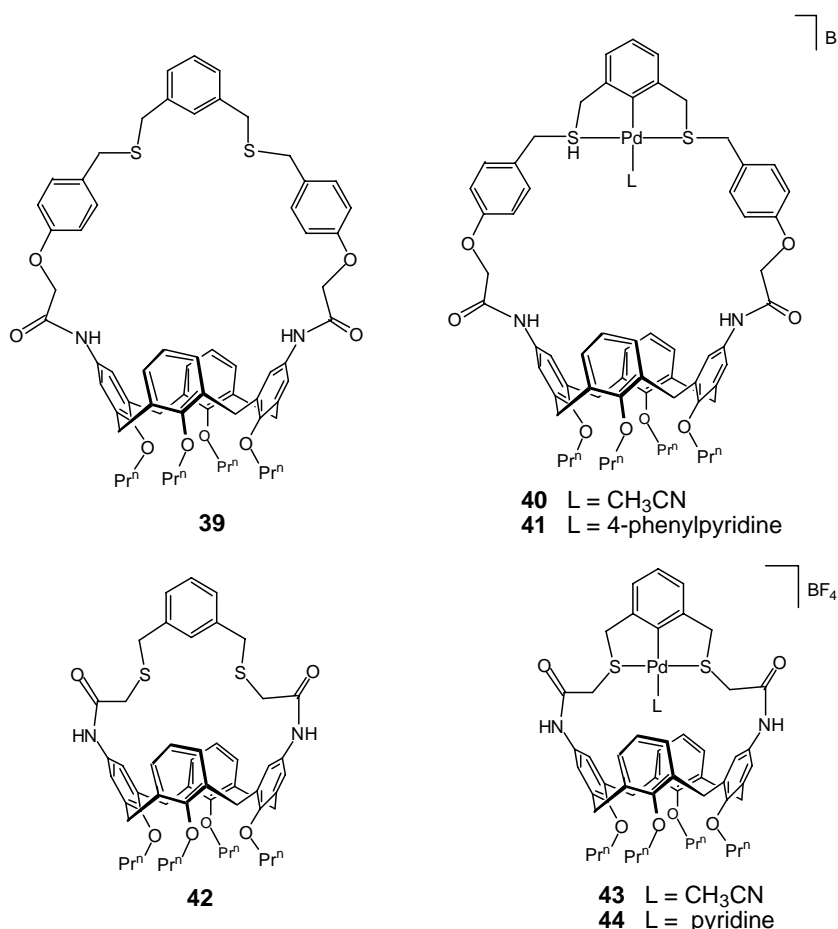
Multimetal complexation via phenolic oxygen atoms of calix[4]resorcinarenes is seen in the reaction of [MoTp(NO)I₂] (Tp = hydrotris(pyrazol-1-yl)borate) with tetrahexylcalix[4]resorcinarene **35** (resH₄). This reaction afforded a mixture of

metallomacrocycles from which $[\{\text{MoTp}(\text{NO})\}_2(\text{resH}_4)]$ **36**, $[\{\text{MoTp}(\text{NO})\}_3(\text{resH}_2)]$ **37**, and $[\{\text{MoTp}(\text{NO})\}_4(\text{res})]$ **38** could be isolated.¹⁹



2.2 Complexes having a metal centre bound to oxygen or sulfur atoms belonging to pendent functional groups

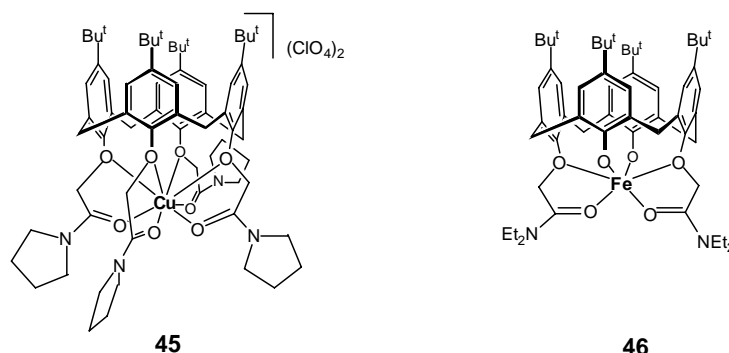
An example of a metallo-receptor in which the metal centre may be held at a cavity entrance is the upper-rim functionalised calix[4]arene **39**.^{20,21} This ligand reacts with $[\text{Pd}(\text{MeCN})_4](\text{BF}_4)_2$ to yield the palladium complex **40**. The ^1H NMR spectrum indicates that the methyl group is nested in the calix cavity. Replacement of the acetonitrile molecule by 4-phenylpyridine afforded complex **41**. Inclusion of the *p*-aryl ring within the cavity was inferred from an upfield shift of 3.90 and 2.78 ppm of the corresponding *p*-*H* and *m*-*H* protons, respectively.



Related complex **43** was easily obtained from calixarene **42** containing a shorter dithio cap. The coordinated acetonitrile was readily displaced by pyridine yielding complex **44**. NMR spectroscopy indicates an asymmetric structure (the two *m*-H of the phenoxy rings bearing amide groups are non-equivalent) possibly because pyridine is too large to be included in the receptor cavity and therefore lies outside. The asymmetry disappears with increasing temperature, indicating a fluxional process in which the pyridine probably moves across the cavity from one orientation "out of the cavity" to the other on the opposite side. Complex **40** displays a remarkable selectivity for complexation of 4-phenylpyridine over that of 3-phenylpyridine, reflecting the good shape fit with the receptor.

Calixarenes with pendant oxygen-containing donor groups have been widely used for solvent extraction.² Many efforts have been made to define the coordinative properties of such podands. Thus, in the tetraamide complex **45**, the copper(II) atom lies in an O_8 environment.²² An X-ray-study showed that the molecule has fourfold symmetry in the solid state and that the Cu atom lies significantly closer to the four carbonyl oxygen atoms ($\text{Cu}\cdots\text{O}$ 1.926 (6) Å) than to the ethereal oxygen atoms (2.963 (6)

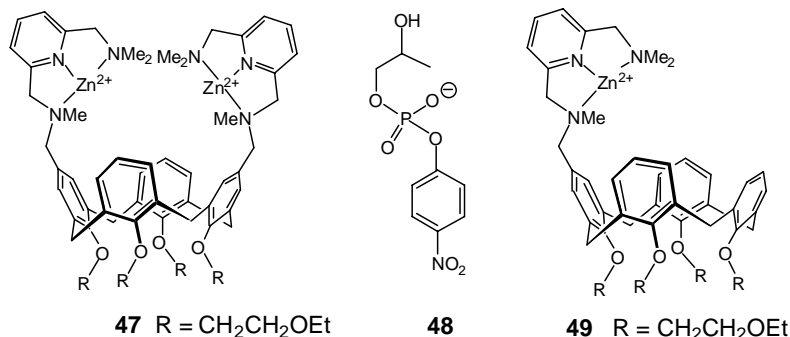
Å). In complex **46**, the iron atom is bonded to 6 oxygen atoms, the shortest bonds being those to the phenolic O atoms ($\text{Fe}\cdots\text{O}$ 1.802(8) and 1.830(7) Å), the next longest being the bonds to the carbonyl oxygens (2.058(7) and 2.031(7) Å), the longest being those to the etheral oxygen atoms (2.230(7) and 2.312(7) Å).²³

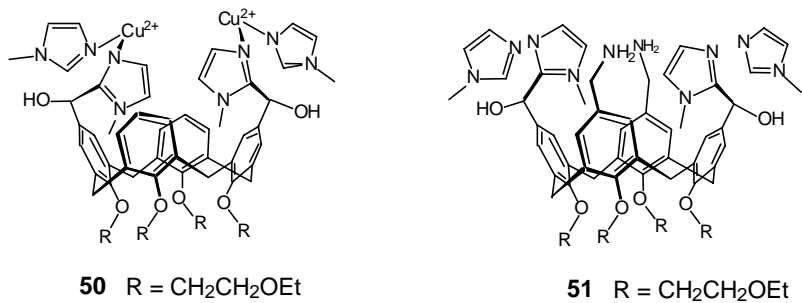


3 Calixarene complexes with metals bound to N donor atoms

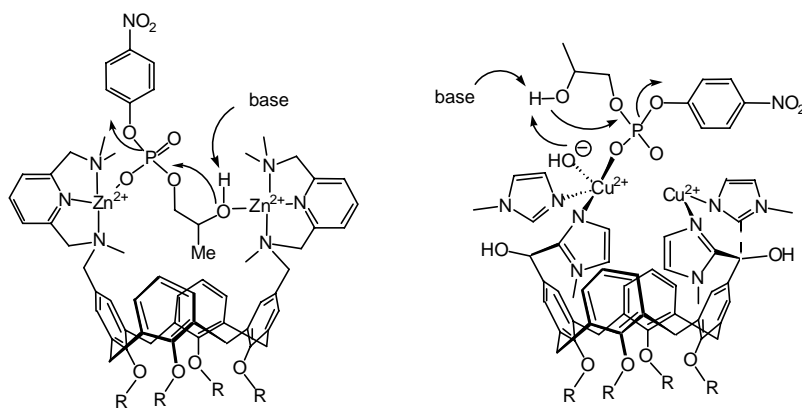
3.1 Attempts to prepare metallo-enzyme models

Metallo-calixarene **47** bearing two distal Zn(II) centres linked to the upper rim via bis(aminomethyl)pyridyl ligands constitutes the first example of a dinuclear complex showing both strong binding to a phosphate diester substrate and high catalytic hydrolysis activity.²⁴ Thus the presence of **47** triggers a 23000-fold rate enhancement in the catalytic cyclisation of the RNA model substrate 2-(hydroxypropyl)-*p*-nitrophenylphosphate **48**.





Comparative studies with the monozinc complex **49** (for which the activity is ca. 50 times lower), shows that the Zn centres in **47** operate synergistically. Possibly, one Zn atom acts as Lewis acid activator of a P-O bond, while the second one activates the hydroxyl group, hence facilitating its deprotonation (Scheme 4).

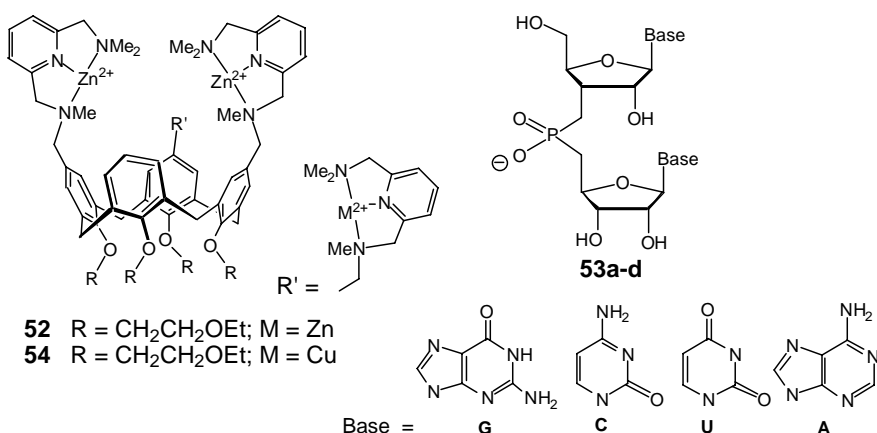


Scheme 4.

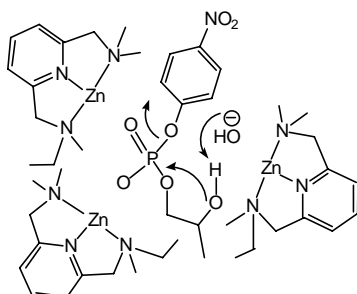
Extension of this work led to the design of another binuclear enzyme model, namely the Cu(II) complex **50**, in which the metal ions are complexed by a bis(methylimidazolyl) chelator.²⁵ The use of this complex for transesterification of **48** induces a rate acceleration of 10^4 , less than that of the Zn(II) complex **47**. The proposed mechanism of catalysis by the copper complex **50** is different from that for the zinc complex **47**. In this case, the phosphate is simultaneously activated by both Cu(II) centres as shown in Scheme 4, while an hydroxy group attached to one of the copper atoms facilitates activation of the neighbouring β -hydroxyl group (bifunctional catalysis).²⁶

Remarkable trinuclear cooperativity was found with the complex **52** mimicking phosphodiesterases (cleavage of RNA dinucleotides **53a-d**).²⁷ Rate accelerations over the uncatalyzed reaction are $\sim 10^4$ - 10^5 and large differences in rate were observed for different nucleobases in the dinucleotides: GpG>>UpU>>ApA. The trinuclear complex is a factor 10, 19 and 160 more active than the dinuclear complex **47** for the cleavage of

CpC, UpU, and GpG, respectively. The higher activity probably originates from favourable substrate binding and cooperative catalytic behaviour of all three Zn(II) ions.

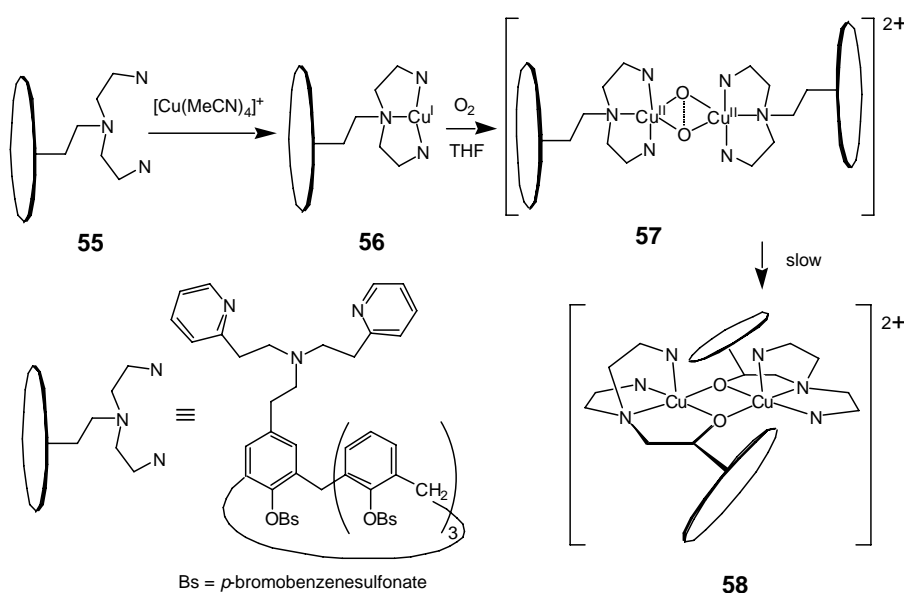


The heterotrinuclear metallo-phosphoesterase mimic **54** is even more active. The catalytic cleavage of **48** brought about by the trinuclear complex was also investigated. Under conditions similar to those for the transesterification of **48** by **47**, **52** induces a rate acceleration of 32 000.²⁸ The proposed mechanism involves two Zn centres that activate the phosphoryl group while the third activates the β-hydroxyl group (Scheme 5).

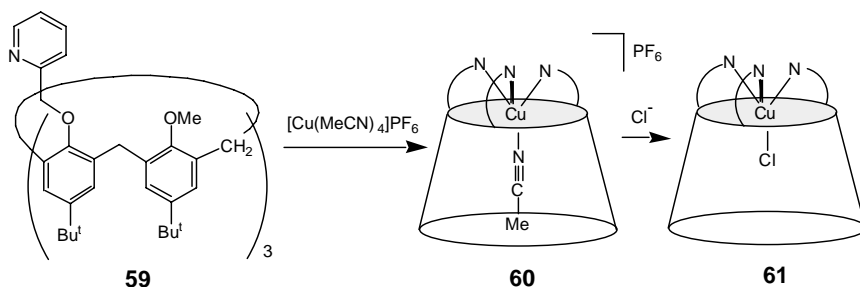


Scheme 5. Possible mechanism for the cleavage of 48 by 52

Receptors such as the amino-dipyridyl-calixarene **55** have been used to prepare dinuclear oxidation catalysts.²⁹ Reaction of **55** with [Cu(CH₃CN)₄] gave **56**, which reacted with oxygen to give a complex with the presumed structure **57** (Scheme 6). **57** slowly converted into **58**, which corresponds to an oxidation of the benzylic carbons of the arms linking the N₃ ligands and the calixarene unit.

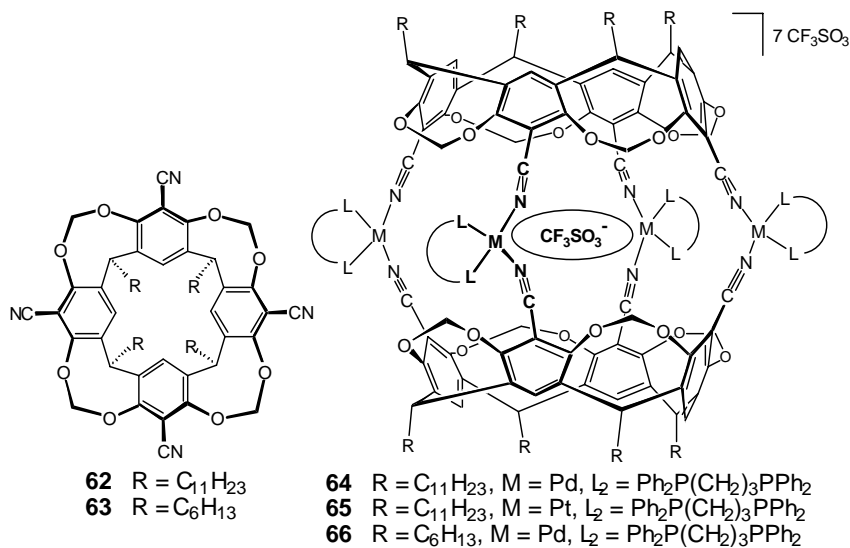
**Scheme 6.**

A calix[6]arene pocket has been used to provide a location for Cu(I) in the monometallic enzyme model **60** (Scheme 7).³⁰ The metal atom is bonded to the three pyridine units of ligand **59**, the fourth ligand being an acetonitrile molecule located in the cavity. The coordinated acetonitrile can easily be exchanged for other linear nitriles. Substitution by the chloride anion afforded complex **61**.³¹ In solution it exists as two equilibrating helical enantiomers. As shown by NMR experiments in the presence of a chiral shift reagent, the chirality is transmitted to the calixarene skeleton at low temperature, thus providing a chiral cavity around one coordination site.

**Scheme 7.**

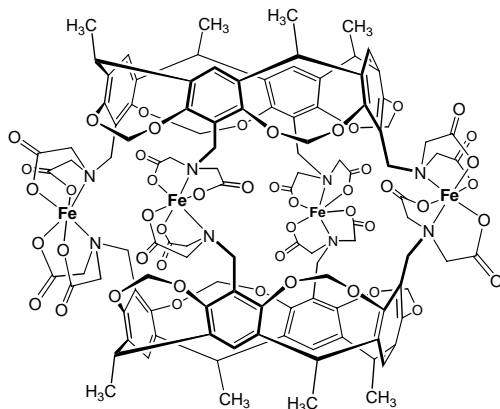
3.2 Complexes formed from resorcinarenes containing pendant nitrogen ligands

Binding of transition metal centres can be used to assemble capsules from appropriately functionalised calixarenes. One strategy capitalises on the fact that square planar cations of the type $[M(dppp)]^+$ ($M = Pd, Pt$; dppp = $\text{Ph}_2\text{P}(\text{CH}_2)_3\text{PPh}_2$) can assemble two ligands in a 90° spatial arrangement.³² Thus, reaction of the tetrafunctionalised resorcinarenes **62** and **63** with $[\text{Pd}(\text{dppp})](\text{CF}_3\text{SO}_3)_2$ (stoichiometry 2L : 4M) gave respectively the cage compounds **64** and **66**. Reaction of **62** with $[\text{Pt}(\text{dppp})](\text{CF}_3\text{SO}_3)_2$ afforded **65**. As shown by NMR, the capsules possess D_{4h} symmetry. The highest peaks observed in the ESI-MS spectrum correspond to the $[\text{M} - 2 \text{CF}_3\text{SO}_3]$ cations. The presence of a CF_3SO_3^- anion lying inside the capsule was inferred from the ^{19}F NMR spectrum (for **64**, $\delta = -81.5$ ppm vs. -78.2 ppm for the external anions), and was shown by an X-ray crystal structure determination.



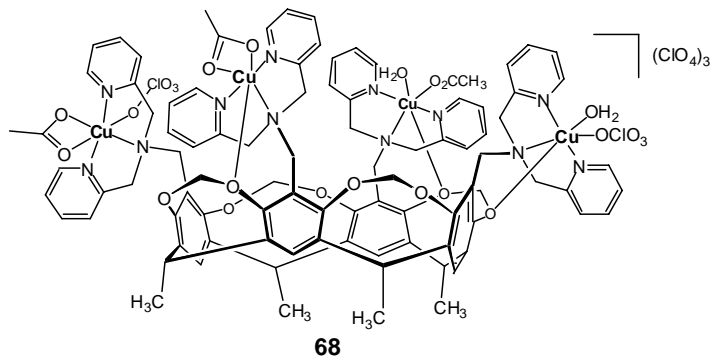
The paramagnetic $\text{Fe}(\text{II})$ cage complex **67** was formed by reaction of an iminodiacetic acid-functionalised resorcinarene precursor with FeCl_2 in aqueous solution above pH 5.³³ X-ray crystallographic analysis showed that the iminodiacetate ligands are coordinated in an N,N -*cis fac* manner; an N,N -*trans fac* coordination would not result in the formation of a container molecule. When **67** is formed in water, six water molecules occupy its cavity. Conduct of the synthesis in the presence of bromobenzene resulted instead in the inclusion of this molecule within the capsule. NMR studies showed that the cavity forms also host-guest complexes with molecules

that do not contain metal binding atoms, such as pentane, cyclohexane, benzene, and fluorobenzene.



67

The tetranuclear complex **68** (having the formulation $[\text{Cu}_4(\text{resorcinarene})(\text{CH}_3\text{CO}_2)_3(\text{ClO}_4)_2(\text{H}_2\text{O})_2](\text{ClO}_4)_3$) was obtained in 74 % yield by reaction of the corresponding tetra-tridentate N_3 ligand with copper(II) acetate and NaClO_4 .³⁴ Although the four Cu centres are structurally different, they all possess a meridional N_3 environment. The Cu centres behave as magnetically isolated entities.

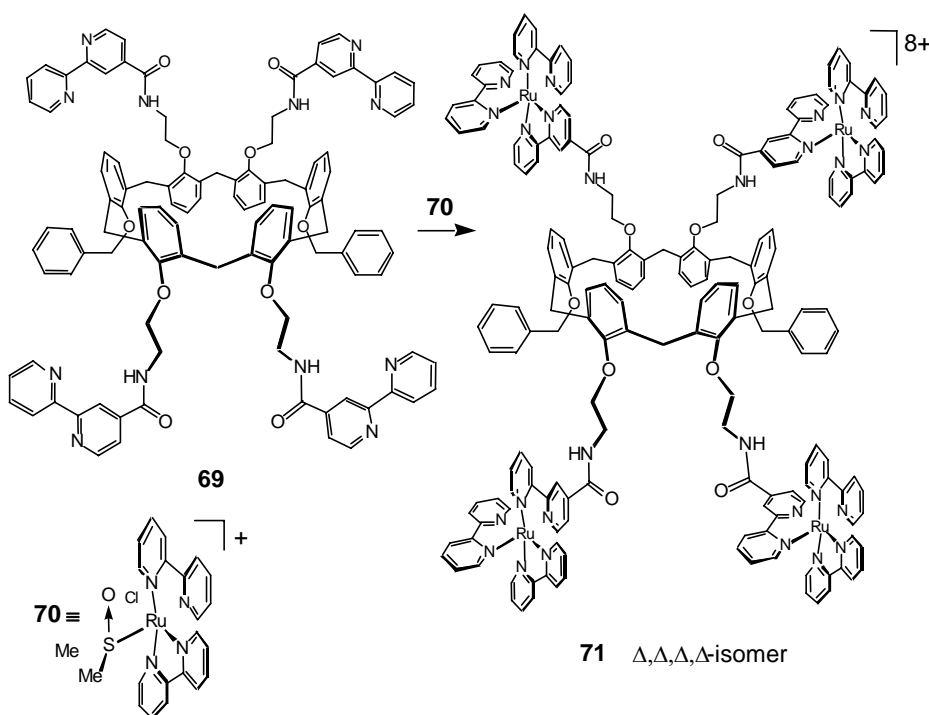


3.3 Other complexes obtained from calix[n]arenes substituted by nitrogen-containing ligands

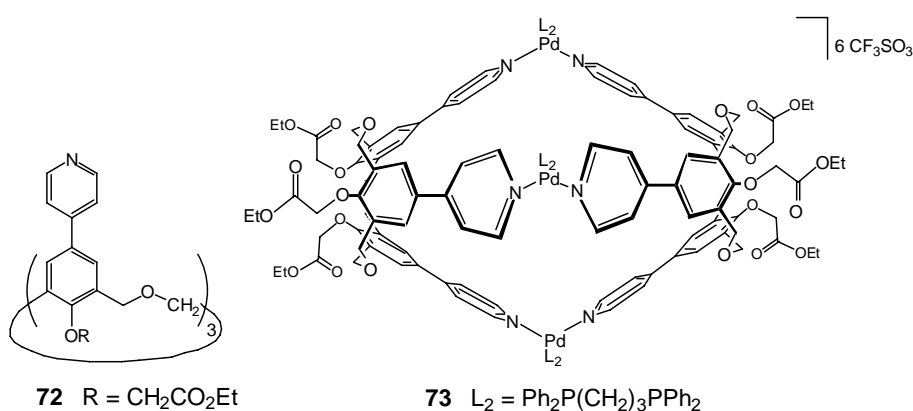
Over the last decade, there has been continuing interest in using calixarenes for the preparation of luminescent or electrochemical sensors able to detect anions or cations. To avoid the formation of complicated isomeric mixtures, tetra-Ru complex **71** was obtained by reaction of the tetrpyridine precursor **69** with the resolved precursor *cis*- Δ -[Ru(bpy)₂(DMSO)Cl]PF₆ **70** (98.6 % ee).³⁵ The precise yield of $\Delta,\Delta,\Delta,\Delta$ -product

could not be determined exactly but was assessed to be ca. 90 %, based on CD spectroscopy and HPLC (Scheme 8).

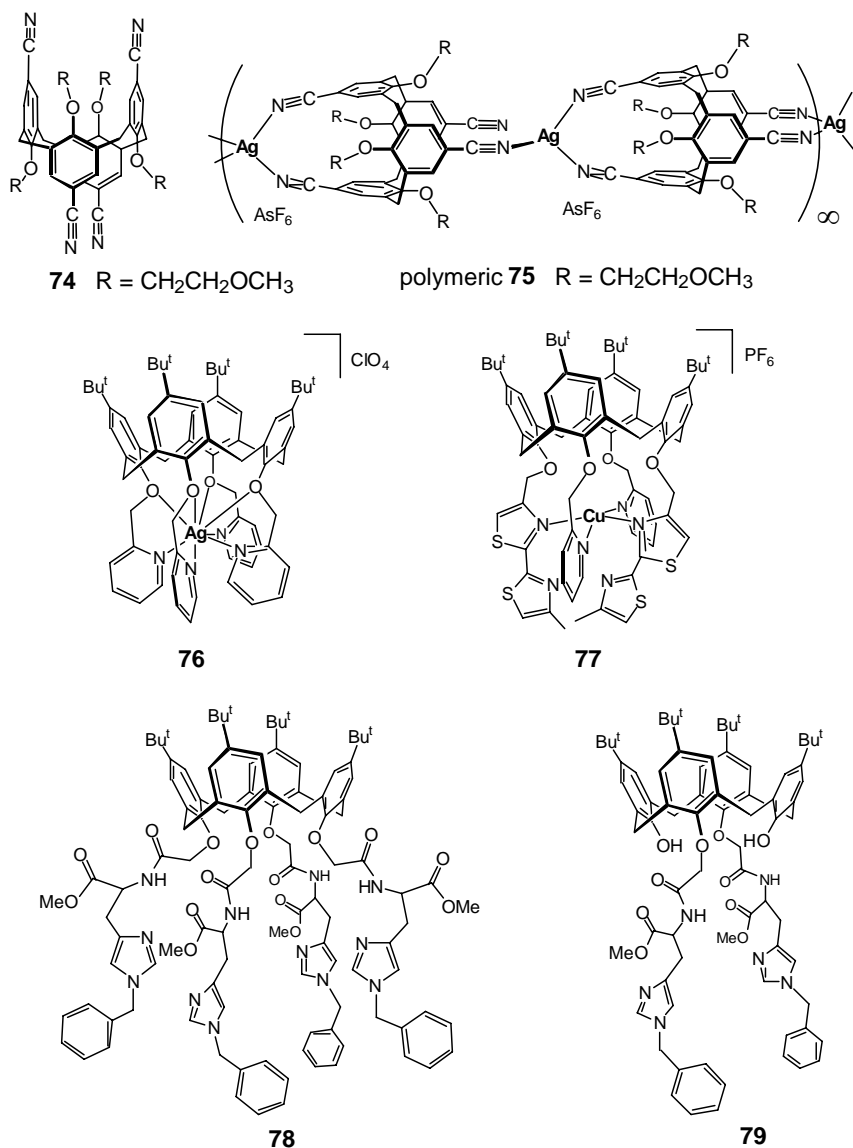
Reaction of the *cone* conformer of the homooxacalix[3]arene-derived trispyridine compound **72**³⁶ with [Pd(dppp)][(CF₃SO₃)₂] gave complex **73** in high yield when the 2calix : 3Pd stoichiometry applied precisely. The NMR spectra, which are consistent with a *D*_{3h}-symmetrical structure, indicate that the phenyl units are more flattened than in the starting compound. Formation of a compound of formula [Pd₃(calix)₂](CF₃SO₃)₆ was inferred from osmometry. Mass spectrometry indicates that the cage is able to encapsulate two molecules of CD₂Cl₂.



Scheme 8.



Metal-controlled assembly of functionalised calixarenes has also recently been applied to 1,2-alternate calixarenes bearing two sets of divergent nitrile arrays. This strategy leads to inorganic polymers. For instance, slow diffusion of a solution of tetranitrile **74**, into a solution of AgAsF_6 afforded complex **75** the polymeric solid-state structure of which was established by an X-ray diffraction study.³⁷ The structure consists of stacked calixarene units linked by tetrahedral silver ions that are bonded to two pairs of nitrile ligands ($\text{C}-\text{N}-\text{Ag}$ 144 °).



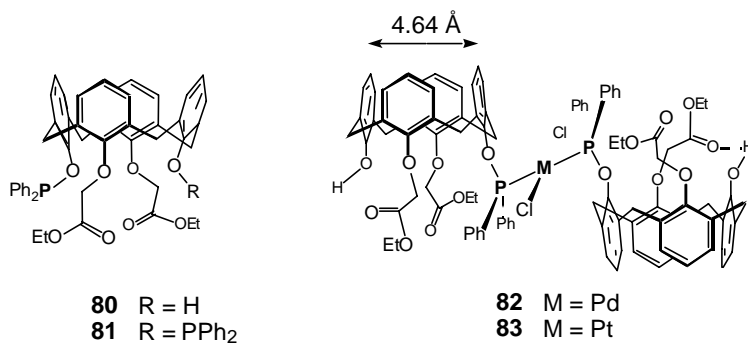
Ag(I) is found in a N_4O_4 environment in complex **76**, where the calixarene matrix adopts a highly symmetrical cone conformation which favours enclathration of an acetonitrile molecule within the hydrophobic pocket.³⁸ The silver ion sits at the centre of a square antiprism ($\text{Ag}\cdots\text{O} : 2.923(3)$; $\text{Ag}\cdots\text{N} : 2.483(5)$ Å).

Cu(I) appears to be encapsulated by a hybrid bis(pyridine)-bis(thiazole) calix[4]arene to give a complex for which the structure 77 has been proposed on the basis of ^{15}N NMR spectroscopy.³⁹ Complexation studies with the two histidyl podands **78** and **79** unambiguously showed that these ligands are able to bind one (paramagnetic) CoCl_2 unit, but the exact nature of the complexes formed could not be detailed because of lack of crystals suitable for an X-ray diffraction study.⁴⁰

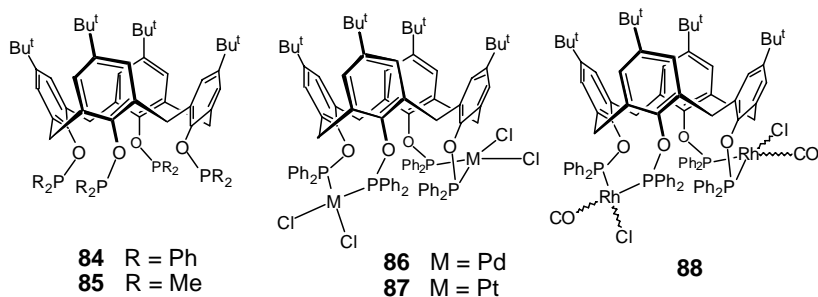
4 Calixarene complexes obtained from phosphorus ligands

4.1 Complexes from calixarenes with phosphorus atoms tethered to the lower rim

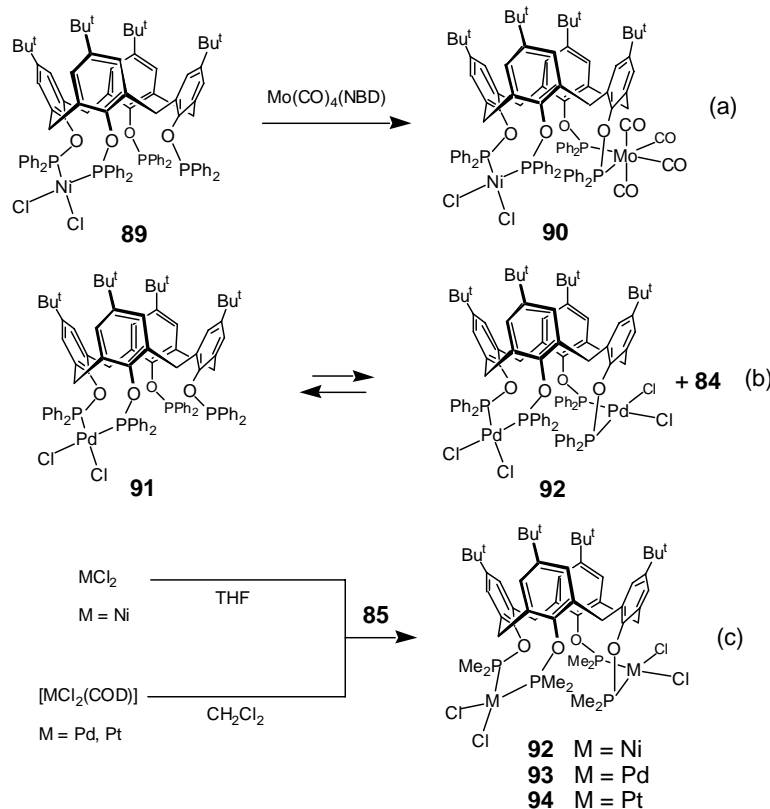
Monophosphinite **80** reacts with $[\text{MCl}_2(\text{PhCN})_2]$ ($\text{M} = \text{Pd, Pt}$) to form the isomorphous MCl_2L_2 complexes **82** and **83**.⁴¹ The selective formation of *trans* compounds can be assigned to the bulkiness of the ligand. In the solid state the phosphino groups adopt the position that causes minimal steric perturbation to the calixarene units and the two calixarenes moieties adopt a divergent spatial array. Each phosphinated aryl ring is pushed towards the centre of the cavity. The C···C separation between the *p*-carbon atoms of the phenol ring and the phosphinated one is only 4.64 Å. Reaction of the diphosphinite **81** with $[\text{PtCl}_2(\text{PhCN})_2]$ afforded sparingly soluble oligomeric material. The formation of tetrameric structures has previously been established with soluble forms of **81**.⁴²



The ligands **84** and **85** readily form chelate complexes involving proximal phosphinites.⁴³ The homodimetallic complexes **86** and **87** have been obtained in high yield from the corresponding $[MCl_2(COD)]$ precursor ($M = Pd, Pt$, COD = cycloocta-1,5-diene) and **84**. The dirhodium complex **88** was obtained from $[Rh(CO)_2Cl]_2$, but the exact relative stereochemistry about the two metal centres is unknown. A remarkable downfield shift was observed for the *endo*-ArCH proton of the metallocyclic units of complexes **86–88**. Similar observations were made within related but somewhat larger metallo-macrocycles (vide infra⁴⁴).



Reaction of **84** with $NiCl_2$ gave the monometallic chelate complex **89**.⁴³ This is useful for the preparation of heterobimetallic systems, such as the Ni-Mo complex **90** (Scheme 9a). The monometallic palladium complex **91** could be obtained from $[PdCl_2(COD)]$ using a 1Pd:1L stoichiometry, but this complex slowly disproportionates into **84** and the corresponding dipalladium complex **86** (Scheme 9b).



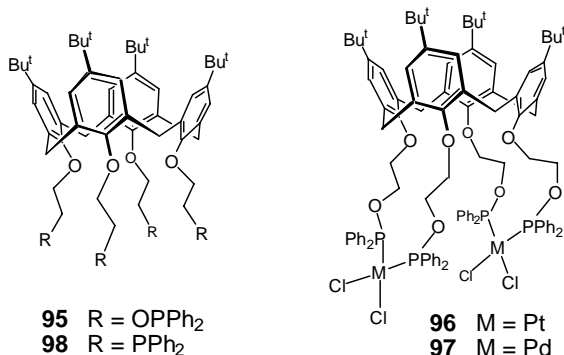
Scheme 9.

Bis-chelate complexes (for $\text{M} = \text{Ni}, \text{Pd}, \text{Pt}$) were easily obtained from the less sterically demanding and more basic tetraphosphinite **85** (Scheme 9c).⁴³ The nickel centres in **92** undergo planar-tetrahedral interconversion. As shown by X-ray diffraction studies of complexes **93** and **94**, the P-M bonds point away from the cavity.

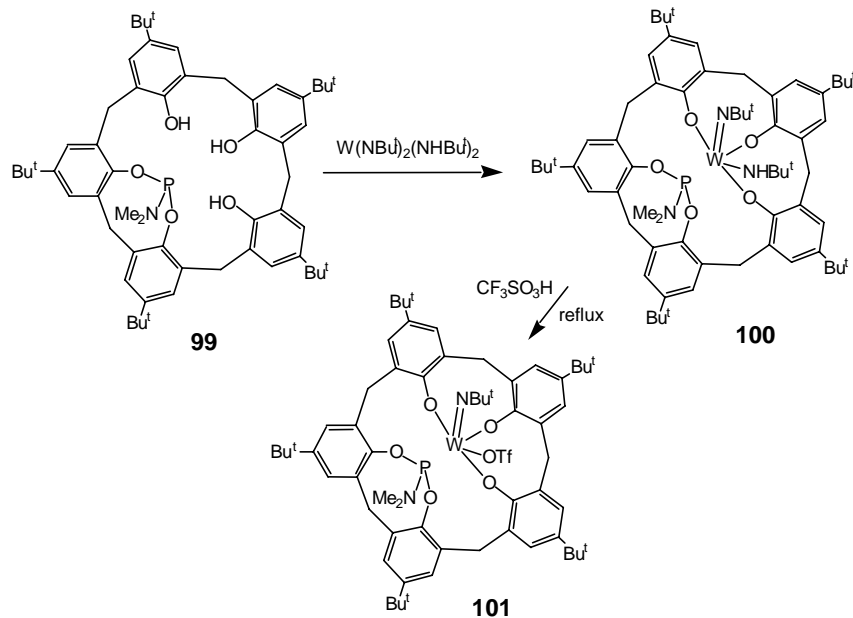
Despite the long separation between two adjacent phosphorus centres, the reaction of **95** with $[\text{PtCl}_2(\text{PhCN})_2]$ afforded the bis-chelate complex **96** in high yield. When $[\text{PdCl}_2(\text{PhCN})_2]$ was used as a starting compound, the related di-palladium complex **97** was formed in 91 % yield along with some oligomeric material.⁴⁵ In the presence of SnCl_2 , complex **96** catalyses the hydroformylation of styrene, but the catalytic activity of this system is much lower than that of conventional $\text{PtCl}(\text{SnCl}_3)(\text{diphos})$ catalysts. However, a slightly higher regioselectivity (+ 10 %) towards branched/aldehyde was observed. The catalytic activity of **97** in the hydroalkoxycarbonylation of styrene ($\text{PhCH=CH}_2 + \text{CO}/\text{ROH}, 130^\circ\text{C}, 140 \text{ bar}$) is weak owing to alcoholysis of the PO bonds.⁴⁵

The activities of $[\text{RhCl}_2(\text{NBD})]_2/\textbf{95}$ and $[\text{RhCl}_2(\text{NBD})]_2/\textbf{98}$ mixtures towards the hydroformylation of styrene were found to be slightly lower than the usual

Rh/phosphine systems. The aldehyde selectivities are comparable to the best rhodium catalysts.⁴⁵

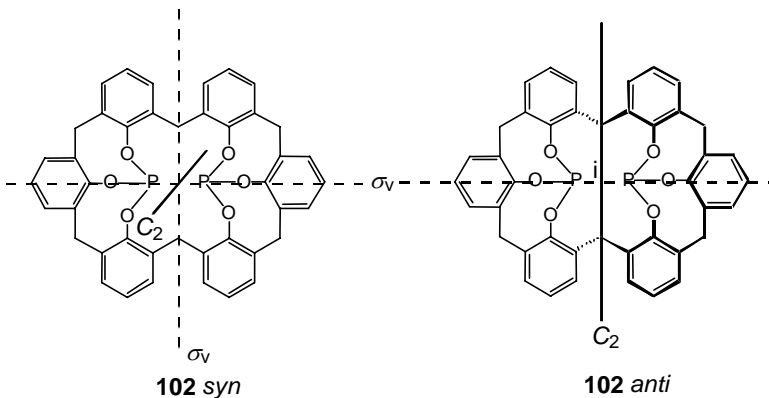


Positioning of a tungsten unit at the entrance of a calix[5]arene was achieved by reacting the aminophosphite 99 with [W(NBu^t)₂(NHBu^t)₂], giving 100.⁴⁶



Scheme 10.

The tungsten atom adopts a square-pyramidal geometry, while the calixarene backbone is rather flattened. The phosphorus lone pair points towards the sixth coordination site with a P···W distance of 3.15 Å that is far outside the usual range found for P-W bonds. Nevertheless, both atoms are close enough to exhibit a small through-space coupling of 43 Hz in the NMR spectrum. Substitution of the butylamido ligand by OTf gave complex 101. The change of electron density at the metal centre induces a significant shortening of the P-W bond (2.74 Å in 101), and the imido ligand is now located inside the calix cavity.



Two reports have appeared that illustrate the relevance of calixarene-derived phosphites in homogeneous catalysis. The chelate complexes $[(syn\text{-}102)\text{MCl}_2]$ ($\text{M} = \text{Pd}$, **103**; $\text{M} = \text{Pt} = \text{104}$), $[(syn\text{-}102)\text{M}(\text{CH}_3)\text{Cl}]$ ($\text{M} = \text{Pd}$, **105**; $\text{M} = \text{Pt} = \text{106}$), $[(syn\text{-}102)\text{M}(\text{CH}_3)(\text{CH}_3\text{CN})]\text{CF}_3\text{SO}_3$ (**107**) and $[(syn\text{-}102)_2\text{Pd}(0)]$ (**108**), all display a *cis* arrangement of the phosphorus atoms,⁴⁷ thus leaving two adjacent sites on Pd available for catalytic action. The structure of **103** (Figure 1) determined by X-ray crystallography showed that the ligand bite angle in this chiral complex is 94° .

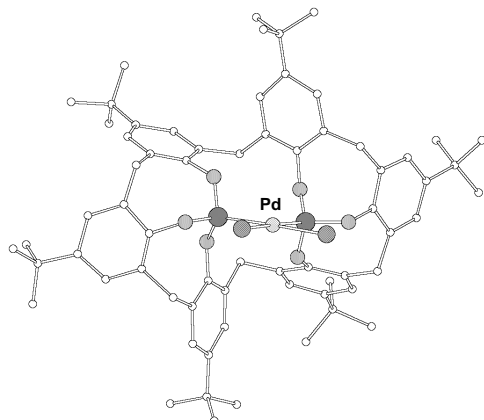
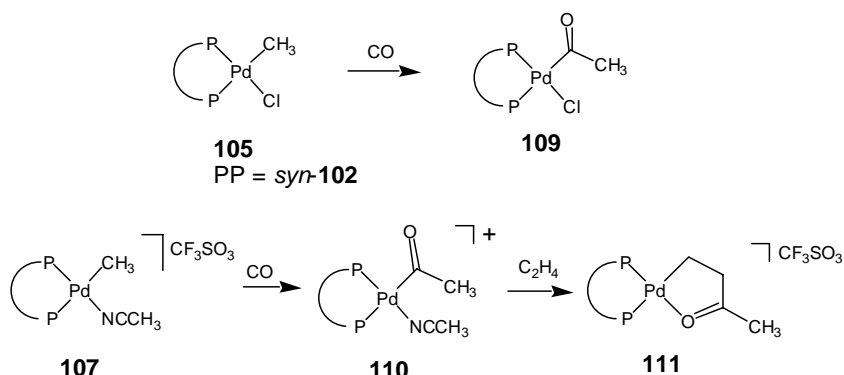


Figure 1. Molecular structure of 103

Both complexes **105** and **107** react with CO to afford the insertion products **109** and **110**, respectively. Only the cationic complex **110** reacts further with ethylene to yield the five-membered ring species **111** (Scheme 11). This behaviour made complex **110** a potential candidate for the catalytic co-polymerisation of CO/ethylene, although catalysis of this type was thought not to be operative when phosphites are used. Remarkably, complex **110** is the first reported complex based on a diphosphite that displays activity in the copolymerization of ethylene and carbon monoxide. The turnover frequencies lie in the range of $850\text{-}5300 \text{ mol}\cdot\text{mol}^{-1}\cdot\text{h}^{-1}$ (25°C , 20 bar

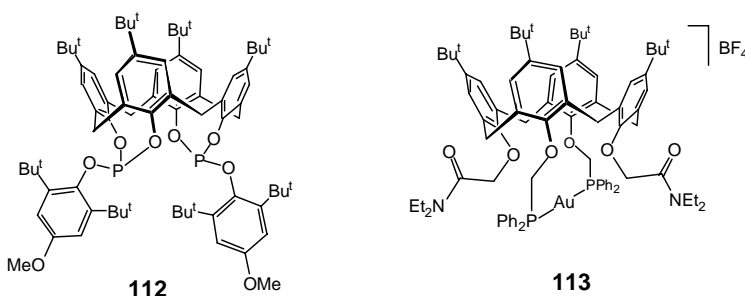
C_2H_4/CO). The $\langle M_n \rangle$ of the polymers obtained was ca. 34 000 with a polydispersivity index of 2.3. These findings are not uncommon for runs using active Pd/phosphine complexes.⁴⁷



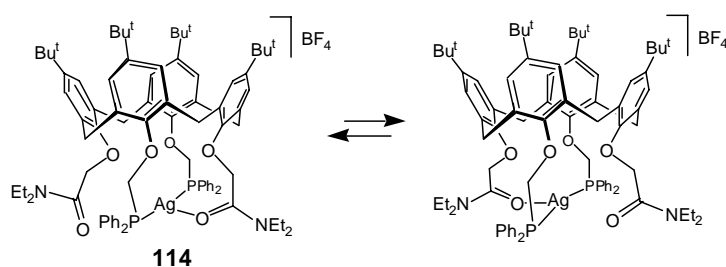
Scheme 11.

Very high regioselectivities in favour of *n*-nonanal were found in the rhodium-catalysed hydroformylation of 1-octene using **112**.⁴⁸ A reaction time of eight hours (1-octene:Rh = 4000, P(H₂-CO) = 20 bar, 100 °C, solvent : 2,2,4-trimethyl-1,3-pentanediol isobutyrate) resulted in 63% conversion and an aldehyde selectivity of 61 % (12% *n*-octenes and 27 % octane). The *n/iso* ratio was 200:1, representing the highest regioselectivity observed to date. Molecular modelling shows that the *P*₂-chelated rhodium atom is blocked between the two sterically demanding 2,6-di-Bu^t-phenoxy groups in such a manner that the olefin approach is difficult. This explains the relatively low reaction rate. Furthermore, the steric hindrance strongly favours the formation of the 1-octyl-rhodium intermediate over the 2-octyl complex, hence the high proportion of *linear* nonanal. It was verified that removal of the two Bu^t substituents of the aryloxy group opens the structure and therefore increases the activity, but this was also accompanied by a selectivity drop.

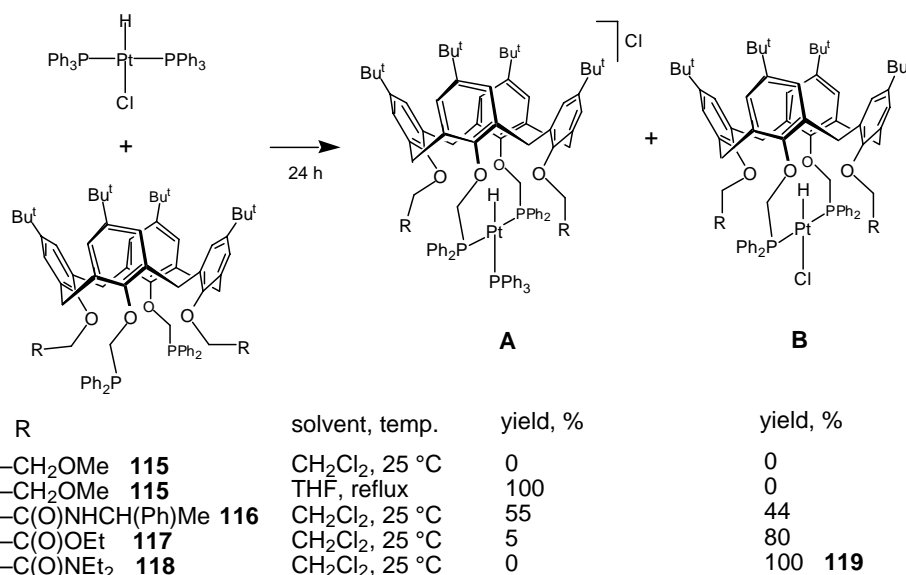
The coordinative properties of calixarenes bearing two distally-positioned —CH₂PPh₂ arms have been investigated towards a series of precious metals.⁴⁹ Diphosphines of this family are able to behave as *trans*-spanning ligands, as *e.g.* in the cationic complexes **113** and **114**.



While the metal centre in **113** appears to be in a linear PMP arrangement, the silver atom of **114** is probably in a T-shaped P_2O_{amide} coordination environment. NMR spectra being in agreement with a C_{2v} -symmetrical structure suggest a fast exchange between the coordinated and the free amide in solution.

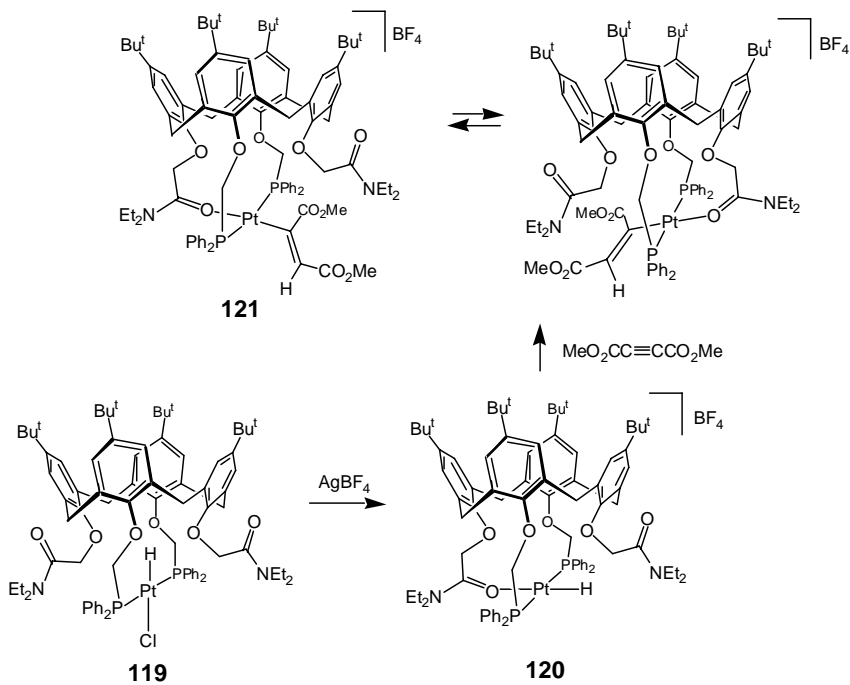


The rate of chelate formation using such diphosphines was found to strongly depend on the nature of the functional groups linked to the other two phenolic oxygen atoms. Diphosphines **115-118** bearing side arms with oxygen donor functionalities, react with the hydrido complex $[\text{PtHCl}(\text{PPh}_3)_2]\text{BF}_4$, to afford a mixture of *trans* complexes, as shown in Scheme 12.



Scheme 12. Anchimeric assistance of the functional side groups in the reaction between calix-diphosphines and $[\text{PtHCl}(\text{PPh}_3)_2]$

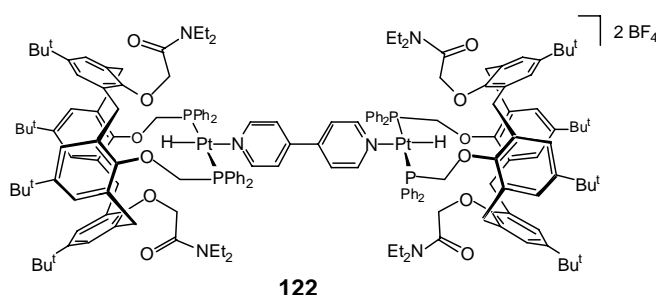
With diphosphines bearing weakly coordinating side groups, compounds of type A with a remaining PPh_3 ligand are formed slowly but preferentially, whereas with strong donors such as $-\text{C}(\text{O})\text{NEt}_2$ both PPh_3 ligands are rapidly substituted (type B complexes are the major compounds). In these reactions, A-type complexes are first formed and then are slowly converted into complexes of type B. Bearing in mind that with **115**, which has weak ether donors, no reaction at all takes place at room temperature, it is plausible that the phosphine moieties on their own cannot initiate the substitution reaction, probably for steric reasons. The substitution must therefore be initiated by the sterically less demanding side-functions. The ease of formation of B-type complexes increases with the donor properties of the auxiliary function. With diamide **118**, only formation of a B-type complex (**119**) was observed. In all the complexes formed, the platinum-hydrogen bond points inside the calixarene cavity. Because of the steric protection of the hydride, the Pt-H bond displays a rather high stability towards potential reagents, such as *e. g.* $\text{MeO}_2\text{CC}\equiv\text{CCO}_2\text{Me}$, which normally insert into the Pt-H bond.



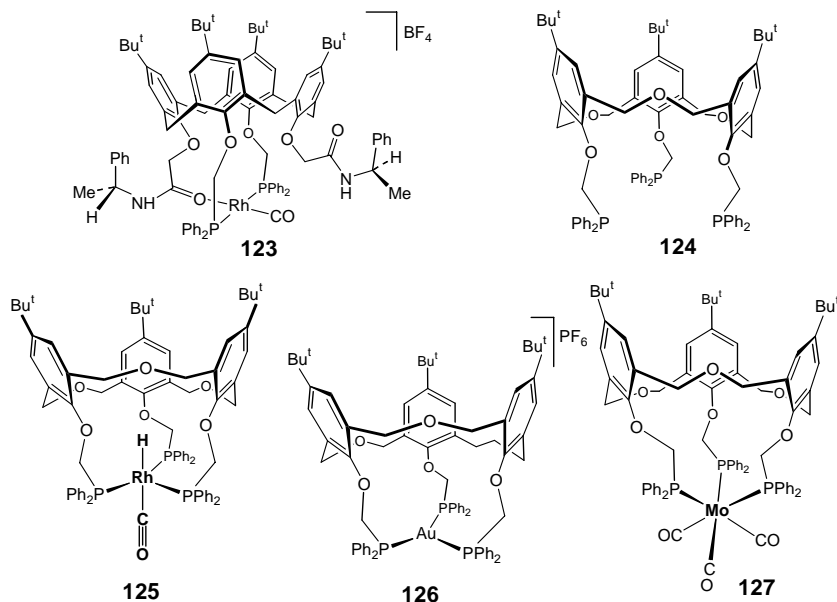
Scheme 13.

Under forcing conditions and again with the help of the auxiliary group, the direction of the Pt-H vector can be modified. Thus, the reaction of **119** with AgBF_4 results in the formation of complex **120** in which the Pt-H bond points towards the

exterior of the cavity (Scheme 13). In this structure, the metal plane closes the cavity.⁴⁹ In other terms, the ligand behaves as a hemispherical ligand that caps the metal plane. In this arrangement, the hydride becomes also much more reactive. With MeO₂CC≡CCO₂Me for example, the platinum alkenyl insertion product **121** is formed. The high *trans* influence of the Pt-C(alkenyl) bond labilises the platinum amide bond and favours the substitution at the free co-ordination site by the opposite amide. This results in a fast pendulum motion as shown in Scheme 13, the exchange possibly occurring via a transient penta-coordinated platinum species. Substitution of the co-ordinated amide of **120** by strong donors allows the repositioning of the hydride inside the cavity, as illustrated by the reaction with 4,4'-bipyridine, leading to **122**.



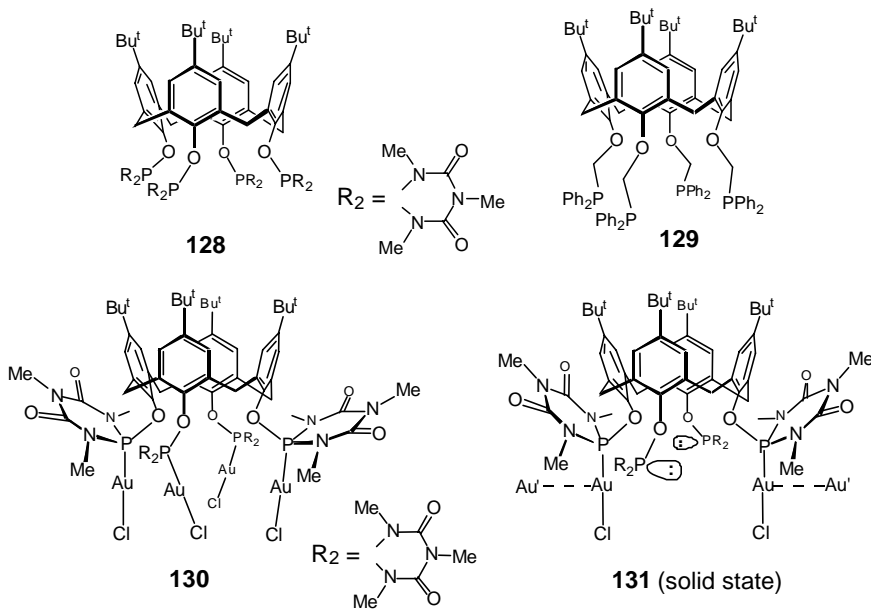
In complex **123** no pendulum motion was observed, indicating a strong metal-amide bond.⁴⁹ Complex **123** was tested as hydroformylation catalyst of styrene (40 bar CO/H₂, 40 °C, toluene-CH₂Cl₂), but its properties were unexceptional.



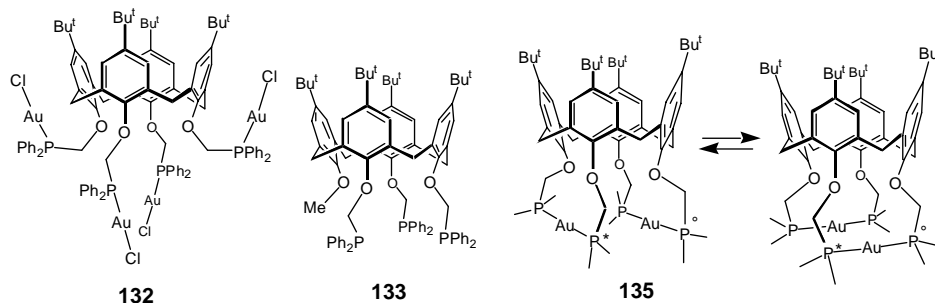
Stereoselectivity around an H-Rh-CO rod has been realised by reaction of the hexahomotrioxocalix[3]arene-derived C_{3v} -symmetrical triphosphine **124**, with $[\text{Rh}(\text{acac})(\text{CO})_2]$ under 20 bar CO/H_2 .⁵⁰ This reaction results in formation of a trigonal

bipyramidal hydrido carbonyl complex with the Rh-H vector directed inside the cavity (**125**). C_{3v} -Symmetrical complexes derived from **124** were also obtained for gold (**126**) and molybdenum (**127**).

Synthesis of multinuclear species can be achieved using tetrapodes **128** and **129**.⁵¹ The addition of four equiv. of $[\text{AuCl}(\text{SC}_4\text{H}_8)]$ to **128** gave the tetragold complex **130**. NMR data indicate an almost C_4 -symmetrical structure for the complex in solution. However careful examination of the ^1H NMR spectrum shows that the resonances of the C(O)NMe groups display a complex pattern. It is likely that rotation of the relatively bulky heterocycles around the phosphorus atoms is restricted, so that the four phosphorinane fragments adopt various orientations with respect to the calix axis. Di-auration of **128** was observed when the latter was reacted with 2 equiv. of $[\text{AuCl}(\text{SC}_4\text{H}_8)]$. The gold moieties of the complex formed (**131**) are bonded to two distal P atoms. Interestingly, the P lone pairs of the uncomplexed phosphorinane moieties point roughly in the same direction so that the two methyl groups of these heterocycles are formally non equivalent. As a result of short intermolecular Au···Au' contacts (3.288(1) Å), a loose polymeric structure emerges in the solid state.

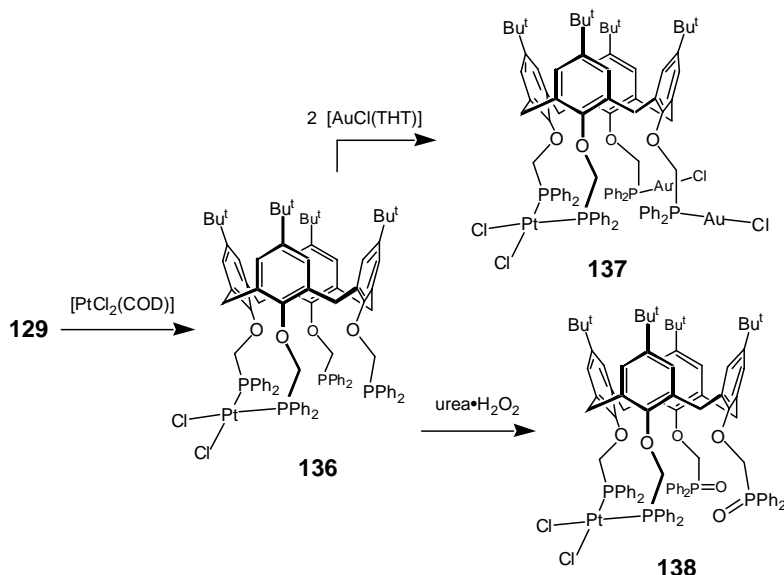


Reaction of **129** with $[\text{AuCl}(\text{SC}_4\text{H}_8)]$ yields the complex **132**⁵¹ which has a C_{4v} -symmetric structure in solution. In the solid state, two opposite Au-Cl units are oriented parallel to their appended phenoxy rings, whilst the other two lie approximately orthogonal to the calixarene axis. Reacting the tridentate ligand **133** with excess $[\text{AuCl}(\text{SC}_4\text{H}_8)]$ led to the trimetallic complex **133}•(AuCl)₃** (**134**).



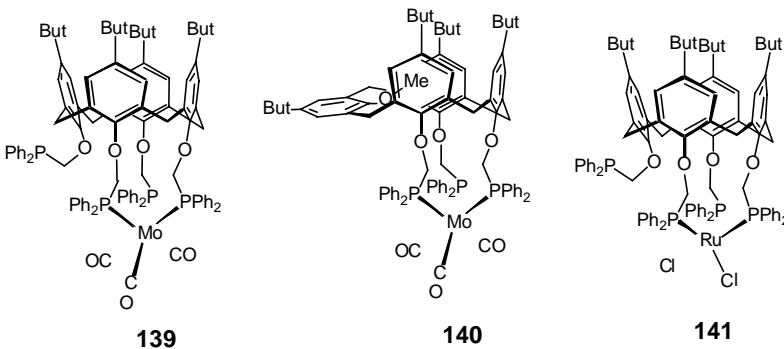
Treatment of **129** with excess $[\text{Au}(\text{solvent})_2]\text{BF}_4$ gave the cationic digold complex **135**.⁵¹ This complex displays dynamic behaviour in solution, the two gold atoms rotating simultaneously on the P_4 surface as shown in the drawing.

Another potential application of ligand **129** is the preparation of heterometallic complexes.⁴⁴ Reaction of **129** with $[\text{PtCl}_2(\text{COD})]$ afforded the chelate complex **136** where the metal is selectively bonded to two proximal phosphines. This complex was further reacted with two equiv. of $[\text{AuCl}(\text{SC}_4\text{H}_8)]$ to afford the PtAu_2 complex **137**. Complex **136** could not be isolated since polymerisation occurred during concentration. A simple way to prevent this phenomenon consists in either complexing the P donors or oxidising them, this latter reaction leading then to complex **138** (Scheme 14).

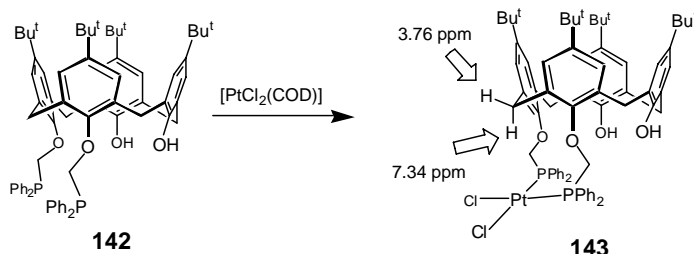


Scheme 14.

Facial P₃ coordination of **129** and **133** is found in complexes **139-141**.⁴⁴ The ruthenium complex **141** binds reversibly two molecules of acetonitrile.



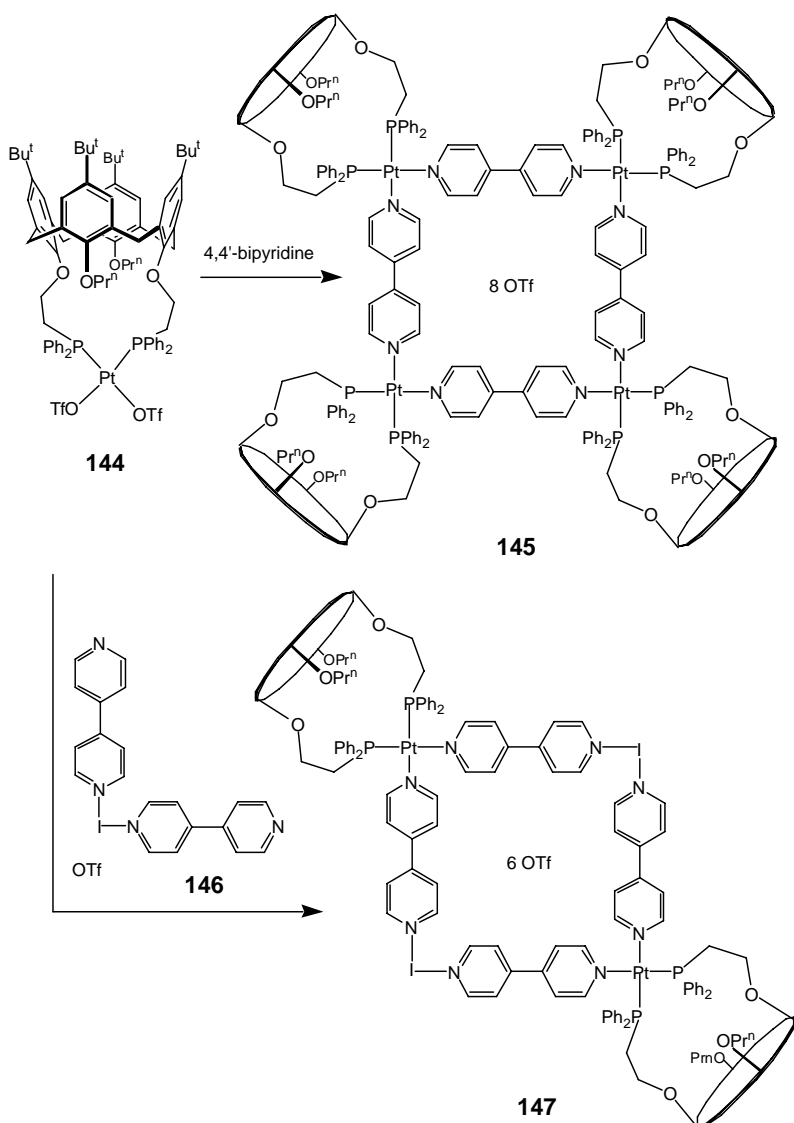
The chelate complex **143** was obtained by reacting diphosphine **142** with [PtCl₂(COD)] (Scheme 15).⁴⁴ In the solid state the PPt vectors point away from the calixarene axis. A striking feature of the NMR spectrum of **143** is the large splitting of the A and B parts of the ArCH₂ group lying between the two phosphines ($\Delta\delta = 3.6$ ppm !), with the axial-CH signal appearing at 7.34 ppm. This effect could arise from a ring current generated by the metallo-macrocycle that opposes the external field. An interaction between the axial CH atom and *both* neighbouring oxygen atoms may also be involved. Note, in the solid state the axial ArCH is exactly apically sited above the platinum atom, with a H···Pt separation of only 2.5 Å, so that the deshielding could possibly also be caused by an interaction with the metal d_{z²} orbital. A similar geometrical relationship was found for complex **137** in the solid state.⁵²



Scheme 15.

Complex **143** displays dynamic behaviour in solution, which can be rationalized as follows: (i) a fast flip-flop motion of both hydroxyl groups at low temperature, alternately forming hydrogen bonds with each of the neighbouring ether oxygen atoms; (ii) a reversible inversion of the phenol rings through the lower-rim annulus, triggered by cleavage of the hydrogen bonds at higher temperature.

Calixarenes have also been used in the construction of "molecular squares".⁵³ The reaction of **144** with 4,4'-bipyridine (Scheme 16) gave **145** and reaction with the bis(heterodiaryliodonium salt **146** gave another square, **147**, which contains two platinum atoms in the central macrocyclic structure.

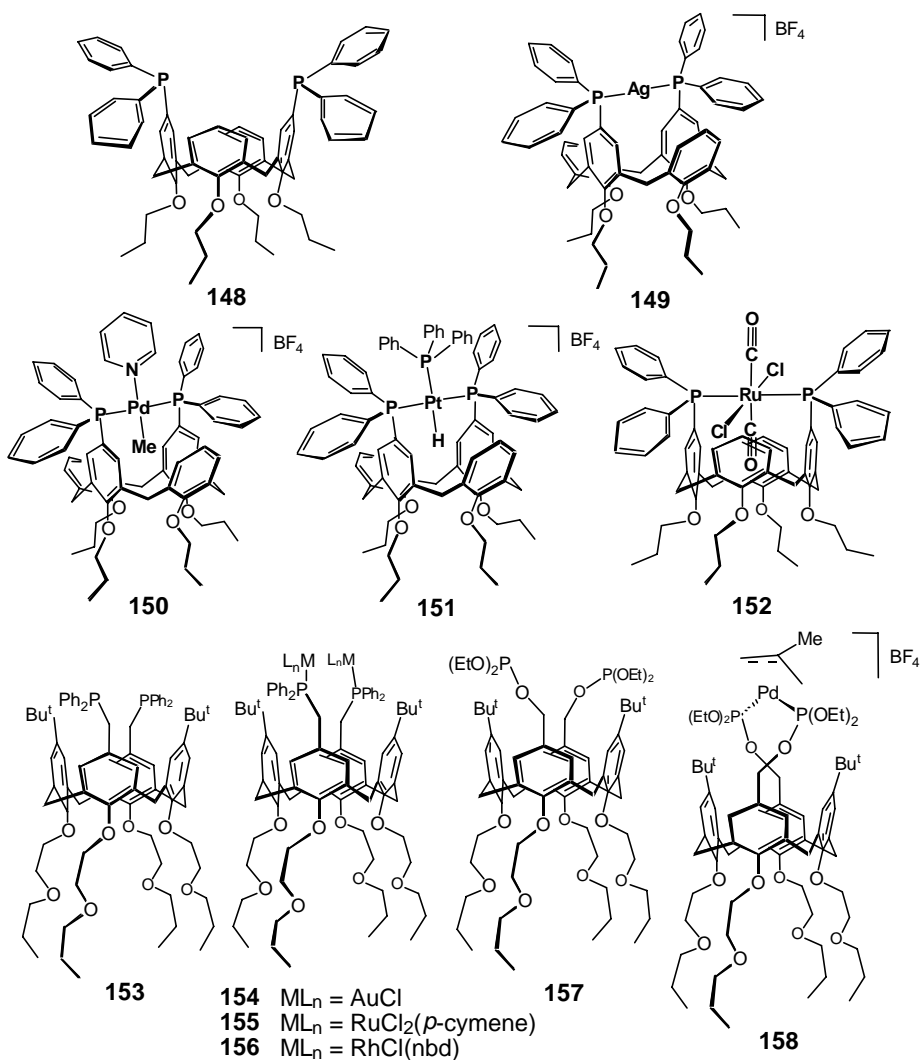


Scheme 16.

4.2 Complexes of calixarenes with upper rim P substituents

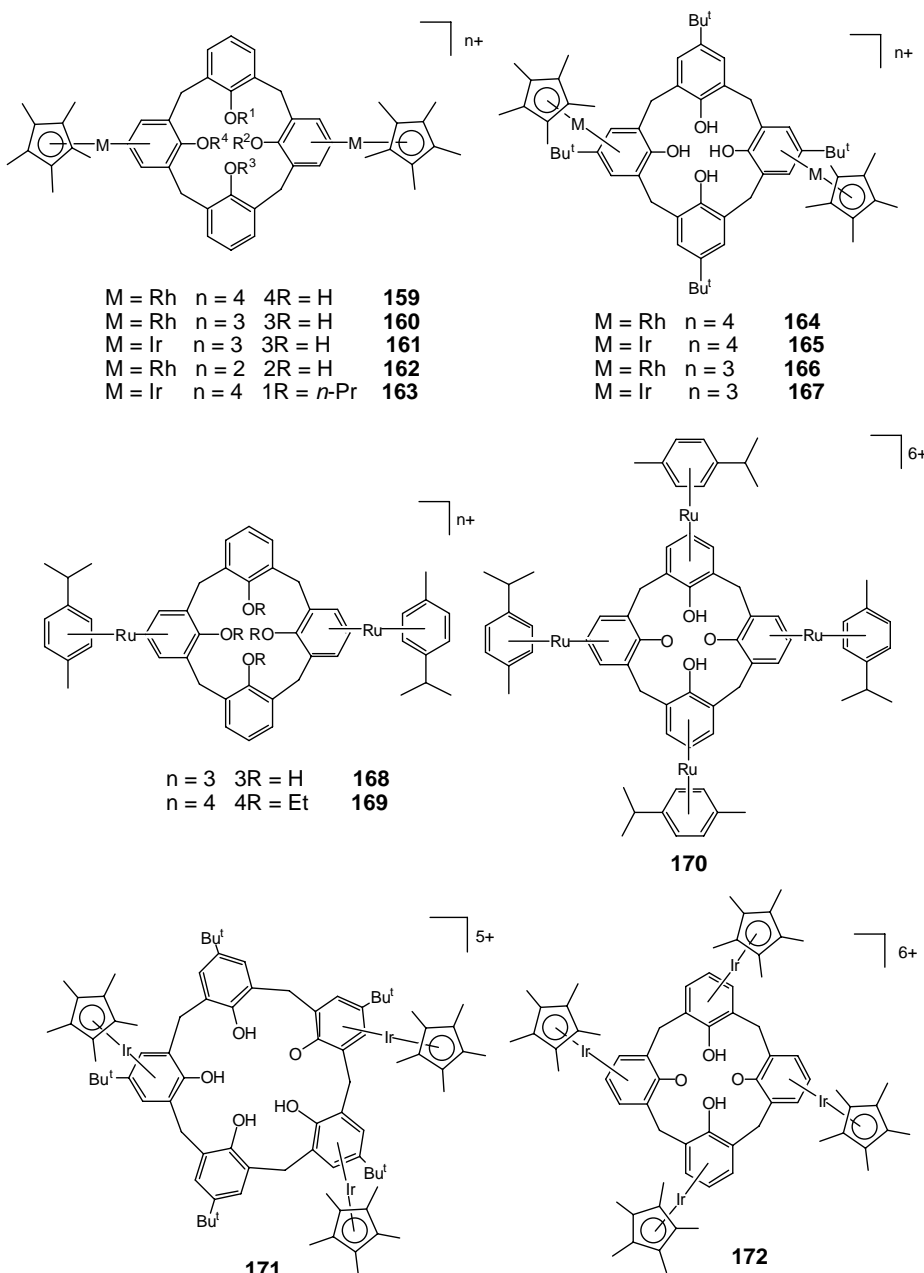
Entrapment of organometallic fragments inside a calix[4] cavity was achieved with the cage compound **148**.⁵⁴ In the complexes **149-152**, the diphosphine acts as a *trans*-spanning ligand which positions the metal centre above the wider entrance. The Pd-Me moiety of complex **150** and the Pt-H bond of **151** are located inside the calix

cavity. Upon formation of the ruthenium complex **152**, one M-CO fragment nests itself between two parallel aryl rings that are separated by only 5.5 Å. Clearly, such complexes open new perspectives for intra-cavity catalysis. With ligand **153** which has somewhat longer phosphorus arms, the binuclear complexes **154-156** were obtained.⁵⁵ In contrast, the reaction of diphosphite **157** with $[\text{Pd}(\eta^3\text{-Me-allyl})(\text{THF})_2]\text{BF}_4$ afforded the mononuclear chelate complex **158**.⁵⁵ The activity of **156** in the hydroformylation of olefins is comparable to that of conventional Rh-PPh₃ systems.



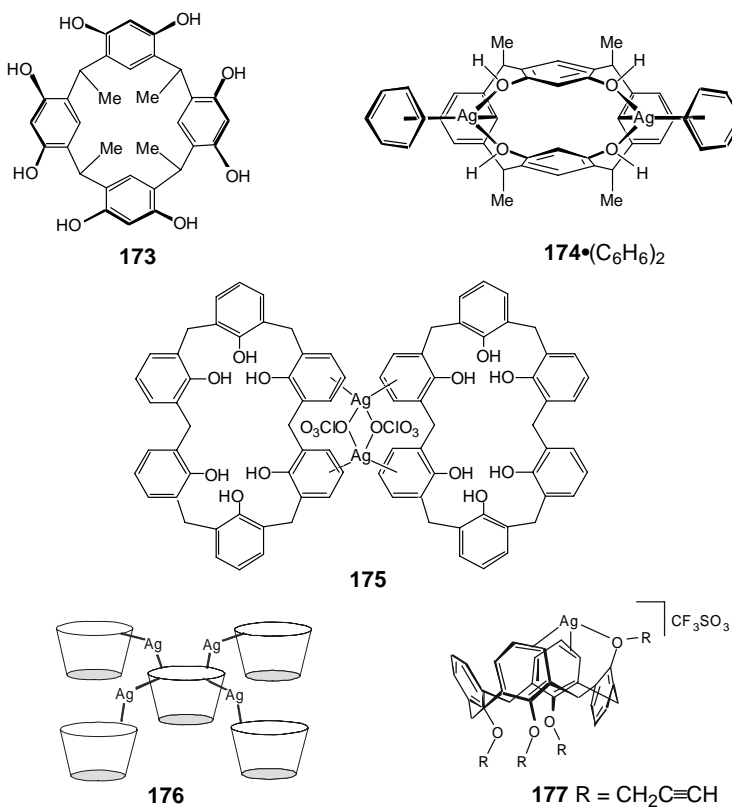
5 Metallocalixarenes with metal centres bonded to π -donor units

Reactions of neutral calixarene precursors and cationic metal arene or metal cyclopentadienyl complexes have provided a series of cationic π -metalated calixarenes (**159-172**).⁵⁶



The trimetallic iridium cation **171**, for example, was synthesised by reacting *p*-Bu^t-calix[5]arene with excess [Ir(η^5 -C₅Me₅)(acetone)₃](BF₄)₂ in refluxing CF₃CO₂H. In all these complexes the presence of the transition metal centre makes the lower rim

hydroxyl functionalities more acidic than that of the starting calixarene. Furthermore, anionic guests can now be included in the cavity. As unambiguously shown by X-ray diffraction studies, the tetrametallic cation **170** is able to bind following anions: BF_4^- , SO_4^{2-} and I^- , while with **172**, inclusion compounds were found with BF_4^- and HSO_4^- . Anion-host contacts as low as 2.85 Å ($\text{BF}_4^- \cdots \text{C}_{\text{calix}}$) were found in **170**• BF_4^- . The anion binding properties of **170** in H_2O have been investigated by NMR titration experiments, leading to binding constants in the range of 100–550 M⁻¹ for nitrate and halide ions. The halide binding decreases in the order $\text{Cl}^- > \text{Br}^- > \text{I}^-$. Interestingly, anion binding is significantly enhanced in non-aqueous media.

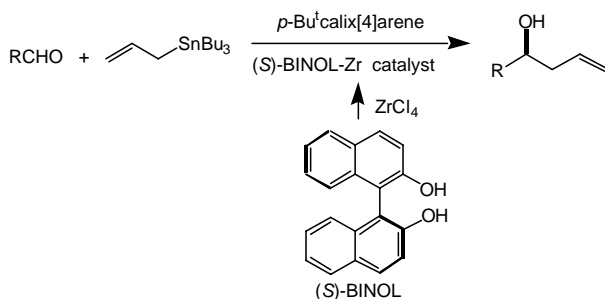


The reaction of AgClO_4 with *C*-methylcalix[4]resorcinarene **173** results in the formation of complex **174**•(C₆H₆)₂.⁵⁷ The dinuclear cation is twofold symmetric, each silver ion being bonded to two OH groups, one carbon atom of an aromatic resorcinarene ring (π interaction) and one carbon atom of a benzene molecule. Reacting calix[6]arene with AgClO_4 afforded the dimeric complex **175**. The reaction of AgClO_4 with calix[4]arene was also examined. This leads to $[\text{Ag}_2(\text{calixarene})(\text{ClO}_4)]$ **176** a complex that possesses a polymeric structure based on cation π interactions. In the solid state each calixarene is π -bonded to four silver atoms, two of which lie above the cavity and the other two outside. Silver ions lying above a calixarene unit are connected to the

outer face of a neighbouring cavity (and *vice versa*) so as to generate a two-dimensional polymeric framework. All calixarene units have the same orientation. In the partial cone calixarene complex **177**, Ag(I) is bound to both hard" and "soft" donor centres as in **174**.⁵⁸

6 Special uses of calixarenes in catalysis

Calixarenes have recently been used as additives in the zirconium-BINOL catalysed enantioselective allylation of aldehydes. The addition of *p*-Bu^t-calix[4]arene to a mixture of BINOL, ZrCl₄(thf)₂, and allyltributyltin (Scheme 17) strongly activates the catalytic system.⁵⁹ Much higher ee's (up to 96% in the case of *n*-C₇H₁₅CHO) were obtained compared to the system without additives. Characterisation of the species responsible for these outstanding results has not been achieved.



Scheme 17.

Modified calix[n]arenes ($n = 4, 5$) may also be used as external donors in late-generation Ziegler-Natta catalysis.⁶⁰ A general result is that the addition of calixarenes to Ti/Al catalysts significantly increases the amount of isotactic polypropylene in the bulk polymerization of propylene. These promising results will certainly trigger new research in the ever evolving field of olefin polymerisation.

7 Conclusion

The particular research reviewed therein illustrates some new possibilities arising from the combination of calixarenes and transition metals. Most of these topics

rely on two major properties associated to calixarene units, namely the possibility to generate sophisticated coordination spheres by multiple functionalisation and the ability to entrap organic or organometallic fragments inside their cavities or pockets. The fascinating discoveries made recently in the fields of homogeneous catalysis, anion complexation, and supramolecular sensors as well as large cage compound synthesis fully justify further research in the rapidly expanding field of metallo-calixarenes.

8 References

1. C. D. Gutsche, *Calixarenes Revisited*, Monographs in Supramolecular Chemistry (Ed. J. F. Stoddart), Royal Society of Chemistry, Cambridge, 1998.
2. *Calixarenes 2001*, Asfari Z., Böhmer V., Harrowfield J., and Vicens J. (eds.), Kluwer, Dordrecht, **2001**.
3. V. Böhmer, *Angew. Chem. Int. Ed.* 1995, **34**, 713-745.
4. C. Wieser, C. Dieleman, D. Matt, *Coord. Chem. Rev.* 1997, **165**, 93-161.
5. C. Floriani, *Chem. Eur. J.* 1999, **5**, 19-23.
6. A. Zanotti-Gerosa, E. Solari, L. Giannini, C. Floriani, A. Chiesi-Villa, C. Rizzoli, *J. Am. Chem. Soc.* 1998, **120**, 437-438.
7. V. C. Gibson, C. Redshaw, W. Clegg, M. R. J. Elsegood, *Chem. Commun.* 1997, 1605-1606.
8. V. C. Gibson, C. Redshaw, W. Clegg, M. R. J. Elsegood, *Chem. Commun.* 1998, 1969-1970.
9. U. Radius, J. Attner, *Eur. J. Inorg. Chem.* 1999, 2221-2231.
10. U. Radius, A. Friedrich, *Z. Anorg. Allg. Chem.* 1999, **625**, 2154-2159.
11. O. V. Ozerov, F. T. Ladipo, B. O. Patrick, *J. Am. Chem. Soc.* 1999, **121**, 7941-7942.
12. O. V. Ozerov, N. P. Rath, F. T. Ladipo, *J. Organomet. Chem.* 1999, **586**, 223-233.
13. W. Clegg, M. R. J. Elsegood, S. J. Teat, C. Redshaw, V. C. Gibson, *J. Chem. Soc., Dalton Trans.* 1998, 3037-3039.
14. G. D. Andreotti, G. Calestani, F. Ugozzoli, A. Arduini, E. Gidini, A. Pochini, R. Ungaro, *J. Incl. Phenom.* 1987, **5**, 123-126.
15. U. Radius, J. Attner, *Eur. J. Inorg. Chem.* 1998, 299-303.
16. M. H. Chisholm, K. Folting, W. E. Streib, D.-D. Wu, *Chem. Commun.* 1998, 379-380.
17. M. H. Chisholm, K. Folting, W. E. Streib, D.-D. Wu, *Inorg. Chem.* 1999, **38**, 5219-5229.
18. G. Mislin, E. Graf, M. W. Hosseini, A. Bilyk, A. K. Hall, J. M. Harrowfield, B. W. Skelton, A. H. White, *Chem. Commun.* 1999, 373-374.

19. F. S. McQuillan, T. E. Berridge, H. Chen, T. A. Hamor, C. J. Jones, *Inorg. Chem.* 1998, *37*, 4959-4970.
20. B. R. Cameron, S. J. Loeb, *Chem. Commun.* 1996, 2003-204.
21. B. R. Cameron, S. J. Loeb, G. P. A. Yap, *Inorg. Chem.* 1997, *36*, 5498-5504.
22. F. Arnaud-Neu, G. Barrett, D. Corry, S. Cremin, G. Ferguson, J. F. Gallagher, S. J. Harris, M. A. McKervey, M.-J. Schwing-Weill, *J. Chem. Soc., Perkin Trans. 2* 1997, 575-579.
23. P. D. Beer, M. G. B. Drew, P. B. Leeson, M. I. Ogden, *Inorg. Chim. Acta* 1996, *246*, 133-141.
24. P. Molenveld, S. Kapsabelis, J. F. J. Engbersen, D. N. Reinhoudt, *J. Am. Chem. Soc.* 1997, *119*, 2948-2949.
25. P. Molenveld, J. F. J. Engbersen, H. Kooijman, A. L. Spek, D. N. Reinhoudt, *J. Am. Chem. Soc.* 1998, *120*, 6726-6737.
26. P. Molenveld, J. F. J. Engbersen, D. N. Reinhoudt, *J. Org. Chem.* 1999, *64*, 6337-6341.
27. P. Molenveld, J. F. J. Engbersen, D. N. Reinhoudt, *Angew. Chem. Int. Ed.* 1999, *38*, 3189-3192.
28. P. Molenveld, J. F. J. Engbersen, D. N. Reinhoudt, *Eur. J. Org. Chem.* 1999, 3269-3275.
29. D. Xie, C. D. Gutsche, *J. Org. Chem.* 1998, *63*, 9270-9278.
30. S. Blanchard, L. Le Clainche, M.-N. Rager, B. Chansou, J.-P. Tuchagues, A. F. Duprat, Y. Le Mest, O. Reinaud, *Angew. Chem. Int. Ed.* 1998, *37*, 2732-2735.
31. S. Blanchard, M.-N. Rager, A. F. Duprat, O. Reinaud, *New J. Chem.* 1998, 1143-1146.
32. P. Jacopozzi, E. Dalcanale, *Angew. Chem. Int. Ed. Engl.* 1997, *36*, 613-615.
33. O. D. Fox, N. K. Dalley, R. G. Harrison, *Inorg. Chem.* 1999, *38*, 5860-5863.
34. O. D. Fox, N. K. Dalley, R. G. Harrison, *Inorg. Chem.* 2000, *39*, 620-622.
35. D. Hesek, Y. Inoue, S. R. L. Everitt, M. Kunieda, H. Ishida, M. G. B. Drew, *Tetrahedron Asymmetry* 1998, *9*, 4089-4097.
36. A. Ikeda, M. Yoshimura, F. Tani, Y. Naruta, S. Shinkai, *Chem. Lett.* 1998, 587-588.
37. G. Mislin, E. Graf, M. W. Hosseini, A. De Cian, N. Kyritsakas, J. Fischer, *Chem. Commun.* 1998, 2545-2546.

38. A. F. Danil de Namor, O. E. Piro, L. E. Pulcha Salazar, A. F. Aguilar-Cornejo, N. Al-Rawi, E. E. Castellano, F. J. Sueros Velarde, *J. Chem. Soc., Faraday Trans.* 1998, **94**, 3097-3104.
39. S. Pellet-Rostaing, J.-B. Regnouf-de-Vains, R. Lamartine, B. Fenet, *Inorg. Chem. Commun.* 1999, **2**, 44-47.
40. Y. Molard, C. Bureau, H. Parrot-Lopez, R. Lamartine, J.-B. Regnouf-de-Vains, *Tetrahedron Lett.* 1999, **40**, 6383-6387.
41. P. Faidherbe, C. Wieser, D. Matt, A. Harriman, A. De Cian, J. Fischer, *Eur. J. Inorg. Chem.* 1998, 451-457.
42. C. Loeber, D. Matt, P. Briard, D. Grandjean, *J. Chem. Soc., Dalton Trans.* 1996, 513-524.
43. M. Stolmàr, C. Floriani, A. Chiesi-Villa, C. Rizzoli, *Inorg. Chem.* 1997, **36**, 1694-1701.
44. C. B. Dieleman, C. Marsol, D. Matt, N. Kyritsakas, A. Harriman, J.-P. Kintzinger, *J. Chem. Soc., Dalton Trans.* 1999, 4139-4148.
45. Z. Csòk, G. Szalontai, G. Czira, L. Kollár, *J. Organomet. Chem.* 1998, **570**, 23-29.
46. M. Fan, H. Zhang, M. Lattman, *Chem. Commun.* 1998, 99-100.
47. F. J. Parlevliet, M. A. Zuideveld, C. Kiener, H. Kooijman, A. L. Spek, P. C. J. Kamer, P. W. N. M. van Leeuwen, *Organometallics* 1999, **18**, 3394-3405.
48. R. Paciello, L. Siggel, M. Röper, *Angew. Chem. Int. Ed.* 1999, **38**, 1920-1923.
49. C. Wieser, D. Matt, J. Fischer, A. Harriman, *J. Chem. Soc., Dalton Trans.* 1997, 2391-2402.
50. C. B. Dieleman, D. Matt, I. Neda, R. Schmutzler, A. Harriman, R. Yaftian, *Chem. Commun.* 1999, 1911-1912.
51. C. B. Dieleman, D. Matt, I. Neda, R. Schmutzler, H. Thönnessen, P. G. Jones, A. Harriman, *J. Chem. Soc., Dalton Trans.* 1998, 2115-2121.
52. C. Dieleman, D. Matt, *unpublished results*
53. P. J. Stang, D. H. Cao, K. Chen, G. M. Gray, D. C. Muddiman, R. D. Smith, *J. Am. Chem. Soc.* 1997, **119**, 5163-5168.
54. C. Wieser-Jeunesse, D. Matt, A. De Cian, *Angew. Chem. Int. Ed.* 1998, **37**, 2861-2864.
55. I. A. Bagatin, D. Matt, H. Thönnessen, P. G. Jones, 1999, **38**,

56. M. Staffilani, K. S. B. Hancock, J. W. Steed, K. T. Holman, J. L. Atwood, R. K. Juneja, R. S. Burkhalter, *J. Am. Chem. Soc.* 1997, **119**, 6324-6335.
57. M. Munakata, L. P. Wu, T. Kuroda-Sowa, M. Maekawa, Y. Suenaga, K. Sugimoto, I. Ino, *J. Chem. Soc., Dalton Trans.* 1999, 373-378.
58. W. Xu, J. J. Vittal, R. J. Puddephatt, *Can. J. Chem.* 1996, **74**, 766-774.
59. S. Casolari, P. G. Cozzi, P. Orioli, E. Tagliavini, A. Umani-Ronchi, *Chem. Commun.* 1997, 2123-2124.
60. R. A. Kemp, D. S. Brown, M. Lattman, J. Li, *J. Molec. Cat. A: Chem.* 1999, **149**, 125-133.

***METALLOCALIXARENES. MISE AU POINT COUVRANT
LA PERIODE 2000-2003.***

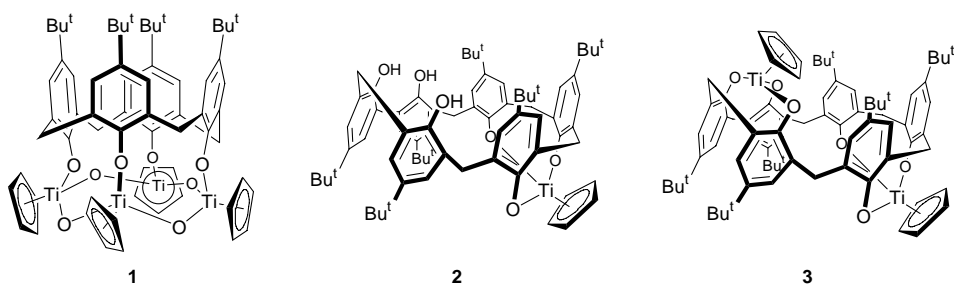
Le présent sous-chapitre complète le document précédent qui couvrait la période 1997-2000. Il est organisé comme suit:

1	Métallocalixarènes comportant des centres métalliques directement liés à des atomes d'oxygène phénoliques	40
1.1	Complexes obtenus avec des métaux du groupe IV	40
1.2	Complexes contenant des métaux du groupe V	43
1.3	Complexes contenant des métaux du groupe VI	44
1.4	Complexes contenant des métaux du groupe VII	51
1.5	Complexes contenant des métaux du groupe VIII	52
1.6	Complexes construits à partir de thiocalixarènes	53
2	Complexation par des calixarènes substitués au niveau du bord supérieur par des groupes fonctionnels contenant des atomes d'oxygène	54
3	Complexes formés à partir de calixarènes à fonctionnalités hybrides (N, O) ou (N, S)	54
4	Complexation par des calixarènes substitués par des groupes fonctionnels azotés	58
5	Complexes d'intérêt biomimétique	64
6	Complexes métalliques formés à partir d'isocyanocalixarènes	66
7	Complexes formés à partir de calixarènes substitués par des bras phosphorés	67
7.1	Calixarènes substitués au niveau du bord inférieur	67
7.2	Formation de liaisons P-M au niveau du bord supérieur	73
8	Calixarènes substitués par des unités ferrocéniques	79
9	Complexes π mettant en jeu un noyau aromatique du calixarène	79
10	Calixarènes en catalyse homogène	80
11	Références	82

1 Métallocalixarènes comportant des centres métalliques directement liés à des atomes d'oxygène phénoliques

1.1 Complexes obtenus avec des métaux du groupe IV

Le complexe téranucléaire **1**,[‡] décrit par Raston *et coll.*, et a été obtenu avec 45 % de rendement par réaction de TiCp_2Cl_2 avec *p*-*tert*-butyl-calix[4](OLi)₄. Il comporte une couronne de huit maillons alternant titane et oxygène localisée à la base du calixarène. A l'état cristallin, les distances Ti-O sont quasiment égales (Ti-O(phénol) = 1.8209(14)–1.8224(14) Å, Ti-O(μ -oxo) = 1.8159(14)–1.8165(16) Å). Un ligand cyclopentadiényle complète l'environnement tétraédrique de chaque atome de Ti(IV) et empêche ainsi la formation d'un bis-calixarène ponté par un Ti.¹ Le rôle protecteur du groupe Cp est également mis à profit lors de la synthèse des complexes mononucléaire **2** et dinucléaire **3**, construits sur une matrice calix[6]arène. Dans ces complexes, chaque entité TiCp pente trois atomes d'oxygène consécutifs du macrocycle. A l'état solide, les distances Ti-O sont comprises entre 1.815(3) et 1.865(3) Å dans **2**. Elles sont sensiblement plus faibles dans le complexe **3** (Ti-O = 1.806(2)–1.857(2) Å).²

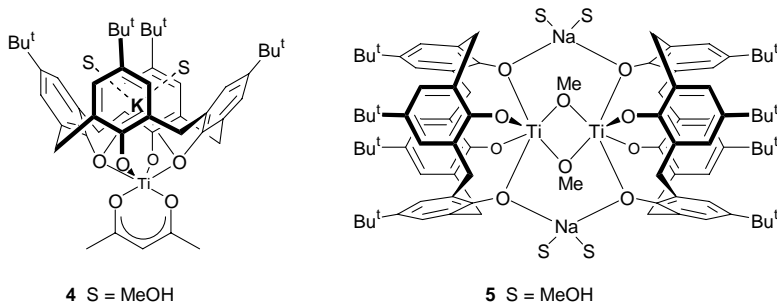


Raston *et coll.* ont également décrit plusieurs complexes associant du titane à des métaux alcalins. Ainsi, le complexe **4** a été obtenu par réaction de *p*-*tert*-butyl-calix[4]arène avec du potassium métallique et $[\text{Ti}(\text{acac})_2(\text{O}^{\text{i}}\text{Pr})_2]$. L'atome de titane est dans un environnement octaédrique constitué de six atomes d'oxygène, quatre provenant du calixarène et deux du fragment acétylacétonato. La cavité calixarénique comporte

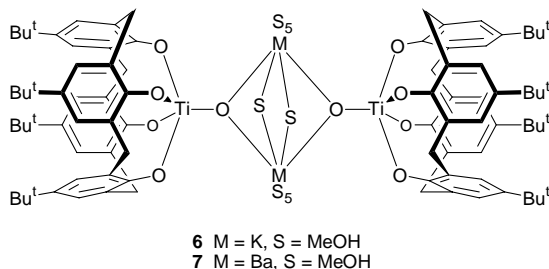
[‡] La numérotation de ce sous-chapitre redémarre à 1.

une entité $K(MeOH)_2$ liée à deux atomes d'oxygène phénoxy ainsi qu'à deux noyaux aromatiques en interaction π . Un analogue "césium" a également été synthétisé.

La réaction du *p*-*tert*-butyl-calix[4]arène avec deux équivalents de sodium et un équivalent de $[Ti(O^iPr)_4]$ conduit au dimère **5**. Chaque atome de titane est dans un environnement octaédrique constitué de six atomes d'oxygène, dont quatre proviennent d'un même calixarène, les deux autres étant ceux de groupes μ_2 -OMe pontant les atomes de titane. Cet édifice dimérique est consolidé par deux ponts μ -Na entre deux oxygènes de deux calixarènes distincts.



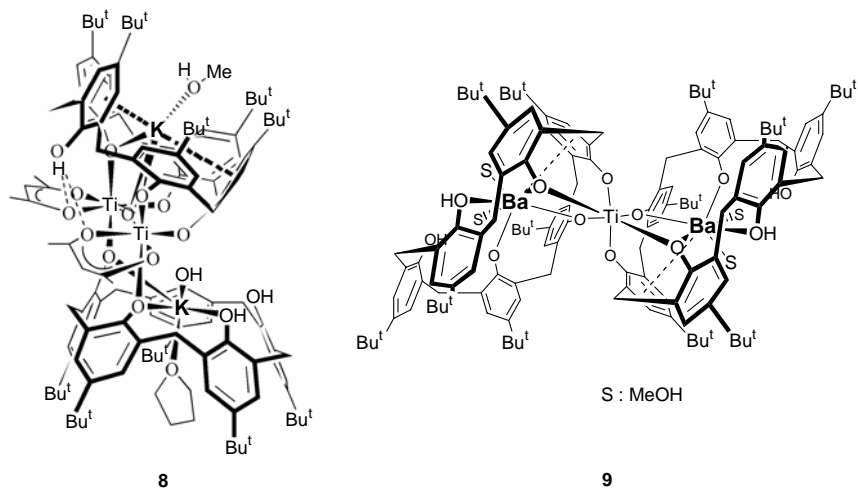
La réaction précédente a également été effectuée avec K/TMEDA et Ba/TMEDA. Ces réactions conduisent respectivement aux dimères **6** et **7**, où les atomes de titane sont cette fois dans un environnement de type pyramide à base carrée, le sommet de la pyramide étant occupé par un atome d'oxygène provenant vraisemblablement de traces d'eau présentes dans le milieu.^{3,4}



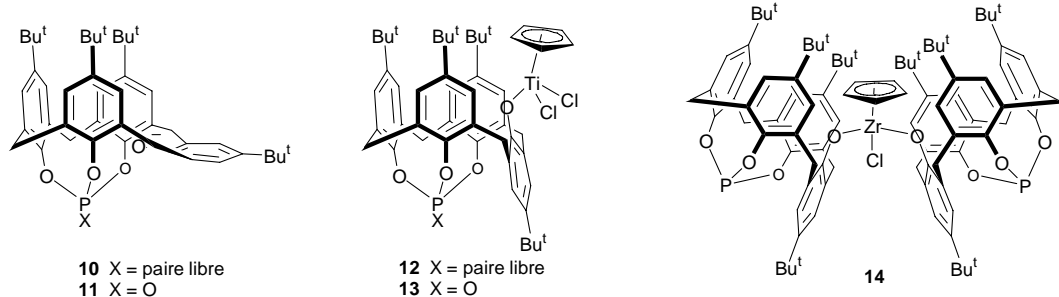
La réaction du *p*-*tert*-butyl-calix[5]arène avec du potassium métallique et $[Ti(acac)_2(O^iPr)_2]$ (stoechiométrie 1:1:1) conduit au complexe **8**. Deux entités calixarène y sont reliées par deux centres Ti(IV) dans un environnement octaédrique. Chaque atome de titane est chélaté par deux phénols d'un même calixarène et associé à la seconde matrice par un oxygène d'un groupement phénoxy. Les centres métalliques sont également reliés par un pont μ -oxo, l'angle TiOTi étant de $151.5(2)^\circ$. A noter que

chaque calixarène complexe en son sein un atome de potassium ainsi qu'une molécule de solvant.⁵

Le traitement d'une matrice plus grande, le *p*-*tert*-butyl-calix[6]arène, par du baryum et $[\text{Ti}(\text{O}^{\text{i}}\text{Pr})_4]$ conduit au complexe bis-calixarène **9**. L'environnement octaédrique du titane permet de complexer deux calixarènes par des ponts μ_3 -oxo. Le titane est dans un environnement octaédrique de six atomes d'oxygène dont trois proviennent du premier calixarène, les trois autres du second. Chaque calixarène comporte un atome de baryum lié à celui-ci par trois oxygènes phenoxy et un oxygène phénolique. L'atome de baryum est, de plus, coordonné à un noyau aromatique par une interaction π . A l'état cristallin, les distances Ti-O sont toutes comparables (Ti-O = 1.930(4)–1.944(4) Å).⁶

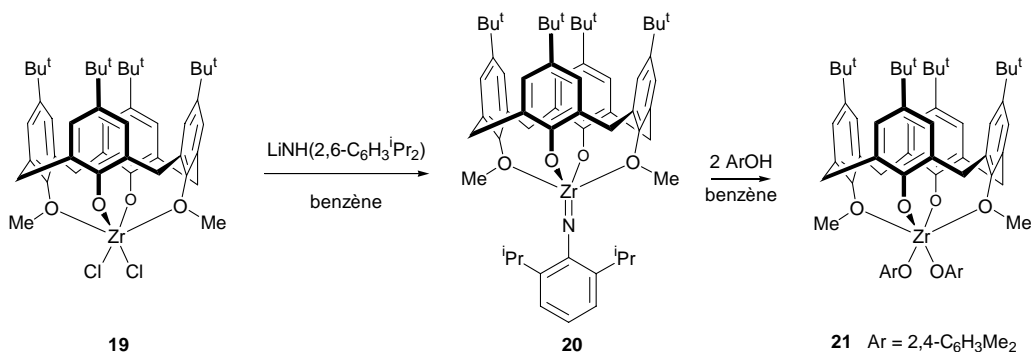


Lattman *et coll.* ont décrit la synthèse des complexes **12** et **13**, obtenus respectivement par réaction des ligands anioniques **10** et **11** avec $[\text{TiCpCl}_3]$. Lorsque **10** est traité avec $[\text{ZrCpCl}_3]$, on forme le complexe **14** où un fragment ZrCpCl ponte deux calixarènes distincts.⁷



Le complexe titane-imido **15** réagit avec CO_2 et CS_2 pour donner respectivement **16** et **17** dans lesquels, les calixarènes sont reliés par une entité Ti_2X_2 ($\text{X} = \text{O}, \text{S}$). Le composé **18** est obtenu à chaud par réaction de **15** avec la diamine $\text{CH}_2(4\text{-C}_6\text{H}_4\text{NH}_2)_2$.

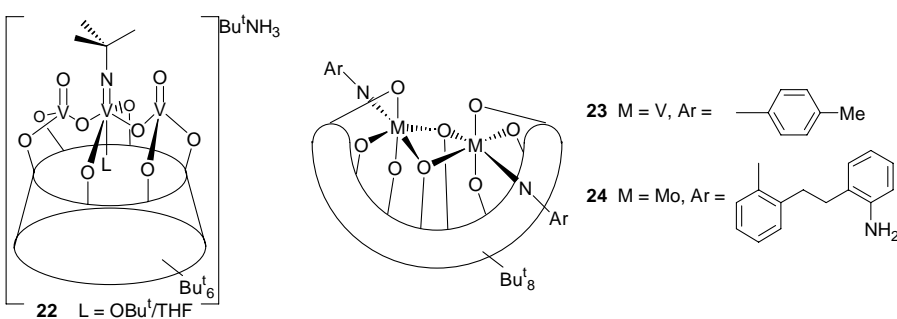
Le complexe de zirconium **19** réagit avec l'amidure $\text{LiNH}(2,6\text{-C}_6\text{H}_3^{\text{iPr}}_2)$ en donnant le complexe imido **20**. Celui-ci peut être converti en **21** par réaction avec le 2,6-diméthylphénol. Une étude structurale par diffraction des rayons X du composé **21** montre que le zirconium présente une géométrie octaédrique très déformée. Cette étude indique également que le complexe **21** cristallise avec une molécule de CH_2Cl_2 incluse dans la cavité.⁸



1.2 Complexes contenant des métaux du groupe V

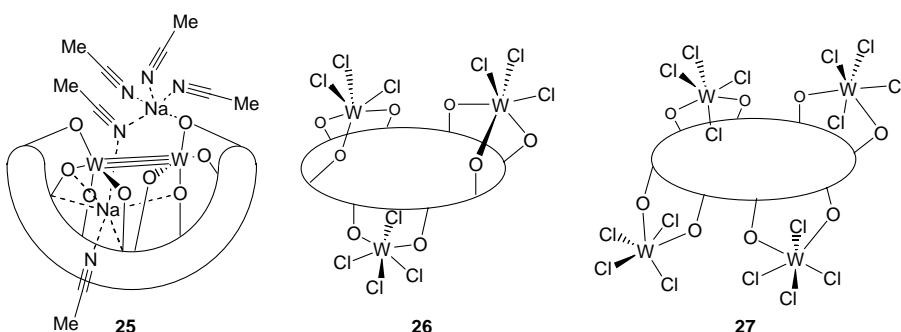
Les deux seuls exemples de métallocalixarènes appartenant à cette catégorie sont les complexes trimétallique **22** (calix[6]arène) et bimétallique **23** (calix[8]arène) décrits par Redshaw *et coll.* Le premier a été obtenu par réaction du complexe imido $[\text{V}(\text{NBu}^{\text{t}})-(\text{OBu}^{\text{t}})_3]$ avec le *p*-*tert*-butyl-calix[6]arène, le second par réaction du complexe imido $[\text{V}(\text{N}-\text{p-tolyl})-(\text{OBu}^{\text{t}})_3]$ avec le *p*-*tert*-butyl-calix[8]arène. Comme le montre une étude radiocristallographique, la matrice calix[6]arène de **22**, qui héberge trois centres métalliques, est soumise à une distorsion considérable. Dans les deux groupements vanadyle, l'atome métallique adopte une géométrie tétraédrique, inédite pour VO. Dans le complexe **23**, l'entité $(\mu_2\text{-O})_2\text{M}_2$ est confinée dans une sorte de cuvette permettant au calix[8]arène de fonctionner comme une pince par rapport au fragment M_2O_2 . A signaler qu'une structure analogue a été observée pour le complexe de molybdène **24**,

mais pour ce dernier, la cuvette subit une déformation supplémentaire qui peut être considérée comme une torsion hélicoïdale du réceptacle.^{9,10}



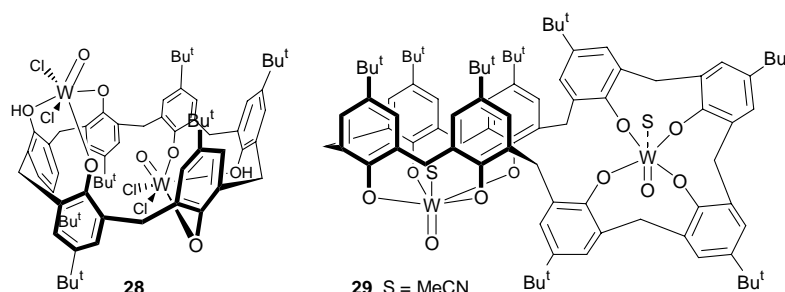
1.3 Complexes contenant des métaux du groupe VI

Redshaw *et coll.* ont également étudié la réaction du *p*-*tert*-butyl-calix[8]arène avec deux équivalents de WCl₆, suivie d'une réduction par Na/Hg. Cette séquence conduit au complexe **25** dans lequel une entité W≡W (W≡W = 2.2976(6) Å) relie les huit atomes d'oxygènes de la matrice, quatre à quatre. Les centres métalliques sont, ici encore, enfouis dans une sorte de cuvette. La réaction du *p*-*tert*-butyl-calix[8]arène avec trois équivalents de WCl₆ conduit au mélange des complexes tri et tétramétallique **26** (majoritaire) et **27** comportant chacun des entités chlorotungsténiques indépendantes.¹¹

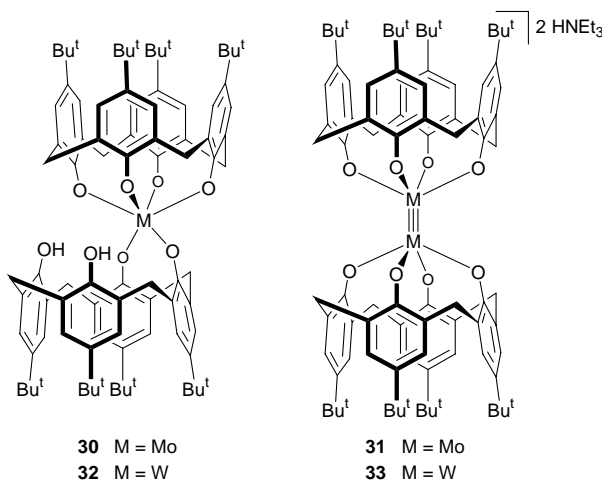


Les complexes **28** et **29** ont été synthétisés par réaction des *p*-*tert*-butyl-calix[6,8]arènes avec WOCl₄. Les atomes de tungstène y sont tous dans un environnement octaédrique, O₄Cl₂ dans **28** et O₅(NCMe) dans **29**. L'unité calix[6]arène de **28** adopte une conformation *uuuddd* (u = up, d = down).¹² Dans le complexe **29**, chaque unité W=O est liée à quatre phenoxy consécutifs dont trois sont *syn*-orientés. La structure du cœur calix[8]arène est similaire à celle du complexe

$[\text{Mo}(\text{NAr})(\text{NCMe})]_2[\text{calix}[8]\text{-O}_8]$ décrit en 1995 par les mêmes auteurs.¹³ Les longueurs des liaisons W=O sont toutes voisines de 1.70 Å.¹⁴

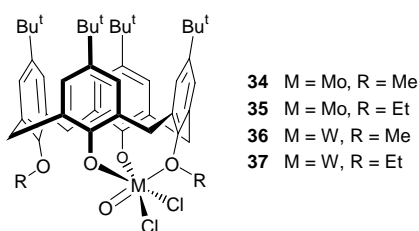


La réaction de $[\text{MoCl}_4(\text{SEt}_2)_2]$ avec le *p*-*tert*-butyl-calix[4]arène conduit au mélange des composés mononucléaire **30** et binucléaire **31**. Les deux calixarènes de **32** sont reliés par un atome de molybdène fixé à six groupements phénoliques, quatre provenant d'un premier calixarène, les deux autres appartenant au second. Ce composé est un exemple rare de complexe de type M-(O_{phénolique})₆. Dans **31**, c'est une liaison triple Mo≡Mo (Mo≡Mo = 2.241(1) Å) qui relie les deux entités calixaréniques. Chaque métal est coordonné à quatre atomes d'oxygène de l'un des calixarènes. Les variantes "tungstène" de ces complexes, **32** et **33**, ont été synthétisées par une voie similaire, mais en partant de $[\text{WCl}_4(\text{SEt}_2)_2]$.¹⁵

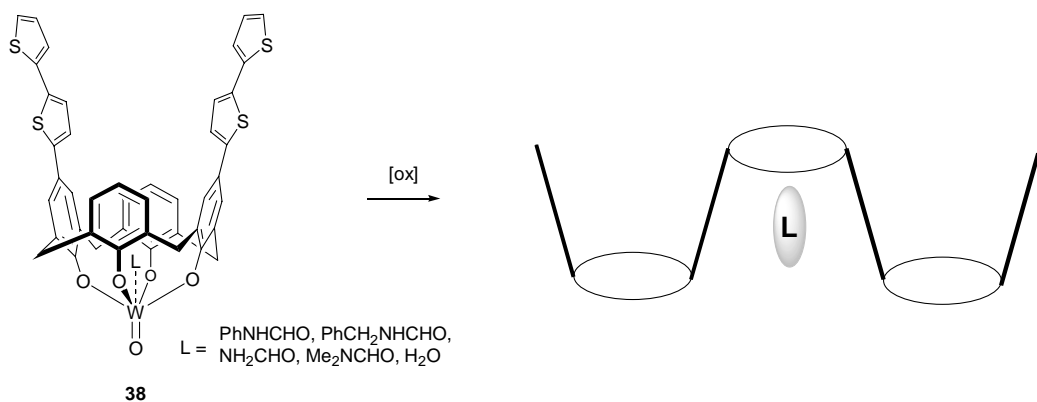


Des complexes du molybdène et du tungstène où le métal est triplement pontant ont également été synthétisés. Ainsi, les composés **34-37** ont été obtenus par réaction de MOCl_4 (M = Mo, W) avec les *p*-*tert*-butyl-calix[4]arènes dialkylés calix[4]-(OR)₂-(OH)₂ appropriés (R = Me, Et). Dans chaque complexe, le métal présente un environnement octaédrique déformé. Les distances M=O sont conformes aux données

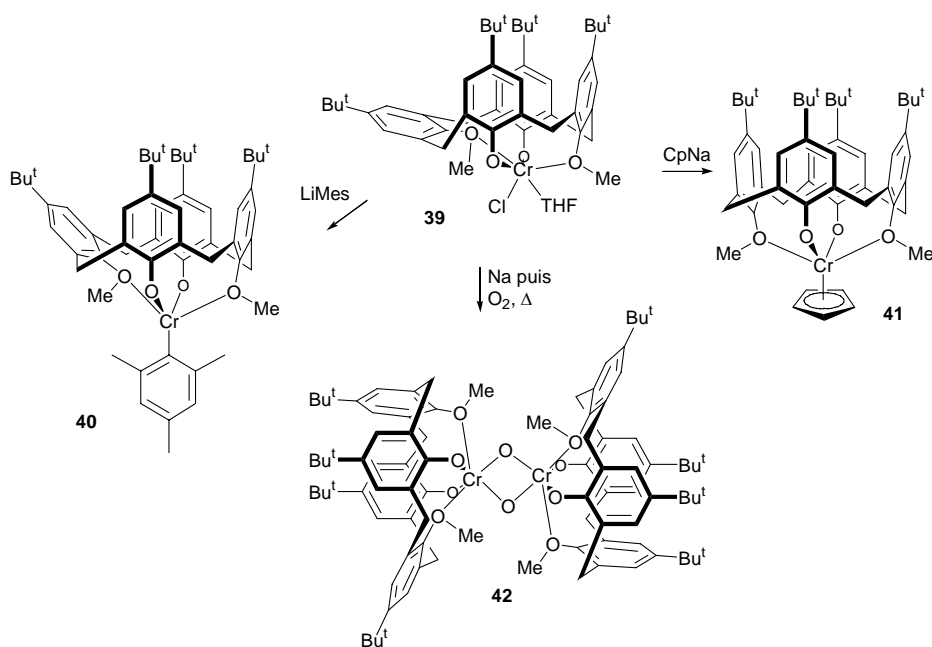
de la littérature ($\text{Mo-O} = 1.650(3)$ et $\text{W-O} = 1.673(3)$ Å). Les liaisons M-O en *trans* du ligand oxo sont de 2.371(2) et 2.339(3) Å, respectivement dans **35** et **36**.¹⁶



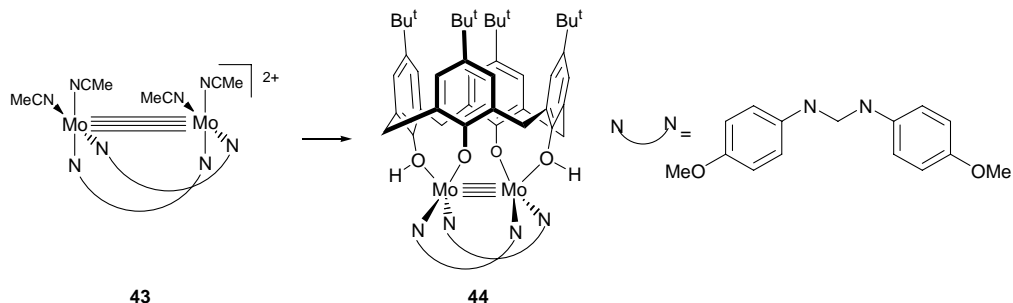
Dans le calixarène **38**, substitué au niveau supérieur par des unités thiophènes, la matrice a été rigidifiée par un pont μ_4 -(W=O). A l'état cristallin, le tungstène complexe une molécule de DMSO venant se positionner à l'intérieur du calixarène. A signaler que d'autres solvants (amides, H_2O) peuvent également être incorporés au sein de la cavité. Les parties thiophènes du complexe peuvent être dimérisées. Le polymère issu de l'oxydation électrochimique du complexe **38** présente des conductivités qui dépendent du ligand inclus dans le calixarène.¹⁷



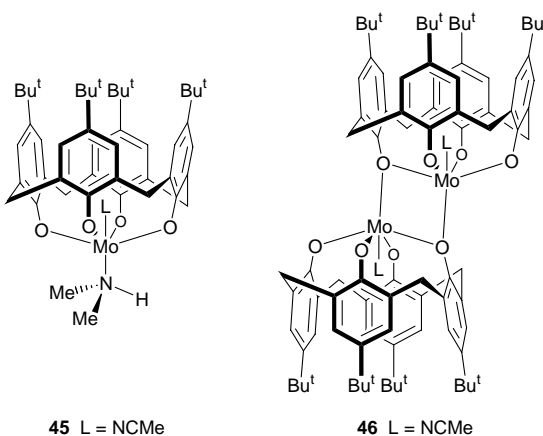
Le complexe **39** a été obtenu en faisant réagir le *p*-*tert*-butyl-calix[4]arène 1,3-diméthylé sur le bord inférieur avec le précurseur $[\text{CrCl}_3(\text{THF})_3]$. Dans ce complexe, la géométrie du chrome est très proche de celle d'un octaèdre idéal. Le calixarène adopte une conformation cône, un des cycles phenoxy étant pratiquement perpendiculaire à l'axe du calixarène. La réaction de **39** avec LiMes (Mes = 2,4,6-Me₃-C₆H₂) ou CpNa fournit respectivement les complexes σ -mesityle **40** et η^5 -cyclopentadienyle **41**. La réduction du chrome(III) de **39** par du sodium, suivie d'une oxydation avec $\frac{1}{2}$ équivalent d'oxygène moléculaire conduit au dimère **42**, où deux ponts μ -oxo relient les centres métalliques.¹⁸



Cotton *et coll.* ont étudié la réaction du cation **43**, contenant une liaison quadruple Mo-Mo, avec l'anion [*p*-*tert*-butyl-calix[4]-()₂-(O)₂]²⁻. Celle-ci conduit au complexe bimétallique **44** où l'unité Mo≡Mo est conservée et où chaque centre métallique est coordonné à deux oxygènes proximaux (Mo-Mo = 2.122(3) Å).¹⁹



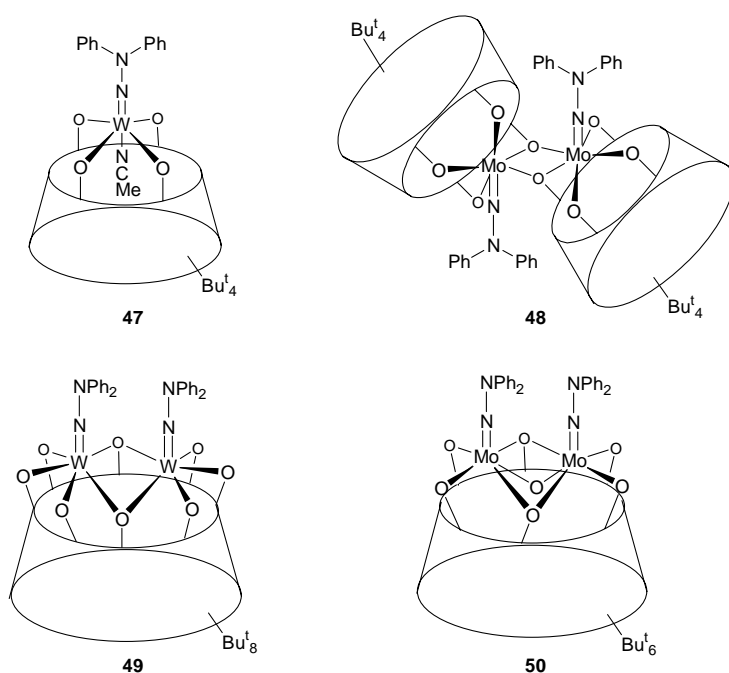
Les complexes **45** et **46** ont été obtenus par réaction du *p*-*tert*-butyl-calix[4]arène avec le précurseur [Mo(NMe₂)₄]. Le site vacant du molybdène dans **45** est occupé par un ligand amine formé lors de la réaction. Dans le dimère **46**, c'est un atome d'oxygène d'un calixarène voisin qui vient stabiliser le métal. Une molécule d'acétonitrile incluse dans le calixarène complète la sphère de coordination de chaque atome de molybdène de ces complexes.²⁰



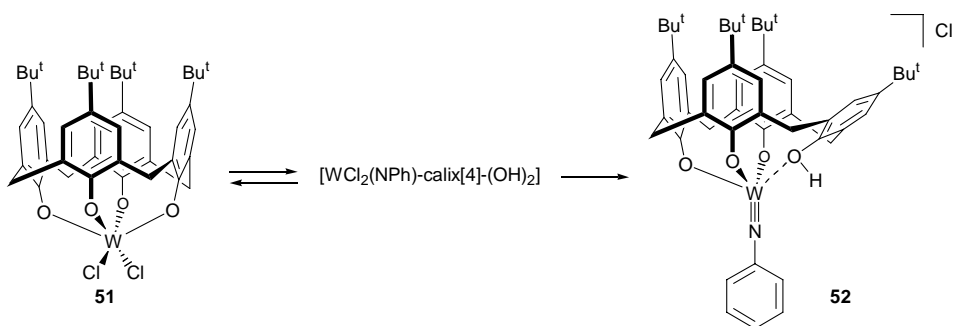
Redshaw *et coll.* ont étudié le comportement de complexes hydrazydo du molybdène ou du tungstène vis-à-vis de calix[n]arènes. Ainsi, la réaction de $[W(=NNPh_2)(OBu^t)_4]$ avec le *p*-*tert*-butyl-calix[4]arène conduit au complexe **47**, premier exemple connu de métallocalixarène à fonctionnalité hydrazydo. A l'état solide, le centre métallique est situé à 0.248 Å du plan O₄ et comporte un ligand acétonitrile piégé à l'intérieur de la cavité.

Le complexe bis-calix[4]arène **48** est formé lors de la réaction entre $[Mo(=NNPh_2)_2Cl_2(DME)]$ et le *p*-*tert*-butyl-calix[4]arène. Ce complexe centrosymétrique résulte formellement de la perte de deux molécules de diphenylhydrazine•chlorhydrate, Ph₂NNH₂•HCl. Les cavités calixarène du complexe adoptent une conformation *d,d,d,out*²¹ et les ligands hydrazydo sont situés à l'extérieur des cavités.

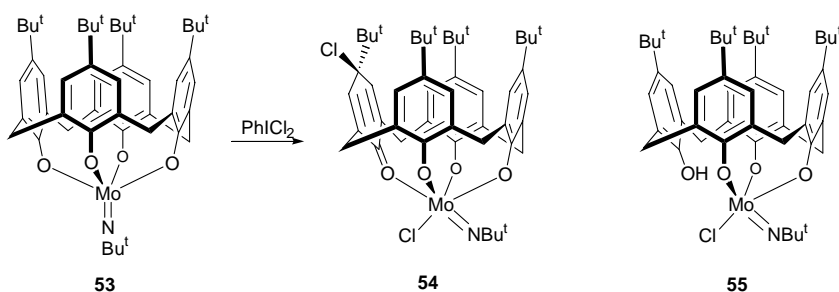
Lorsque la réaction conduisant à **47** est reproduite avec du *p*-*tert*-butyl-calix[8]arène, on obtient le composé binucléaire **49**. Une réaction analogue mettant en présence le *p*-*tert*-butyl-calix[6]arène et le précurseur $[Mo(=NNPh_2)(OBu^t)_3]$ conduit à **50**, un complexe binucléaire du molybdène. Contrastant avec le complexe **49** où les seuls atomes reliant directement les deux centres métalliques sont des oxygènes "phénoxy", le complexe **50** comporte non seulement des atomes d'oxygène de ce type, mais également un atome μ_2 -oxo. Ce dernier provient vraisemblablement du solvant utilisé, Et₂O.²²



Le dérivé imidocalix[4]arène **52**, un complexe du tungstène(VI), peut être obtenu par réaction du *p*-*tert*-butyl-calix[4]arène et $[WCl_4(NPh)]$. Ce calixarène adopte une conformation cône partiellement aplati. Les auteurs suggèrent que le mécanisme de formation de **52** implique le passage par l'intermédiaire $[WCl_2(NPh)\text{-calix}[4]\text{-(OH)}_2]$. Celui-ci pourrait une fois formé évoluer soit en formant **51** par élimination de H_2NPh , soit en donnant **52** par perte de HCl . **52** peut également être obtenu par réaction directe de **51** avec l'aniline avec 65 % de rendement. Cette dernière voie a permis de synthétiser des analogues de **52** où l'unité NPh a été remplacée par N-C₆H₄-Me (ortho, méta ou para).²³



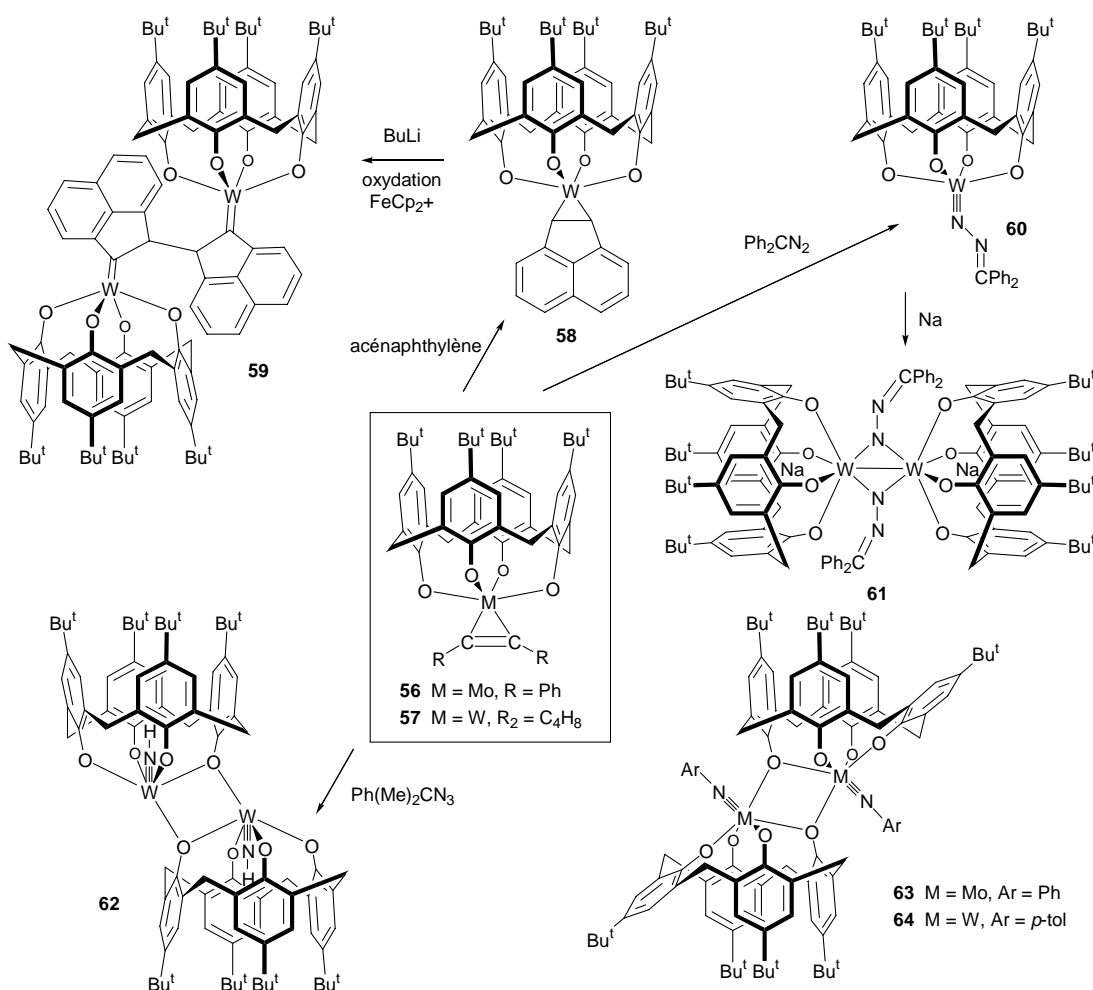
Radius et Attner ont montré que l'oxydation de **53** par $PhICl_2$ permet d'introduire deux atomes de chlore dans la molécule, l'un sur le centre métallique, l'autre sur l'un des noyaux aromatiques, qui devient ainsi une chloro-cyclohexadiènone (formation de **54**). L'addition de HCl au complexe **53** conduit réversiblement à **55**.²⁴



L'équipe de Floriani a, jusqu'à récemment, poursuivi ses recherches sur les métallocalixarènes, en s'attachant à montrer que ces macrocycles constituent de bons modèles de surface métal-oxo. Une mise au point détaillée de ses travaux a été présentée dans "Calixarenes 2001".²⁵ Une présentation sommaire en est faite ci-après.

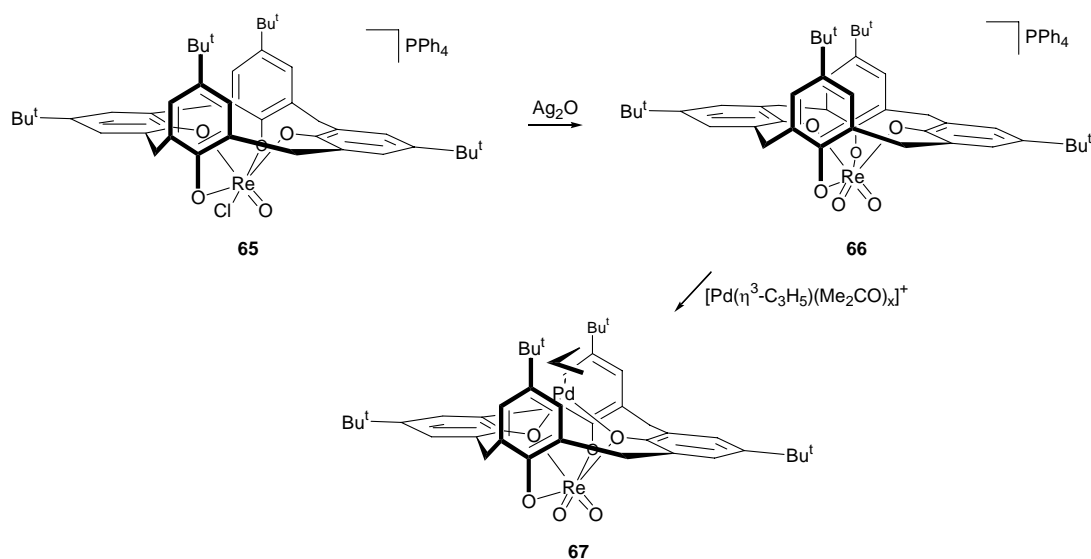
Un travail important concerne la réactivité des métallacyclopropènes **56** et **57**. Le coordinat C₂R₂ de **57** peut facilement être déplacé par de l'acénaphthylène pour former le métallacyclopropane **58**. Ce dernier peut alors être converti en **59** en deux étapes: a) déprotonation du cycle WC₂; b) couplage oxydant par FeCp₂⁺. Le ligand C₂R₂ de **57** peut également être déplacé par le diphenyldiazométhane, conduisant alors à la métallohydrazone **60**. La réduction de **60** par du sodium induit la formation du dimère **61** où deux entités calix-W sont liées entre elles par des ponts μ-NR. Une liaison métal-métal complète le nuage électronique des atomes de tungstène (W-W = 2.646(1) Å). A noter que chaque cavité de **61** incorpore un atome de sodium.

La réaction de **57** avec l'azoture Ph(Me)₂CN₃ produit le dimère **62**. Dans celui-ci, chaque cavité calixarène héberge un ligand imido N-H. Dans les complexes dimères **63** et **64**, obtenus par réaction de Ar-N=N-Ar (Ar = Ph ou *p*-tolyl) avec *p*-*tert*-butyl-calix[4]-(OM)₄ (M = Li ou Na), la situation est différente: là, les ligands imido pointent vers l'extérieur de la cavité.²⁶⁻²⁸



1.4 Complexes contenant des métaux du groupe VII

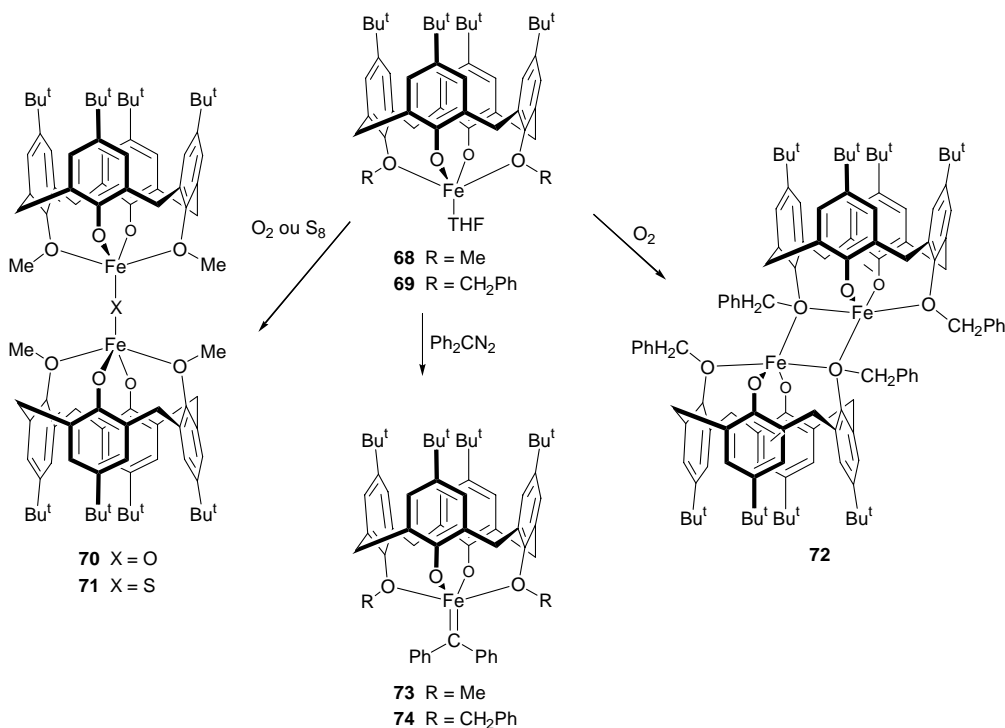
La réaction du *p*-*tert*-butyl-calix[4]arène avec [PPh₄][ReOCl₄] en présence de n-BuLi conduit au complexe de rhénium **65**, un calixarène très aplati où deux atomes d'oxygène pénètrent dans la cavité. Par oxydation avec Ag₂O, le complexe peut être converti en **66** qui présente la même particularité structurale. L'orientation particulière de deux atomes d'oxygène pénétrant dans la cavité, peut être mise à profit pour positionner des groupements organométalliques à l'intérieur du calixarène: ainsi, par exemple, la réaction de **66** avec [Pd(allyl)S]⁺ conduit au complexe **67** où le palladium, coordonné par les deux oxygènes endo-orientés, est maintenu piégé entre deux arènes cofaciaux. A noter que l'entité ReO₂Pd est plane.²⁹



1.5 Complexes contenant des métaux du groupe VIII

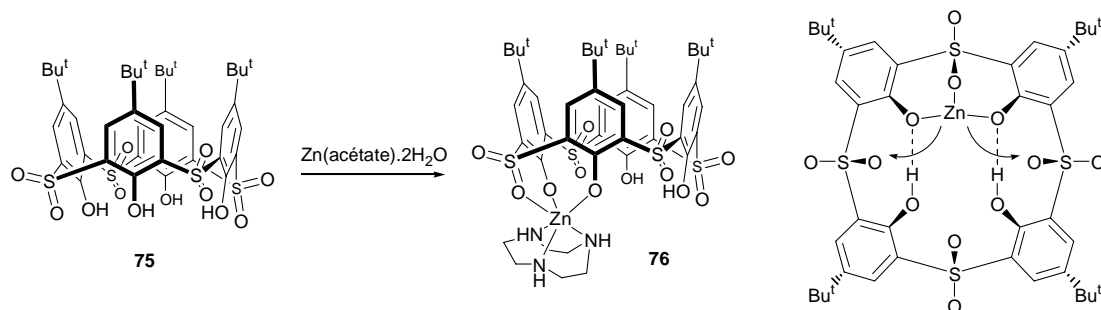
Les complexes **68** et **69** ont été obtenus par réaction de [FeMes₂] (Mes = 2,4,6-Me₃-C₆H₂) avec les *p*-*tert*-butyl-calix[4]arènes di-O-alkylés appropriés. **68** réagit avec de l'oxygène moléculaire ou du soufre en produisant respectivement les complexes **70** et **71**. Le pont μ-oxo reliant les centres métalliques de **70** est quasi linéaire (Fe-O-Fe = 177.3(1)°). La réaction de **69** avec l'oxygène moléculaire aboutit, quant à elle, au dimère **72**. Chaque atome de fer est pris en griffe par les quatre atomes d'oxygène d'un même calixarène, tout en restant coordonné à un oxygène benzylique de l'autre cavité.

La réaction de **68** et **69** avec le diphenyldiazométhane conduit respectivement aux complexes carbéniques **73** et **74**. La longueur de la liaison Fe=C dans **73** est de 1.943(8) Å.³⁰



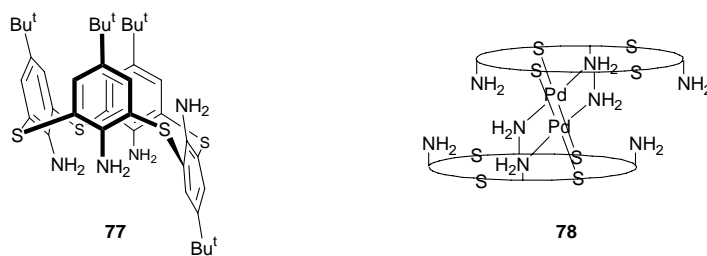
1.6 Complexes construits à partir de thiocalixarènes

Le *p*-*tert*-butyl-sulfonylcalix[4]arène **75**, composé hydrosoluble, forme avec Zn(acétate) \cdot 2H₂O et TACN (1,4,7-triazacyclononane), le complexe **76**. Le centre métallique présente un environnement octaédrique constitué de deux atomes d'oxygène phénoxy, d'un oxygène d'un groupe sulfonyle et des trois atomes d'azote du ligand N₃. Ce complexe, qui présente une symétrie apparente C_{4v}, est dynamique en solution. Le fragment ZnN₃ glisse le long des huit atomes d'oxygène constituant la "surface inférieure" du calixarène.³¹



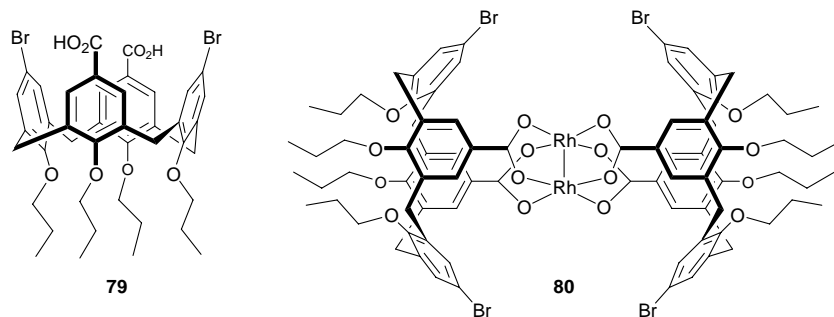
Le dimère **78** a été obtenu par réaction de [Pd(OAc)₂] avec le thiocalixarène-(NH₂)₄ **77** (rendement 23 %). Dans ce complexe, chaque atome de palladium est chélaté

par deux unités (*N, S*), ces deux unités n'appartenant pas au même calixarène. Les deux unités calixarènes adoptent une conformation "cône partiellement aplati".³²



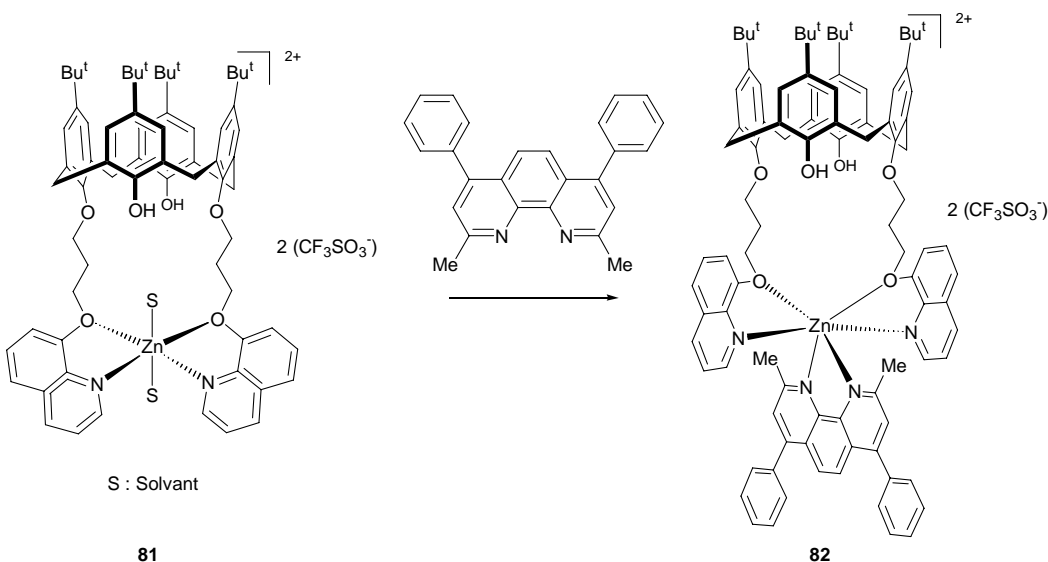
2 Complexation par des calixarènes substitués au niveau du bord supérieur par des groupes fonctionnels contenant des atomes d'oxygène

En utilisant le double acide carboxylique **79**, Seitz et Maas ont pu synthétiser le premier exemple de complexe di-rhodium-tétra-acétate **80** où l'entité Rh₂ est confinée dans une capsule. Chaque calixarène de ce complexe adopte une conformation "cône aplati", avec un angle entre les plans ArCO₂ de 24.5°, et de 112° entre les deux autres plans distaux.³³

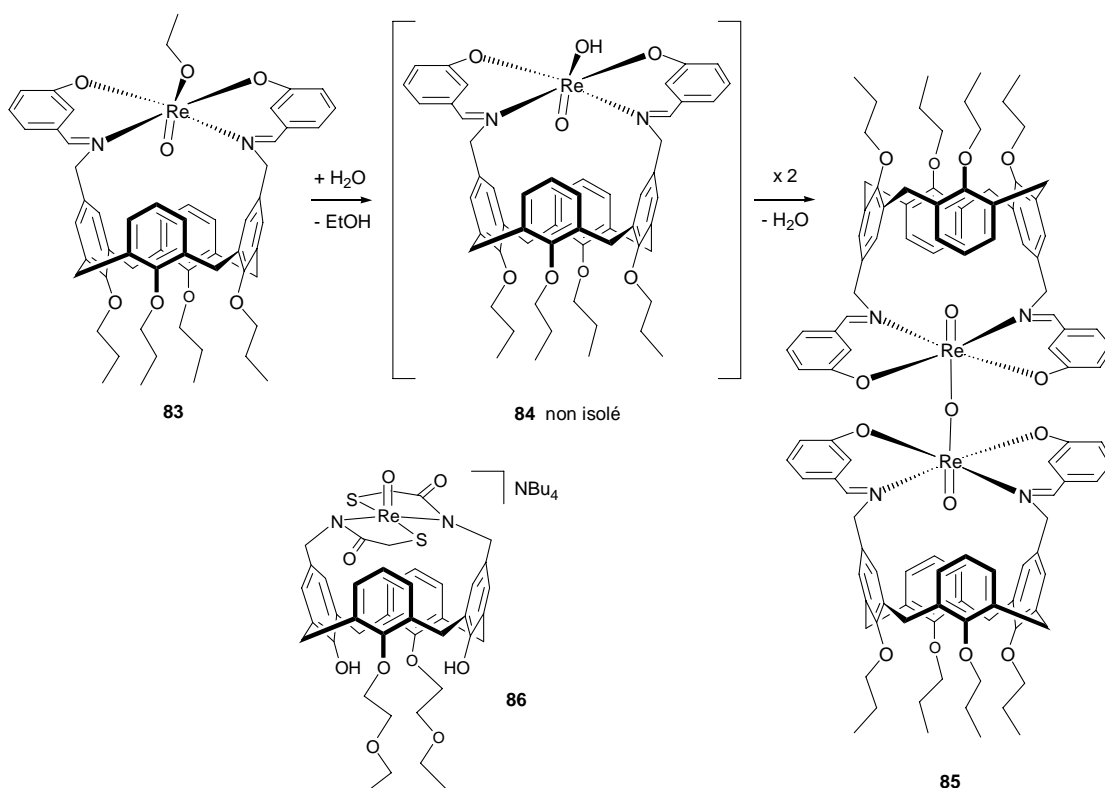


3 Complexes formés à partir de calixarènes à fonctionnalités hybrides (*N, O*) ou (*N, S*)

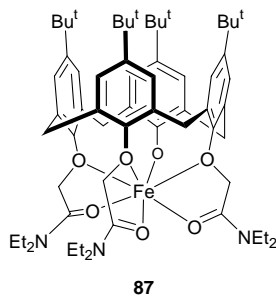
Le complexe cationique **81** a été obtenu par réaction de $[\text{Zn}(\text{CF}_3\text{SO}_3)_2]$ avec un *p-tert*-butyl-calix[4]arène distalement substitué par deux groupements prop-(8-oxy-quinoléine). La présence de zinc induit un changement caractéristique des propriétés d'absorption et de fluorescence par rapport au ligand libre. Le zinc empêche un transfert d'énergie efficace entre le fragment calixarène et les quinoléines. L'addition d'un ligand batho-phénanthroline provoque une exaltation de la luminescence, mettant en évidence la participation des molécules de phénanthroline dans le processus d'excitation de transfert d'énergie dans **82**.³⁴



Reinhoudt *et coll.* ont synthétisés une série de complexes calix-*salen* ou analogue (salen = N_2O_2) du rhénium (**83-86**). Ces complexes sont des marqueurs biomédicaux potentiels. Le complexe bis-chélate **83** s'est avéré relativement instable; il conduit en effet très facilement au composé binucléaire **85**. Ce dernier résulte de la perte d'une molécule d'eau à partir de deux molécules de **84** (intermédiaire non isolé issu d'un échange du fragment éthoxy avec de l'eau). Contrairement à **83**, le composé soufré **86** présente une bonne stabilité en solution tamponnée (MeOH/phosphate) proche du milieu physiologique.³⁵

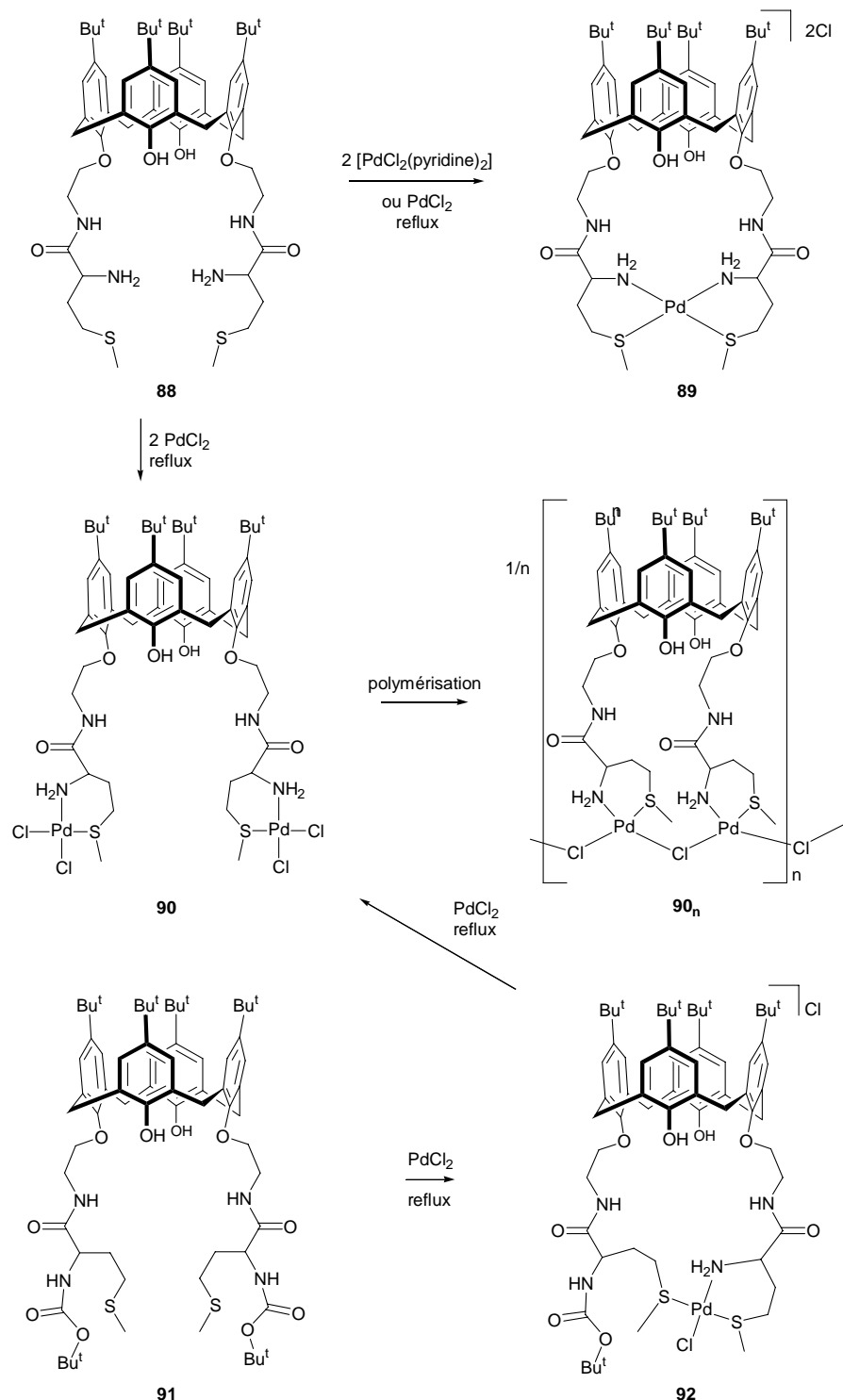


Ogden *et coll.* ont décrit la synthèse du complexe tris-amide **87** où l'atome de fer est crypté par sept atomes d'oxygène. Une étude radiocristallographique a montré que le fer est plus proche des oxygènes des fonctions amide que des oxygènes de type éther [(Fe-O_{amide} 2.064(2), 1.999(2) et 2.045(2) Å), (Fe-O_{ether} 2.300(4), 2.495(2) et 2.365(2) Å), (Fe-O_{phenoxy} 1.792(2) Å)].³⁶



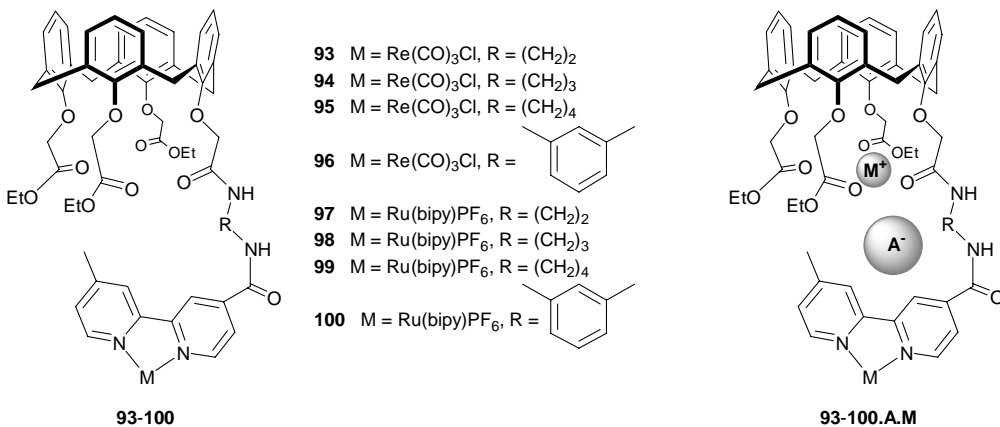
Le complexe bis-chélate **89**, synthétisé par Zhu *et coll.*, a été obtenu par réaction du calixarène **88** à chaud avec deux équivalents de [PdCl₂(pyridine)₂] ou un équivalent de [PdCl₂] à reflux. Si on répète la réaction avec deux équivalents de [PdCl₂], on forme le complexe binucléaire **90**. A l'interface air-eau, ce composé forme une monocouche par suite de la formation d'un polymère de type **90_n**. Celle-ci est remarquablement stable, probablement en raison de la grande stabilité des ponts chlorures. Le complexe **90** peut également être préparé en deux étapes à partir de **91**. Ce dernier réagit avec

[PdCl₂] pour donner **92** avec 75 % de rendement. En faisant réagir **92** avec [PdCl₂] dans le méthanol à reflux, on forme **90**.^{37,38}

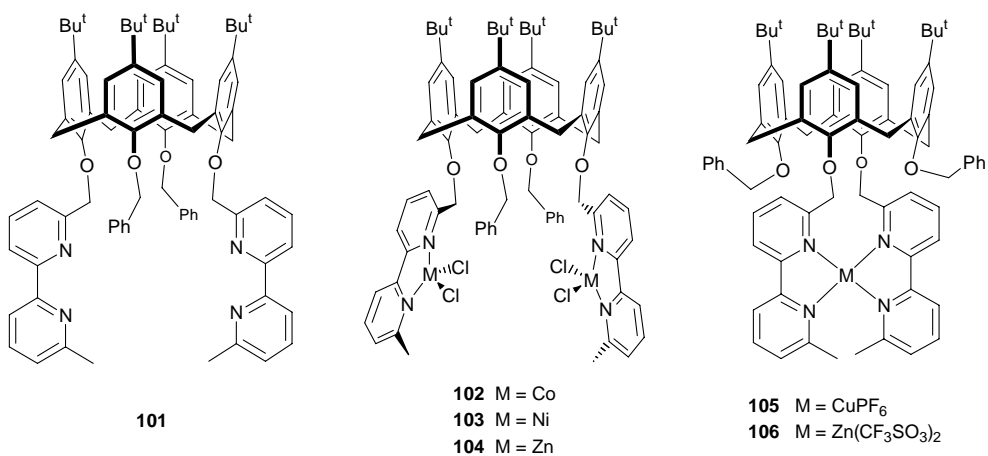


4 Complexation par des calixarènes substitués par des groupes fonctionnels azotés

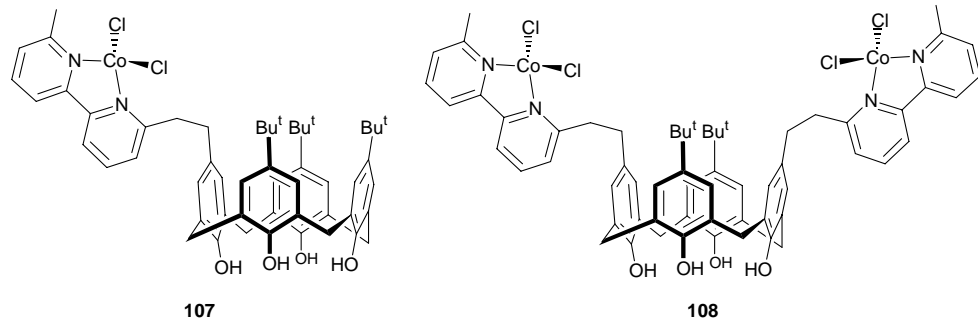
Beer *et coll.* ont étudié les propriétés des complexes **93-100**, contenant soit du rhénium soit du ruthénium. Ces composés sont capables de complexer des paires d'ions constituées d'un cation alcalin (Li^+ , Na^+) et d'un halogénure (Br^- , I^-). Des titrations suivies par RMN montrent que dans CH_3CN , la complexation de l'ion alcalin se fait dans la cavité tétraester et que celle-ci exalte la fixation de l'halogénure.³⁹



Regnouf-de-Vains *et coll.* ont décrit la synthèse des complexes binucléaires **102-104** à partir du calixarène **101**. Dans ces complexes, les deux centres métalliques sont dans un environnement tétraédrique. Contrairement à ce qui a été observé par Milstein (*vide infra*) pour des complexes obtenus à partir d'un ligand similaire, mais avec des métaux de configuration d^8 , les deux entités bipyridine du calixarène **103** ne donnent pas lieu à une interaction $\pi-\pi$ à l'état solide. Par contre, l'une de ces entités bipyridine s'associe à une bipyridine d'une molécule voisine en donnant naissance à une supramolécule dont le motif est répété indéfiniment. Les complexes *bis-chélate* **105** et **106** sont obtenus à partir du même ligand, respectivement par réaction avec un équivalent de $\text{Cu}(\text{MeCN})_4\text{PF}_6$ et de $\text{Zn}(\text{CF}_3\text{SO}_3)_2$. Dans ces complexes, les entités CH_2 -bipyridine s'enroulent hélicoïdalement autour des centres métalliques. L'obtention de tels complexes mononucléaires illustre, non seulement la flexibilité de la matrice calixarène, mais également la très bonne préorganisation du ligand.⁴⁰

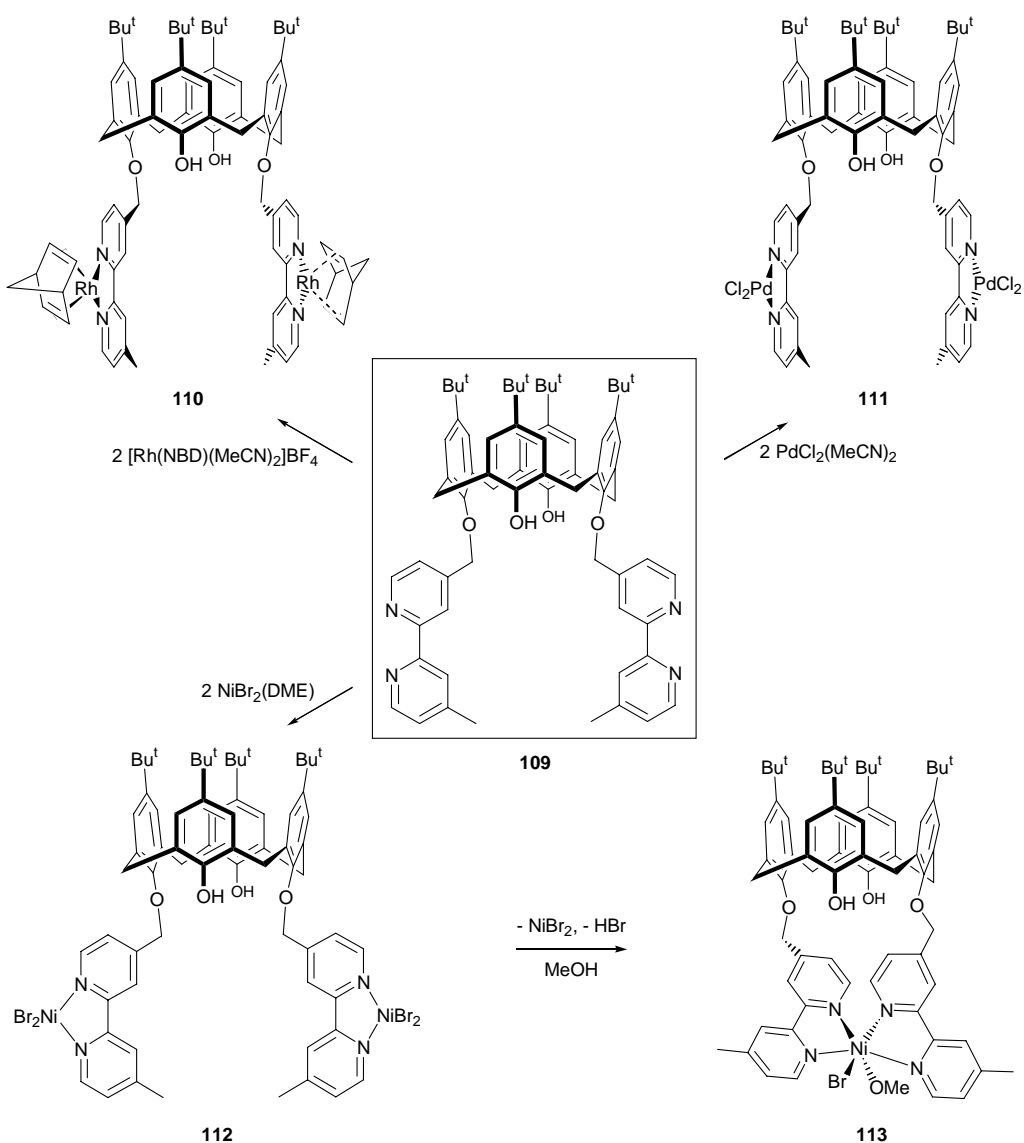


Les mêmes auteurs ont décrit des calixarènes substitués par des groupes (6'-Me)(6-éthylène)-(6,6'-bipyridine) au niveau du bord supérieur. Ces derniers ont été utilisés pour la préparation de complexes tétraédriques, tels que **107** et **108**.⁴¹

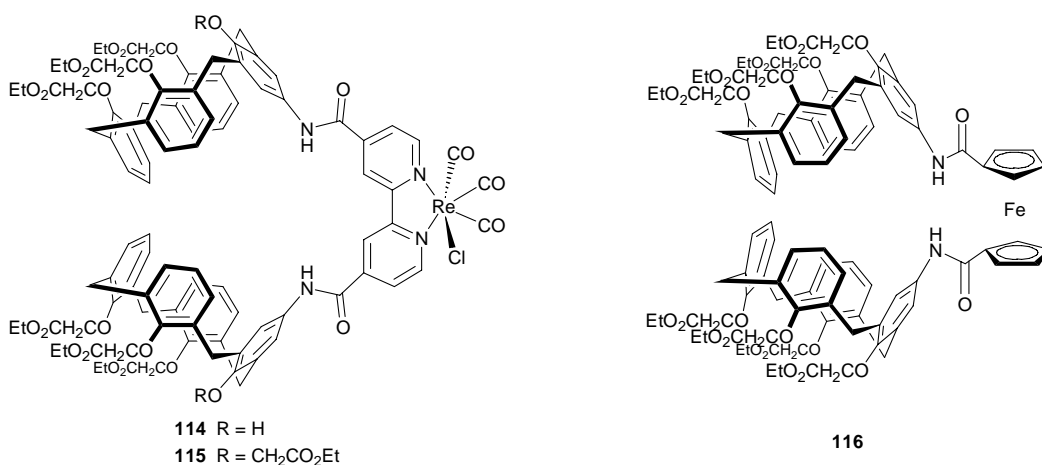


Plus récemment, Milstein *et coll.* ont utilisé le calixarène-bipyridine **109** pour la synthèse des complexes **110-112**. Des études radiocristallographiques menées pour les complexes **110** et **111** montrent qu'à l'état solide, les plans bipyridine de la molécule sont parallèles et que les atomes métalliques pointent dans des directions opposées. La faible séparation entre les deux plans bipyridine suggère l'existence d'interactions π .

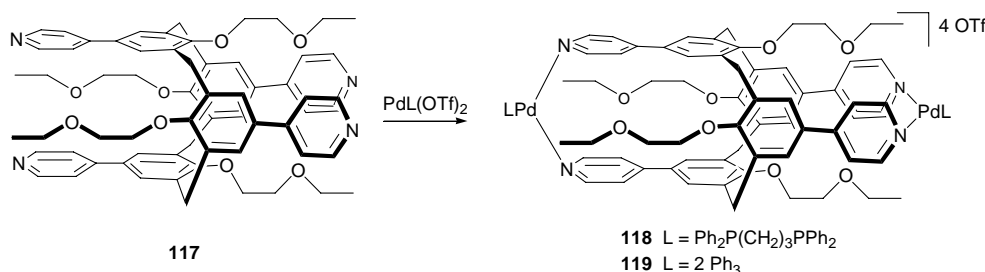
La dissolution de **112** dans du méthanol conduit à la décomplexation de l'un des atomes de nickel avec formation du complexe octaédrique **113**. En raison de la forte influence *trans* du brome, la longueur de la liaison Ni-N située en *trans* de l'halogénure est plus longue (2.148(4) Å) que les autres distances Ni-N de la molécule (Ni-N : 2.057(4) à 2.081(4) Å).⁴²



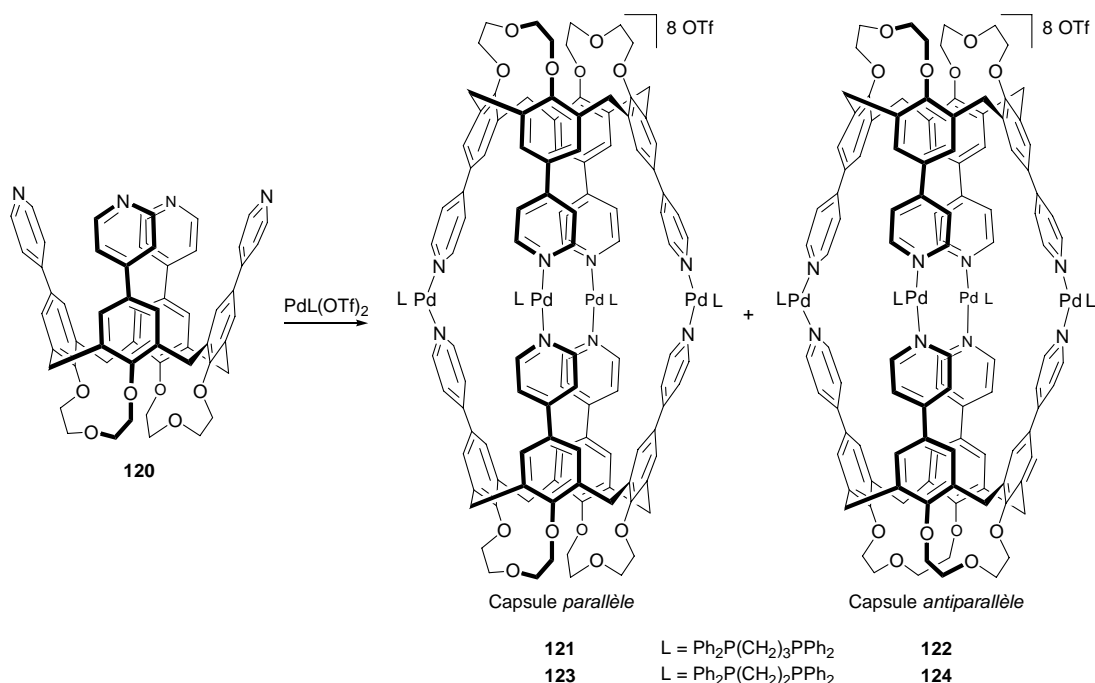
Les récepteurs hétéroditopiques bis-calixarène **114-116** sont capables de fixer des anions à la partie supérieure des unités calixarène et des cations alcalins au niveau des esters des parties inférieures. La complexation des ions alcalins provoque une exaltation des capacités réceptrices de l'ion iodure en milieu acétonitrile, l'effet de coopération étant très marqué lorsqu'on utilise **115** associé à Na^+ . Le composé ferrocénique **116** s'avère efficace pour la reconnaissance électrochimique des anions carboxylates et halogénures. C'est en présence de Li^+ que la réponse électrochimique de **116** est la plus forte vis-à-vis de l'ion bromure.⁴³



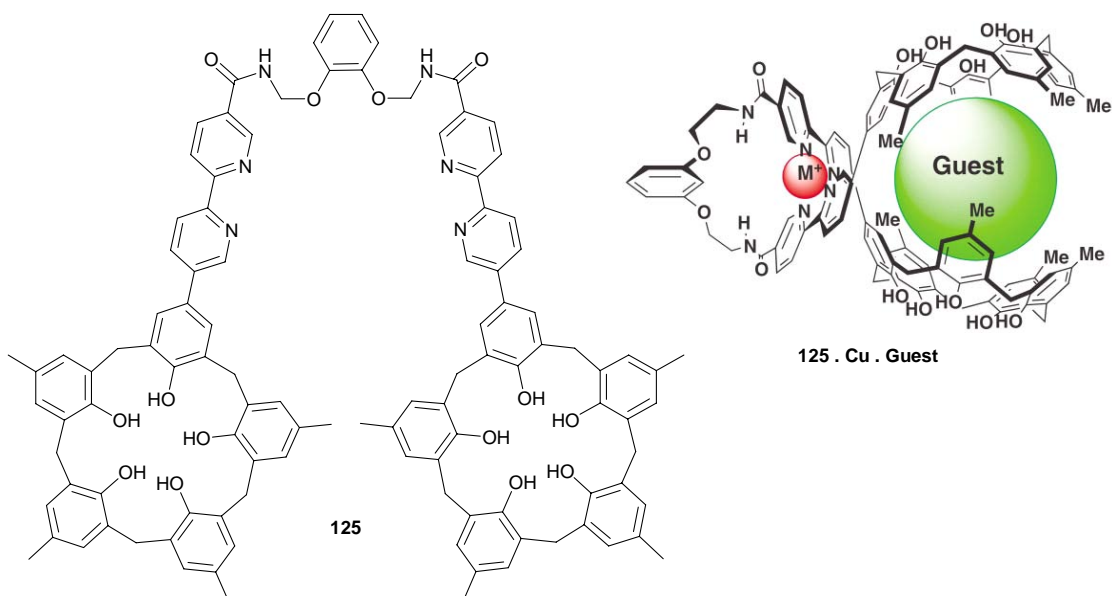
Contrairement à leurs attentes, Shinkai *et coll.* ne sont pas parvenus à générer un tube moléculaire en faisant réagir le calixarène 1,3-alterné **117** avec l'un ou l'autre des cations *cis*-[Pd{Ph₂P(CH₂)₃PPh₂}](OTf)₂] et *trans*-[Pd(PPh₃)₂(OTf)₂]; ces réactions conduisent respectivement aux complexes *bis-chélate* **118** et **119** qui ont été caractérisés uniquement par spectrométrie de masse.



La réaction de [Pd{Ph₂P(CH₂)₃PPh₂}](OTf)₂] avec le calixarène-*tétra*-pyridine *cône*-**120** conduit au mélange des capsules **121** et **122**, la première de symétrie *D*_{2h}, la seconde de symétrie *C*_i. La formation de ces assemblages a été démontrée par spectrométrie de masse et RMN. Un résultat analogue a été obtenu en partant de [Pd{Ph₂P(CH₂)₂PPh₂}](OTf)₂] (formation du mélange de **123** et **124**).⁴⁴

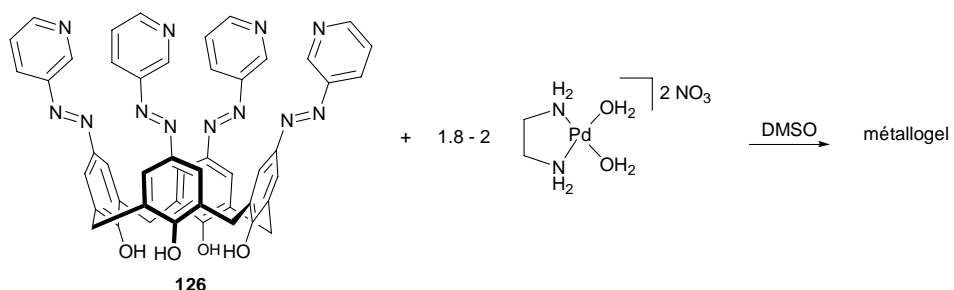


Un effet allostérique se produit lors de la complexation du fullerène C_{60} par le bis (calix[5]arène-bipyridine) **125** en présence de cuivre(I). En effet, comme l'ont montré Fukazawa *et coll.*, la constante d'association du complexe de **125**• CuPF_6 avec le C_{60} est 40 fois plus forte qu'avec **125** seul. Ce résultat traduit la bonne prédisposition des cavités calix[5]arène par suite de l'enroulement des unités bipyridine autour du cuivre.⁴⁵

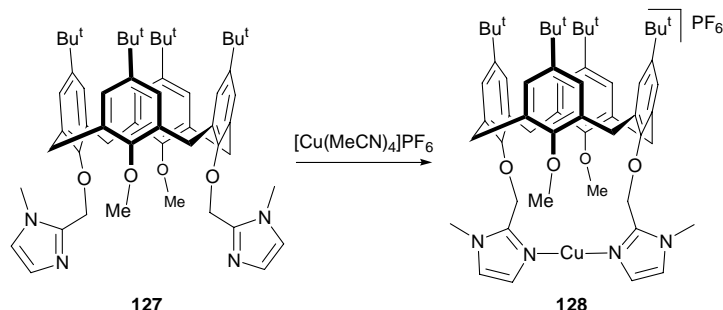


La réaction du ligand tétra-pyridine **126** avec $[\text{Pd}(\text{en})(\text{H}_2\text{O})_2](\text{NO}_3)_2$ ($\text{en} =$ éthylènediamine) conduit à la formation d'un polymère organométallique incorporant

des molécules de solvant en formant un gel. Ce "métallogel" est stable et insoluble dans l'eau sur une large plage de pH (1 à 13). Cette stabilité est maintenue jusqu'à 100 °C.⁴⁶

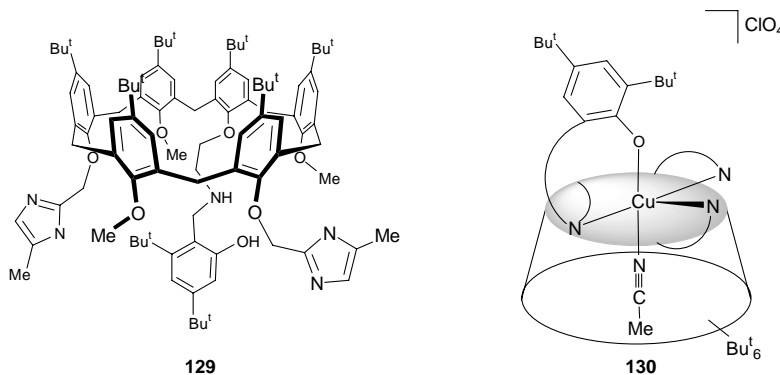


Reinaud *et coll.* ont réussi à positionner un atome de cuivre(I) près de la partie inférieure du calix[4]arène-imidazolyl **127**. Dans le complexe formé, **128**, l'environnement du cuivre est quasiment linéaire (angle N-Cu-N = 178.5(4)°). Cette géométrie confère une grande stabilité au cuivre vis-à-vis de l'oxydation par l'oxygène moléculaire, y compris en solution.⁴⁷



Poursuivant leurs études sur les ligands azotés dérivés de calixarènes, les mêmes auteurs ont examiné les propriétés complexes de calix[6]arènes substitués par le même fragment imidazolyl.

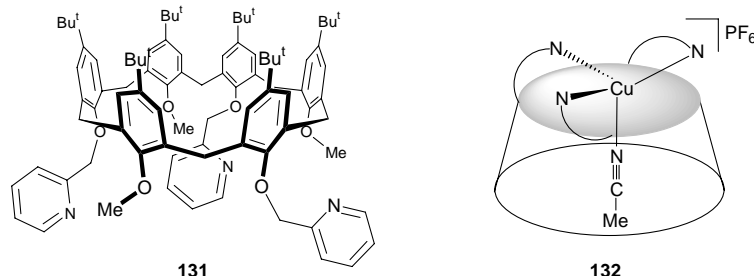
La réaction du calix[6]arène **129** avec $[\text{Cu}(\text{H}_2\text{O})_6](\text{ClO}_4)_2$ conduit à **130**. Dans ce complexe, le centre métallique qui adopte une géométrie de type pyramide à base carrée, est à nouveau positionné à l'entrée de la cavité. La base de la pyramide est constituée d'un imidazole, du chélate amino-phénolate N,O ainsi qu'une molécule d'acétonitrile. Le second bras imidazole occupe le sommet de la pyramide.⁴⁸



5 Complexes d'intérêt biomimétique

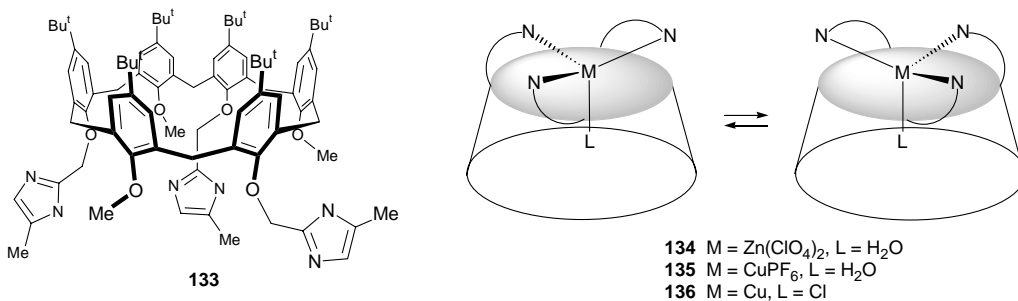
Reinaud et coll. ont montré que l'unité calix[6]arène constituait une excellente cavité hydrophobe pour le confinement d'entités métallo-organiques. Dans ces molécules on dispose d'un site de coordination localisé au fond d'un entonnoir, autrement dit d'un site très protégé. De petits ligands peuvent naturellement accéder à ce site. Dans le complexe **132**, obtenu par réaction de **131** avec [Cu(MeCN)₄](PF₆), le ligand acétonitrile inclus dans la cavité peut être échangé avec d'autres nitriles tels que le benzonitrile.

Le complexe **132** a été évalué vis-à-vis de l'oxydation catalytique de l'éthanol et du benzène, avec H₂O₂. Les produits d'oxydation (éthanal et acide acétique d'une part, phénol et benzoquinone d'autre part) sont formés plus rapidement qu'avec le système Cu(pyridine)₃/H₂O₂, mettant ainsi en évidence l'influence favorable de la cavité du calixarène et démontrant que ces systèmes sont des modèles valables de cupro-enzymes.^{49,50}

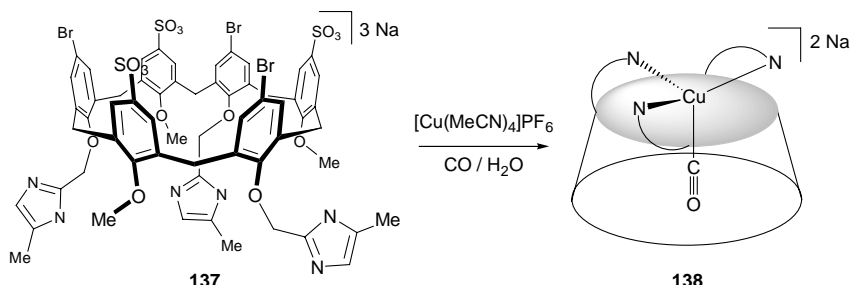


Le dérivé tris-imidazole **133** conduit facilement aux complexes **134** et **135**, respectivement par réaction avec [Zn(H₂O)₆](ClO₄)₂ et [Cu(H₂O)₆]PF₆.⁵¹⁻⁵³ En solution,

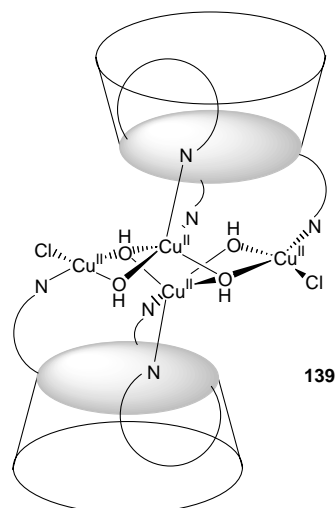
le calixarène décrit un mouvement de balancier autour de l'axe M–L.⁵³ Chacun de ces entonnoirs est capable d'incorporer divers petits ligands (alcool, amine, nitrile⁵⁴ ou carbonyle). Dans certains cas, les parois de la matrice peuvent augmenter la stabilité du complexe ainsi formé par le biais d'interactions CH/π entre les parois aromatiques et la molécule invitée.⁵⁵



Le complexe hydrosoluble **138** a été obtenu à partir de **137**, version hydrosoluble de **133**, par réaction avec $[\text{Cu}(\text{MeCN})_4]\text{PF}_6$ et CO, en solution aqueuse ou alcoolique. A souligner que ce complexe est stable vis-à-vis de l'oxydation par l'air et ne donne lieu à aucune disproportionation. Cette stabilité remarquable est due à l'environnement des trois imidazoles imitant ainsi les sites tris-(histidine) de cupro-enzymes, sites connus pour effectivement stabiliser le cuivre(I) dans l'eau.⁵⁶

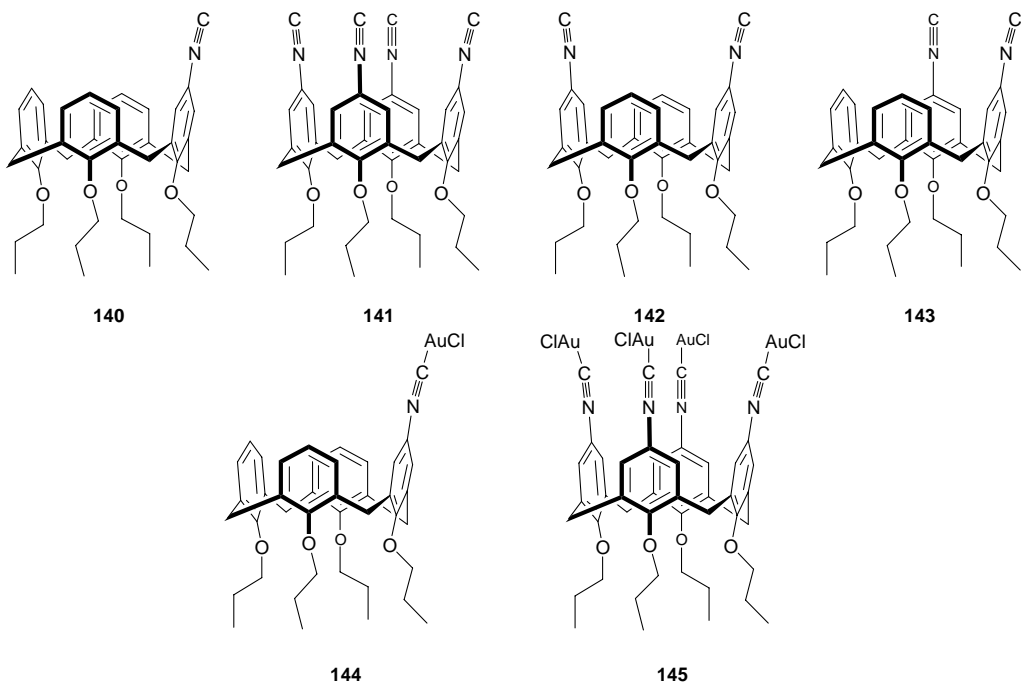


En faisant réagir le complexe **136** avec $[\text{Cu}(\text{MeCN})_4]\text{PF}_6$ en présence de dioxygène, on forme le complexe bis-calixarène **139** où quatre atomes de cuivre sont localisés entre les deux calixarènes. La formation de **139** provoque le basculement d'une entité phénolique porteuse d'un imidazole en incluant ce dernier dans la cavité. Dans ce complexe, les quatre atomes de cuivre sont au degré d'oxydation 2.⁵⁷

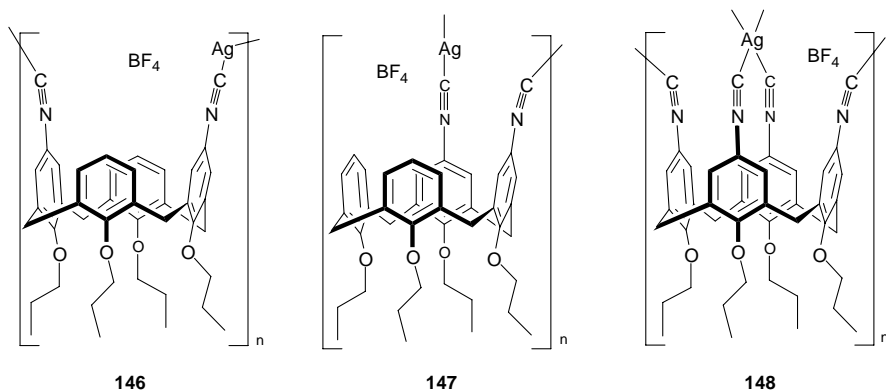


6 Complexes métalliques formés à partir d'isocyanocalixarènes

Harvey *et coll.* ont décrit la synthèse des isonitriles **140** et **141** et ont étudié les propriétés photochimiques des complexes de l'or(I) **144** et **145** obtenus à partir de ces ligands. Les auteurs aboutissent à la conclusion qu'en solution, il n'existe aucune interaction aurophilique dans le complexe tétranucléaire **145**.⁵⁸



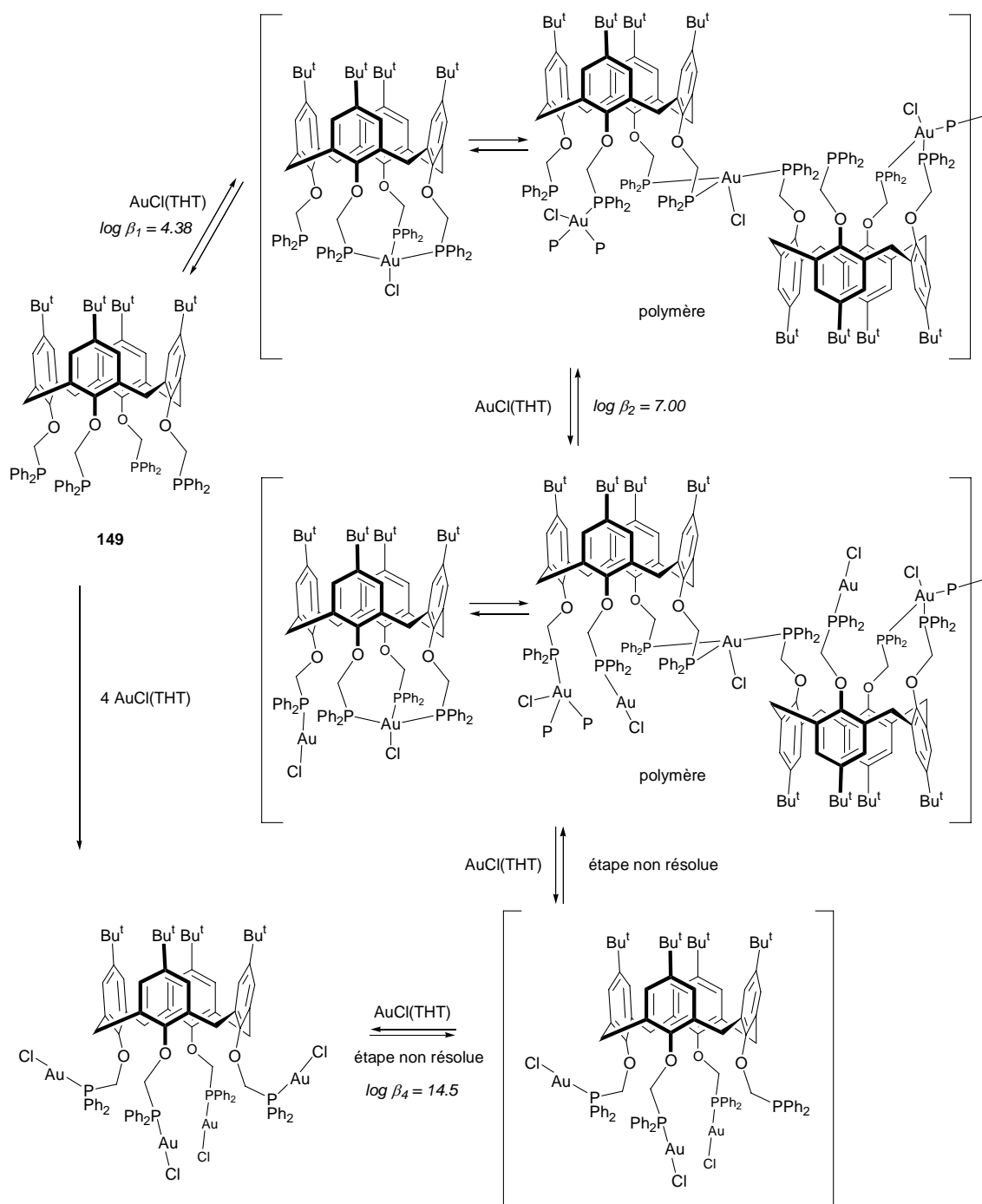
Le même groupe de recherche a étudié la complexation de l'ion Ag^+ par les isonitriles **141-143**. Ces réactions conduisent à des oligomères et polymères inorganiques, **146-148**, mais leur structure précise n'a pas été déterminée.⁵⁹



7 Complexes formés à partir de calixarènes substitués par des bras phosphorés

7.1 Calixarènes substitués au niveau du bord inférieur

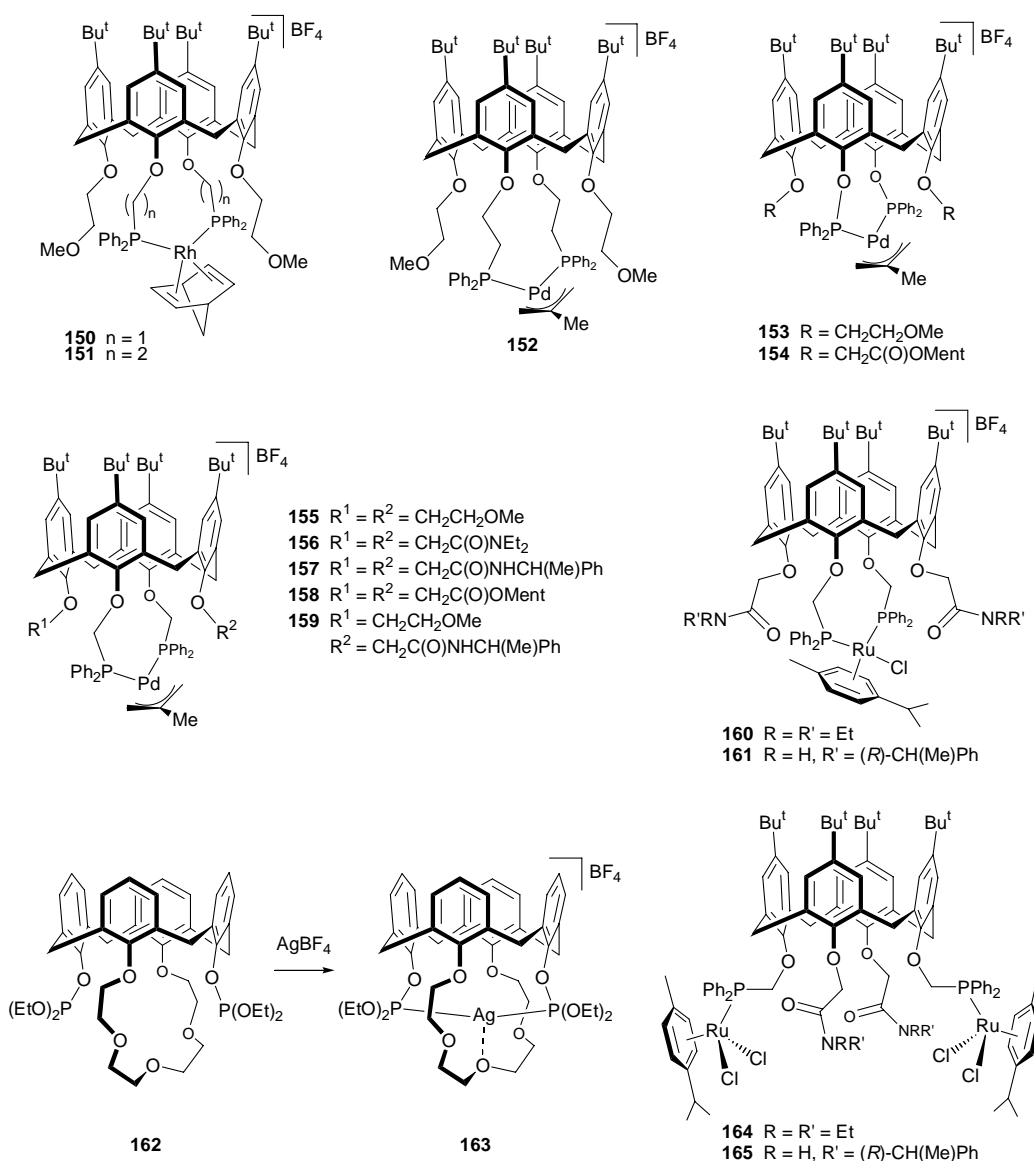
Une étude spectrophotochimique jumelée avec une étude par RMN a mis en évidence que la complexation de quatre unités AuCl par la téraphosphine **149** s'effectue en trois étapes identifiables. Le processus de complexation a lieu en moins d'une seconde. Selon l'étape considérée, l'introduction d'une nouvelle entité AuCl peut soit faciliter (coopération positive), soit ralentir l'étape suivante. Au cours de ces processus, les fragments "AuCl" effectuent des sauts intra- ou intermoléculaire entre les différents atomes de phosphore. La possibilité de former des polymères a été mise en évidence par une étude radiocristallographique effectuée pour l'une des espèces formées pendant la complexation.⁶⁰



Jeunesse, Dieleman *et coll.* ont étudié les possibilités de former des complexes chélatés à partir de calixarènes-diphosphines dans lesquels les atomes de phosphore sont portés par des substituants distaux. Ils ont montré qu'on peut très facilement aboutir à une chélation dès lors qu'on effectue ces réactions de complexation avec des espèces métalliques stabilisées par des ligands labiles, notamment avec des cations métalliques générés *in situ* dans un solvant de type THF ou CH₂Cl₂. En appliquant cette stratégie, les complexes **150-161** et **163** ont pu être obtenus avec des rendements quasi

quantitatifs. Une étude radiocristallographique réalisée pour le complexe calix-couronne **163** révèle un angle de chélation P-Ag-P anormalement grand ($134.74(4)^\circ$). Il faut signaler ici que ce type de diphosphite (**162**) pourrait trouver des applications intéressantes en hydroformylation d'oléfines où des diphosphines à grand angle de chélation se sont parfois avérées utiles pour augmenter la sélectivité en aldéhyde linéaire.⁶¹

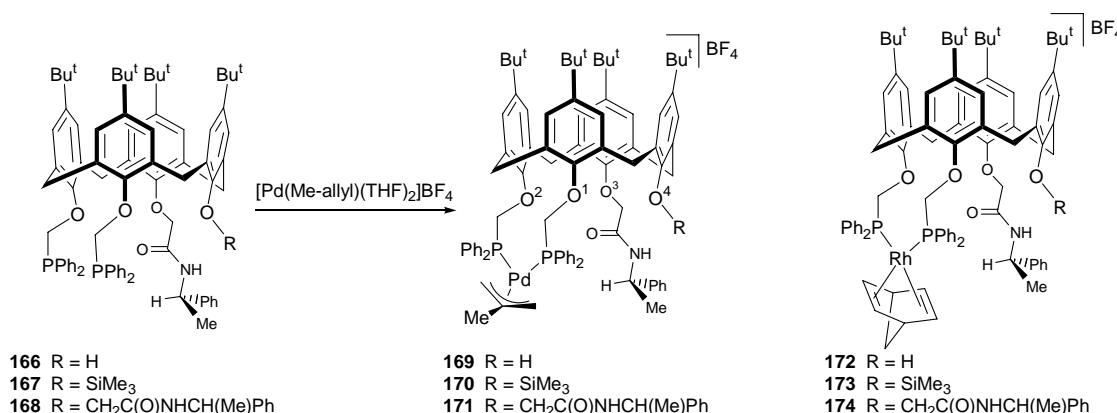
Bien entendu, les ligands du type étudié dans ce paragraphe peuvent également servir à la complexation de deux centres métalliques distincts (ex: complexes **164** et **165**).⁶²



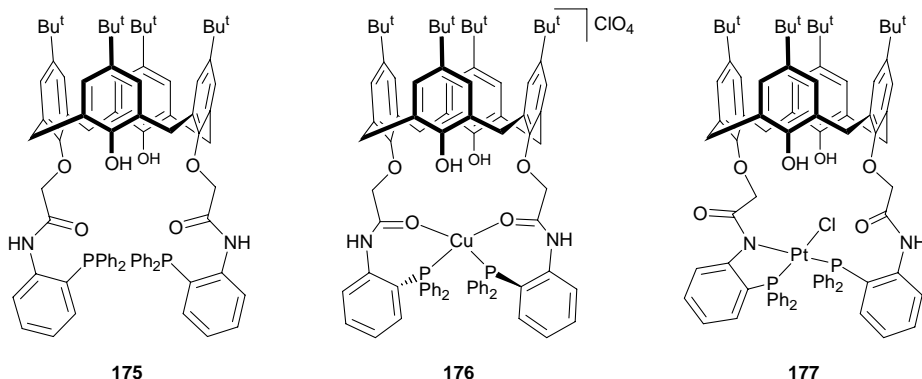
Les phosphines **166-168** ont été employées pour la préparation des complexes optiquement actifs du palladium **169-171**.

Ces complexes sont d'excellents catalyseurs d'alkylation allylique. Les excès énantiométriques observés restent cependant en deçà des meilleurs systèmes existants. Il s'avère que l'induction asymétrique observée est fortement dépendante de la différence de taille entre les deux substituants greffés sur les positions 3 et 4, les meilleurs résultats (*ee* = 67 %) ayant été obtenus avec le ligand **166** (*R* = H). Cette différence de taille entraîne une dissymétrie du cœur du calixarène, elle même provoquant une meilleure transmission de l'information chirale.

Les mêmes effets ont été observés lors de l'hydrogénéation asymétrique de l'itaconate de diméthyle avec les complexes cationiques **172-174**.⁶³

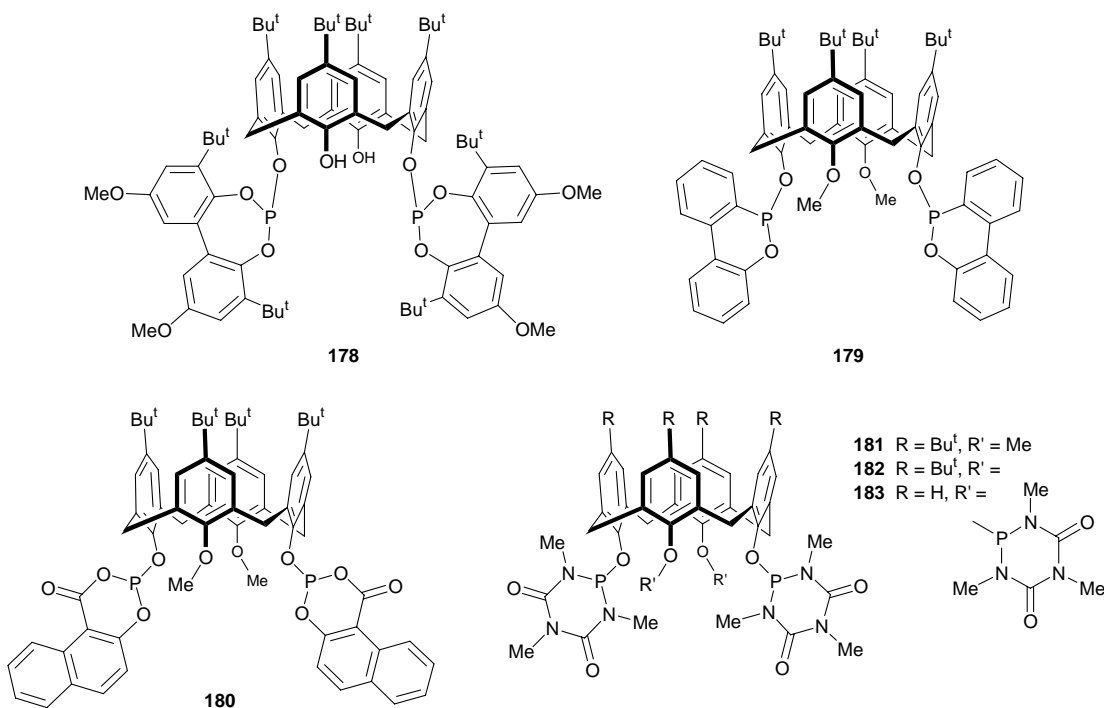


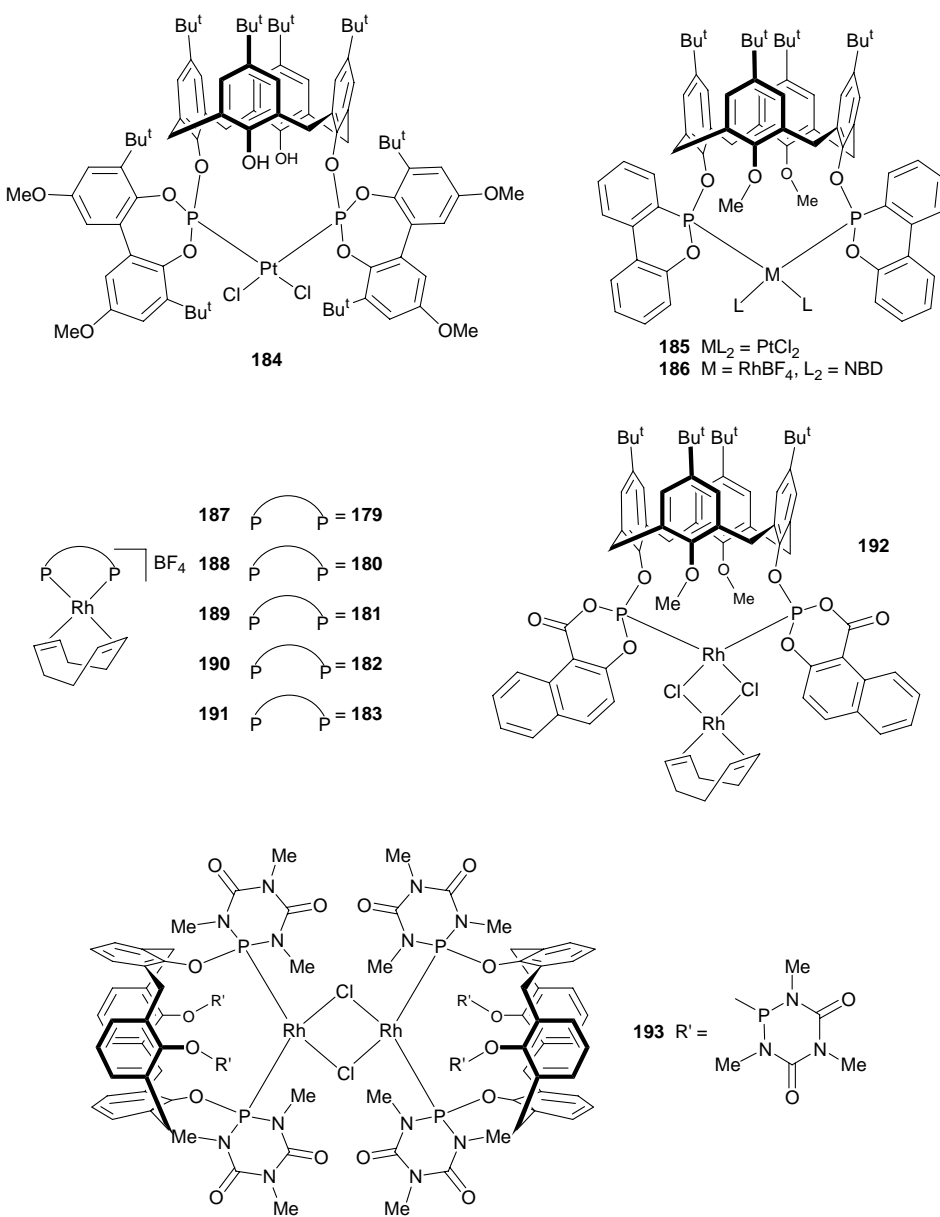
Le ligand **175** a été utilisé, par Zhang et coll., pour la synthèse des complexes chélates **176** et **177** où les calixarènes conservent la conformation cône du produit de départ. Seul le cuivre permet de construire un système doublement chélaté. La géométrie tétraédrique du cuivre(I) dans **176** est très déformée comme en témoigne la valeur des angles P-Cu-P (136.85(8) $^\circ$) et O-Cu-O (109.79(19) $^\circ$).⁶⁴



Schmutzler, Börner et coll. ont étudié les propriétés complexantes des calixarènes **178-183**, tous porteurs de deux atomes de phosphore trivalent liés à des oxygènes distaux. Avec $[\text{PtCl}_2(\text{COD})]$ (COD = 1,5-cyclooctadiène), **178** et **179**

conduisent respectivement aux complexes **184** et **185** de configuration cis. Un comportement cis-chélatant est également observé dans les complexes rhodiés **186** (issu de la réaction de **179** avec $[(\text{NBD})\text{Rh}(\text{acac})]/\text{HBF}_4$ (NBD = norbornadiène)) et **187-191**, obtenus respectivement par réaction des ligands **179-183** avec $[(\text{COD})\text{Rh}(\text{acac})]/\text{HBF}_4$. Pour aucun de ces complexes l'angle de chélation P-M-P n'a pu être déterminé. Les seuls complexes chélates ayant fait l'objet d'études radiocristallographiques sont les complexes **192** et **193**, formés respectivement lors de la réaction de **180** et **183** avec $[\text{RhCl}(\text{COD})]_2$. Les angles de chélation sont respectivement de $101.09(5)^\circ$ dans **192** et $104.73(4)^\circ$ dans **193**, valeurs nettement supérieures à ce qu'on attend pour un complexe de stéréochimie plan carré. Les ligands **178-183**, associés à du rhodium, montrent d'*excellentes* activités en d'hydroformylation d'octène ($\text{TOF} = 2400-5000 \text{ mol(octène).mol(Rh)}^{-1}.\text{h}^{-1}$). Curieusement, aucune sélectivité particulière L/B (L = nonanal, B = 2-méthyoctanal) n'a été observée ($L/B \approx 0.9-1.7$) pour ces ligands à angle de pince important.⁶⁵⁻⁶⁷

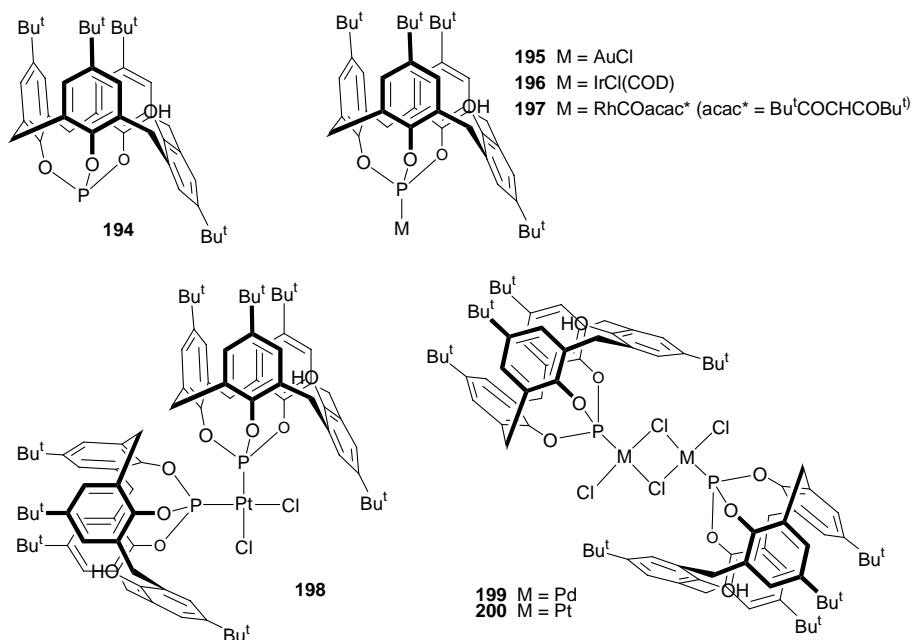




Le calixarène **194**, synthétisé en 1991 par Lattman,⁶⁸ a été utilisé par Pringle *et coll.* pour la synthèse des complexes **195-200**.^{69,70} Lors de la complexation, la conformation initiale, *cône partiel*, est conservée. Les études par diffraction des rayons X réalisées pour **196**, **199** et **200** montrent que dans chacune de ces structures, le noyau phénolique anti-orienté bloque un site axial de l'atome métallique. Ces études permettent également de déterminer l'angle de cône de ce ligand, 176°. Dans la version dé-terbutylée de **194** (non dessiné), cet angle est de 160°. Le ligand **194** a été testé en hydroformylation d'hexène. Il conduit à des activités de l'ordre de 100 mol(hexène).mol(Rh)⁻¹.h⁻¹ (ce résultat est probablement sous estimé) et des rapports L/B proches de 1. La forte proportion de l'isomère branché serait due à un taux

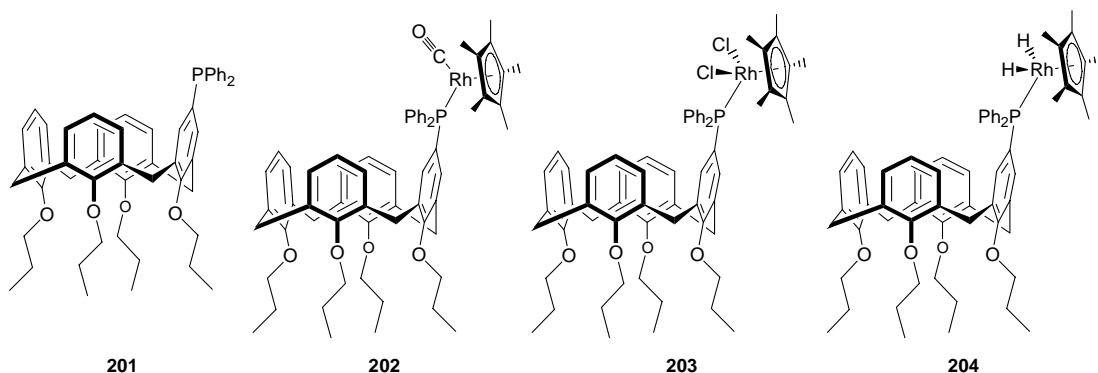
d'isomérisation élevé provoqué par la présence d'un rhodium insaturé (et donc très actif).⁷⁰

Des variantes alkylées de **194** existent, mais ces composés adoptent une conformation cône. Utilisés en hydroformylation de l'octène, ces phosphites conduisent à des catalyseurs très actifs en hydroformylation (TOF = 2500-8000 mol(octène).mol(Rh)⁻¹.h⁻¹). Les rapports L/B sont compris entre 1,2 et 2,1.²¹ L'introduction d'une fonction auxiliaire coordinante a été étudiée lors de ce travail de thèse. On constate une nette influence de cette fonction en hydroformylation d'octène (voir chapitre 2).⁷¹

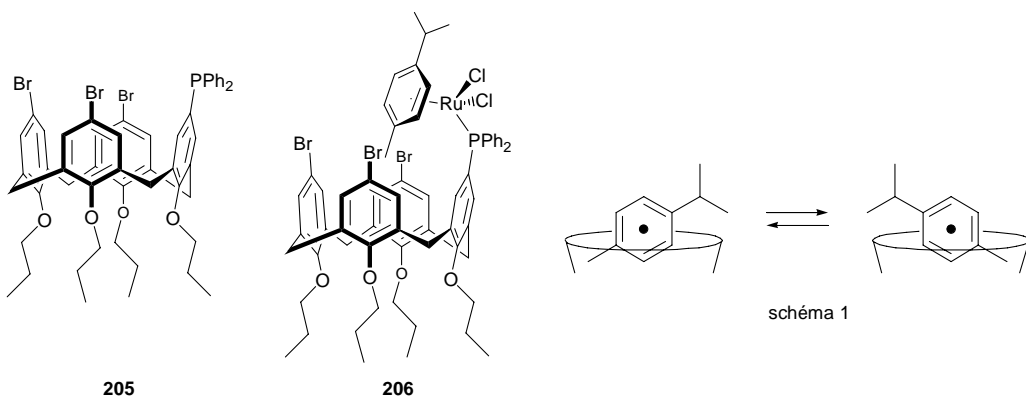


7.2 Formation de liaisons P-M au niveau du bord supérieur

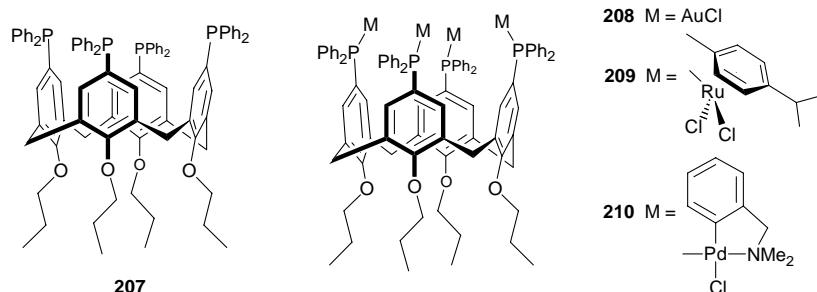
La monophosphine **201** réagit avec $[\text{Cp}^*\text{Rh}(\text{CO})_2]$ et $[(\text{Cp}^*\text{RhCl}_2)_2]$ ($\text{Cp}^* = \text{C}_5\text{Me}_5$) en donnant les complexes monophosphine **202** et **203**, respectivement. Une étude par diffraction des rayons X montre qu'à l'état solide, le vecteur P-Rh de **203** est orienté vers l'extérieur de la cavité. En traitant **203** avec NaBH_4 , on forme le dihydrure **204**.^{72,73}



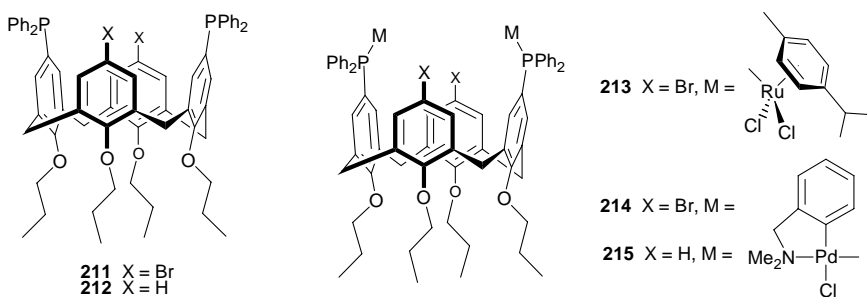
La monophosphine **205** présente un comportement très différent de **201**. Sa réaction avec $[\text{RuCl}_2(p\text{-cymène})]_2$ conduit au complexe monophosphine **206**. A l'état solide, comme en solution, le fragment $[\text{Ru}(p\text{-cymène})\text{Cl}_2]$ reste ici piégé à l'intérieur de la cavité. Les atomes de brome empêchent la rotation complète du fragment métallique autour de l'axe P–C_{calixarène}. Par ailleurs, l'unité *p*-cymène décrit un mouvement oscillatoire autour de l'axe de coordination tout en maintenant le groupe méthyle orienté vers l'intérieur de la cavité (schéma 1).



La tétraphosphine **207** conduit aux complexes tétranucléaires **208**, **209** et **210** par réaction avec $[\text{AuCl}(\text{THT})]$ (THT = tétrahydrothiophène), $[\text{Ru}(p\text{-cymène})\text{Cl}_2]_2$ et $[\text{PdCl}(\text{DMBA})]_2$ (DMBA = diméthylbenzylamine), respectivement.



Les complexes dinucléaires **213**, **214** et **215** peuvent être obtenus facilement à partir des diphosphines **211** et **212**.



Les complexes *cis*-chélates **216** et **217** sont formés lors de la réaction, à haute dilution, de $[\text{PtCl}_2(\text{COD})]$ avec, respectivement, les diphosphines **211** et **212**. A l'état cristallin, le centre métallique pointe vers l'un des noyaux X-substitué. L'angle P-Pt-P est d'environ 100° . Ces complexes donnent lieu, en solution, à deux dynamiques distinctes: a) un basculement rapide du plan métallique de part et d'autre de l'axe du calixarène; b) une oscillation des groupes PPh_2 autour de l'axe P–métal, ce mouvement positionnant en alternance les deux groupes Ph(P) endo-orientés près de l'entrée du calixarène (schéma 2). Des dynamiques identiques ont été observées pour les complexes **218**, **219**, **220** et **221**. A signaler que la réaction de **212** avec $[\text{PtCl}_2(\text{PhCN})_2]$ conduit au complexe monomère **222** (stéréochimie *trans*), alors que **223** réagit avec $[\text{PdCl}_2(\text{COD})]$ en donnant le dimère **224** (stéréochimie *trans* pour chacun des centres métalliques).^{74,75}

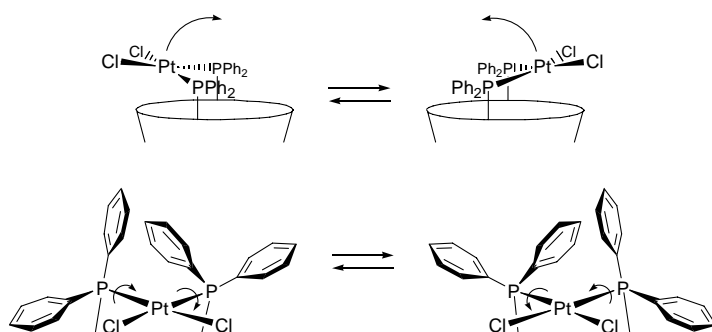
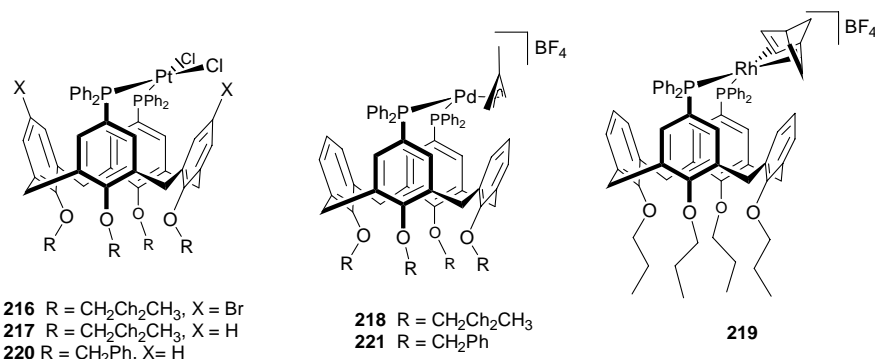
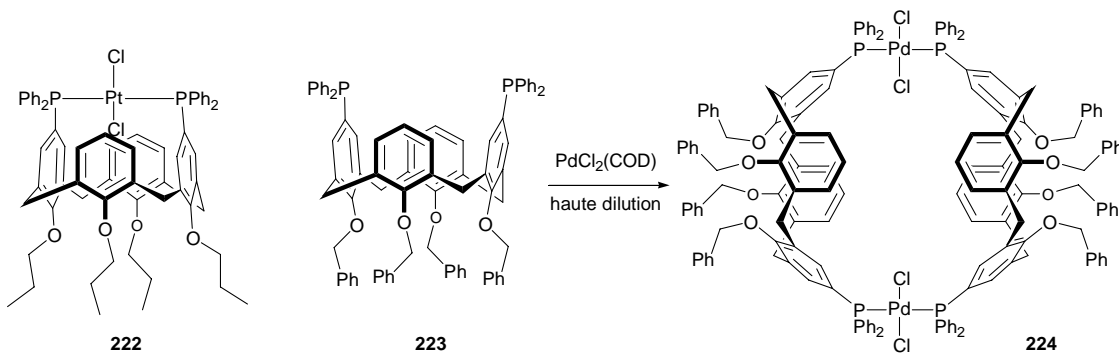
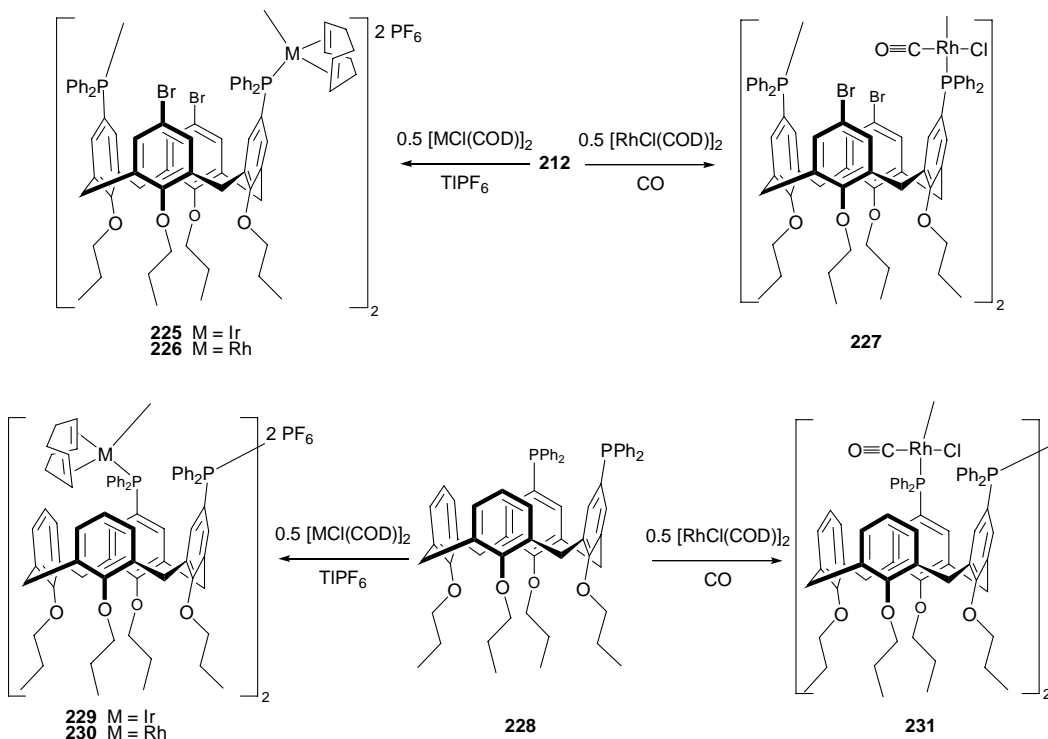


schéma 2

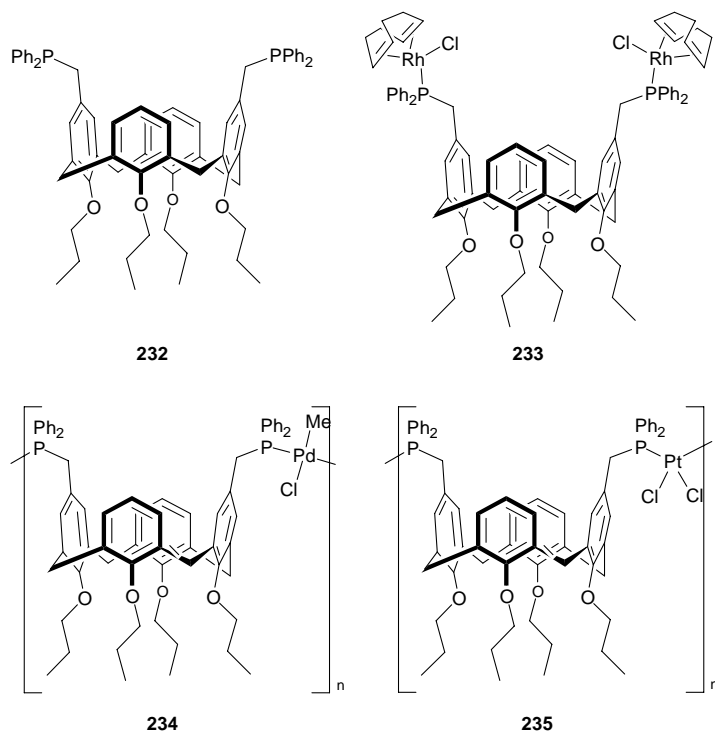


Harvey *et coll.* ont également étudié les propriétés complexantes de la diphosphine **212**, mais en s'intéressant au rhodium et à l'iridium. Ils ont montré que la réaction de **212** avec $[MCl(COD)]_2/TlPF_6$ ($M = Rh, Ir$) conduisait à des dimères (complexes **225** et **226**). La tendance marquée de **212** à former des composés dimères a également été observée lors de la réaction de **212** avec le complexe neutre $[RhCl(COD)]_2$, qui conduit à **227**. Des résultats comparables ont aussi été obtenus à partir de la diphosphine **228**, construite sur un calixarène où les atomes de phosphores sont portés par deux unités phénoliques adjacentes. Cette diphosphine a notamment permis de synthétiser les complexes **229**, **230** et **231**.⁷⁶

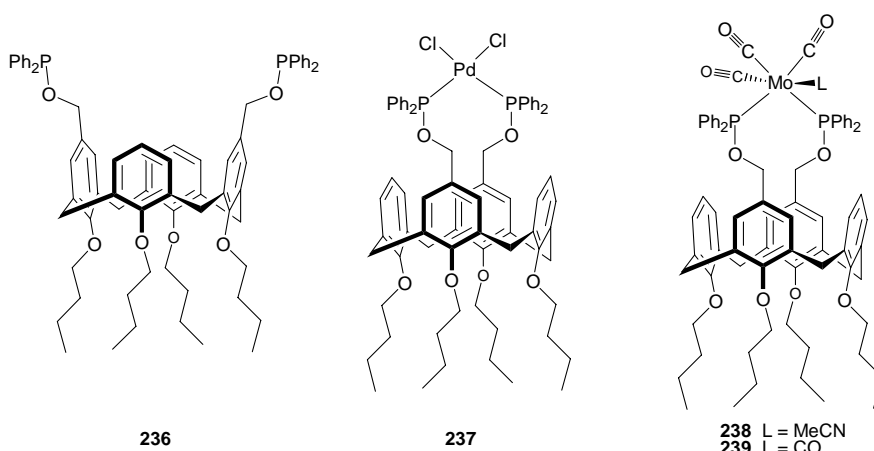


Le complexe dinucléaire **233** a été obtenu par réaction de la diphosphine **232** avec $[RhCl(COD)]_2$. Ce dernier a été employé en hydroformylation de l'octène et du styrène (55 bar, 70°, NEt_3). Les sélectivités observées sont proches de celles attendues

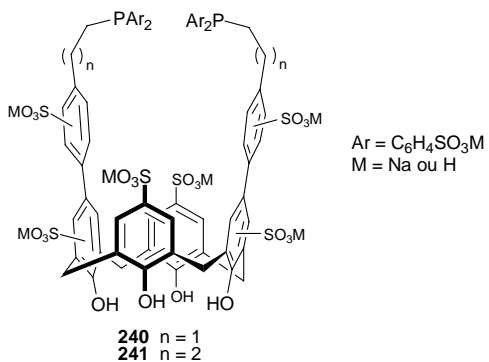
pour ce type de complexe. Ainsi, les rapports L/B sont respectivement de 2.2 (octène) et 0.16 (14/86, styrène). La réaction de **232** avec $[\text{PdClMe}(\text{COD})]$ ou $[\text{PtCl}_2(\text{COD})]$ conduit à des espèces polymériques (complexes **234** et **235**).⁷⁷



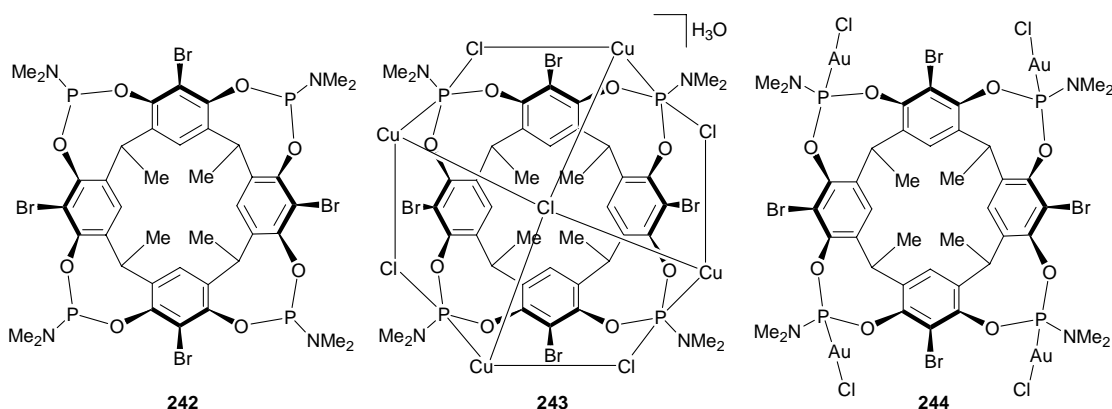
Le diphosphinite **236** forme avec $[\text{PdCl}_2(\text{PhCN})_2]$ le monomère **237**. Dans ce complexe, l'angle de chélation est de $97.46(3)^\circ$. Un autre chélate, le complexe **238**, a été obtenu par réaction de **236** avec $[\text{Mo}(\text{CO})_3(\text{toluène})]$ dans l'acétonitrile. Ce composé peut être converti en **239** par action du monoxyde de carbone. Dans **239**, l'angle de chélation ($\text{P-Mo-P} = 100.42(5)^\circ$) est légèrement supérieur à celui observé pour **237**. Dans chacune de ces structures, le plan PMP, parallèle à l'axe du calixarène, coupe le macrocycle au niveau de deux liaisons $\text{Ar}-\text{CH}_2-\text{Ar}$ diamétralement opposées, conférant ainsi à la structure une symétrie C_2 . En solution, ce plan décrit un mouvement oscillatoire autour de l'axe du calixarène.⁷⁸



Les diphosphines sulfonées **240** et **241** ont été utilisées pour l'hydroformylation de l'octène en milieu biphasique. Elles s'avèrent environ quatre fois plus efficaces que TPPTS / β -CD (TPPTS = triphénylphosphine trisulfonate, β -CD = β -cyclodextrine; l'utilisation de β -CD, dans ce cas, est nécessaire pour assurer le transfert de l'oléfine en phase aqueuse), tout en conduisant aux mêmes sélectivités ($L/B = 1.7\text{-}3$).⁷⁹ Lors de l'hydroformylation d'oléfines internes (2 ou 4-octène), l'activité et la sélectivité en aldéhyde linéaire ($L/B = 0.3$ à 0.4) baissent consécutivement à la forte isomérisation du substrat.⁸⁰

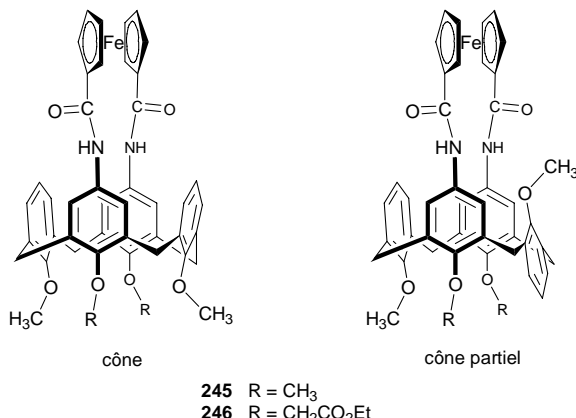


Le résorcinarene tétraphosphoramide **242** conduit par réaction avec CuCl au complexe tétranucléaire **243** où les atomes de cuivre sont liés entre eux par des ponts Cl. La réaction de **242** avec [AuCl(THT)] produit le complexe **244** qui présente une symétrie C_{4v} en solution. A l'état solide, cette symétrie n'est pas conservée: un des vecteurs PAu est approximativement parallèle au plan de référence, alors que les trois autres pointent vers l'axe du résorcinarene.⁸¹



8 Calixarènes substitués par des unités ferrocéniques

Chacun des complexes ferrocène **245** et **246** existe en solution sous la forme de deux conformères, *cône* et *cône partiel*, en équilibre. Une étude préliminaire par RMN montre qu'ils peuvent sélectivement fixer certains anions, notamment (Cl⁻ et H₂PO₄⁻).⁸²



9 Complexes π mettant en jeu un noyau aromatique du calixarène

Ishii *et coll.* ont étudiés la formation des complexes π **247-249**, à partir des calixarènes génériques et de [(COD)M(μ -OMe)]₂ (M = Rh, Ir). Dans ces complexes, le

métal est toujours fixé à l'extérieur du calixarène. L'addition d'un fragment "Rh(COD)" supplémentaire fournit les complexes **250-252**, respectivement, où le second atome de rhodium se coordine à deux atomes d'oxygène proximaux. En solution, l'atome de rhodium coordiné à des atomes d'oxygène ponte tantôt le couple (O^1, O^2), tantôt (O^2, O^3). Ce comportement fluxionnel est représenté sur le schéma 3.⁸³

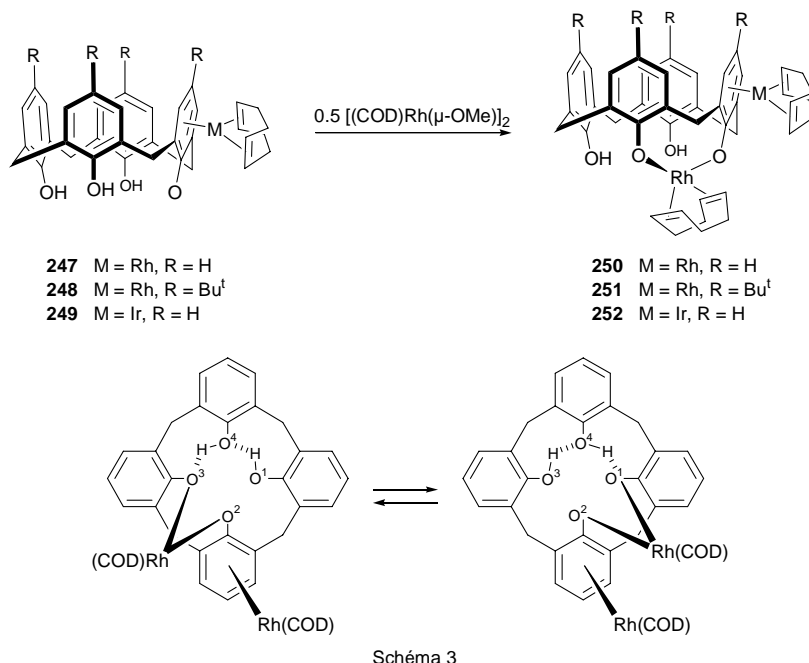


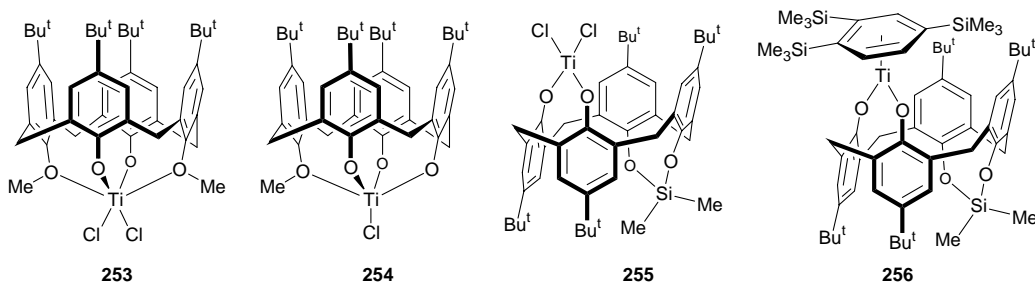
Schéma 3

10 Calixarènes en catalyse homogène

Plusieurs complexes calixaréniques bien définis ont été utilisés pour la formation de liaisons C–C. Ainsi, le complexe **23**, associé à Me₂AlCl ou du méthylaluminoxane (MAO), converti l'éthylène en polyéthylène. L'activité observée, 50 g.mmol⁻¹.h⁻¹.bar⁻¹, est six fois plus grande que celle obtenue en présence de MAO.⁹ Le complexe **253** est lui aussi un catalyseur de polymérisation de l'éthylène (0.23 g. mmol⁻¹.h⁻¹.bar⁻¹, activation réalisée avec le MAO).⁸⁴ A signaler que ce dernier, de même que **254**, catalyse également l'époxydation d'alcool en présence de zéolithes.⁸⁵

D'autres complexes associant des lanthanides à des calixarènes génériques (calix[4,6,8]) se sont avérés efficaces pour la polymérisation d'éthylène. Les activités les plus élevées ont été obtenues avec le calix[6]arène-(OH)₆.⁸⁶

Le complexe Ti-arène **256**, obtenu à partir du calixarène *1,2-alterné*-**255**, effectue efficacement (sélectivités en trimère supérieures à 90 %) la cyclotrimérisation d'alcyne vrais.⁸⁷



Dans plusieurs publications, des catalyseurs calixaréniques ont été formés *in situ*. Ainsi, par exemple, l'utilisation du mélange $\text{Ti}(\text{OPr})_4/\text{calix}[4,6,8]\text{arène}$ augmente d'un facteur 20 les rendements des réactions de couplage entre un diène et le benzaldéhyde par rapport à la réaction sans ajout de calixarène (schéma 4).⁸⁸

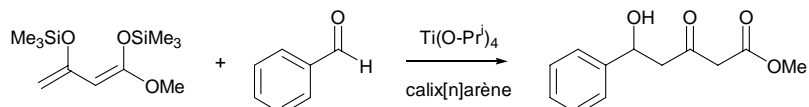


schéma 4

Les propriétés de transfert de phase de calix[4,6,8]arènes aminés hydrosolubles ont été utilisées pour augmenter de manière significative les rendements de certaines réactions. Ainsi, en milieu biphasique, les rendements de réaction d'alkylation de méthylènes activés (par ex. en α de carbonyle ou d'alcool) par des halogénures d'alkyles sont décuplés par la présence d'une quantité catalytique d'un calixarène hydrosoluble.⁸⁹

De même, l'utilisation du calixarène hydrosoluble **257** permet de multiplier par 12 la vitesse du couplage de Suzuki entre l'acide phényl boronique et le iodobenzène (schéma 5).⁹⁰

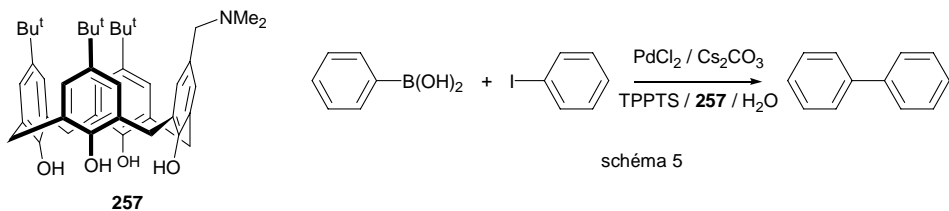


schéma 5

On peut constater qu'à ce jour les calixarènes restent relativement peu utilisés en catalyse homogène.

11 Références

1. A. J. Petrella, N. K. Roberts, C. L. Raston, M. Thornton-Pett and R. N. Lamb, *Chem. Commun.*, 2003, 1238-1239.
2. A. J. Petrella, N. K. Roberts, D. C. Craig, C. L. Raston and R. N. Lamb, *Chem. Commun.*, 2003, 1014-1015.
3. A. J. Petrella, D. C. Craig, R. N. Lamb, C. L. Raston and N. K. Roberts, *Dalton Trans.*, 2003, 4590-4597.
4. A. J. Petrella, N. K. Roberts, C. L. Raston, D. C. Craig, M. Thornton-Pett and R. N. Lamb, *Eur. J. Inorg. Chem.*, 2003, 4153-4158.
5. A. J. Petrella, N. K. Roberts, D. C. Craig, C. L. Raston and R. N. Lamb, *Chem. Commun.*, 2003, 1728-1729.
6. A. J. Petrella, N. K. Roberts, D. C. Craig, C. L. Raston and R. N. Lamb, *Chem. Commun.*, 2003, 2288-2289.
7. M. Fan, H. Zhang and M. Lattman, *Phosphorus, Sulfur and Silicon*, 2002, **177**, 1549-1551.
8. S. R. Dubberley, A. Friedrich, D. A. Willman, P. Mountford and U. Radius, *Chem. Eur. J.*, 2003, **9**, 3634-3654.
9. V. C. Gibson, C. Redshaw and M. R. J. Elsegood, *J. Chem. Soc., Dalton Trans.*, 2001, 767-769.
10. V. C. Gibson, C. Redshaw and M. R. J. Elsegood, *New J. Chem.*, 2002, **26**, 16-19.
11. V. C. Gibson, C. Redshaw and M. R. J. Elsegood, *Chem. Commun.*, 2002, 1200-1201.
12. U. Lüning, F. Löffler and J. Eggert, in *Calixarenes 2001*, Asfari Z., Böhmer V., Harrowfield J., and Vicens J. (eds.), Kluwer, Dordrecht, **2001**, pp. 71-88.
13. V. C. Gibson, C. Redshaw, W. Clegg and M. R. J. Elsegood, *J. Chem. Soc., Chem. Commun.*, 1995, 2371-2372.
14. C. Redshaw and M. R. J. Elsegood, *Eur. J. Inorg. Chem.*, 2003, 2071-2074.
15. J. Attner and U. Radius, *Chem. Eur. J.*, 2001, **7**, 783-790.
16. A. J. Millar, J. M. White, C. J. Doonan and C. G. Young, *Inorg. Chem.*, 2000, **39**, 5151-5155.
17. A. Vigalok and T. M. Swager, *Adv. Mater.*, 2002, **14**, 368-371.
18. J. Hesschenbrouck , E. Solari, C. Floriani, N. Re, C. Rizzoli and A. Chiesi-Villa,

- J. Chem. Soc., Dalton Trans.*, 2000, 191-198.
19. F. A. Cotton, L. M. Daniels, C. Lin and C. A. Murillo, *Inorg. Chim. Acta*, 2003, **347**, 1-8.
 20. J. Attner and U. Radius, *Z. Anorg. Allg. Chem.*, 2002, **628**, 2345-2352.
 21. F. J. Parlevliet, C. Kiener, J. Fraanje, K. Goubitz, M. Lutz, A. L. Spek, P. C. J. Kamer and P. W. N. M. Van Leeuwen, *J. Chem. Soc., Dalton Trans.*, 2000, 1113-1122.
 22. C. Redshaw and M. R. J. Elsegood, *Inorg. Chem.*, 2000, **39**, 5164-5168.
 23. M. Brown and C. Jablonski, *Can. J. Chem.*, 2001, **79**, 463-471.
 24. U. Radius and J. Attner, *Eur. J. Inorg. Chem.*, 2002, 161-164.
 25. C. Floriani and R. Floriani-Moro, in *Calixarenes 2001*, Asfari Z., Böhmer V., Harrowfield J., and Vicens J. (eds.), Kluwer, Dordrecht, **2001**, pp. 536-560.
 26. G. Guillemot, E. Solari, R. Scopelliti and C. Floriani, *Organometallics*, 2001, **20**, 2446-2448.
 27. G. Guillemot, E. Solari, C. Floriani, N. Re and C. Rizzoli, *Organometallics*, 2000, **19**, 5218-5230.
 28. G. Guillemot, E. Solari, C. Floriani and C. Rizzoli, *Organometallics*, 2001, **20**, 607-615.
 29. K. Iwasa, T. Kochi and Y. Ishii, *Angew. Chem. Int. Ed.*, 2003, **42**, 3658-3660.
 30. V. Esposito, E. Solari, C. Floriani, N. Re, C. Rizzoli and A. Chiesi-Villa, *Inorg. Chem.*, 2000, **39**, 2604-2613.
 31. T. Kajiwara, S. Yokozawa, T. Ito, N. Iki, N. Morohashi and S. Miyano, *Angew. Chem. Int. Ed.*, 2002, **41**, 2076-2078.
 32. H. Katagiri, N. Morohashi, N. Iki, C. Kabuto and S. Miyano, *Dalton Trans.*, 2003, 723-726.
 33. J. Seitz and G. Maas, *Chem. Commun.*, 2002, 338-339.
 34. I. A. Bagatin, E. S. De Souza, A. S. Ito and H. E. Toma, *Inorg. Chem. Commun.*, 2003, **6**, 288-293.
 35. K. J. C. Van Bommel, W. Verboom, R. Hulst, H. Kooijman, A. L. Spek and D. N. Reinhoudt, *Inorg. Chem.*, 2000, **39**, 4099-4106.
 36. M. I. Ogden, B. W. Skelton and A. H. White, *J. Chem. Soc., Dalton Trans.*, 2001, 3073-3077.
 37. W. He, F. Liu, Y. Mei, Z. Guo and L. Zhu, *New J. Chem.*, 2001, **25**, 1330-1336.

38. W. He, F. Liu, Z. Ye, Y. Zhang, Z. Guo, L. Zhu, X. Zhai and J. Li, *Langmuir*, 2001, **17**, 1143-1149.
39. J. B. Cooper, M. G. B. Drew and P. D. Beer, *J. Chem. Soc., Dalton Trans.*, 2001, 392-401.
40. J.-O. Dalbavie, J.-B. Regnouf-de-Vains, R. Lamartine, M. Perrin, S. Lecocq and B. Fenet, *Eur. J. Inorg. Chem.*, 2002, 901-909.
41. J.-O. Dalbavie, J.-B. Regnouf-de-Vains, R. Lamartine, S. Lecocq and M. Perrin, *Eur. J. Inorg. Chem.*, 2000, 683-691.
42. R. Dorta, L. J. W. Shimon, H. Rozenberg, Y. Ben-David and D. Milstein, *Inorg. Chem.*, 2003, **42**, 3160-3167.
43. J. B. Cooper, M. G. B. Drew and P. D. Beer, *J. Chem. Soc., Dalton Trans.*, 2000, 2721-2728.
44. Z. Zhong, A. Ikeda, M. Ayabe, S. Shinkai, S. Sakamoto and K. Yamaguchi, *J. Org. Chem.*, 2001, **66**, 1002-1008.
45. T. Haino, Y. Yamanaka, H. Araki and Y. Fukazawa, *Chem. Commun.*, 2002, 402-403.
46. B. Xing, M.-F. Choi and B. Xu, *Chem. Commun.*, 2002, 362-363.
47. L. Le Clainche, M. Giorgi and O. Reinaud, *Eur. J. Inorg. Chem.*, 2000, 1931-1933.
48. O. Sénèque, M. Campion, B. Douziech, M. Giorgi, Y. Le Mest and O. Reinaud, *Dalton Trans.*, 2003, 4216-4218.
49. L. Le Clainche, Y. Rondelez, O. Sénèque, S. Blanchard, M. Campion, M. Giorgi, A. F. Duprat, Y. Le Mest and O. Reinaud, *C. R. Acad. Sci., Chimie, Série IIc*, 2000, **3**, 811-819.
50. Y. Rondelez, M.-N. Rager, A. Duprat and O. Reinaud, *J. Am. Chem. Soc.*, 2002, **124**, 1334-1340.
51. O. Sénèque, Y. Rondelez, L. Le Clainche, C. Inisan, M.-N. Rager, M. Giorgi and O. Reinaud, *Eur. J. Inorg. Chem.*, 2001, 2597-2604.
52. L. Le Clainche, M. Giorgi and O. Reinaud, *Inorg. Chem.*, 2000, **39**, 3436-3437.
53. Y. Rondelez, O. Sénèque, M.-N. Rager, A. F. Duprat and O. Reinaud, *Chem. Eur. J.*, 2000, **6**, 4218-4226.
54. O. Sénèque, M.-N. Rager, M. Giorgi and O. Reinaud, *J. Am. Chem. Soc.*, 2000, **122**, 6183-6189.

55. O. Sénèque, M. Giorgi and O. Reinaud, *Chem. Commun.*, 2001, 984-985.
56. Y. Rondelez, G. Bertho and O. Reinaud, *Angew. Chem. Int. Ed.*, 2002, **41**, 1044-1046.
57. O. Sénèque, M. Campion, N. Douziech, M. Giorgi, E. Rivière, Y. Journaux, Y. Le Mest and O. Reinaud, *Eur. J. Inorg. Chem.*, 2002, 2007-2014.
58. J. Gagnon, M. Drouin and P. D. Harvey, *Inorg. Chem.*, 2001, **40**, 6052-6056.
59. P. Mongrain and P. D. Harvey, *Can. J. Chem.*, 2003, **81**, 1246-1254.
60. C. B. Dieleman, D. Matt and A. Harriman, *Eur. J. Inorg. Chem.*, 2000, 831-834.
61. P. C. J. Kamer, J. N. H. Reek and P. W. N. M. Van Leeuwen, in *Rhodium Catalyzed Hydroformylation*, Van Leeuwen, P. W. N. M. and Claver C. (eds.), Kluwer, Dordrecht, **2000**, pp. 35-62.
62. C. Jeunesse, C. Dieleman, S. Steyer and D. Matt, *J. Chem. Soc., Dalton Trans.*, 2001, 881-892.
63. C. Dieleman, S. Steyer, C. Jeunesse and D. Matt, *J. Chem. Soc., Dalton Trans.*, 2001, 2508-2517.
64. X.-X. Han, L.-H. Weng, X.-B. Leng and Z.-Z. Zhang, *Polyhedron*, 2001, **20**, 1881-1884.
65. C. Kunze, D. Selent, I. Neda, M. Freytag, P. G. Jones, R. Schmutzler, W. Baumann and A. Börner, *Z. Anorg. Allg. Chem.*, 2002, **628**, 779-787.
66. C. Kunze, I. Neda, M. Freytag, P. G. Jones and R. Schmutzler, *Z. Anorg. Allg. Chem.*, 2002, **628**, 545-552.
67. C. Kunze, D. Selent, I. Neda, R. Schmutzler, A. Spannenberg and A. Börner, *Heteroatom Chem.*, 2001, **12**, 577-585.
68. D. V. Khasnis, J. M. Burton, M. Lattman and H. Zhang, *J. Chem. Soc., Chem. Commun.*, 1991, 562-563.
69. C. J. Cobley, D. D. Ellis, A. G. Orpen and P. G. Pringle, *J. Chem. Soc., Dalton Trans.*, 2000, 1101-1107.
70. C. J. Cobley, D. D. Ellis, A. G. Orpen and P. G. Pringle, *J. Chem. Soc., Dalton Trans.*, 2000, 1109-1112.
71. S. Steyer, C. Jeunesse, D. Matt, R. Welter and M. Wesolek, *J. Chem. Soc., Dalton Trans.*, 2002, 4264-4274.
72. M. Vézina, J. Gagnon, K. Villeneuve, M. Drouin and P. D. Harvey, *Chem. Commun.*, 2000, 1073-1074.

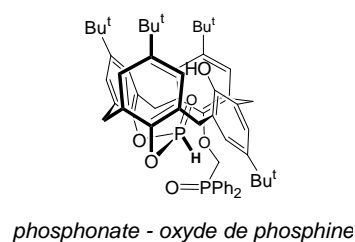
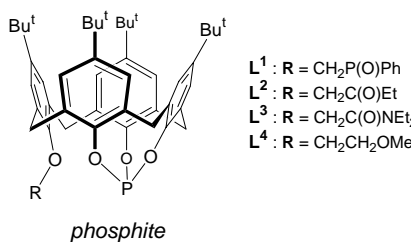
73. M. Vézina, J. Gagnon, K. Villeneuve, M. Drouin and P. D. Harvey, *Organometallics*, 2001, **20**, 273-281.
74. M. Lejeune, C. Jeunesse, D. Matt, N. Kyritsakas, R. Welter and J.-P. Kintzinger, *J. Chem. Soc., Dalton Trans.*, 2002, 1642-1650.
75. K. Takenaka, Y. Obora, L. H. Jiang and Y. Tsuji, *Organometallics*, 2002, **21**, 1158-1166.
76. F. Plourde, K. Gilbert, J. Gagnon and P. D. Harvey, *Organometallics*, 2003, **22**, 2862-2875.
77. X. Fang, B. L. Scott, J. G. Watkin, C. A. G. Carter and G. J. Kubas, *Inorg. Chim. Acta*, 2001, **317**, 276-281.
78. D. R. Evans, M. Huang, J. C. Fettinger and T. L. Williams, *Inorg. Chem.*, 2002, **41**, 5986-6000.
79. S. Shimizu, S. Shirakawa, Y. Sasaki and C. Hirai, *Angew. Chem. Int. Ed.*, 2000, **39**, 1256-1259.
80. S. Shirakawa, S. Shimizu and Y. Sasaki, *New J. Chem.*, 2001, **25**, 777-779.
81. P. Sakhaii, I. Neda, M. Freytag, H. Thönnessen, P. G. Jones and R. Schmutzler, *Z. Anorg. Allg. Chem.*, 2000, **626**, 1246-1254.
82. B. Tomapatanaget and T. Tuntulani, *Tetrahedron Lett.*, 2001, **42**, 8105-8109.
83. Y. Ishii, K.-I. Onaka, H. Hirakawa and K. Shiramizu, *Chem. Commun.*, 2002, 1150-1151.
84. C. Capacchione, P. Neri and A. Proto, *Inorg. Chem. Commun.*, 2003, **6**, 339-342.
85. A. Massa, A. D'ambrosi, A. Proto and A. Scettri, *Tetrahedron Lett.*, 2001, **42**, 1995-1998.
86. Y. Chen, Y. Zhang, Z. Shen, R. Kou and L. Chen, *Eur. Polym. J.*, 2001, **37**, 1181-1184.
87. O. V. Ozerov, B. O. Patrick and F. T. Ladipo, *J. Am. Chem. Soc.*, 2000, **122**, 6423-6431.
88. A. Soriente, M. Fruilo, L. Gregoli and P. Neri, *Tetrahedron Lett.*, 2003, **44**, 6195-6198.
89. S. Shimizu, T. Suzuki, S. Shirakawa, Y. Sasaki and C. Hirai, *Adv. Synth. Catal.*, 2002, **344**, 370-378.
90. M. Baur, M. Frank, J. Schatz and F. Schildbach, *Tetrahedron*, 2001, **57**, 6985-6991.

***HETEROFUNCTIONALISED PHOSPHITES BUILT ON A
CALIX[4]ARENÉ SCAFFOLD AND THEIR USE IN
1-OCTENE HYDROFORMYLATION. FORMATION OF
12-MEMBERED P,O-CHELATE RINGS.***

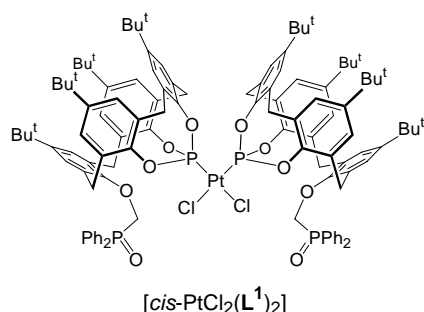
Résumé	2
1 Introduction	4
2 Results and discussion	5
2.1 Synthesis and stability of the ligands	5
2.2 Complexes obtained from phosphites L ¹ -L ³	11
2.3 Hydroformylation with heterodifunctional calix phosphites	19
3 Conclusion	22
4 References	23
5 Experimental	26
5.1 General procedures	26
5.2 Syntheses	27
5.3 Hydroformylation experiments	49
5.4 X-Ray crystallography	49

Résumé

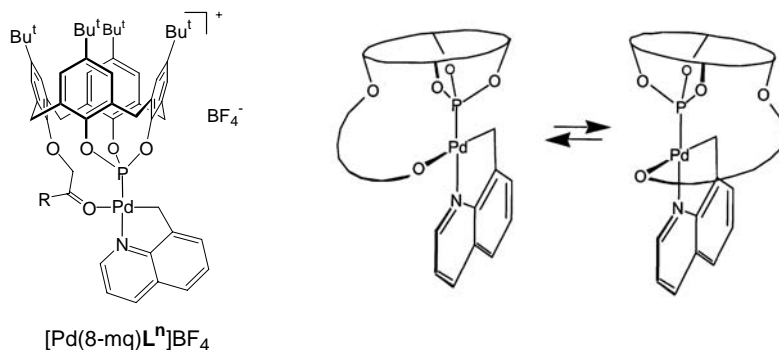
Ce chapitre étudie la possibilité d'accéder à des phosphites encombrés par pontage de trois groupes hydroxy d'un calixarène monofonctionnalisé du type *cône*-calix[4]arène-(OH)₃-(OR) par un atome de phosphore. Les calixphosphites **L¹-L⁴** ont été obtenus par réaction du mélange PCl₃/NEt₃ avec les calixarènes monofonctionnalisés suivants: *p*-*tert*-butyl-calix[4]arène-(OH)₃-OR (R = -CH₂P(O)Ph₂ (**L¹**), -CH₂CO₂Et (**L²**), -CH₂CONEt₂ (**L³**), -CH₂CH₂OMe (**L⁴**)). Ces phosphites adoptent tous la conformation "cône". En raison de la présence d'une fonctionnalité oxygénée dans le quatrième substituant phénolique, ils constituent potentiellement des ligands *P,O*-chélatants. Le phosphite **L¹** est relativement robuste puisque stable en présence de soude; en revanche, au contact d'une solution acide il est immédiatement converti en phosphonate. L'oxydation lente de **L¹** par l'air conduit à un composé hybride phosphate-oxyde de phosphine.



Dans les complexes suivants, [RuCl₂(*p*-cymène)**L¹**], [*cis*-PtCl₂(**L¹**)₂], [*trans*-PdCl₂(**L¹**)₂], [Pd(8-mq)Cl(**Lⁿ**)] (8-mqH = 8-methylquinoléine, n = 1-3), [Pd(dmba)Cl(**L¹**)] (dmbaH = *N,N*-dimethylbenzylamine), [Pd(η^3 -C₄H₇)Cl(**L²**)], [Rh(acac)(CO)**Lⁿ**] (n = 1-3) et [RhCl(CO)(**L¹**)₂], les ligands phosphites ont un comportement κ^1P (coordination monodentate). L'encombrement marqué de **L¹** est manifeste dans le complexe bis-phosphite [*cis*-PtCl₂(**L¹**)₂] pour lequel on observe un empêchement de la rotation des deux ligands autour des axes Pt-P. Une étude structurale par diffraction des rayons X non seulement établit que le phosphite possède un angle de cône supérieur à 180°, mais fait également apparaître la forte déformation subie par la matrice calix[4]arène par suite du P-pontage.



La bonne préorganisation de ces ligands permet d'obtenir des complexes chélates impliquant l'atome de phosphore et l'atome d'oxygène de la fonction auxiliaire. Une telle situation est notamment rencontrée dans les complexes $[Pd(8\text{-mq})L^n]BF_4$ ($n = 1\text{-}3$), (8-mqH = 8-méthylquinoléine). Une étude par diffraction des rayons X montre que dans le complexe $[Pd(8\text{-mq})L^2]BF_4$ la boucle P,O (incorporant la matrice calixarène) est située en dehors du plan métallique. En solution, la molécule présente un comportement dynamique, la boucle P,O basculant en alternance de part et d'autre du plan de coordination. Ce mouvement est facilité par la grande flexibilité du cœur calixarénique.



Les quatre phosphites $L^1\text{-}L^4$, associés à du rhodium, ont été testés en hydroformylation d'octène. Ces systèmes sont rapides (ex. TOF = 4400 mol(octène).mol(Rh) $^{-1}\cdot h^{-1}$ pour L^4) et les activités correspondent à celles attendues pour des phosphites d'encombrement moyen. Une diminution de l'activité est observée lorsque le caractère donneur de la fonction auxiliaire augmente: $L^4 > L^1 > L^2 > L^3$. Ceci suggère une coordination (transitoire) de cette dernière durant le processus catalytique, entraînant des modifications de la géométrie du calixarène et par voie de conséquence des propriétés électroniques et stériques du phosphite. La nature du groupement auxiliaire a également un impact sur la sélectivité en aldéhyde linéaire, la proportion de ce dernier augmentant sensiblement avec le caractère donneur du groupe auxiliaire (ex.

$L/B = 3.6$ avec \mathbf{L}^2 et $L/B = 1.4$ avec \mathbf{L}^4). Il est raisonnable de considérer que la coordination de la fonction latérale, lorsqu'elle se produit, modifie les interactions stériques entre le ligand et le substrat coordonné.

1 Introduction

Ligands which combine a P(III) centre with an oxygen-donor functionality have been intensively investigated over the last twenty years.¹⁻⁶ Prominent applications for such ligands are, e.g. the nickel-catalysed oligomerisation of ethylene with enolato-phosphine complexes⁷⁻⁹ or the hydroformylation of propene with rhodium complexes made water-soluble with sulfonatophosphines.¹⁰ Hybrid P,O-ligands offer distinct advantages over conventional phosphines or diphosphines. For example, they may act towards naked d⁸ metal ions as unsymmetrical chelates capable of directing an incoming substrate specifically towards one of the two opposite coordination sites, *i.e.* *trans* to P or *trans* to O.¹¹ Another important feature of mixed P,O-ligands concerns their ability to display hemilabile behaviour, a property which is frequently observed for neutral P,O-chelators in which the oxygen atom is a weak donor (*e.g.* an ether group) and, therefore, may reversibly be substituted.¹²⁻¹⁶ Such bidentate ligands have proved useful for increasing the rate of catalytic reactions by stabilisation of transient key intermediates.^{17,18} It should also be mentioned that P,O-ligands in which the oxygen atom is part of a water-solubilising fragment have attracted much attention in recent years owing to their potential utility in biphasic catalysis. Interestingly, to date, most mixed P,O-ligands are based on tertiary phosphines, while phosphite ligands comprising additional oxygen donors have scarcely been studied.¹⁹⁻²¹ This is rather surprising considering the above-mentioned industrial applications of P,O-phosphine ligands.

The present work deals with the synthesis, characterisation and co-ordinative properties of phosphite ligands that contain a secondary "oxygen" function (amide, ester, phosphine oxide, ether). The new ligands are based on a calix[4]arene scaffold on which the auxiliary function has been introduced prior to P-functionalisation. This work also reports the first example of a structurally characterised chelate complex derived from a calixarene-based phosphite. The new P,O-phosphites, which may form 12-membered chelate complexes, were used in octene hydroformylation and the influence

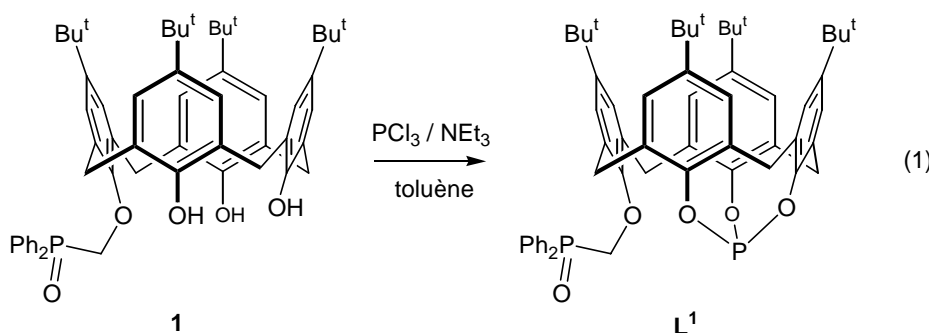
of the side group was determined. Phosphites based on a calix[4]arene scaffold were first reported by Lattman *et al.*²² Recent publications by the groups of Pringle,^{23,24} van Leeuwen^{25,26} and Röper²⁷ report the coordination and catalytic chemistry of other calix[n]arene phosphites ($n = 4, 6$), but none of these ligands is suitable for the formation of an unsymmetrical chelate.

2 Results and discussion

2.1 Synthesis and stability of the ligands

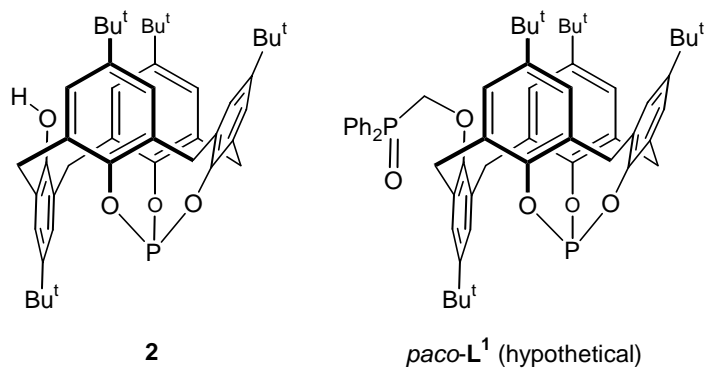
In this work, the nomenclature "*m*-H" specifically refers to aromatic protons in *meta* positions on phenolic rings of the calixarene backbone. The following results illustrate how a calix[4]arene bearing a single substituent tethered at the lower rim can be used for the preparation of functional phosphites. All calixarene phosphites presented herein adopt a cone conformation.

Reaction of the mono-functionalised calixarene **1**²⁸ with $\text{PCl}_3/\text{NEt}_3$ in toluene afforded phosphite **L**¹ in quantitative yield (eqn. 1).

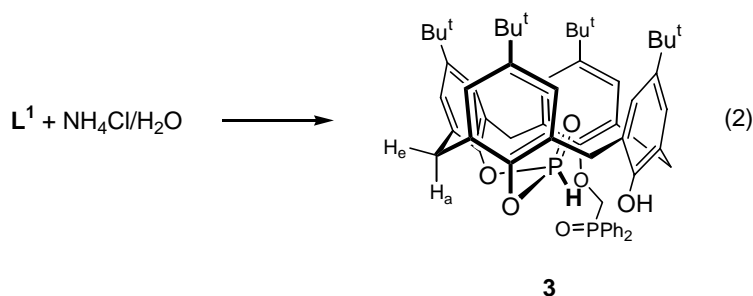


Compound **L**¹ is highly soluble in all common organic solvents, a property that makes recrystallisation difficult. It turned out that after careful elimination of NEt_3HCl and NEt_3 from the reaction mixture (see Experimental section), the product did not require further purification. The ^{31}P NMR spectrum of **L**¹ shows two signals, at 107 and 26.1 ppm, corresponding to the phosphite and phosphine oxide fragments, respectively (*cf.* 128 ppm for $\text{P}(\text{OPh})_3$ and 23 ppm for $\text{O}=\text{PPh}_3$). The ^1H NMR spectrum, which

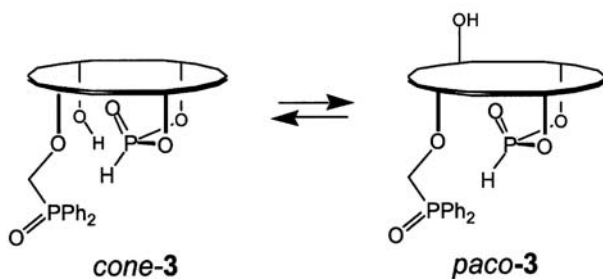
displays three Bu^t signals of relative intensity 1:1:2 and two AB patterns for the ArCH_2 groups, is consistent with the existence of a symmetry plane. As revealed by 2D ROESY experiments, the *m*-H protons of the calixarene unit correlate exclusively with *equatorial* ArCH_2Ar atoms. This observation unambiguously establishes the cone structure of **L**¹. Note that this conformation contrasts with that of Lattman's calixarene **2**, obtained by reacting *p*-*tert*-butyl-calix[4]arene with hexamethylphosphorus triamide/ $\text{CF}_3\text{CO}_2\text{-H}$.²² Clearly, the steric crowding of the phosphine oxide group in precursor **1** prevents *trans* annulus inversion and, hence, leads to the selective formation of a cone conformer. It should be stressed that the use of $\text{PCl}_3/\text{NEt}_3$ for the preparation of *cone*-**L**¹ does not result in the formation of a second (isomeric) product, in contrast to the observations made by Parlevliet *et al.*, who applied the same methodology to the synthesis of other calix-phosphites.²⁶ Thus, starting from a monoprotected calixarene appears to be advantageous for synthesising calix-[4]arene-based phosphites. Molecular mechanics calculations have shown that the calixarene core of *cone*-**L**¹ is significantly more strained than the hypothetical partial-cone analogue, *paco*-**L**¹.²⁹ Corroborating the observations made by Pringle *et al.* for another calixarene phosphite,²³ we found that dichloromethane solutions of **L**¹ were quite stable towards aqueous NaOH. However, **L**¹ decomposes instantly on treatment with slightly acidic water (*vide infra*).



Treatment of a dichloromethane solution of **L**¹ with aqueous NH_4Cl results in cleavage of a P-O bond and selective formation of phosphonate **3** (eqn. 2).



This compound was characterised by ^1H , ^{13}C , ^{31}P and IR spectroscopy. The phosphonate signal appears at 1.4 ppm in the ^{31}P NMR spectrum, while the PH proton gives a characteristic doublet at 6.01 ppm ($J(\text{PH}) = 792$ Hz). The ^1H NMR spectrum shows four distinct AB patterns for the ArCH_2 bridging units. All AB separations were found to be ≥ 0.7 ppm, suggesting a cone conformation. However, 2D NOESY experiments clearly indicate that a cone \rightleftharpoons partial cone exchange, as shown in Scheme 1, takes place.



Scheme 1. Proposed dynamics for compound **3**.

This was easily deduced from the number of correlations involving the two methylene groups bordering the phenol ring; indeed, both possess a CH atom correlating with two aromatic *m*-H protons of the calixarene core, while the other CH correlates with a single *m*-H (Fig. 1).

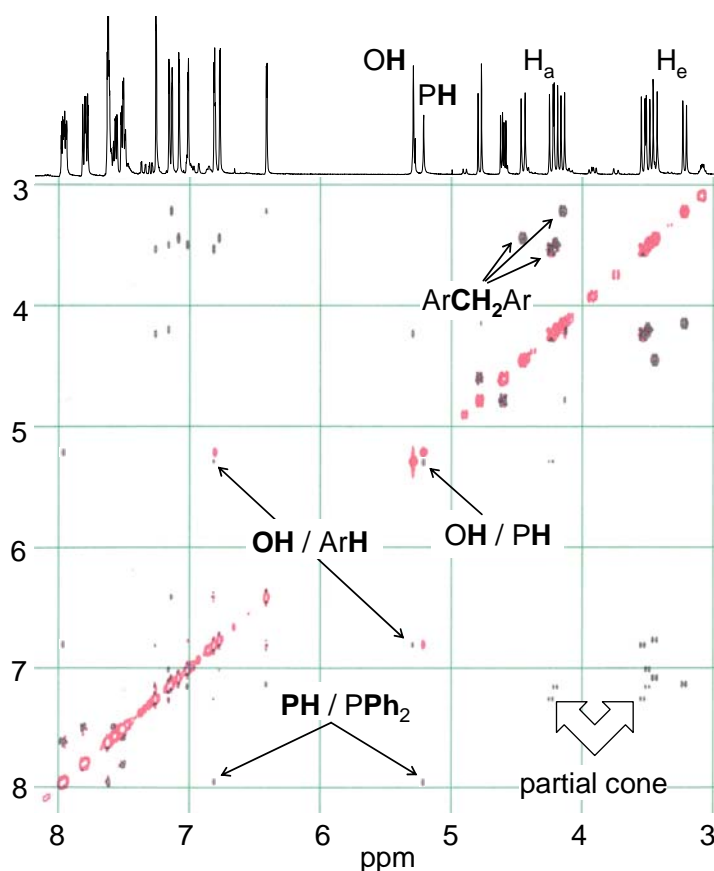
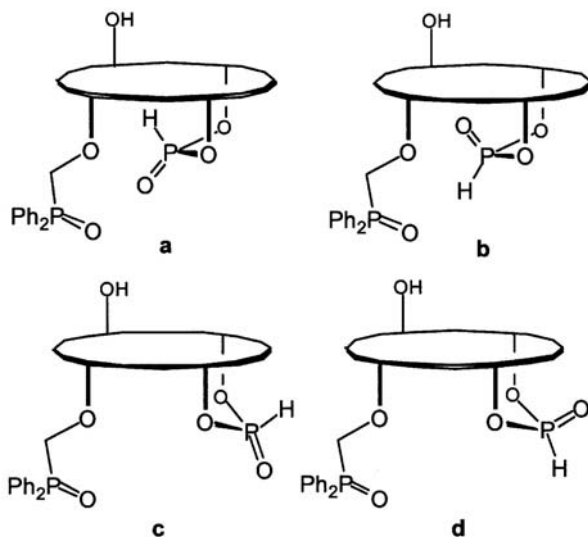


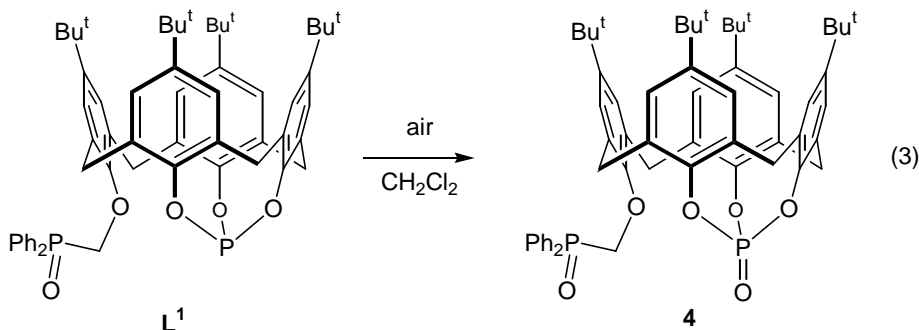
Fig. 1. ROESY spectrum of phosphonate **3** (CDCl_3).

The other two methylene groups show NOEs, exactly as expected for CH_2 groups linking *syn*-oriented aryl rings (*i.e.* the equatorial CH_e atoms correlate with two *m*-H protons, while no cross-peaks involving axial CH_a atoms are observed). The same 2D experiment also revealed a spatial proximity between the PH group and the hydroxy group, indicating that the phosphorus atom is positioned below the cavity. Finally, the 2D spectrum established a proximity between the PH group and the PPh_2 protons. These data allow assignment of structure b (Scheme 2). Note, **3** is a chiral molecule and therefore exists as a mixture of two enantiomers (not drawn).

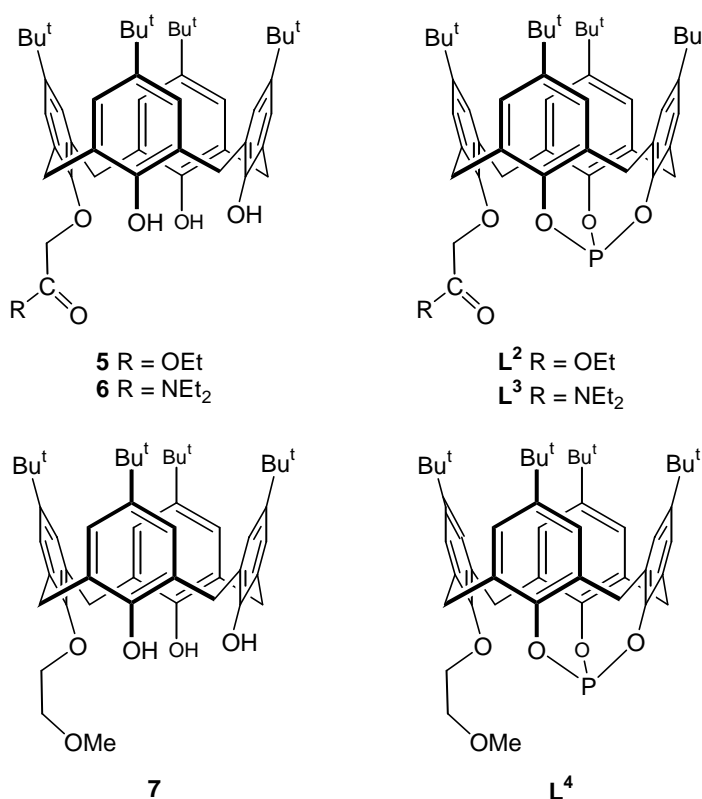


Scheme 2. The four possible orientations of the phosphonate group in *paco*-3.

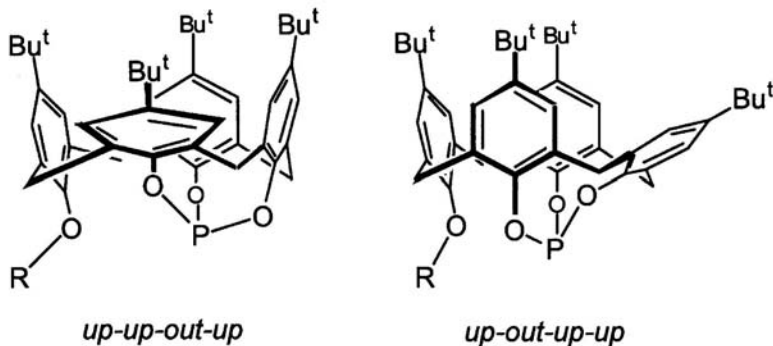
Slow oxidation occurred when a solution of **L**¹ was allowed to stand in air for several days, affording the mixed phosphine oxide-phosphate **4** (eqn. 3). The phosphate unit is characterised by a peak at -23.3 ppm in the ³¹P NMR spectrum. As expected, the IR spectrum of **4** shows a strong phosphate band near 1300 cm⁻¹ ($\nu(P=O)$).



The related ligands **L**², **L**³ and **L**⁴ were prepared by a method similar to that outlined for **L**¹, but starting from the monofunctionalised *cone*-calixarenes **5**,³⁰ **6** and **7**,³¹ respectively (see Experimental section). As for **L**¹, the three ³¹P{¹H} NMR spectra show a phosphite signal near 106 ppm and the ¹H NMR spectra are in keeping with cone conformations. The IR spectrum of **L**² displays a strong absorption band at 1760 cm⁻¹, typical for an ester function, while the amide stretch vibration of **L**³ appears at 1653 cm⁻¹.



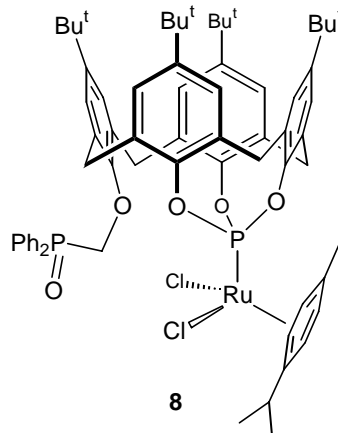
As already mentioned, the four calixarenes **L¹-L⁴** possess a conical shape. Many studies have established that, for *syn ArCH₂Ar* arrangements, the ¹³C chemical shift of the bridging methylene carbon lies between *ca.* 29 and 33 ppm, while for an *anti* arrangement, the methylene signal appears in the 37-39 ppm region.^{31,32} Interestingly, for each of the four *C_s*-symmetrical ligands described in this work, one ArCH₂ signal lies exactly between these two regions (near 36.5 ppm), while the other one appears in the range expected for *syn*-arranged ArCH₂Ar moieties (*ca.* 33 ppm). The observation of a signal with an "intermediate" chemical shift may be interpreted in terms of partial flattening of the calix core as a consequence of the strain imposed by the very short μ₃-P capping unit. Shape modification of calixarenes through μ₃-P caps has already been described in detail, including for larger calixarenes.^{23,26,33} In fact, the observed ³¹P chemical shifts, near 106 ppm, suggest that calixarenes **L¹-L⁴** adopt a so-called *up-up-out-up* rather than an *up-out-up-up* conformation (Scheme 3). As shown by van Leeuwen *et al.*, higher δ values are expected (*ca.* 116 ppm) for the latter conformation.²⁶



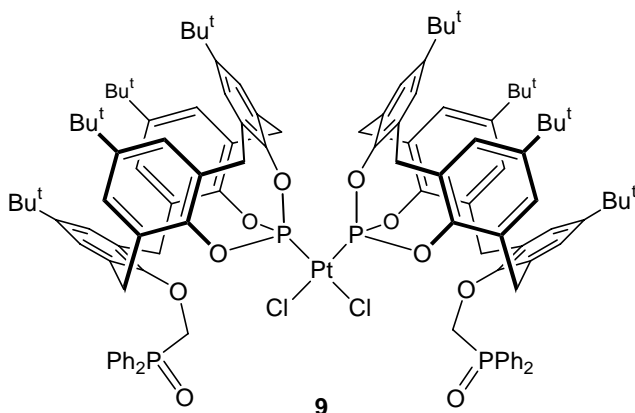
Scheme 3. The two known cone conformations of calix[4]arene phosphites.

2.2 Complexes obtained from phosphites L^1-L^3

L^1 reacts with $[\text{RuCl}_2(p\text{-cymene})]_2$ to quantitatively afford the red phosphite complex **8** characterised by a singlet at 92.6 ppm in the ^{31}P NMR spectrum. This signal is *highfield*-shifted with respect to that of free L^1 (107 ppm), but this is not unusual for coordinated phosphites.³⁴ Furthermore, no significant shift was observed for the phosphine oxide signal upon complexation, hence ruling out bonding of the phosphoryl unit.



Reaction of L^1 with $[\text{PtCl}_2(1,5\text{-cyclooctadiene})]$ afforded complex **9** in high yield. Its ^{31}P NMR spectrum shows a singlet at 32.7 ppm with the corresponding Pt satellites. The observed $J(\text{PPt})$ coupling constant, 6736 Hz, is nearly identical to the value (6629 Hz) recently reported by Pringle *et al.* for *cis*- $[\text{PtCl}_2(p\text{-ac}-2')]_2$ (**2'** is the non-butylated analogue of **2**).²³



An X-ray diffraction study (*vide infra*) confirmed the *cis* stereochemistry. Unlike that of **L**¹, the ^1H NMR spectrum of **9** shows four distinct AB patterns for the bridging methylene units, as well as an AB spectrum for the PCH_2 protons, in keeping with two calixarene subunits that are no longer C_s -symmetric. This observation reflects the important steric crowding of the two calixarene fragments, preventing the *cis*-arranged phosphites freely rotating about the MP bonds. Fig. 2 shows the solid state structure of the complex. The platinum centre has, as expected, a planar coordination environment, the metal lying only *ca.* 0.010 Å out of the least-squares P_2Cl_2 plane. The PPtP angle lies 6° over the ideal 90° value. The Pt-P bond lengths (2.218(2) and 2.224(2) Å) are comparable to those found in other $[\text{PtCl}_2(\text{phosphite})_2]$ complexes.^{35,36} Both calixarene cores adopt a cone conformation, but are highly distorted with respect to calix[4]arenes containing uncapped phenol units. Thus, as anticipated, each calixarene contains an aryl-OP ring whose orientation approaches that of the calixarene reference plane (dihedral angles 26.2(2) and 27.9(3)°), resulting in an *up-up-out-up*²⁶ conformation (Fig. 2). The fact that rotation of a particular phosphite about its Pt-P axis is hindered by the neighbouring ligand becomes obvious if one considers the spatial expansion of the ligands. The latter is particularly important in the region containing the phosphine oxide arm. For example, the P(1)-Pt-C(47) angle is 123°. Thus, virtual rotation of the ligands about their coordination axis generates a cone having an opening angle (Ω) larger than 180°, hence implying mutual steric hindrance between the phosphites. Finally, we note that both calixarene cavities contain an acetonitrile guest. This is not unusual with calix[4]arenes that are somewhat flattened.³⁷ The molecule crystallises with three further CH_3CN molecules as well as a water molecule.

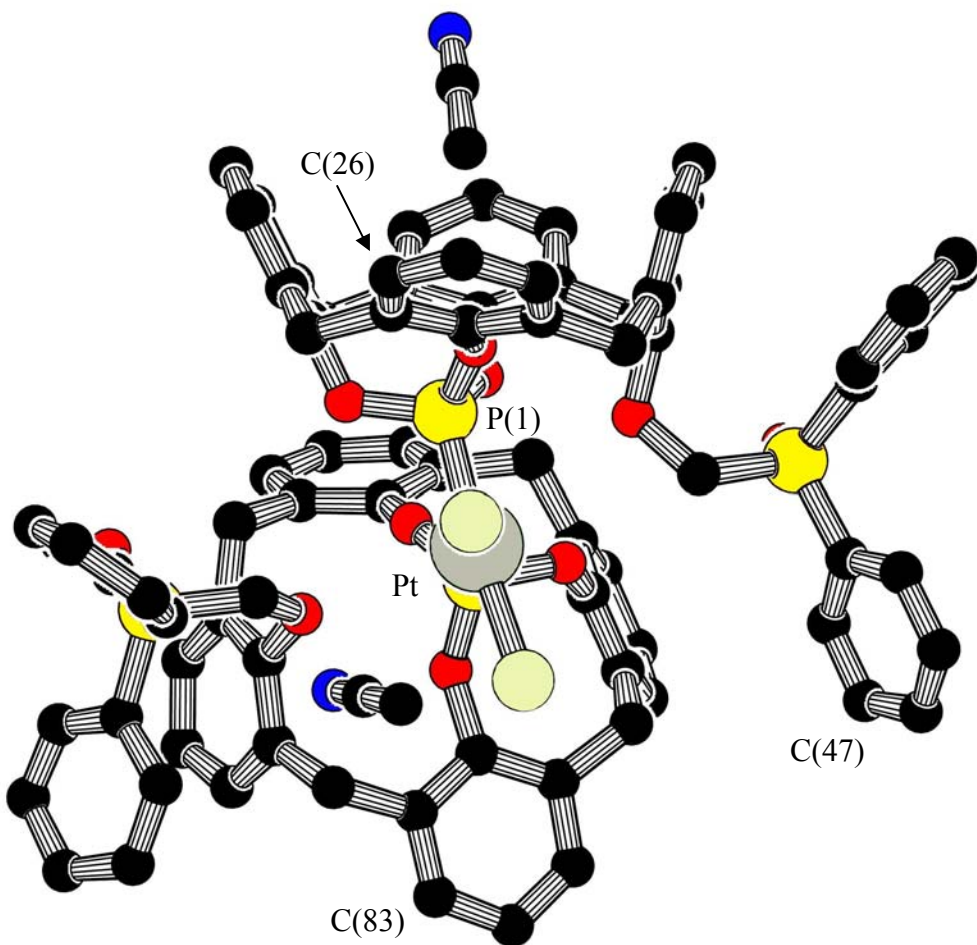
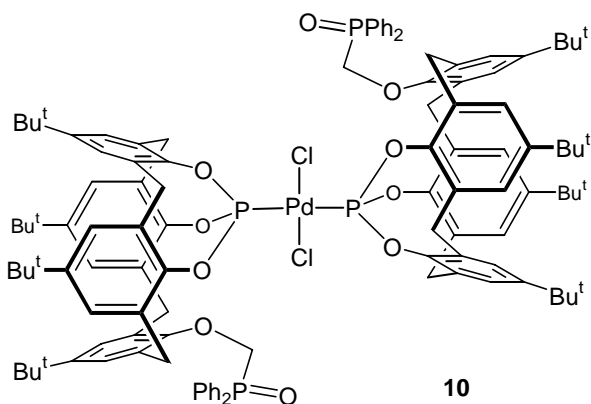
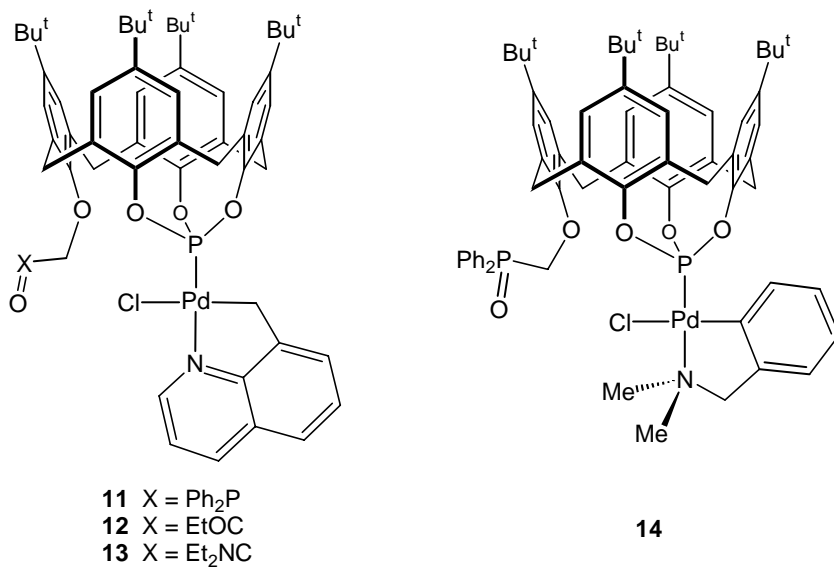


Fig. 2. Molecular structure of $\text{cis}-[\text{PtCl}_2(\mathbf{L}^1)_2]$. Each calixarene contains an acetonitrile molecule (other solvents not shown). The Bu^\ddagger groups have been omitted for clarity. The most inclined phenol units are those containing C(26) and C(83). Selected bond lengths (\AA): Pt-Cl(1) 2.342(1), Pt-Cl(2) 2.339(1), Pt-P(1) 2.217(1), Pt-P(3) 2.224(1).

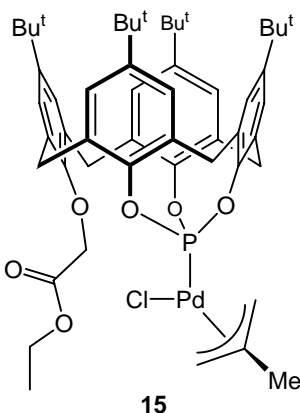
Reaction of \mathbf{L}^1 with $[\text{PdCl}_2(1,5\text{-cyclooctadiene})]$ yielded complex *trans*-**10** quantitatively. The assignment of a *trans* stereochemistry was inferred from the NMR spectra which show that the calixarene fragments retain a C_s -symmetrical structure upon complexation. Obviously, owing to the large separation between the two calixarene fragments, there is, in this case, no barrier to rotation about the M-P bond.



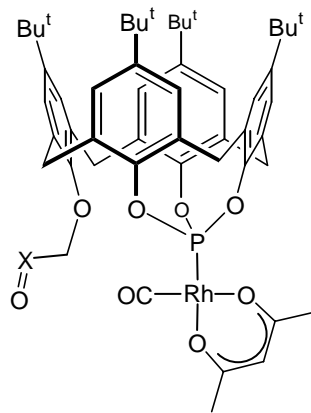
Further examples where the ligand symmetry remains unaffected upon complexation are the complexes **11-13**, obtained by reaction of $[\text{Pd}(8\text{-mq})\text{Cl}]_2$ (8-mqH = 8-methylquinoline) with **L¹**, **L²** and **L³**, respectively, and complex **14** resulting from the reaction of **L¹** with the cyclometallated Pd(II) complex $[\text{PdCl}(\text{o-C}_6\text{H}_4\text{CH}_2\text{NMe}_2)]_2$.



Reaction of **L²** with $[\text{PdCl}(\eta^3\text{-C}_4\text{H}_7)]$ afforded the allylic complex **15**. The metal plane is not a symmetry element of this molecule, hence the corresponding ^1H NMR spectrum exhibits four distinct ArCH₂Ar groups and an AB pattern for the methylenic OCH₂CO₂Et protons.

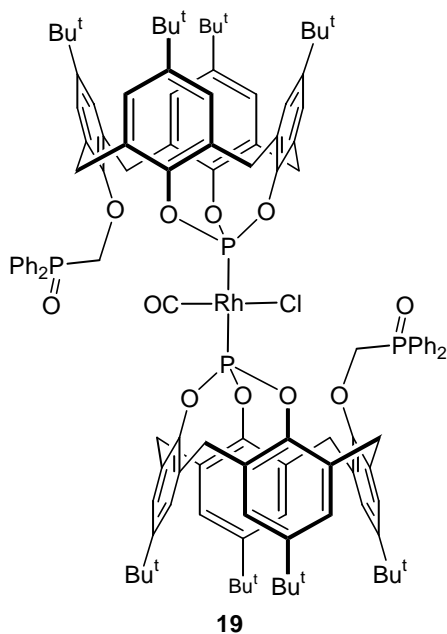


Reaction of $[\text{Rh}(\text{acac})(\text{CO})_2]$ with one equiv. of \mathbf{L}^1 - \mathbf{L}^3 gave the highly soluble complexes **16**, **17** and **18**, respectively. Phosphite bonding in these complexes was deduced from the presence of a doublet in their ^{31}P NMR spectra [$J(\text{PRh}) = \text{ca. } 305 \text{ Hz}$]. The corresponding IR spectra show a strong $\nu(\text{CO})$ carbonyl band near 2000 cm^{-1} .

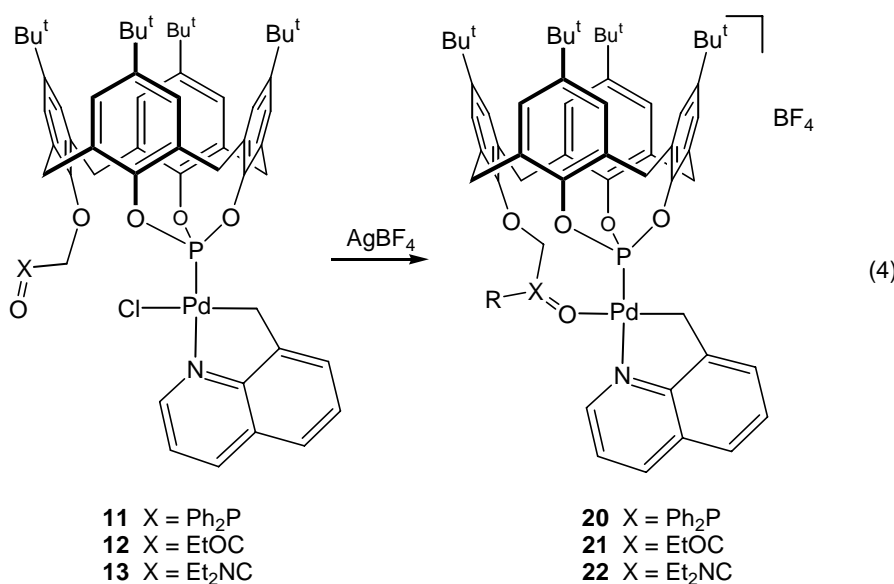


16 $X = \text{Ph}_2\text{P}$
17 $X = \text{EtOC}$
18 $X = \text{Et}_2\text{NC}$

The bis-phosphite **19** was obtained in high yield by reaction of $[\text{RhCl}(\text{CO})_2]_2$ with 4 equiv. of \mathbf{L}^1 . Characterisation data are reported in the Experimental section. It is worth mentioning here that small amounts of **19** were formed in hydroformylation experiments (*vide infra*) when using insufficiently purified samples of \mathbf{L}^1 , *i.e.* containing residual amounts of NEt_3HCl .



In order to force bonding of the auxiliary groups, the three complexes **11-13** were treated with silver tetrafluoroborate (eqn. 4). These reactions afforded the cationic complexes **20-22**, respectively, which were authenticated by elemental analysis and mass and multinuclear NMR spectroscopies. Coordination of the carbonyl functions of **21** and **22** was inferred from their IR spectra. Thus, the $\nu(\text{C}=\text{O})$ stretching vibrations of these two complexes are lowered by more than 50 cm^{-1} when compared to the corresponding starting complexes, **12** and **13**, respectively. In the ^{31}P NMR spectrum of complex **20**, the phosphine oxide signal underwent a downfield shift of *ca.* 5 ppm upon complexation, in accord with bonding of the phosphoryl fragment. Owing to the presence of broad calixarene bands in the $\nu(\text{P}=\text{O})$ region, we were unable to confirm by IR the coordination of the phosphoryl unit.



The ultimate proof for chelate formation in complex **22** came from a single crystal X-ray diffraction study. The molecular structure of the complex is shown in Fig. 3. Again, the calixarene core adopts an *up-up-out-up* cone conformation ("out" refers to the phenol ring bearing O(3)), but the deviation from a typical cone is more pronounced than in **9**, as revealed by the dihedral angle of only 10° between the O(3) phenol ring and the calix reference plane. The coordination plane is strongly inclined with respect to the calix reference plane (dihedral angle *ca.* 68°). All metal-ligand bond distances are normal, but, as frequently observed in chelate complexes, the palladium stereochemistry deviates somewhat from an ideal square planar coordination geometry. Thus, the P-Pd-O angle is 7° greater than 90° , reflecting the strain imposed on the P,O-chelate by amide coordination. In fact, Pd-O bond formation forces the amide plane to be nearly perpendicular to the coordination plane, so as to optimise overlap of an oxygen lone pair with the in-plane metal d-orbital. Incidentally, the particular orientation of the amide induces an increased distortion of the calixarene shape, as revealed by the strong inclination of the O(5) phenol plane with respect to the calix reference plane (dihedral angle *ca.* 80° vs. 61° for the O(1) phenol plane).

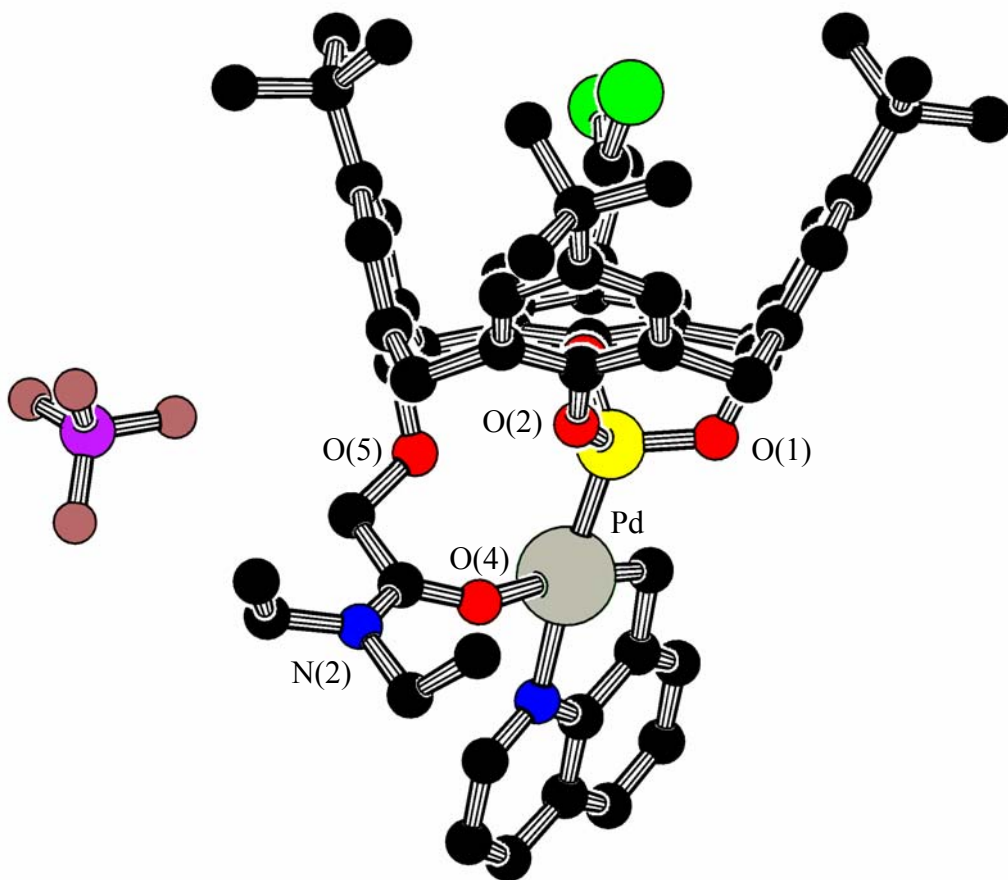
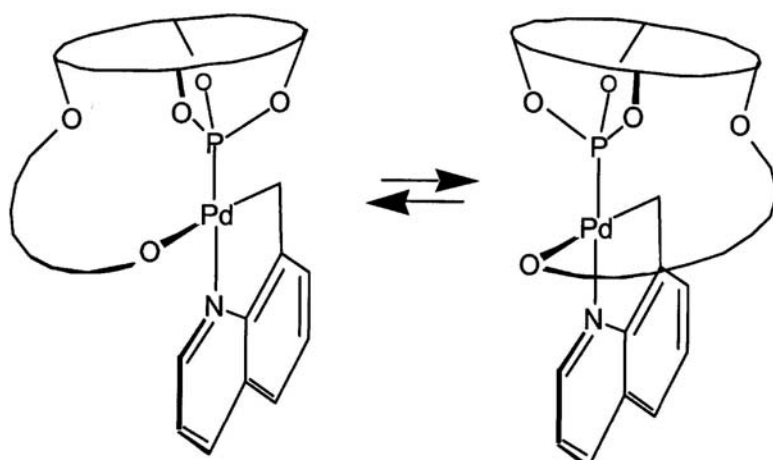


Fig. 3. Molecular structure of the chelate complex **22**. The calixarene contains a CH_2Cl_2 guest. The O(3) atom is opposite to O(2). Selected bond lengths (\AA): Pd-N(1) 2.089(3), Pd-O(4) 2.148(3), Pd-P 2.2041(11).

Complex **22** displays an apparent C_s symmetry in solution, in keeping with the dynamics shown in Scheme 4, in which the chelate loop rapidly swings from one side of the metal plane to the other. This motion implies restricted rotation of the two chelate ends about the Pd-P and Pd-O(4) bonds, respectively, as well as a structural rearrangement of the calixarene core, rendering the O(2) and O(3) phenol rings equivalent on the NMR timescale. It is noteworthy that equilibrating *up-up-out-up/out-up-up-up* conformations of calix[4]arenes have already been evidenced by van Leeuwen *et al.*²⁶ It appears very plausible that this fluxionality induces the displacement of the amide arm from one side of the coordination plane to the other. As verified by IR spectroscopy (in CH_2Cl_2 and CH_3CN), there is no amide labilisation during this process, ruling out hemilabile³⁸ ligand behaviour.



Scheme 4. Swinging of the P-O(amide) loop from one side of the metal plane to the other.

2.3 *Hydroformylation with heterodifunctional calix phosphites*

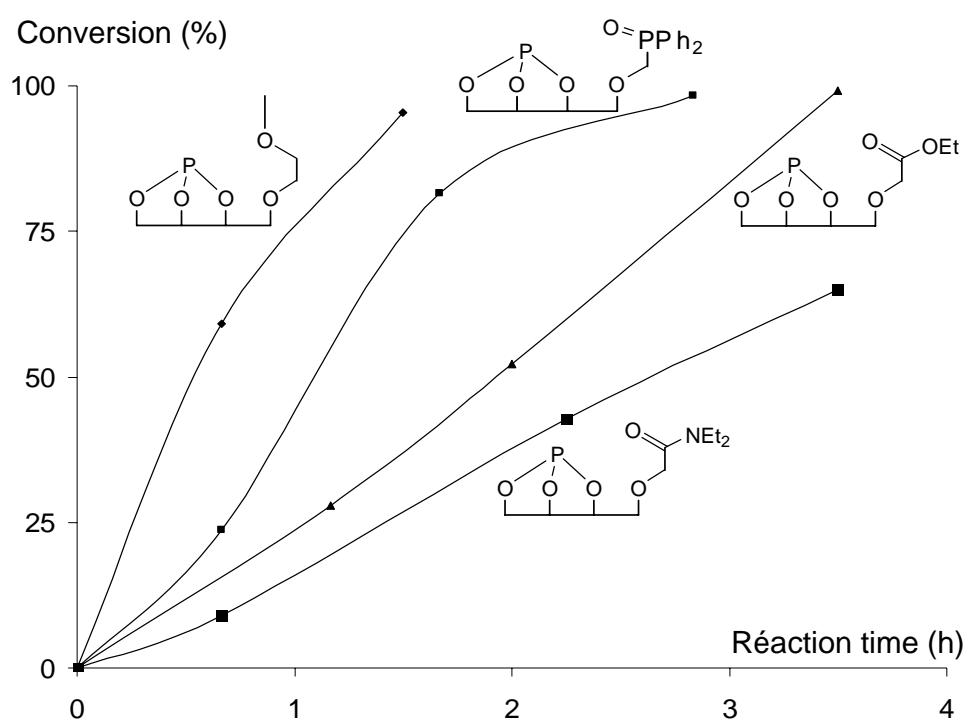
In the present study, 1-octene was hydroformylated in toluene at 80 °C under 22 bar CO-H₂ pressure (initial pressure at 80 °C). The phosphite:metal:substrate ratio was 10:1:5000. The results obtained for the four phosphites are summarised in Table 1 and Fig. 4. It should be emphasised that these experiments were carried out with rigorously pure samples of phosphites, free of NEt₃HCl in particular. The presence of the latter in ligand samples resulted in the formation of undesirable side products, *e.g.* **19** (when starting from **L¹**).

As expected for bulky phosphites, the reaction rates were higher than those observed using P(OPh)₃. The higher activity is generally explained by a lower number of coordinated phosphites. The fastest catalysis occurred with the ether phosphite **L⁴**. The corresponding activity (TOF *ca.* 4500) is, however, 1.6 times lower than that recently reported by van Leuwen *et al.* for the related phosphite **23** bearing an ⁱPr group instead of -CH₂CH₂OMe. For comparison, the TOF found for PPh₃ under similar conditions is 2200 (L/B = 2.8), while the highest rates reported to date were those for the bulky phosphite **24** (*ca.* 40 000 mol.mol(Rh)⁻¹.h⁻¹; L/B = 1.9).³⁹

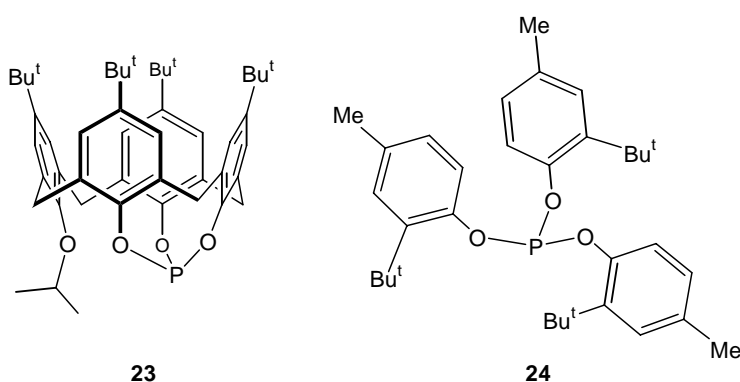
Table 1. Hydroformylation of 1-octene with calixarene phosphites^a.

Ligand	TOF ^b	L/B ^c	L/all products ^d (%)	Isomerisation ^e (%)
PPh ₃	2200	2.8		1.5
P(OPh) ₃	—	2.8 ^f		—
Alkylphosphite 23	7300	1.4	54	6
Ether phosphite L ⁴	4400	1.4	53	3.5
PV(O)-phosphite L ¹	2450	2.4	58	11.2
Ester phosphite L ²	1300	3.6	57	9.6
Amide phosphite L ³	950	2.7	57	13.6

^a Conditions: L/Rh = 10, 1-octene/Rh = 5000, [Rh] = ca. 0.11 mM, initial pressure (at 20 °C) P = 20 bar CO-H₂ (1:1), T = 80 °C, toluene-*n*-decane (15 cm³, 0.5 cm³). ^b Turnover frequency, determined at *ca.* 30% conversion. ^c The L/B ratio takes into account all possible branched aldehydes. ^d At *ca.* 95% conversion. ^e Isomerised 1-octene/all octenes. ^f At 40 bar. See also Experimental section.

**Fig. 4.** Conversion of 1-octene as a function of time using phosphites **L**¹-**L**⁴.

Interestingly, the activity decreases in the order **L⁴** > **L¹** > **L²** > **L³**, that is, with increasing donor strength of the oxygen-containing side group. The aldehyde selectivity also changes significantly, those of ligands **L¹-L³** being higher than those observed for **23** and **L⁴**. The reason for these variations is a matter for discussion. A logical explanation for an activity decrease is that conformational changes within the calixarene backbone occur during catalysis which incidentally changes the electronic and steric properties of the ligand. Such a shape modification appears, however, questionable since ligands **23** and **L⁴** have similar structures but different activities. Note in particular that both ligands adopt an *up-up-out-up* conformation, at least at room temperature.²⁶ The observed changes could also arise from the formation of P,O-chelate [‡] complexes during catalysis. Indeed, it should be recalled that, as shown by Lindner and Norz, ether phosphines may act as transient chelate ligands when used in methanol carbonylation.¹⁷ Furthermore, Alper *et al.* recently established that phosphine oxides may coordinate to rhodium centres during olefin hydroformylation.⁴⁰ Note that the L/B variation (Table 1) does not rigorously parallel the donor strength of the side group (ether < phosphine oxide < ester < amide). The reason why ester **L²** gives a higher L/B ratio than amide **L³** (the amide is a stronger donor than the ester group) remains unclear and suggests that other factors (probably steric) have to be taken into account. At the end of the catalytic runs performed with **L¹**, the reaction mixture contained, beside unmodified **L¹**, trace amounts of compounds **3** and **4**.



[‡] Molecular mechanics calculations show that for a hypothetical chelate complex [RhH(CO)₂(P-O)] with tbp structure, the bis-equatorial P,O-coordination (ee) is favoured over equatorial apical (ae) coordination.²⁹ For this calculation, the calixarene was maintained in an *up-up-out-up* conformation.

3 Conclusion

In the present study we have described the high yield synthesis of four new heterofunctionalised P,O-phosphites based on a calix[4]arene backbone. The mixed phosphine oxide–phosphite **L¹** is stable towards aqueous NaOH, but decomposes instantly in the presence of slightly acidic water. All calixarenes adopt a cone conformation, making the phosphites potential chelating systems. The ability to behave as a P,O-chelate was unambiguously demonstrated for three of them, **L¹-L³**, which form 12-membered palladacycles with the "Pd(8-mq)⁺" unit. In the latter complexes, the chelating P,O-loop swings from one side of the metal plane to the other, the whole dynamics possibly being facilitated by the flexibility of the calixarene. In keeping with their steric crowding, the rates of hydroformylation for the ligands are higher than those observed for P(OPh)₃, but remain lower than that found for the bulky phosphite P{O(2-Bu^t,4-MeC₆H₃)₃}. The activity decreases with the donor strength of the oxo side group, suggesting that, during catalysis, P,O-chelates are formed. Furthermore, with the "good" O-donors, the L/B ratios are significantly higher than with the ether phosphite **L⁴**. However, the observed selectivities cannot be explained solely in terms of the donor properties of the side group and further experiments, including IR studies under CO/H₂, with other heterofunctionalised phosphites need to be performed to ascertain the reasons for these observations.

4 References

1. A. Bader and E. Lindner, *Coord. Chem. Rev.*, 1991, **108**, 27.
2. C. S. Slone, D. A. Weinberger and C. A. Mirkin, *Prog. Inorg. Chem.*, 1999, **48**, 233.
3. E. Engeldinger, D. Armsbach and D. Matt, *Angew. Chem., Int. Ed.*, 2001, **40**, 2526.
4. J. Holz, M. Quirmbach and A. Börner, *Synthesis*, 1997, **9**, 983.
5. A. M. Z. Slawin, J. D. Woollins and Q. Zhang, *J. Chem. Soc., Dalton Trans.*, 2001, 621.
6. P. Braunstein, J. Fischer, D. Matt and M. Pfeffer, *J. Am. Chem. Soc.*, 1984, **106**, 410.
7. W. Keim, F. H. Kowaldt, R. Goddard and C. Krüger, *Angew. Chem., Int. Ed. Engl.*, 1978, **17**, 466.
8. D. Matt, M. Huhn, J. Fischer, J. De Cian, W. Kläui, I. Tkatchenko and M. C. Bonnet, *J. Chem. Soc., Dalton Trans.*, 1993, 1173.
9. D. Matt, M. Huhn, M. C. Bonnet, I. Tkatchenko, U. Englert and W. Kläui, *Inorg. Chem.*, 1995, **34**, 1288.
10. B. Cornils and W. A. Herrmann, *Aqueous Homogeneous Catalysis with Organometallic Compounds*, ed. B. Cornils and W. A. Herrmann, Wiley-VCH, Weinheim, 1998.
11. T. Hosokawa, Y. Wakabayashi, K. Hosokawa, T. Tsuji and S.-I. Murahashi, *Chem. Commun.*, 1996, 859.
12. (a) P. Braunstein, D. Matt, F. Mathey and D. Thavard, *J. Chem. Res.*, 1978, (S) 232-233; (b) P. Braunstein, D. Matt, F. Mathey and D. Thavard, *J. Chem. Res.*, 1978, (M) 3041-3063.
13. J. C. Jeffrey and T. B. Rauchfuss, *Inorg. Chem.*, 1979, **18**, 2658.
14. P. Steinert and H. Werner, *Chem. Ber.*, 1997, **130**, 1591.
15. H. Yang, M. Alvarez-Gressier, N. Lugan and R. Mathieu, *Organometallics*, 1997, **16**, 1401.
16. C. S. Slone, C. A. Mirkin, G. P. A. Yap, I. A. Guzei and A. L. Rheingold, *J. Am. Chem. Soc.*, 1997, **119**, 10743.

17. E. Lindner and H. Norz, *Chem. Ber.*, 1990, **123**, 459.
18. D. Selent, K.-D. Wiese, D. Röttger and A. Börner, *Angew. Chem., Int. Ed.*, 2000, **39**, 1639.
19. M. Hariharasarma, C. H. Lake, C. L. Watkins and G. M. Gray, *J. Organomet. Chem.*, 1999, **580**, 328.
20. L. A. Barg, R. W. Byrn, M. D. Carr, D. H. Nolan, B. N. Storhoff and J. C. Huffman, *Organometallics*, 1998, **17**, 1340.
21. C. Roch-Neirey, N. Le Bris, P. Laurent, J.-C. Clément and H. des Abbayes, *Tetrahedron Lett.*, 2001, **42**, 643.
22. D. V. Khasnis, M. Lattman and C. D. Gutsche, *J. Am. Chem. Soc.*, 1990, **112**, 9422.
23. C. J. Cobley, D. D. Ellis, A. G. Orpen and P. G. Pringle, *J. Chem. Soc., Dalton Trans.*, 2000, 1101.
24. C. J. Cobley, D. D. Ellis, A. G. Orpen and P. G. Pringle, *J. Chem. Soc., Dalton Trans.*, 2000, 1109.
25. F. J. Parlevliet, M. A. Zuideveld, C. Kiener, H. Kooijman, A. L. Spek, P. C. J. Kamer and P. W. N. M. van Leeuwen, *Organometallics*, 1999, **18**, 3394.
26. F. J. Parlevliet, C. Kiener, J. Fraanje, K. Goubitz, M. Lutz, A. L. Spek, P. C. J. Kamer and P. W. N. M. van Leeuwen, *J. Chem. Soc., Dalton Trans.*, 2000, 1113.
27. R. Paciello, L. Siggel and M. Röper, *Angew. Chem., Int. Ed.*, 1999, **38**, 1920.
28. C. B. Dieleman, D. Matt and P. G. Jones, *J. Organomet. Chem.*, 1997, **545-546**, 461.
29. MACSPARTAN, version 1.1.8, Wavefunction, Inc., Irvine, CA, USA, 1998.
30. L. C. Groenen, B. H. M. Ruël, A. Casnati, W. Verboom, A. Pochini, R. Ungaro and D. N. Reinhoudt, *Tetrahedron*, 1991, **47**, 8379.
31. C. Jeunesse, C. Dieleman, S. Steyer and D. Matt, *J. Chem. Soc., Dalton Trans.*, 2001, 881.
32. C. Jaime, J. de Mendoza, P. Prados, P. M. Nieto and C. Sánchez, *J. Org. Chem.*, 1991, **56**, 3372.
33. J. Gloede, S. Ozegowski, D. Matt and A. De Cian, *Tetrahedron Lett.*, 2001, **42**, 9139.
34. C. Cobley and P. G. Pringle, *Inorg. Chim. Acta*, 1997, **265**, 107.
35. A. Crispini, K. N. Harrison, A. G. Orpen, P. G. Pringle and J. R. Wheatcroft, *J.*

- Chem. Soc., Dalton Trans.*, 1996, 1069.
- 36. S. Cserépi-Szücs, G. Huttner, L. Zsolnai and J. Bakos, *J. Organomet. Chem.*, 1999, **586**, 70.
 - 37. M. Baaden, G. Wipff, M. Burgard and D. Matt, *J. Chem. Soc., Perkin Trans 2*, 2000, 1315-1321.
 - 38. P. Braunstein and F. Naud, *Angew. Chem., Int. Ed.*, 2001, **40**, 680.
 - 39. A. van Rooy, E. N. Orij, P. C. J. Kamer and P. W. N. M. van Leeuwen, *Organometallics*, 1995, **14**, 34.
 - 40. H. J. Clark, R. Wang and H. Alper, *J. Org. Chem.*, 2002, **67**, 6224.
 - 41. OpenMoleN, Interactive Structure Solution, Nonius B.V., Delft, The Netherlands, 1997.
 - 42. G. M. Sheldrick, SHELX-97, Program for the Refinement of Crystal Structures, University of Göttingen, Germany, 1997.

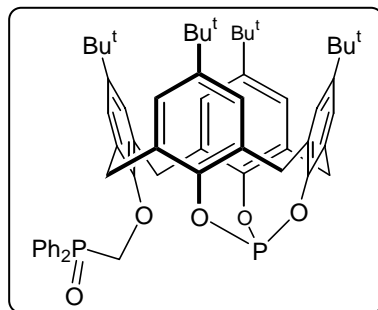
5 Experimental

5.1 General procedures

Unless otherwise stated, materials were obtained from commercial suppliers and used without further purification. Solvents were dried over suitable reagents and freshly distilled under dry nitrogen before use. CDCl_3 was passed through a 5 cm thick alumina column and stored under N_2 over molecular sieves (4 Å). All reactions were carried out using modified Schlenk tube techniques under a dry nitrogen atmosphere. IR spectra were recorded on a Perkin-Elmer 1600 spectrometer ($4000\text{-}400 \text{ cm}^{-1}$). Routine ^1H , $^{13}\text{C}\{^1\text{H}\}$ and $^{31}\text{P}\{^1\text{H}\}$ NMR spectra were recorded on Bruker AC-200 (^1H : 200.1 MHz; ^{13}C : 50.3 MHz), AC-300 (^1H : 300.1 MHz; ^{31}P : 121.5 MHz) and ARX-500 (^1H : 500.1 MHz) spectrometers. The 2D (^1H - ^1H NOESY and ROESY) NMR spectra were recorded on a Bruker ARX-500 using a standard pulse sequence and Bruker software for treatment of the acquired data. Proton chemical shifts are reported relative to residual protiated solvents (CHCl_3 , δ 7.26). The ^{13}C chemical shifts are referenced relative to deuterated solvents (CDCl_3 , δ 77.00) and the ^{31}P NMR data are given relative to external H_3PO_4 . A positive sign denotes a value downfield from the reference. Abbreviations used are s = singlet, d = doublet, t = triplet, q = quartet, br = broad. The mass spectra were recorded on a ZAB HF VG analytical spectrometer using m-nitrobenzyl alcohol as a matrix. For column chromatography, Geduran SI (E. Merck, 0.040-0.063 mm) was used. Routine thin layer chromatographic analyses were carried out using plates coated with Merck Kieselgel 60 GF₂₅₄. Elemental analyses were performed by the Service de Microanalyse, Centre de Recherche Chimie, Université Louis Pasteur, Strasbourg. Melting points were determined with a Büchi 535 capillary melting point apparatus and are uncorrected. The abbreviation 8-mq stands for the 8-methyl-quinolinyl fragment.

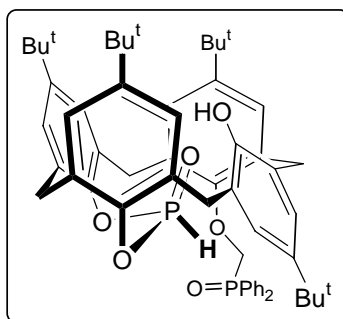
5.2 Syntheses

5,11,17,23-Tetra-*tert*-butyl-25-(diphenylphosphinoyl-methoxy)-26,27,28-(μ_3 -phosphorustrioxo)calix[4]arene (L^1).



To a cold (-40 °C) solution of 1 (1.000 g, 1.16 mmol) in a NEt₃-toluene mixture (2 cm³, 14.35 mmol NEt₃; 100 cm³ toluene) was added dropwise a solution of PCl₃ (0.1 cm³, 1.16 mmol) in toluene (5 cm³) maintained at *ca.* -40 °C. The mixture was then heated at 80 °C for 20 h. The NEt₃HCl salt formed was removed by filtration, first through a bed of Celite, then through a 2 cm layer of SiO₂ and finally washed with cold toluene (2 × 10 cm³). Filtration over SiO₂ was required for complete removal of the ammonium salt. The filtrate and washing solutions were evaporated under vacuum. Drying under vacuum for 2 h is sufficient for complete removal of the remaining amine. Yield: 1.000 g, 1.12 mmol, 97%. Mp 105 °C. IR (KBr) $\nu_{\text{max}}/\text{cm}^{-1}$: 1194 (s, P=O, tentative assignment). ¹H NMR (500 MHz, CDCl₃): δ 8.11-8.07 and 7.45-7.37 (10 H, P(O)Ph₂), 7.10 and 7.01 (AB q, ⁴J = 2.5 Hz, 2H each, *m*-ArH), 7.02 (s, 2H, *m*-ArH), 6.66 (s, 2H, *m*-ArH), 4.58 (d, ²J = 7.7 Hz, 2H, P(O)CH₂), 4.38 and 3.45 (AB q, ²J = 14.7 Hz, 4H, ArCH₂Ar), 4.11 and 3.34 (AB q, ²J = 14.4 Hz, 4H, ArCH₂Ar), 1.36 (s, 18H, C(CH₃)₃), 1.16 (s, 9H, C(CH₃)₃), 0.86 (s, 9H, C(CH₃)₃). ¹³C{¹H} NMR (50 MHz, CDCl₃): δ 153.38-124.56 (aryl C), 73.48 (d, J(PC) = 83 Hz, P(O)CH₂), 36.42 (s × 2, ArCH₂Ar), 34.23 (s, C(CH₃)₃), 34.03 (s × 2, C(CH₃)₃), 33.86 (s, C(CH₃)₃), 33.11 (s × 2, ArCH₂Ar), 31.42 (s × 3, C(CH₃)₃), 30.94 (s, C(CH₃)₃). ³¹P{¹H} NMR (121 MHz, CDCl₃): δ 107.0 (s, P(OAr)₃), 26.1 (s, P(O)Ph₂). Found: C, 76.04; H, 7.44; calc. for C₅₇H₆₄O₅P₂·H₂O (M_r = 900.07): C, 76.06; H, 7.28%.

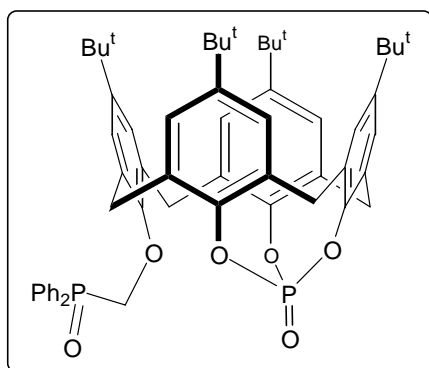
Racemic mixture of 5,11,17,23-tetra-*tert*-butyl-25-(diphenylphosphinoylmethoxy)-(μ_2 -26,27-phosphonato)-28-hydroxycalix-[4]arene and 5,11,17,23-tetra-*tert*-butyl-25-(diphenylphosphinoylmethoxy)-26-hydroxy-(μ_2 -27,28-phosphonato)-calix[4]arene (3**).**



A solution of **L¹** (1.000 g, 1.13 mmol) in CH₂Cl₂ (20 cm³) was shaken in the presence of a 0.1 M solution of NH₄Cl in water (20 cm³). After 0.5 h, the organic component was separated and washed twice with water (2 × 10 cm³). The organic phase was then dried over MgSO₄. After filtration, the solution was evaporated to dryness. Recrystallisation from CH₂Cl₂-pentane at -78 °C afforded **3** as a white, analytically pure solid. Yield: 0.803 g, 0.88 mmol, 78%. Mp 175-182 °C. IR (KBr) $\nu_{\text{max}}/\text{cm}^{-1}$: 1194 (P=O, tentative assignment). ¹H NMR (500 MHz, CDCl₃): δ 8.00-7.93, 7.83-7.77 and 7.64-7.33 (10H, P(O)Ph₂), 7.27 and 7.16 (AB q, ⁴J = 2.2 Hz, 2H, m-ArH), 7.14 and 7.08 (AB q, ⁴J = 2.0 Hz, 2H, m-ArH), 7.02 and 6.42 (AB q, ⁴J = 2.2 Hz, 2H, m-ArH), 6.82 and 6.77 (AB q, ⁴J = 2.4 Hz, 2H, m-ArH), 6.01 (d, J(PH) = 792 Hz, 1H, P(OAr)₂(O)H), 5.27 (s, 1H, OH, exchanges with D₂O), 4.79 and 4.60 (ABX system with X = P, ²J_{AB} = 13.2 Hz, ²J_{AX} = 7.6 Hz, ²J_{BX} = 0 Hz, 2H, P(O)CH₂), 4.47 and 3.45 (AB q, ²J = 14.7 Hz, 2H, ArCH₂Ar), 4.25 and 3.54 (AB q, ²J = 14.0 Hz, 2H, ArCH₂Ar), 4.20 and 3.50 (AB q, ²J = 14.0 Hz, 2H, ArCH₂Ar), 4.16 and 3.22 (AB q, ²J = 14.4 Hz, 2H, ArCH₂Ar), 1.33 (s, 9H, C(CH₃)₃), 1.25 (s, 9H, C(CH₃)₃), 1.06 (s, 9H, C(CH₃)₃), 0.84 (s, 9H, C(CH₃)₃). ¹³C{¹H} NMR (50 MHz, CDCl₃): δ 152.98-125.06 (aryl C), 73.92 (d, J(PC) = 82 Hz, P(O)CH₂), 35.83 (s × 2, ArCH₂Ar), 34.19 (s, C(CH₃)₃), 34.03 (s, ArCH₂Ar), 33.93, 33.83, 33.76 (s × 3, C(CH₃)₃), 33.53 (s, ArCH₂Ar), 31.60, 31.40, 31.11, 30.79 (s × 4, C(CH₃)₃). ³¹P{¹H} NMR (121 MHz, CDCl₃): δ 25.8 (s, P(O)Ph₂), 1.4 (s, P(OAr)₂(O)H). ³¹P NMR (121 MHz, CDCl₃): δ 25.9 (br s, P(O)Ph₂), 1.4 (d, J(PH) = 792 Hz,

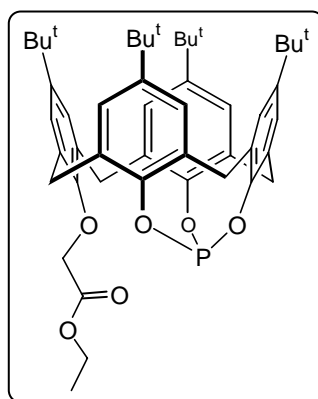
$\text{P(OAr)}_2(\text{O})\text{H}$. Found: C, 75.12; H, 7.48; calc. for $\text{C}_{57}\text{H}_{64}\text{O}_6\text{P}_2$ ($M_r = 909.08$): C, 75.31; H, 7.44%.

5,11,17,23-Tetra-*tert*-butyl-25-(diphenylphosphinoylmethoxy)-26,27,28-(μ_3 -phosphato)-calix[4]arene (4).



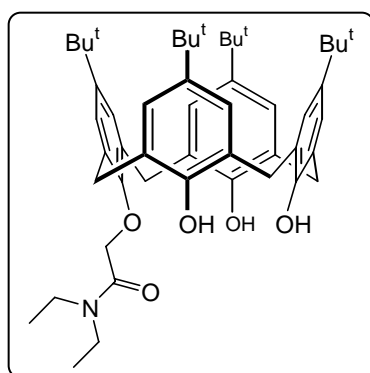
A CH_2Cl_2 -ethanol solution (1:1, v/v, 50 cm³) of **L**¹ (3.000 g, 3.37 mmol) was left standing in air for 4 days. The solvent was then evaporated and the residue was subjected to flash chromatography using AcOEt-hexane (40:60, v/v) as eluent. Unreacted **L**¹ eluted first ($R_f = 0.50$, AcOEt-hexane, 40:60, v/v) followed by **4** ($R_f = 0.30$, AcOEt-hexane, 40:60, v/v). Analytically pure **4** (white solid) was obtained by recrystallisation in CH_2Cl_2 -pentane. Yield: 0.600 g, 0.66 mmol, 19%. Mp > 240 °C. IR (KBr) $\nu_{\text{max}}/\text{cm}^{-1}$: 1307 (s, P=O_{phosphate}), 1187 (s, P=O_{phosphine oxide}, tentative assignment). ¹H NMR (300 MHz, CDCl_3): δ 8.37-8.31 and 7.50-7.48 (10 H, $\text{P}(\text{O})\text{Ph}_2$), 7.10 and 7.06 (AB q, ⁴*J* = 2.2 Hz, 4H, *m*-ArH), 7.06 (s, 2H, *m*-ArH), 6.48 (s, 2H, *m*-ArH), 4.55 (d, ²*J* = 7.7 Hz, 2H, $\text{P}(\text{O})\text{CH}_2$), 4.53 and 3.51 (AB q, ²*J* = 14.6 Hz, 4H, ArCH₂Ar), 4.24 and 3.27 (AB q, ²*J* = 14.8 Hz, 4H, ArCH₂Ar), 1.35 (s, 18H, $\text{C}(\text{CH}_3)_3$), 1.15 (s, 9H, $\text{C}(\text{CH}_3)_3$), 0.71 (s, 9H, $\text{C}(\text{CH}_3)_3$). ¹³C{¹H} NMR (50 MHz, CDCl_3): δ 155.11-124.72 (aryl C), 74.08 (d, *J*(PC) = 84 Hz, $\text{P}(\text{O})\text{CH}_2$), 35.36 (s × 2, ArCH₂Ar), 34.38 (s, $\text{C}(\text{CH}_3)_3$), 34.16 (s × 2, $\text{C}(\text{CH}_3)_3$), 33.76 (s, $\text{C}(\text{CH}_3)_3$), 32.31 (s × 2, ArCH₂Ar), 31.36 (s × 3, $\text{C}(\text{CH}_3)_3$), 30.82 (s, $\text{C}(\text{CH}_3)_3$). ³¹P{¹H} NMR (121 MHz, CDCl_3): δ 24.9 (s, $\text{P}(\text{O})\text{Ph}_2$), -23.3 (s, $\text{P}(\text{O})(\text{OAr})_3$). Found: C, 75.67; H, 7.35; calc. for $\text{C}_{57}\text{H}_{64}\text{O}_6\text{P}_2$ ($M_r = 907.06$): C, 75.48; H, 7.11%.

5,11,17,23-Tetra-*tert*-butyl-25-(ethoxycarbonylmethoxy)-26,27,28-(μ_3 -phosphorus-trioxy)calix[4]arene (\mathbf{L}^2).



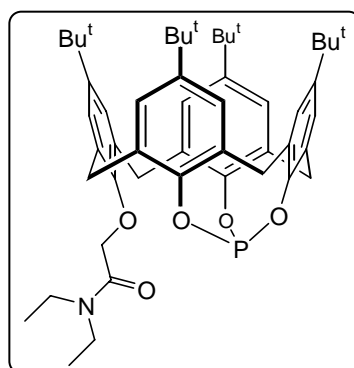
PCl_3 (0.17 cm³, 1.94 mmol) was added dropwise to a solution of 5 (1.420 g, 1.93 mmol) and NEt_3 (2.0 cm³, 14.35 mmol) in toluene (100 cm³). The mixture was stirred at room temperature for 4 days. The NEt_3HCl salt formed was filtered off using a bed of Celite and washed with toluene (2 × 10 cm³). The filtrate and washing solutions were evaporated under vacuum. Analytically pure \mathbf{L}^2 was obtained as a white solid by recrystallisation from CH_2Cl_2 -methanol at -78 °C. Yield: 0.984 g, 1.29 mmol, 67%. Mp > 240 °C. IR (KBr) $\nu_{\text{max}}/\text{cm}^{-1}$: 1760 (m s, C=O). ^1H NMR (300 MHz, CDCl_3): δ 7.17-7.10 (m, 4H, *m*-ArH), 7.04 (s, 2H, *m*-ArH), 6.77 (s, 2H, *m*-ArH), 4.73 and 3.56 (AB q, $^2J = 14.4$ Hz, 4H, ArCH₂Ar), 4.56 (s, 2H, OCH₂CO₂), 4.39 and 3.44 (AB q, $^2J = 14.3$ Hz, 4H, ArCH₂Ar), 4.25 (q, $^3J = 7.1$ Hz, 2H, CH₂CH₃), 1.36 (s, 18H, C(CH₃)₃), 1.30 (t, $^3J = 7.1$ Hz, 3H, CH₂CH₃), 1.19 (s, 9H, C(CH₃)₃), 0.94 (s, 9H, C(CH₃)₃). $^{13}\text{C}\{\text{H}\}$ NMR (50 MHz, CDCl_3): δ 169.44 (s, CO₂), 148.13-124.60 (aryl C), 72.04 (s, OCH₂CO₂), 61.00 (s, CH₂CH₃), 36.57 (s × 2, ArCH₂Ar), 34.32 (s, C(CH₃)₃), 34.09 (s × 2, C(CH₃)₃), 33.99 (s, C(CH₃)₃), 33.86 (s, C(CH₃)₃), 33.86 (s × 2, ArCH₂Ar), 31.51 (s × 3, C(CH₃)₃), 31.14 (s, C(CH₃)₃), 14.29 (s, CH₂CH₃); $^{31}\text{P}\{\text{H}\}$ NMR (121 MHz, CDCl_3): δ 106.3 (s, P(OAr)₃). Found: C, 75.61; H, 7.88; calc. for C₄₈H₅₉O₆P ($M_r = 762.95$): C, 75.56; H, 7.79%.

5,11,17,23-Tetra-*tert*-butyl-25-(diethylcarbamoylmethoxy)-26,27,28-trihydroxy calix[4]arene (6**).**



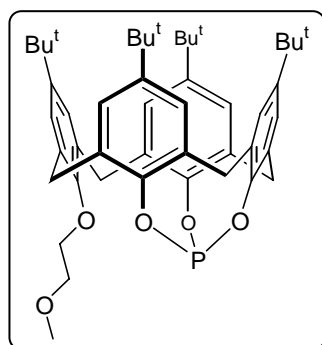
A suspension of *p*-*tert*-butylcalix[4]arene (1.000 g, 1.54 mmol) and K₂CO₃ (0.115 g, 0.83 mmol) in acetonitrile (50 cm³) was refluxed for 2 h. 2-Bromo-*N,N*-diethylacetamide (1.000 g, 5.15 mmol) was then added and the mixture refluxed for a further 10 days. After cooling, the solvent was removed under reduced pressure. The residue was taken up in CH₂Cl₂ (30 cm³) and washed with 1 M HCl (30 cm³), then with water (30 cm³). The organic layer was dried over MgSO₄, filtered and evaporated. The crude product was purified by column chromatography using AcOEt-hexane (30:70, v/v) as eluent. Unreacted *p*-*tert*-butyl-calix[4]arene eluted first followed by **6** (SiO₂, *R*_f = 0.38, AcOEt-hexane, 30:70, v/v). After evaporation, the residue was taken up in CH₂Cl₂. Addition of ethanol at -78 °C afforded the product as a white powder. Yield: 0.274 g, 0.36 mmol, 23%. Mp 149 °C. IR (KBr) ν_{max} /cm⁻¹: 1653 (s, C=O). ¹H NMR (300 MHz, CDCl₃): δ 10.43 (s, 1H, OH, exchanges with D₂O), 9.73 (s, 2H, OH, exchanges with D₂O), 7.08 (s, 2H, *m*-ArH), 7.04 (m, 4H, *m*-ArH), 6.95 (d, ⁴J = 2.4 Hz, 2H, *m*-ArH), 4.96 (s, 2H, OCH₂), 4.60 and 3.37 (AB q, ²J = 12.9 Hz, 4H, ArCH₂Ar), 4.34 and 3.40 (AB q, ²J = 13.6 Hz, 4H, ArCH₂Ar), 3.55 (q, ³J = 7.2 Hz, 2H, NCH₂CH₃), 3.29 (q, ³J = 7 Hz, 2H, NCH₂CH₃), 1.29-1.20 (overlapping signals, 42H, C(CH₃)₃ and NCH₂CH₃); ¹³C{¹H} NMR (50 MHz, CDCl₃): δ 168.85 (s, C=O), 148.31, 142.76, 134.03, 127.95 (s × 4, aromatic C_{quat}), 126.34-125.61 (aryl C), 72.26 (s, OCH₂CO), 40.68 and 40.42 (s × 2, CH₂CH₃), 33.96 (s, C(CH₃)₃), 33.16 (s × 2, ArCH₂Ar), 32.94 (s × 2, ArCH₂Ar), 31.50 (s, C(CH₃)₃), 31.33 (s, C(CH₃)₃), 14.06 and 12.94 (s × 2, CH₂CH₃). Only one C(CH₃)₃ signal could be detected. Found: C, 78.71; H, 8.83; N, 1.77; calc. for C₅₀H₆₇NO₅ (M_r = 762.07): C, 78.80; H, 8.86; N, 1.84%.

5,11,17,23-Tetra-*tert*-butyl-25-(diethylcarbamoylmethoxy)-26,27,28-(μ_3 -phosphorustrioxo)calix[4]arene (L^3).



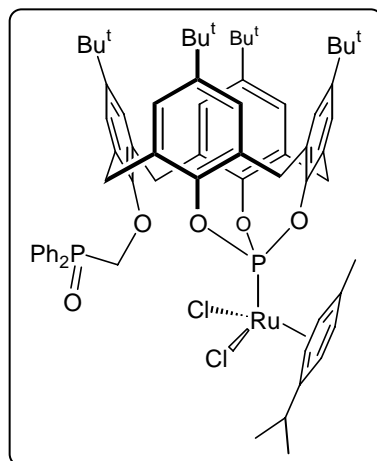
To a solution of **6** (0.611 g, 0.802 mmol) in an NEt_3 -toluene mixture (NEt_3 , 1 cm^3 , 7.17 mmol; toluene, 50 cm^3) was added dropwise PCl_3 (0.070 cm^3 , 0.802 mmol) under stirring. After 3 h, the NEt_3HCl salt formed was removed by filtration through a bed of Celite and washed with toluene ($2 \times 15 \text{ cm}^3$). The filtrate and washing solutions were evaporated under vacuum. Yield: 0.620 g, 0.79 mmol, 98%. Mp 88-90 °C. IR (KBr) $\nu_{\text{max}}/\text{cm}^{-1}$: 1653 (s, C=O). ^1H NMR (300 MHz, CDCl_3): δ 7.16 (m, 2H, *m*-ArH), 7.09 (d, $^4J = 2.5$ Hz, 2H, *m*-ArH), 7.04 (s, 2H, *m*-ArH), 6.77 (s, 2H, *m*-ArH), 4.64 and 3.43 (AB q, $^2J = 14.1$ Hz, 4H, ArCH₂Ar), 4.55 (s, 2H, OCH₂), 4.39 and 3.56 (AB q, $^2J = 14.3$ Hz, 4H, ArCH₂Ar), 3.58 (q, $^3J = 6.9$ Hz, 2H, NCH₂CH₃), 3.45 (q, $^3J = 7.1$ Hz, 2H, NCH₂CH₃), 1.35 (s, 18H, C(CH₃)₃), 1.24 (t, $^3J = 6.9$ Hz, 3H, NCH₂CH₃), 1.18 (s, 9H, C(CH₃)₃), 1.17 (t, $^3J = 6.9$ Hz, 3H, NCH₂CH₃), 0.95 (s, 9H, C(CH₃)₃). $^{13}\text{C}\{\text{H}\}$ NMR (75 MHz, CDCl_3): δ 167.15 (s, C=O), 155.43-124.54 (aryl C), 74.36 (s, OCH₂CO), 41.54 and 39.90 (s \times 2, CH₂CH₃), 36.49 (s \times 2, ArCH₂Ar), 34.23, 34.00 and 33.90 (s \times 3, C(CH₃)₃), 33.82 (s \times 2, ArCH₂Ar), 31.40 and 31.06 (s \times 2, C(CH₃)₃), 14.40 and 12.83 (s \times 2, CH₂CH₃). $^{31}\text{P}\{\text{H}\}$ NMR (121 MHz, CDCl_3): δ 106.1 (s, P(OAr)₃). Found: C, 76.22; H, 8.65; N, 1.51; calc. for $\text{C}_{50}\text{H}_{64}\text{NO}_5\text{P}$ ($M_r = 790.02$): C, 76.02; H, 8.17; N, 1.77%.

5,11,17,23-Tetra-*tert*-butyl-25-(3-oxabutyloxy)-26,27,28-(μ_3 -phosphorustrioxy)calix[4]arene (L**⁴).**



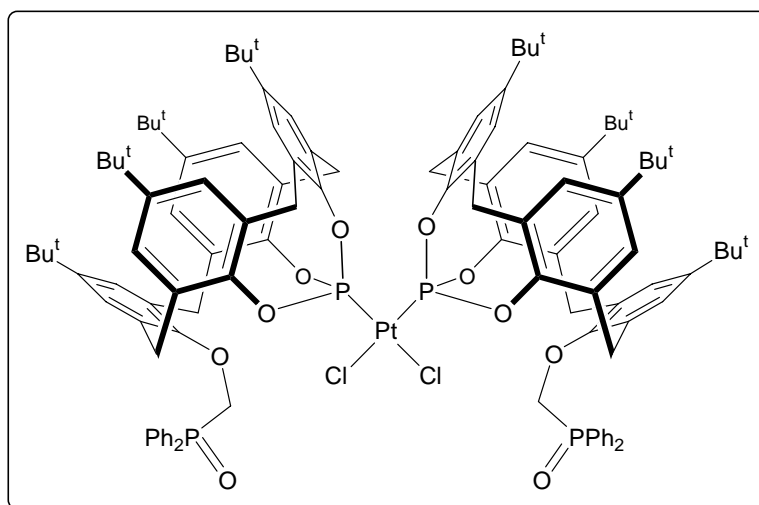
PCl₃ (0.027 cm³, 0.31 mmol) was added dropwise to a toluene (100 cm³) solution containing **7** (0.217 g, 0.31 mmol) and NEt₃ (0.5 cm³, 3.59 mmol). The mixture was stirred at room temperature for 18 h. The NEt₃HCl salt formed was filtered off using a bed of Celite and washed with toluene (2 × 10 cm³). The filtrate and washing solutions were evaporated under vacuum. Yield: 0.194 g, 0.264 mmol, 86%. Mp 91-92 °C. ¹H NMR (200 MHz, CDCl₃): δ 7.18 and 7.11 (AB q, ⁴J = 2.2 Hz, 4H, m-ArH), 7.06 (s, 2H, m-ArH), 6.80 (s, 2H, m-ArH), 4.67 and 3.52 (AB q, ²J = 14.5 Hz, 4H, ArCH₂Ar), 4.45 and 3.48 (AB q, ²J = 14.3 Hz, 4H, ArCH₂Ar), 4.03 (m, 2H, OCH₂), 3.78 (m, 2H, OCH₂), 3.47 (s, 3H, OCH₃), 1.51 (s, 18H, C(CH₃)₃), 1.20 (s, 9H, C(CH₃)₃), 0.98 (s, 9H, C(CH₃)₃). ¹³C{¹H} NMR (50 MHz, CDCl₃): δ 152.22-143.00 and 134.15-124.40 (aryl C), 74.26 (s, OCH₂), 71.67 (s, OCH₂), 59.39 (s, OCH₃), 36.56 (s × 2, ArCH₂Ar), 34.27 (s, C(CH₃)₃), 34.04 (s, C(CH₃)₃), 33.62 (s × 2, ArCH₂Ar), 31.47 (s × 3, C(CH₃)₃), 31.17 (s, C(CH₃)₃). ³¹P{¹H} NMR (121 MHz, CDCl₃): δ 105.6 (s, P(OAr)₃). Found: C, 76.95; H, 8.24; calc. for C₄₇H₅₉O₅P (M_r = 734.942): C, 76.81; H, 8.09%.

(η^6 -*p*-Cymene)dichloro{5,11,17,23-tetra-*tert*-butyl-25-(diphenylphosphinoyl-methoxy)-26,27,28-(μ_3 -phosphorustrioxo)-calix[4]arene}ruthenium(II) (8).



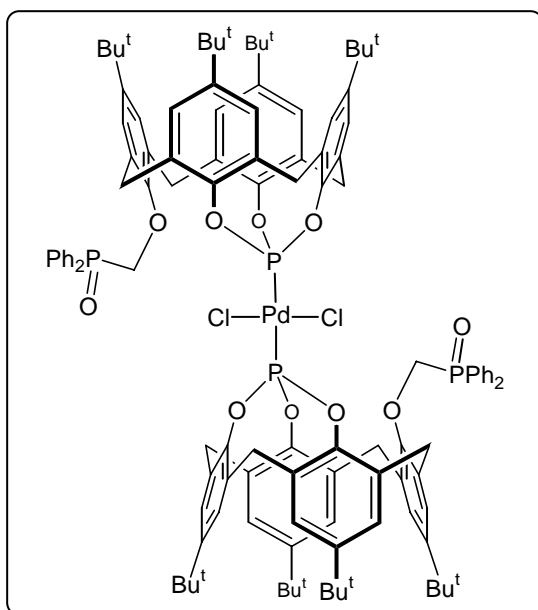
L¹ (0.250 g, 0.28 mmol) was added to a solution of [RuCl₂(*p*-cymene)]₂ (0.086 g, 0.14 mmol) in CH₂Cl₂ (40 cm³). After stirring for 2 h, the solvent was removed under vacuum. Recrystallisation from AcOEt-hexane. Yield: 0.190 g, 0.16 mmol, 57%. Mp 219–223 °C (slow decomp.). IR (KBr) ν_{max} /cm⁻¹: 1195 (P=O, tentative assignment). ¹H NMR (300 MHz, CDCl₃): δ 7.78–7.71 and 7.52–7.42 (10 H, P(O)Ph₂), 7.10 (s, 2H, *m*-ArH), 7.05 (s, 2H, *m*-ArH), 6.88 (s, 2H, *m*-ArH), 6.21 (s, 2H, *m*-ArH), 5.82 and 5.70 (AA'BB' system, ³J = 5.9 Hz, 4H, C₆H₄ of *p*-cymene), 4.90 and 3.50 (AB q, ²J = 14.3 Hz, 4H, ArCH₂Ar), 4.82 (s, 2H, P(O)CH₂), 4.76 and 3.23 (AB q, ²J = 15 Hz, 4H, ArCH₂Ar), 2.76 (m, 1H, CH(CH₃)₂ of *p*-cymene), 1.80 (s, 3H, ArCH₃ of *p*-cymene), 1.33 (s × 2, 18H, C(CH₃)₃), 1.13 (s, 9H, C(CH₃)₃), 1.05 (d, ³J = 6.9 Hz, 6H, CH(CH₃)₂ of *p*-cymene), 0.59 (s, 9H, C(CH₃)₃). ¹³C{¹H} NMR (50 MHz, CDCl₃): δ 148.29–123.87 (aryl C), 108.99 and 96.54 (s × 2, C_{quat} of *p*-cymene), 91.69, 91.56, 87.33 and 87.16 (s × 4, aryl CH of *p*-cymene), 73.28 (d, J(PC) = 80.3 Hz, P(O)CH₂), 35.99 (s, ArCH₂Ar), 34.16 (s, C(CH₃)₃), 33.80 (s, C(CH₃)₃), 33.27 (s, ArCH₂Ar), 31.31 (s, C(CH₃)₃), 31.21 (s × 2, C(CH₃)₃), 30.74 (s, C(CH₃)₃), 21.27 (s, CH(CH₃)₂ of *p*-cymene), 17.93 (s, ArCH₃ of *p*-cymene). ³¹P{¹H} NMR (121 MHz, CDCl₃): δ 92.56 (s, P(OAr)₃), 24.75 (s, P(O)Ph₂). Found: C, 67.47; H, 7.64; calc. for C₆₇H₇₈Cl₂O₅P₂Ru (M_r = 1197.29): C, 67.21; H, 6.57%. Despite several purifications (recrystallisation followed by chromatography), the samples always contained free *p*-cymene.

cis-Dichlorobis{5,11,17,23-tetra-*tert*-butyl-25-(diphenylphosphinoylmethoxy)-26,27,28-(μ_3 -phosphorustrioxo)calix[4]arene}-platinum(II) (9).



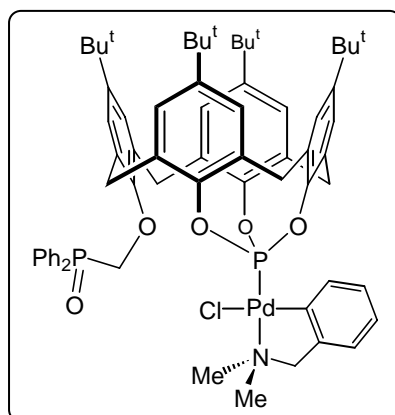
L¹ (0.143 g, 0.16 mmol) was added to a solution of [PtCl₂(1,5-cyclooctadiene)] (0.030 g, 0.08 mmol) in CH₂Cl₂ (30 cm³). After stirring for 1 h, the solution was concentrated under vacuum. Addition of pentane and cooling to -20 °C afforded **9** as a white solid. Yield: 0.130 g, 0.06 mmol, 79%. Mp > 240 °C. IR (KBr) $\nu_{\text{max}}/\text{cm}^{-1}$: 1179.2 (P=O, tentative assignment). ¹H NMR (300 MHz, CDCl₃): δ 7.89-7.68 and 7.46-7.31 (20 H, P(O)Ph₂), 7.06-6.98 (6H, *m*-ArH), 6.91 (4H, *m*-ArH), 6.70 (s, 2H, *m*-ArH), 6.57 (s, 2H, *m*-ArH), 6.45 (s, 2H, *m*-ArH), 5.78 and 5.54 (ABX system with X = P, ²J_{AB} = 12.9 Hz, ²J_{AX} = 0 Hz, ²J_{BX} = 6.5 Hz, 4H, P(O)CH₂), 4.89 and 3.34 (AB q, ²J = 12.8 Hz, 4H, ArCH₂Ar), 4.60 and 3.22 (AB q, ²J = 13.9 Hz, 4H, ArCH₂Ar), 4.60 and 2.90 (AB q, ²J = 12.8 Hz, 4H, ArCH₂Ar), 3.98 and 2.49 (AB q, ²J = 12.2 Hz, 4H, ArCH₂Ar), 1.28 (s, 18H, C(CH₃)₃), 1.23 (s, 18H, C(CH₃)₃), 1.20 (s, 18H, C(CH₃)₃), 0.96 (s, 18H, C(CH₃)₃). ¹³C{¹H} NMR (50 MHz, CDCl₃): δ 150.75-124.07 (aryl C), 71.69 (d, *J*(PC) = 72.6 Hz, P(O)CH₂), 37.76 (s, ArCH₂Ar), 35.40 (s, C(CH₃)₃), 34.81 (s, C(CH₃)₃), 33.27 (s, ArCH₂Ar), 32.27 (s, C(CH₃)₃), 32.07 (s, C(CH₃)₃). ³¹P{¹H} NMR (121 MHz, CDCl₃): δ 32.7 (s with Pt satellites, *J*(PPt) = 6736 Hz, P(OAr)₃), 26.5 (s, P(O)Ph₂). Found: C, 66.70; H, 6.52; calc. for C₁₁₄H₁₂₈Cl₂O₁₀P₄Pt (M_r = 2048.11): C, 66.85; H, 6.30%.

trans-Dichlorobis{5,11,17,23-tetra-*tert*-butyl-25-(diphenylphosphinoylmethoxy)-26,27,28-(μ_3 -phosphorustrioxo)calix[4]arene}palladium(II) (10).



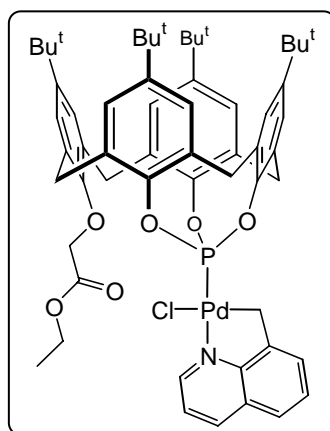
L1 (0.150 g, 0.168 mmol) was added to a solution of [PdCl₂(1,5-cyclooctadiene)] (0.024 g, 0.08 mmol) in CH₂Cl₂ (15 cm³). After stirring for 1 h, the solution was concentrated under vacuum. Addition of pentane and cooling to -20 °C afforded **10** as a pale yellow solid. Yield: 0.224 g, 0.11 mmol, 68%. Mp > 240 °C. IR (KBr) $\nu_{\text{max}}/\text{cm}^{-1}$: 1183.1 (P=O, tentative assignment). ¹H NMR (300 MHz, CDCl₃): δ 7.90-7.84 and 7.23-7.18 (20 H, P(O)Ph₂), 7.05 (s, 4H, *m*-ArH), 7.00 (d, ⁴J = 2.9 Hz, 4H, *m*-ArH), 6.93 (s, 4H, *m*-ArH), 6.60 (s, 4H, *m*-ArH), 5.56 (s, 4H, P(O)CH₂), 4.82 and 3.26 (AB q, ²J = 14.1 Hz, 4H, ArCH₂Ar), 4.45 and 3.18 (AB q, ²J = 14.3 Hz, 4H, ArCH₂Ar), 1.28 (s, 36H, C(CH₃)₃), 1.20 (s, 18H, C(CH₃)₃), 0.93 (s, 18H, C(CH₃)₃). ¹³C{¹H} NMR (50 MHz, CDCl₃): δ 146.43-124.63 (aryl C), 72.88 (d, *J*(PC) = 74 Hz, P(O)CH₂), 36.42 (s, ArCH₂Ar), 35.66 (s, C(CH₃)₃), 34.45 (s, C(CH₃)₃), 33.99 (s, C(CH₃)₃), 33.83 (s, ArCH₂Ar), 31.40 (s × 3, C(CH₃)₃), 31.17 (s, C(CH₃)₃). ³¹P{¹H} NMR (121 MHz, CDCl₃): δ 58.8 (s, P(OAr)₃), 27.6 (s, P(O)Ph₂). Found: C, 69.56; H, 6.58; calc. for C₁₁₄H₁₂₈Cl₂O₁₀P₄Pd (M_r = 1959.45): C, 69.88; H, 6.58%.

Chloro(8-methylquinolinylmethyl-*C,N*){5,11,17,23-tetra-*tert*-butyl-25-(diphenylphosphinoylmethoxy)-26,27,28-(μ_3 -phosphorustrioxy)calix[4]arene}palladium(II) (11**).**



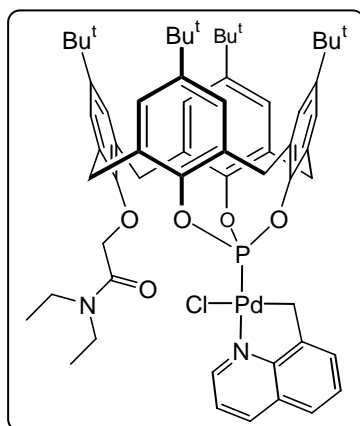
L¹ (0.151 g, 0.169 mmol) was added to a solution of [Pd(8-mq)Cl]₂ (0.048 g, 0.08 mmol) in CH₂Cl₂ (15 cm³). After stirring for 1 h, the solution was concentrated under vacuum. Addition of pentane and cooling to -20 °C afforded **11** as a pale yellow solid. Yield: 0.160 g, 0.136 mmol, 60%. Mp > 168-169 °C (decomp). IR (KBr) $\nu_{\text{max}}/\text{cm}^{-1}$: 1187.3 (P=O, tentative assignment). ¹H NMR (200 MHz, CDCl₃): δ 9.60-9.54 (1H, arom. H of 8-mq), 8.31-8.26 (1H, arom H of 8-mq), 7.65-7.43 and 7.13-6.99 (20 H, P(O)Ph₂, arom. H of 8-mq and *m*-ArH of calix), 6.51 (s, 2H, *m*-ArH), 4.95 (d, ²J = 1.7 Hz, 2H, P(O)CH₂), 4.82 and 3.45 (AB q, ²J = 14 Hz, 4H, ArCH₂Ar), 4.65 and 3.41 (AB q, ²J = 14.1 Hz, 4H, ArCH₂Ar), 1.36 (s, 18H, C(CH₃)₃), 1.18 (s, 9H, C(CH₃)₃), 0.82 (s, 9H, C(CH₃)₃). ¹³C{¹H} NMR (50 MHz, CDCl₃): δ 154.16-121.09 (aryl C), 72.82 (d, *J*(PC) = 80 Hz, P(O)CH₂), 35.99 (s × 2, ArCH₂Ar), 34.35 (s, C(CH₃)₃), 34.03 (s, C(CH₃)₃), 33.70 (s × 2, ArCH₂Ar), 31.40 (s, C(CH₃)₃), 31.01 (s, C(CH₃)₃), 26.39 (s, CH₂ 8-mq); ³¹P{¹H} NMR (121 MHz, CDCl₃): δ 89.8 (s, P(OAr)₃), 26.3 (s, P(O)Ph₂). Found: C, 64.52; H, 6.17; calc. for C₆₇H₇₂ClNO₅P₂Pd·CH₂Cl₂ (M_r = 1260.04): C, 64.82; H, 6.17%.

Chloro(8-methylquinolinylmethyl-*C,N*){5,11,17,23-tetra-*tert*-butyl-25-(ethoxy-carbonylmethoxy)-26,27,28-(μ_3 -phosphorustrioxy)calix[4]arene}palladium(II) (12).



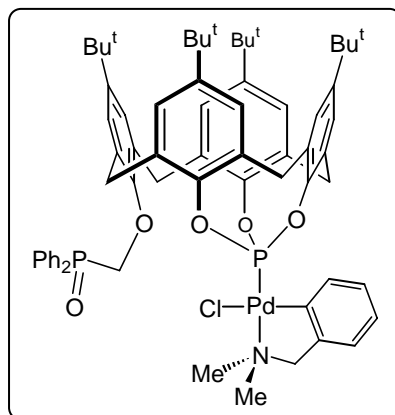
L² (0.175 g, 0.23 mmol) was added to a solution of [Pd(8-mq)Cl]₂ (0.065 g, 0.114 mmol) in CH₂Cl₂ (50 cm³). After stirring for 24 h, the solution was concentrated under vacuum. Addition of MeOH and cooling to -78 °C afforded **12** as a pale yellow solid. Yield: 0.163 g, 0.156 mmol, 68%. Mp > 240 °C. IR (CH₂Cl₂) $\nu_{\text{max}}/\text{cm}^{-1}$: 1755 (C=O). ¹H NMR (300 MHz, CDCl₃): δ 9.64-9.60 (m, 1H, arom. H of 8-mq), 8.28 (d, ³J = 7.1 Hz, 1H, arom. H of 8-mq), 7.61-7.44 (m, 4H, arom. H of 8-mq), 7.21-7.05 (m, 6H, m-ArH), 6.77 (s, 2H, m-ArH), 5.07 and 3.54 (AB q, ²J = 13.9 Hz, 4H, ArCH₂Ar), 4.71 and 3.49 (AB q, ²J = 14.0 Hz, 4H, ArCH₂Ar), 4.71 (s, 2H, OCH₂CO₂), 3.84 (s, 2H, CH₂ of 8-mq), 3.66 (q, ³J = 7.2 Hz, 2H, CH₂CH₃), 1.36 (s, 18H, C(CH₃)₃), 1.22 (s, 9H, C(CH₃)₃), 0.96 (s, 9H, C(CH₃)₃), 0.88 (t, ³J = 7.1 Hz, 3H, CH₂CH₃); ¹³C{¹H} NMR (50 MHz, CDCl₃): δ 169.77 (s, CO), 153.25-121.19 (aryl C), 71.62 (s, OCH₂CO₂), 60.25 (s, CH₂CH₃), 36.12 (s, ArCH₂Ar), 34.42 (s, C(CH₃)₃), 34.12 (s, ArCH₂Ar and C(CH₃)₃), 33.93 (s × 2, C(CH₃)₃), 31.40 (s × 3, C(CH₃)₃), 31.11 (s, C(CH₃)₃), 13.80 (s, CH₂CH₃), the CH₂ signal of 8-mq was not detected. ³¹P{¹H} NMR (121 MHz, CDCl₃): δ 88.7 (s, P(OAr)₃). Found: C, 66.80; H, 6.43; N, 1.42; calc. for C₅₈H₆₇ClNO₆PPd (M_r = 1047.00): C, 66.53; H, 6.45; N, 1.34%.

Chloro(8-methylquinolinylmethyl-*C,N*){5,11,17,23-tetra-*tert*-butyl-25-(diethylcarbamoylmethoxy)-26,27,28-(μ_3 -phosphorustrioxy)calix[4]arene}palladium(II) (13).



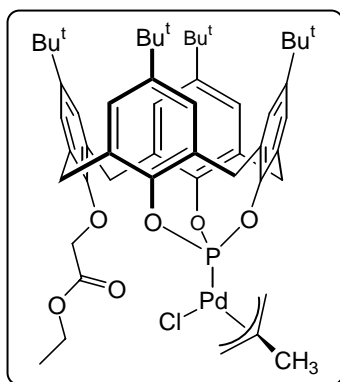
L³ (0.175 g, 0.22 mmol) was added to a solution of [Pd(8-mq)Cl]₂ (0.063 g, 0.111 mmol) in CH₂Cl₂ (20 cm³). After stirring for 24 h, the solution was concentrated under vacuum. Addition of hexane and cooling to -78 °C afforded **13** as a pale yellow solid. Yield: 0.170 g, 0.158 mmol, 71%. Mp > 233 °C (decomp.). IR (CH₂Cl₂) ν_{max} /cm⁻¹: 1655 (C=O). ¹H NMR (300 MHz, CDCl₃): δ 9.66-9.62 (m, 1H, arom. H of 8-mq), 8.29-8.26 (m, 1H, arom. H of 8-mq), 7.61-7.44 (m, 4H, arom. H of 8-mq), 7.20 (br s, 2H, *m*-ArH), 7.12 (s, 2H, *m*-ArH), 7.10 (s, 2H, *m*-ArH), 6.75 (s, 2H, *m*-ArH), 5.10 and 3.56 (AB q, ²J = 13.9 Hz, 4H, ArCH₂Ar), 4.79 (s, 2H, OCH₂CON), 4.70 and 3.49 (AB q, ²J = 14.0 Hz, 4H, ArCH₂Ar), 3.82 (s, 2H, CH₂Pd), 3.07 (q, ³J = 7.1 Hz, 2H, CH₂CH₃), 2.87 (q, ³J = 7.1 Hz, 2H, CH₂CH₃), 1.36 (s, 18H, C(CH₃)₃), 1.21 (s, 9H, C(CH₃)₃), 0.95 (s, 9H, C(CH₃)₃), 0.67 (t, ³J = 7.1 Hz, 3H, CH₂CH₃), 0.48 (t, ³J = 7.1 Hz, 3H, CH₂CH₃). ¹³C{¹H} NMR (50 MHz, CDCl₃): δ 167.64 (s, CO), 153.71-121.19 (aryl C), 72.86 (s, OCH₂), 41.35 and 39.89 (s × 2, CH₂CH₃), 36.16 (s, ArCH₂Ar), 34.45 (s, C(CH₃)₃), 34.31 (s, ArCH₂Ar), 34.10 (s × 2, C(CH₃)₃), 33.93 (s, C(CH₃)₃), 31.48 (s × 3, C(CH₃)₃), 31.15 (s, C(CH₃)₃), 27.12 (s, CH₂ of 8-mq), 13.77 and 12.61 (s × 2, CH₂CH₃); ³¹P{¹H} NMR (121 MHz, CDCl₃): δ 88.1 (s, P(OAr)₃). Found: C, 67.14; H, 6.60; N, 2.48; calc. for C₆₀H₇₂ClN₂O₅PPd (M_r = 1074.07): C, 67.09; H, 6.79; N, 2.61%.

Chloro(*o*-dimethylaminomethylphenyl-*C,N*){5,11,17,23-tetra-*tert*-butyl-25-(diphenylphosphinoylmethoxy)-26,27,28-(μ_3 -phosphorustrioxy)calix[4]arene} palladium(II) (14).



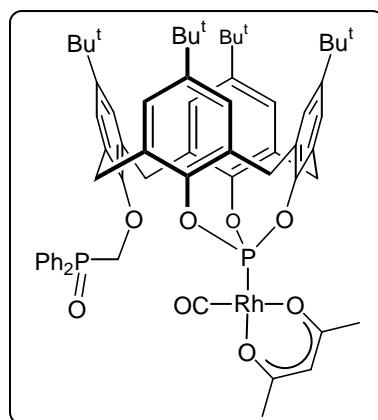
L¹ (0.107 g, 0.12 mmol) was added to a solution of [Pd(*o*-C₆H₄CH₂-NMe₂)Cl]₂ (0.031 g, 0.06 mmol) in CH₂Cl₂ (10 cm³). After stirring for 1 h, the solvent was removed under vacuum. Recrystallisation from CH₂Cl₂-hexane at -78 °C gave **14** as a pale yellow solid. Yield: 0.072 g, 0.062 mmol, 52%. Mp > 186 °C (decomp). IR (KBr) $\nu_{\text{max}}/\text{cm}^{-1}$: 1185 (P=O, tentative assignment). ¹H NMR (200 MHz, CDCl₃): δ 7.64-7.38, 7.28-7.19 and 7.06-6.62 (20 H, arom. H), 6.41 (s, 2H, *m*-ArH of calix), 5.17 (s, 2H, P(O)CH₂), 4.77-4.70 (m, 4H, ArCH₂Ar), 3.93 (s, 2H, NCH₂), 3.44 (d, ²J = 14 Hz, 2H, ArCH₂Ar), 3.01 (d, ²J = 14 Hz, 2H, ArCH₂Ar), 2.76 (d, ⁴J(PH) = 4.2 Hz, 6H, N(CH₃)₂), 1.31 (s, 18H, C(CH₃)₃), 1.19 (s, 9H, C(CH₃)₃), 0.86 (s, 9H, C(CH₃)₃). ¹³C{¹H} NMR (50 MHz, CDCl₃): δ 153.90-122.60 (aryl C), 72.90 (d, ³J(PC) = 4.9 Hz, NCH₂), 72.65 (d, *J*(PC) = 80.8 Hz, P(O)CH₂), 50.38 (s × 2, N(CH₃)₂), 36.16 (s × 2, ArCH₂Ar), 34.32 (s, C(CH₃)₃), 33.93 (s, C(CH₃)₃), 33.67 (s × 2, ArCH₂Ar), 31.34 (s × 3, C(CH₃)₃), 31.01 (s, C(CH₃)₃). ³¹P{¹H} NMR (121 MHz, CDCl₃): δ 82.3 (s, P(OAr)₃), 26.5 (s, P(O)Ph₂). Found: C, 68.10; H, 6.86; N, 1.24; calc. for C₆₆H₇₆ClNO₅P₂Pd (M_r = 1167.13): C, 67.92; H, 6.56; N, 1.20%.

Chloro(η^3 -2-methylallyl){5,11,17,23-tetra-*tert*-butyl-25-(ethoxycarbonylmethoxy)-26,27,28-(μ_3 -phosphorustrioxy)calix[4]arene}palladium(II) (15**).**



L² (0.186 g, 0.244 mmol) was added to a solution of [Pd(η^3 -C₄H₇)Cl]₂ (0.048 g, 0.12 mmol) in CH₂Cl₂ (10 cm³). After stirring for 15 h, the solution was concentrated to ca. 50%. Addition of hexane and cooling to -78 °C gave **15** as a white powder. Yield: 0.160 g, 0.167 mmol, 68%. Mp > 240 °C. IR (nujol) ν_{max} /cm⁻¹: 1734 (C=O). ¹H NMR (400 MHz, CDCl₃): δ 7.22-7.19 and 7.11-7.10 (2 overlapping AB q, 4H, *m*-ArH), 7.07 (s, 2H, *m*-ArH), 6.73 and 6.71 (AB q, 2H, *m*-ArH), 5.01 and 3.54 (AB q, ²J = 14.4 Hz, 2H, ArCH₂Ar), 5.00 and 4.72 (AB q, ²J = 16.4 Hz, 2H, OCH₂CO₂), 4.93 and 3.56 (AB q, ²J = 15.0 Hz, 2H, ArCH₂Ar), 4.45 and 3.46 (AB q, ²J = 13.6 Hz, 2H, ArCH₂Ar), 4.43 (br s, 1H, H-allyl), 4.41 and 3.49 (AB q, ²J = 13.2 Hz, 2H, ArCH₂Ar), 4.14 (q, ³J = 7.2, 2H, OCH₂CH₃), 3.47 (br s, 1H, H-allyl), 3.16 (br s, 1H, H-allyl), 2.55 (br s, 1H, H-allyl), 1.85 (s, 3H, CH₃-allyl), 1.37 (s, 9H, C(CH₃)₃), 1.36 (s, 9H, C(CH₃)₃), 1.25 (t, ³J = 7.2 Hz, OCH₂CH₃), 1.18 (s, 9H, C(CH₃)₃), 0.90 (s, 9H, C(CH₃)₃); ¹³C{¹H} NMR (50 MHz, CDCl₃): δ 170.73 (s, CO₂), 153.77-124.60 (aryl C and C_{quat} allyl), 78.62 and 77.54 (s × 2, CH₂-allyl), 71.95 (s, OCH₂CO₂), 60.73 (s, OCH₂CH₃), 36.31 and 35.99 (s × 2, ArCH₂Ar), 34.45 (s × 2, C(CH₃)₃), 34.18 (s × 2, C(CH₃)₃), 33.98 (s × 2, ArCH₂Ar), 31.49 (s × 3, C(CH₃)₃), 31.11 (s, C(CH₃)₃), 23.27 (s, CH₃-allyl), 14.24 (s, OCH₂CH₃); ³¹P{¹H} NMR (121 MHz, CDCl₃): δ 107.0 (s, P(OAr)₃). Found: C, 67.23; H, 7.10; calc. for C₅₂H₆₆ClO₆PPd (M_r = 959.92): C, 67.06; H, 6.93%.

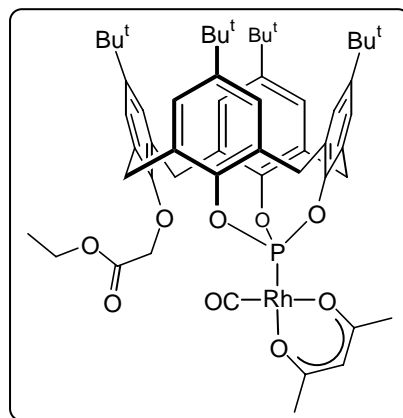
Acetylacetonatocarbonyl{5,11,17,23-tetra-*tert*-butyl-25-(diphenylphosphinoylmethoxy)-26,27,28-(μ_3 -phosphorustrioxo)calix[4]arene}rhodium(I) (16).



L¹ (0.134 g, 0.15 mmol) was added [§] to a solution of [Rh(acac)(CO)₂] [acac = MeC(O)-CHC(O)Me] (0.040 g, 0.151 mmol) in CH₂Cl₂ (30 cm³). After stirring for 12 h, the volatiles were evaporated under vacuum to give **16** as a yellow powder. Owing to its high solubility in all common organic solvents, **16** was not purified further. Yield: 0.156 g, 0.139 mmol, 92%. Mp 76-78 °C. IR (CH₂Cl₂) $\nu_{\text{max}}/\text{cm}^{-1}$: 2004s (CO), 1182 (s, P=O, tentative assignment). ¹H NMR (300 MHz, CDCl₃): δ 8.00-7.93 and 7.53-7.44 (10 H, P(O)Ph₂), 7.05 (s, 4H, *m*-ArH), 7.02 (s, 2H, *m*-ArH), 6.35 (s, 2H, *m*-ArH), 5.37 (s, 1H, CH-acac), 4.79 (d, ²J = 4.4 Hz, 2H, P(O)CH₂), 4.52 and 3.40 (AB q, ²J = 14.6 Hz, 4H, ArCH₂Ar), 4.52 and 3.29 (AB q, ²J = 14.9 Hz, 4H, ArCH₂Ar), 1.99 (s, 3H, CH₃-acac), 1.36 (s, 3H, CH₃-acac), 1.33 (s, 18H, C(CH₃)₃), 1.17 (s, 9H, C(CH₃)₃), 0.70 (s, 9H, C(CH₃)₃). ¹³C{¹H} NMR (75 MHz, CDCl₃): δ 187.23 and 187.00 (s × 2, CO), 146.29-124.13 (aryl C), 101.65 (s, CH-acac), 73.21 (d, *J*(PC) = 56 Hz, P(O)CH₂), 35.83 and 35.34 (s × 2, ArCH₂Ar), 34.08 (s × 2, C(CH₃)₃), 33.63 (s × 2, C(CH₃)₃), 33.11 (s × 2, ArCH₂Ar), 31.42 (s × 3, C(CH₃)₃), 31.33 (s, C(CH₃)₃), 26.94 (CH₃-acac), 25.46 (CH₃-acac). ³¹P{¹H} NMR (121 MHz, CDCl₃): δ 104.0 (d, *J*(PRh) = 300 Hz, P(OAr)₃), 28.0 (s, P(O)Ph₂). Found: C, 67.66; H, 6.53; calc. for C₆₃H₇₁O₈P₂Rh (M_r = 1121.09): C, 67.49; H, 6.38%.

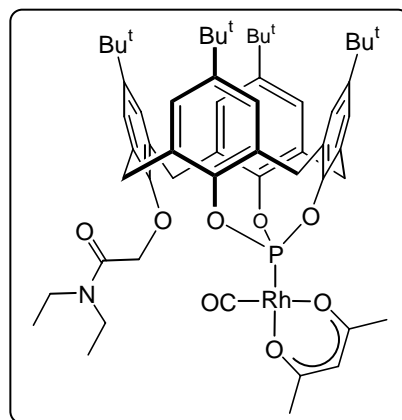
[§] **L¹** needs to be free of NEt₃HCl. The presence of the latter leads to formation of complex **19**.

Acetylacetonatocarbonyl{5,11,17,23-tetra-tert-butyl-25-(ethoxycarbonylmethoxy)-26,27,28-(μ_3 -phosphorustrioxy)calix[4]arene}rhodium(I) (17).



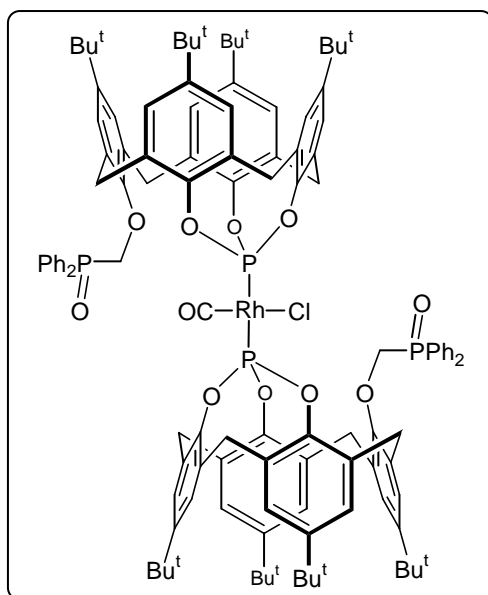
L² (0.111 g, 0.15 mmol) was added to a solution of [Rh(acac)(CO)₂] (0.040 g, 0.15 mmol) in CH₂Cl₂ (30 cm³). After stirring for 12 h, the volatiles were evaporated under vacuum to give **17** as a yellow powder. Yield: 0.135 g, 0.136 mmol, 90%. Mp 109-111 °C. IR (CH₂Cl₂) ν_{max} / cm⁻¹: 2001s (CO), 1755m (C=O ester). ¹H NMR (200 MHz, CDCl₃): δ 7.18 and 7.07 (AB q, ²J = 2.4 Hz, 4H, *m*-ArH), 7.05 (s, 2H, *m*-ArH), 6.59 (s, 2H, *m*-ArH), 5.36 (s, 1H, CH-acac), 4.98 and 3.57 (AB q, ²J = 14.6 Hz, 4H, ArCH₂Ar), 4.64 (s, 2H, OCH₂CO₂), 4.58 and 3.43 (AB q, ²J = 14.6 Hz, 4H, ArCH₂Ar), 4.19 (q, ³J = 7.1 Hz, 2H, OCH₂CH₃), 2.03 (s, 3H, CH₃-acac), 1.45 (s, 3H, CH₃-acac), 1.35 (s, 18H, C(CH₃)₃), 1.28 (t, ³J = 7.1 Hz, 3H, OCH₂CH₃), 1.18 (s, 9H, C(CH₃)₃), 0.79 (s, 9H, C(CH₃)₃). ¹³C{¹H} NMR (75 MHz, CDCl₃): δ 186.91 and 185.70 (s × 2, CO), 170.00 (s, CO₂), 153.61-124.20 (aryl C), 100.85 (s, CH-acac), 71.52 (s, OCH₂CO₂), 60.80 (s, OCH₂CH₃), 36.31 and 36.00 (s × 2, ArCH₂Ar), 34.42 (s × 2, C(CH₃)₃), 34.09 (s × 2, C(CH₃)₃), 33.77 (s × 2, ArCH₂Ar), 31.47 (s × 3, C(CH₃)₃), 31.04 (s, C(CH₃)₃), 26.94 (CH₃-acac), 25.58 (CH₃-acac), 14.25 (s, OCH₂CH₃). ³¹P{¹H} NMR (121 MHz, CDCl₃): δ 103.1 (d, *J*(PRh) = 309 Hz, P(OAr)₃). Found: C, 65.48; H, 6.85; calc. for C₅₄H₆₆O₉PRh (M_r = 992.98): C, 65.32; H, 6.70%.

Acetylacetonatocarbonyl{5,11,17,23-tetra-*tert*-butyl-25-(diethylcarbamoyl-methoxy)-26,27,28-(μ_3 -phosphorustrioxy)calix[4]arene}rhodium(I) (18).



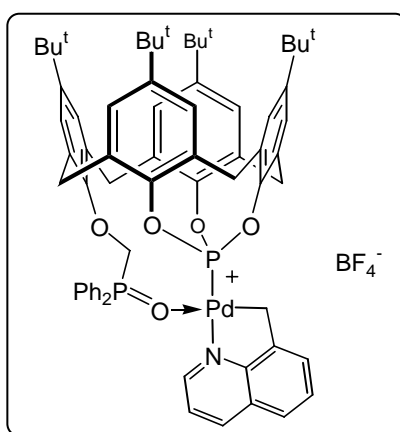
L³ (0.119 g, 0.15 mmol) was added to a solution of [Rh(acac)(CO)₂] (0.040 g, 0.15 mmol) in CH₂Cl₂ (30 cm³). After stirring for 12 h, the volatiles were evaporated under vacuum to afford **18** as a yellow powder. Yield: 0.143 g, 0.14 mmol, 93%. Mp 90-92 °C. IR (CH₂Cl₂) ν_{max} / cm⁻¹: 2000s (CO), 1634 (C=O amide). ¹H NMR (300 MHz, CDCl₃): δ 7.17 and 7.07 (AB q, ²J = 2.5 Hz, 4H, *m*-ArH), 7.05 (s, 2H, *m*-ArH), 6.57 (s, 2H, *m*-ArH), 5.36 (s, 1H, CH-acac), 4.83 and 3.43 (AB q, ²J = 14.3 Hz, 4H, ArCH₂Ar), 4.60 (s, 2H, OCH₂), 4.58 and 3.55 (AB q, ²J = 14.6 Hz, 4H, ArCH₂Ar), 3.77 (q, ³J = 7.1 Hz, 2H, NCH₂CH₃), 3.41 (q, ³J = 7.3 Hz, 2H, NCH₂CH₃), 2.02 (s, 3H, CH₃-acac), 1.40 (s, 3H, CH₃-acac), 1.35 (s, 18H, C(CH₃)₃), 1.24-1.16 (m, 15H, C(CH₃)₃ and NCH₂CH₃), 0.79 (s, 9H, C(CH₃)₃). ¹³C{¹H} NMR (75 MHz, CDCl₃): δ 187.23 and 186.74 (s × 2, CO), 167.69 (s, C(O)N), 153.69-124.12 (aryl C), 101.59 (s, CH-acac), 73.90 (s, OCH₂CONEt₂), 41.92 and 39.90 (s × 2, CH₂CH₃), 35.89 (s × 2, ArCH₂Ar), 34.36 (s, C(CH₃)₃), 34.04 (s × 2, C(CH₃)₃), 33.73 (s, C(CH₃)₃), 33.57 (s × 2, ArCH₂Ar), 31.40 (s × 3, C(CH₃)₃), 30.99 (s, C(CH₃)₃), 26.92 and 25.43 (s × 2, CH₃-acac), 14.26 and 12.88 (s × 2, CH₂CH₃). ³¹P{¹H} NMR (121 MHz, CDCl₃): δ 102.7 (d, *J*(PRh) = 306 Hz, P(OAr)₃). Found: C, 66.22; H, 7.15; N, 1.21; calc. for C₅₆H₇₁NO₈PRh (M_r = 1020.04): C, 65.94; H, 7.02; N, 1.37%.

Chlorocarbonylbis{5,11,17,23-tetra-*tert*-butyl-25-(diphenylphosphinoylmethoxy)-26,27,28-(μ_3 -phosphorustrioxo)calix[4]arene}rhodium(I) (19).



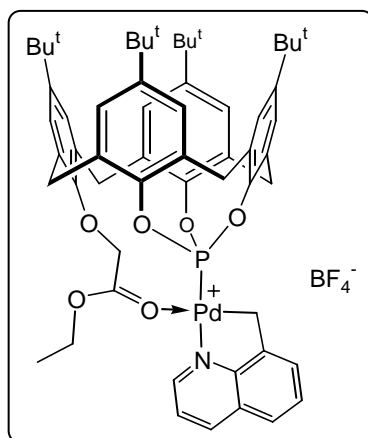
L¹ (0.200 g, 0.11 mmol) was added to a solution of [RhCl(CO)₂] (0.022 g, 0.056 mmol) in CH₂Cl₂ (30 cm³). After stirring for 1 h, hexane was added to precipitate the product. Yield: 0.189 g, 0.097 mmol, 88%. Mp 235-237 °C. IR (KBr) $\nu_{\text{max}}/\text{cm}^{-1}$: 1989s (CO). ¹H NMR (300 MHz, CDCl₃): δ 7.87-6.93 (m, 32H, PPh₂ and *m*-ArH), 6.58 (s, 4H, *m*-ArH), 5.40 (br s, 4H, PCH₂), 4.70 and 3.26 (AB q, ²J = 13.9 Hz, 8H, ArCH₂Ar), 4.45 and 3.23 (AB q, ²J = 14.1 Hz, 8H, ArCH₂Ar), 1.27 (s, 36H, C(CH₃)₃), 1.21 (s, 18H, C(CH₃)₃), 0.91(s, 18H, C(CH₃)₃). ¹³C{¹H} NMR (50 MHz, CDCl₃): δ 152.72-124.46 (aryl C), 72.53 (d, *J*(PC) = 77 Hz, P(O)CH₂), 36.12 (s × 2, ArCH₂Ar), 34.49 (s, C(CH₃)₃), 34.25 (s × 2, ArCH₂Ar), 34.00 (s × 2, C(CH₃)₃), 33.85 (s, C(CH₃)₃), 31.37 (s × 3, C(CH₃)₃), 31.14 (s, C(CH₃)₃). ³¹P{¹H} NMR (121 MHz, CDCl₃): δ 93.4 (d, *J*(PRh) = 223 Hz, P(OAr)₃), 26.9 (s, P(O)Ph₂). FAB mass spectrum: m/z 1021.3 ([M - L¹ - Cl]⁺, 73%), 1884.8 ([M - CO - Cl + H]⁺, 75%), 1919.7 ([M - Cl + H]⁺, 9%). Found: C, 71.05; H, 6.84; calc. for C₁₁₅H₁₂₉O₁₁P₄Rh (M_r = 1948.49): C, 70.89; H, 6.62%.

(8-Methylquinolinylmethyl-*C,N*){5,11,17,23-tetra-*tert*-butyl-25-(diphenylphosphinoylmethoxy)-26,27,28-(μ_3 -phosphorustrioxy)calix[4]arene}palladium(II) tetrafluoroborate (20).



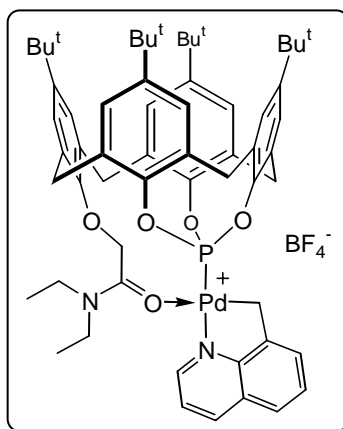
A solution of AgBF₄ (0.016 g, 0.082 mmol) in THF (1 cm³) was added to a solution of **11** (0.100 g, 0.085 mmol) in CH₂Cl₂ (20 cm³). After stirring for 5 min, the solution was filtered through Celite and evaporated to dryness. **20** Was obtained as a pale yellow powder by recrystallisation from an ethyl acetate-hexane mixture at -78 °C. Yield: 0.53 g, 0.043 mmol, 51%. Mp > 163-164 °C (decomp). IR (KBr) $\nu_{\text{max}}/\text{cm}^{-1}$: 1197.5 (P=O, tentative assignment). ¹H NMR (200 MHz, CDCl₃): δ 9.60-9.54 (1H, arom. H of 8-mq), 8.31-8.26 (1H, arom. H of 8-mq), 7.65-7.43 and 7.13-6.99 (20 H, P(O)Ph₂, arom. H of 8-mq and *m*-ArH), 6.51 (s, 2H, *m*-ArH), 4.95 (d, ²J = 1.7 Hz, 2H, P(O)CH₂), 4.82 and 3.45 (AB q, ²J = 14 Hz, 4H, ArCH₂Ar), 4.65 and 3.41 (AB q, ²J = 14.1 Hz, 4H, ArCH₂Ar), 1.36 (s × 2, 18H, C(CH₃)₃), 1.18 (s, 9H, C(CH₃)₃), 0.82 (s, 9H, C(CH₃)₃). ¹³C{¹H} NMR (50 MHz, CDCl₃): δ 154.16-121.09 (aryl C), 72.82 (d, *J*(PC) = 80 Hz, P(O)CH₂), 35.99 (s × 2, ArCH₂Ar), 34.35 (s, C(CH₃)₃), 34.03 (s, C(CH₃)₃), 33.70 (s × 2, ArCH₂Ar), 31.40 (s, C(CH₃)₃), 31.01 (s, C(CH₃)₃), 26.39 (s, CH₂-8-mq). ³¹P{¹H} NMR (121 MHz, CDCl₃): δ 88.5 (s, P(OAr)₃), 31.0 (br s, P(O)Ph₂). Found: C, 63.30; H, 5.96; calc. for C₆₇H₇₂CINO₅P₂Pd·CH₂Cl₂ (M_r = 1283.09) C, 63.34; H, 5.76%.

(8-Methylquinolinylmethyl-*C,N*){5,11,17,23-tetra-*tert*-butyl-25-(ethoxycarbonyl-methoxy)-26,27,28-(μ_3 -phosphorustrioxy)calix[4]arene}palladium(II) tetrafluoroborate (21).



A solution of AgBF₄ (0.017 g, 0.09 mmol) in THF (1 cm³) was added to a solution of **12** (0.093 g, 0.09 mmol) in CH₂Cl₂ (20 cm³). After stirring for 5 min, the solution was filtered through Celite and concentrated under vacuum. Addition of hexane afforded **21** as a pale yellow powder. Yield: 0.080 g, 0.073 mmol, 81%. Mp > 196–197 °C (decomp.). IR (CH₂Cl₂) ν_{max} /cm⁻¹: 1685 (C=O). ¹H NMR (300 MHz, CDCl₃): δ 8.95–8.93 (m, 1H, arom. H of 8-mq), 8.35 (d, ³J = 8.2 Hz, 1H, arom. H of 8-mq), 7.65 (d, ³J = 8.0 Hz, 1H, arom. H of 8-mq), 7.45–7.30 (m, 3H, arom. H of 8-mq), 7.21 and 7.19 (AB q, ⁴J = 0 Hz, 4H, *m*-ArH), 7.13 (s, 2H, *m*-ArH), 6.77 (s, 2H, *m*-ArH), 4.70 (s, 2H, OCH₂CO₂), 4.61 and 3.61 (AB q, ²J = 14.5 Hz, 4H, ArCH₂Ar), 4.56 and 3.61 (AB q, ²J = 14.5 Hz, 4H, ArCH₂Ar), 4.44 (q, ³J = 6.8 Hz, 2H, CH₂CH₃), 3.51 (s, 2H, CH₂ of 8-mq), 1.35 (t, ³J = 6.8 Hz, 3H, CH₂CH₃), 1.35 (s, 18H, C(CH₃)₃), 1.21 (s, 9H, C(CH₃)₃), 0.94 (s, 9H, C(CH₃)₃). ¹³C{¹H} NMR (50 MHz, CDCl₃): δ 150.36–122.89 (aryl C), 71.95 (s, OCH₂CO₂), 63.53 (s, CH₂CH₃), 36.02 (s × 2, ArCH₂Ar), 34.45 (s, C(CH₃)₃), 34.16 (s × 2, C(CH₃)₃), 33.96 (s, C(CH₃)₃), 33.70 (s × 2, ArCH₂Ar), 31.27 (s × 3, C(CH₃)₃), 30.98 (s, C(CH₃)₃), 14.90 (s, CH₂CH₃), the CH₂ signal of 8-mq was not detected. ³¹P{¹H} NMR (121 MHz, CDCl₃): δ 87.8 (s, P(OAr)₃). FAB mass spectrum: m/z 1010.4 ([M - BF₄]⁺, 100%). Found: C, 63.21; H, 6.43; N, 1.32; calc. for C₅₈H₆₇BF₄NO₆PPd (M_r = 1098.354): C, 63.42; H, 6.15; N, 1.28%.

(8-Methylquinolinylmethyl-*C,N*){5,11,17,23-tetra-*tert*-butyl-25-(diethylcarbamoyl-methoxy)-26,27,28-(μ_3 -phosphorustrioxy)calix[4]arene}palladium(II) tetrafluoroborate (**22**).



A solution of AgBF₄ (0.017 g, 0.09 mmol) in THF (1 cm³) was added to a solution of **13** (0.095 g, 0.09 mmol) in CH₂Cl₂ (20 cm³). After stirring for 5 min, the solution was filtered through Celite and concentrated under vacuum. Addition of hexane afforded **22** as a pale yellow powder. Yield: 0.094 g, 0.08 mmol, 95%. Mp > 229 °C (decomp.). IR (CH₂Cl₂) $\nu_{\text{max}}/\text{cm}^{-1}$: 1603 (C=O). ¹H NMR (300 MHz, CDCl₃): δ 8.68-8.64, 8.34-8.31, 7.90-7.85, 7.65-7.61 and 7.44-7.36 (6H, arom. H of 8-mq), 7.19 and 7.15 (AB q, ⁴J = 2.4 Hz, 4H, *m*-ArH), 7.17 (s, 2H, *m*-ArH), 6.98 (s, 2H, *m*-ArH), 4.93 (s, 2H, OCH₂C(O)N), 4.62 and 3.62 (AB q, ²J = 13.9 Hz, 4H, ArCH₂Ar), 4.49 and 3.55 (AB q, ²J = 13.5 Hz, 4H, ArCH₂Ar), 3.72 (q, ³J = 7.2 Hz, 2H, CH₂CH₃), 3.58 (m, 4H, CH₂CH₃ and CH₂ of 8-mq), 1.31 (t, 6H, CH₂CH₃), 1.31 (s, 18H, C(CH₃)₃), 1.24 (s, 9H, C(CH₃)₃), 1.13 (s, 9H, C(CH₃)₃). ¹³C{¹H} NMR (50 MHz, CDCl₃): δ 171.04 (s, CO), 151.47-123.36 (aryl C), 71.14 (s, OCH₂C(O)N), 42.84 and 42.26 (s × 2, CH₂CH₃), 36.32 (s × 2, ArCH₂Ar), 34.60 (s × 2, ArCH₂Ar), 34.50 (s, C(CH₃)₃), 34.22 (s, C(CH₃)₃), 34.15 (s × 2, C(CH₃)₃), 31.32 (s, C(CH₃)₃), 31.24 (s × 3, C(CH₃)₃), 20.02 (s, CH₂-8-mq), 13.87 and 13.14 (s × 2, CH₂CH₃). ³¹P{¹H} NMR (121 MHz, CDCl₃): δ 87.0 (s, P(OAr)₃). Found: C, 63.82; H, 6.46; N, 2.47; calc. for C₆₀H₇₂BF₄N₂O₅PPd (M_r = 1124.424): C, 64.03; H, 6.45; N, 2.49%.

5.3 Hydroformylation experiments

The hydroformylation experiments were carried out in a glasslined, 100 cm³ stainless steel autoclave containing a magnetic stirring bar. In a typical run, the autoclave was charged under nitrogen with 0.5 cm³ of a 4 mM toluene solution of [Rh(acac)(CO)₂], 10 equiv. of ligand (0.02 mmol) and 14.5 cm³ of toluene. Once closed, the autoclave was flushed twice with syngas (CO-H₂ 1:1 v/v), then pressurised with 15 bar of the CO-H₂ mixture and heated for 2 h at 80 °C. The autoclave was then allowed to cool to room temperature and depressurised. A mixture of internal standard (decane, 0.5 cm³, 2.56 mmol) and 1-octene (1.57 cm³, 10 mmol) was then added to the catalyst mixture. The autoclave was pressurised to 20 bar, then heated to 80 °C (leading to a 22 bar pressure). Progress of the reaction was checked by monitoring the pressure decrease. During the experiments, several samples were taken, which were diluted with toluene and analysed by GC. In view of the relatively low isomerisation observed, the reaction was not quenched with P(OBuⁿ)₃ at the end of the catalytic run.

5.4 X-Ray crystallography

Crystal data for **9**. Crystals suitable for X-ray diffraction were obtained by slow evaporation of an acetonitrile solution of the complex: C₁₁₄H₁₂₈Cl₂O₁₀P₄Pt·5CH₃CN·H₂O, $M = 2271.46$, triclinic, space group $\bar{P}\bar{1}$, colourless, $a = 16.3979(1)$, $b = 17.5637(1)$, $c = 24.1629(1)$ Å, $\alpha = 71.905(6)$, $\beta = 84.340(6)$, $\gamma = 65.213(6)$ °, $U = 6001.5(1)$ Å³, $D_c = 1.26$, $Z = 2$, $\mu = 1.325$ mm⁻¹, $F(000) = 2368$. Data were collected on a Nonius KappaCCD diffractometer (graphite Mo-Kα radiation, $\lambda = 0.71073$ Å) at -100 °C. 37630 Reflections collected with (2.5 < θ < 27.53°), 22183 data with $I > 3\sigma(I)$. The structure was solved by direct methods and refined anisotropically on F^2 using the Open-MoleN package.⁴¹ Hydrogen atoms were included using a riding model or rigid methyl groups. No hydrogen atoms were located by Fourier difference for either the acetonitrile or the water molecules. Some atoms were refined isotropically [C(108)-C(113), C(117), C(118), N(2), O(11)]. The molecule crystallises with 5 acetonitrile molecules, two of which are located inside the two calixarene cavities, and one water molecule. Final results: $R(F) = 0.060$, $wR(F) = 0.074$, goodness of fit = 1.077, 1256 parameters, largest difference peak = 1.3 e Å⁻³.

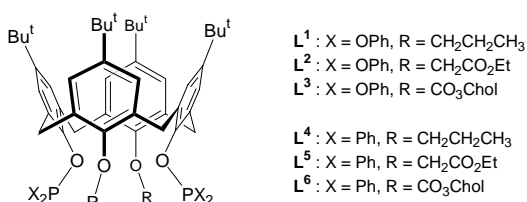
Crystal data for 22. Crystals suitable for X-ray diffraction were obtained by slow diffusion of hexane into a dichloromethane solution of the complex: C₆₀H₇₂BF₄N₂O₅PPd·3CH₂Cl₂·0.5C₆H₁₄, $M = 1423.24$, triclinic, space group $P\bar{1}$, pale yellow, $a = 13.7230(4)$, $b = 14.6378(4)$, $c = 18.4221(6)$ Å, $\alpha = 87.411(2)$, $\beta = 88.7070(13)$, $\gamma = 78.6180(13)^\circ$, $U = 3623.70(19)^3$, $D_c = 1.304$, $Z = 2$, $\mu = 0.555$ mm⁻¹, $F(000) = 1478$. Data were collected on a Nonius KappaCCD diffractometer (graphite Mo-Kα radiation, $\lambda = 0.71073$ Å) at -90 °C. 21214 Reflections collected with $(1.02 < \theta < 27.48^\circ)$, 9432 data with $I > 2\sigma(I)$. The structure was solved by direct methods and refined anisotropically on F^2 using the SHELXL-97 procedure.⁴² Hydrogen atoms were included using a riding model or rigid methyl groups. The hexane molecule has been idealised. Final results: $R(F^2) = 0.063$, $wR(F^2) = 0.176$, goodness of fit = 1.048, 773 parameters, largest difference peak = 1.56 e Å⁻³.

***BIS-PHOSPHITES AND BIS-PHOSPHINITES BASED ON
DISTALLY-FUNCTIONALIZED CALIX[4]ARENES:
COORDINATION CHEMISTRY AND USE IN RHODIUM-
CATALYSED, LOW-PRESSURE OLEFIN
HYDROFORMYLATION.***

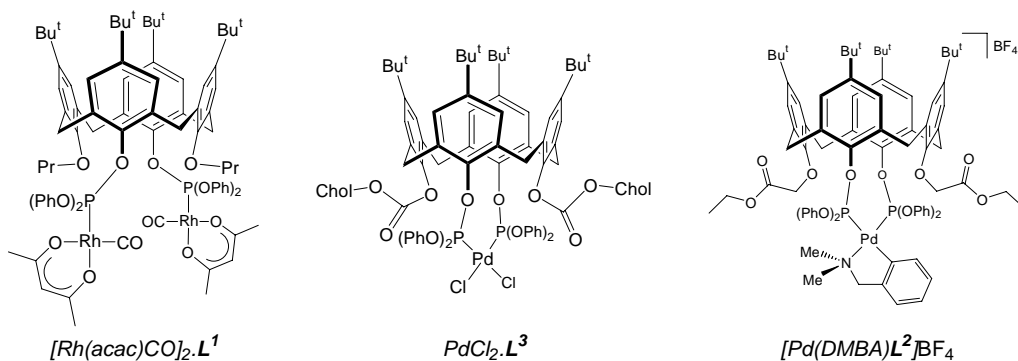
Résumé	2
1 Introduction	3
2 Results and discussion	5
2.1 Ligand syntheses	5
2.2 Catalytic studies	10
2.2.1 Hydroformylation of octene	11
2.2.2 Hydroformylation of styrene	15
3 Conclusion	16
4 References	18
5 Experimental	19

Résumé

La seconde partie de ce mémoire décrit des calixarènes porteurs de deux groupes PX_2 ($X = OPh$ ou Ph) greffés sur des atomes d'oxygène occupant des positions distales de la matrice. Ces ligands (\mathbf{L}^1 - \mathbf{L}^6) ont été obtenus par introduction de deux fragments PX_2 ($X = OPh$ ou Ph) sur des calixarènes 1,3-dialkylés (propoxy, ester, carbonate de cholestéryle). Les ligands formés adoptent tous la conformation "cône". Les diphosphites \mathbf{L}^1 - \mathbf{L}^3 peuvent se comporter soit comme ligands *bis*-monodentates κ^1P , κ^1P' (ex. $\{[Rh(acac)CO]_2\mathbf{L}^1\}$), soit en ligand chélatant par exemple $[PdCl_2\mathbf{L}^3]$ $[Pd(DMBA)\mathbf{L}^2]BF_4$. Ce dernier complexe s'isomérise lentement, en solution, en un oligomère où le phosphite devient ligand pontant. Cette transformation qui s'accompagne d'une diminution des contraintes angulaires autour du centre de coordination, est vraisemblablement induite par la forte influence *trans* de l'atome de carbone métallé du ligand $Me_2NCH_2C_6H_4$.

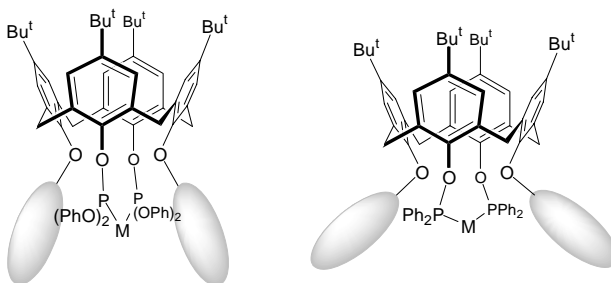


Diphosphites \mathbf{L}^1 - \mathbf{L}^3 et diphosphinites \mathbf{L}^4 - \mathbf{L}^6



Associés à du rhodium, tous les ligands synthétisés se sont avérés actifs en hydroformylation d'oléfines. Dans le cas de l'octène, les phosphinites présentent une activité supérieure aux phosphites (ex. $TOF = 2600 \text{ mol}(octène).\text{mol}(Rh)^{-1}.\text{h}^{-1}$ avec $Rh(acac)(CO)_2/\mathbf{L}^4$). En revanche, les phosphites sont plus sélectifs que les phosphinites

correspondants. Ainsi, alors qu'avec les phosphinites les rapports L/B sont généralement proches de 2, ce rapport est toujours supérieur à 5 avec les phosphites et peut dépasser 10 lorsqu'on emploie des diphosphites porteurs de fonctions auxiliaires carbonylées. La comparaison avec le rapport L/B = 2.8, obtenu avec $\text{P}(\text{OPh})_3$, suggère qu'avec les phosphites une coordination transitoire de la fonction latérale se produit lors de la réaction catalytique. Ce phénomène accentue vraisemblablement la formation d'une poche autour du métal favorisant la formation d'un intermédiaire "Rh(*n*-alkyle)" par rapport à un intermédiaire "Rh(*iso*-alkyle)". A signaler que les modèles moléculaires montrent qu'avec les diphosphites, les fonctions auxiliaires sont plus proches du métal qu'avec les phosphinites. Ce rapprochement est facilité par l'encombrement plus faible des groupes $\text{P}(\text{OPh})_2$ par rapport aux groupes PPh_2 .

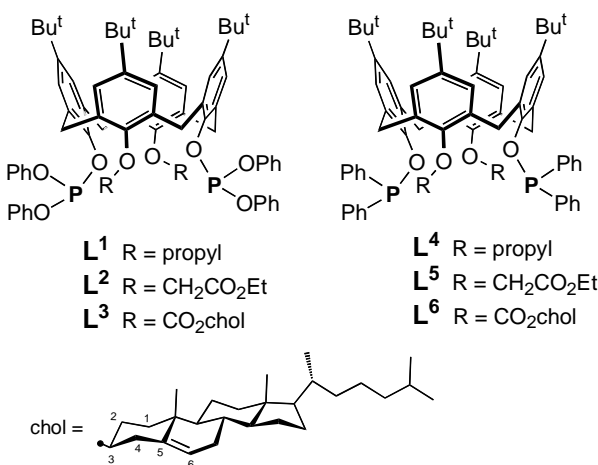


Ces ligands ont également été testés en hydroformylation du styrène. Dans tous les cas, le rapport L/B est supérieur à ce qu'on observe avec PPh_3 (L/B = 5/95). C'est avec les ligands porteurs de groupements carbonyle que cet effet est le plus marqué (ex L/B = 40/60 avec **L⁶**). La quantité anormalement élevée d'aldéhyde linéaire semble confirmer les conclusions déduites de l'étude d'hydroformylation de l'octène. On peut mentionner qu'aucune induction asymétrique n'est observée avec les ligands chiraux **L³** et **L⁶**, probablement parce que les centres stéréogènes sont trop éloignés du centre catalytique.

1 Introduction

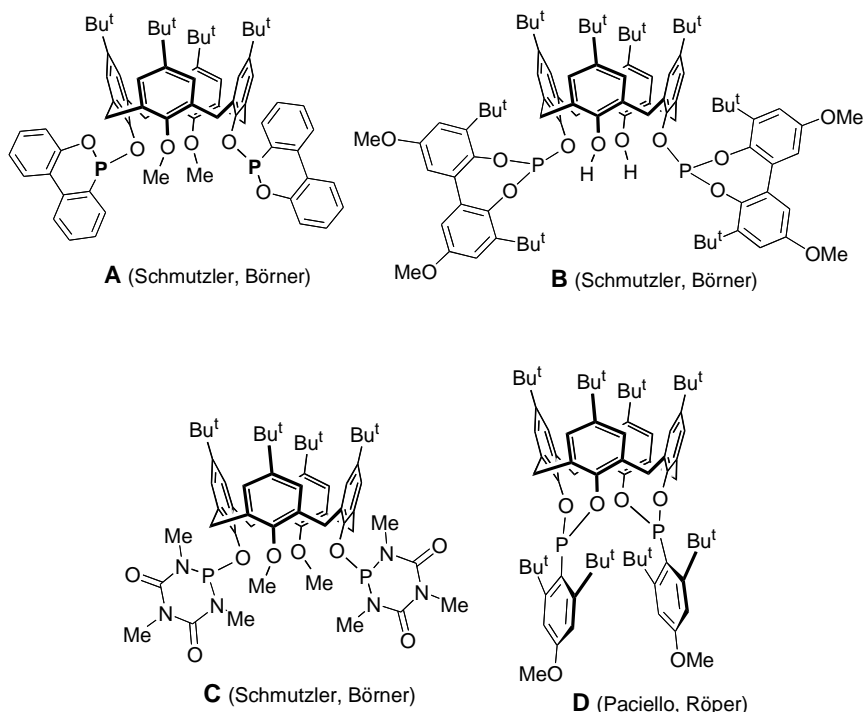
The calix[4]arene platform allows several ligating moieties to be assembled in a convergent manner about one metal centre, thereby forming a complex with a well-defined coordination environment.¹⁻³ Although there are now numerous examples of

multiply P(III)-substituted calixarenes,⁴⁻⁶ catalytic chemistry with such ligands is only at its beginning. Among the most striking contributions in this field are some recent studies dealing with the use of calixarene-phosphites in rhodium-catalysed olefin hydroformylation.⁷⁻¹¹ The importance of phosphites and especially of bulky phosphites in hydroformylation arises from the higher reaction rates they produce in comparison to triphenylphosphine.¹² In the present study, we report the synthesis and coordinative properties of calix[4]arenes in which two non-cyclic PR₂ groups have been tethered at distal phenolic oxygen atoms, the other two phenolic functions being substituted either by a non-coordinating group (e.g. n-Pr as in L¹) or by a podand arm containing a moderately strong coordinating function (CH₂CO₂Et, L²; CO₂cholesteryl, L³). The resulting phosphites were assessed in the hydroformylation of octene and styrene and also compared to the related diphosphinites L⁴-L⁶.



The present study complements an interesting catalytic study recently reported by Schmutzler and Börner, based on the use of the related ligands A-C,^{10,11} in which the P centres, as part of a ring, are sterically considerably more demanding than those of the phosphite centers in L¹-L³.¹³ The catalysts reported by these authors were shown to be highly active in the hydroformylation of 1-octene and to lead to lower linear aldehyde selectivities than conventional Rh/PPh₃ systems. Paciello and Röper reported on another chelating calixarene-diphosphite, D, which displays remarkably high nonanal selectivities (99.5 %) in octene hydroformylation.⁷ Here again, the P atoms are part of a ring. Finally, we wish to mention that calixarene-monophosphites in which the phosphorus atom acts as a triple μ_3 -O,O,O bridge were also used recently in olefin hydroformylation. These phosphites were found to be quite robust and to provide highly

active hydroformylation catalysts.^{8,9,14} It should be recalled that diphosphites are usually preferred over monophosphites in octene hydroformylation since they lead to higher 1:b ratios.¹²



2 Results and discussion

2.1 Ligand syntheses

The present study required the synthesis of the 1,3-difunctionalized calixarenes **1-3**. Precursors **1** and **2** were prepared according to reported procedures, while calixarene **3** was obtained in good yield by reacting *p*-*tert*-butyl-calix[4]arene with cholesteryl chloroformate in the presence of NEt₃. Unlike **1** and **2**, which adopt a stable cone conformation, compound **3** is conformationally mobile, the two unsubstituted phenol rings flipping quickly through the calixarene annulus. This conclusion was inferred from a 2D-NMR study which established a spatial proximity between the *m*-H of the ArOH rings and both methylenic protons of the ArCH₂ groups (Fig. 1). Note that **3** contains 16 asymmetric carbon atoms.

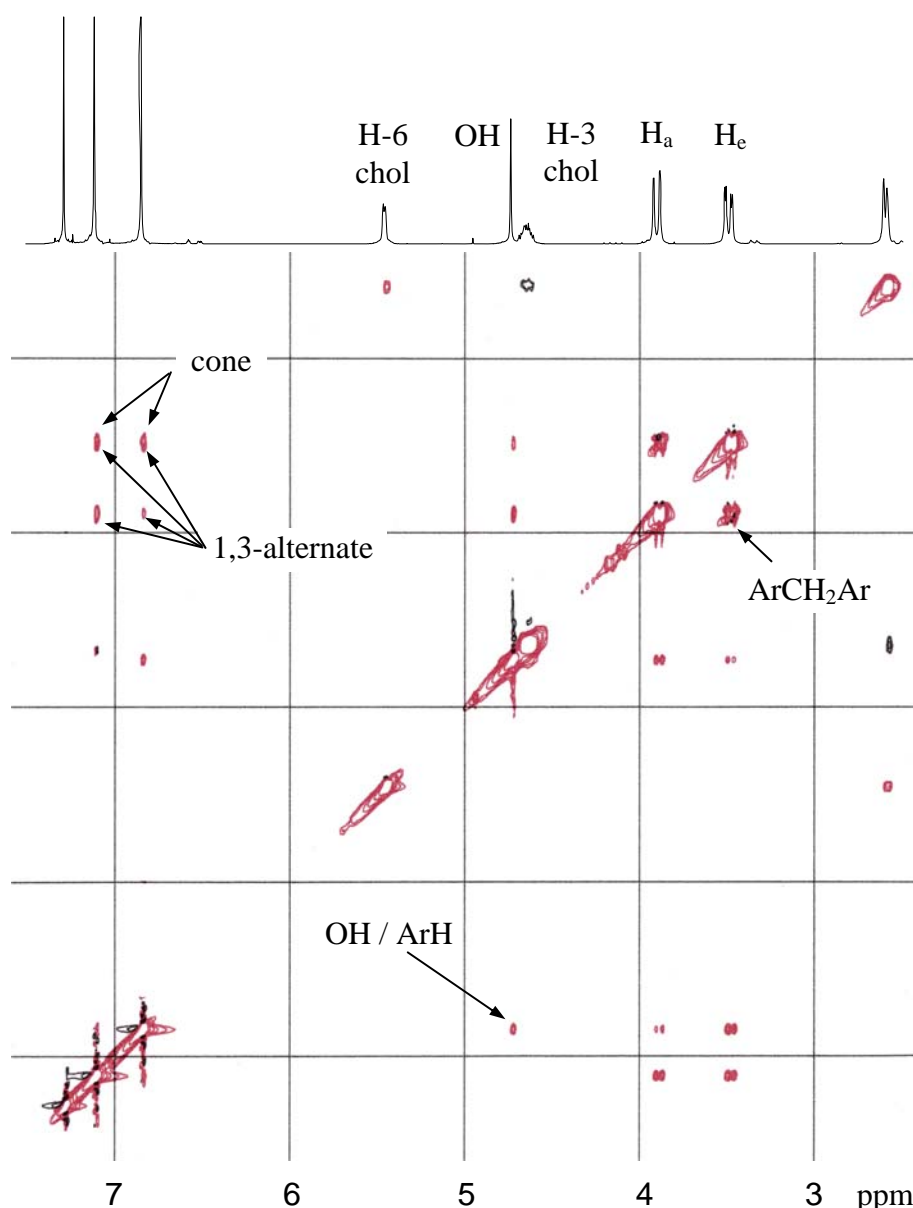
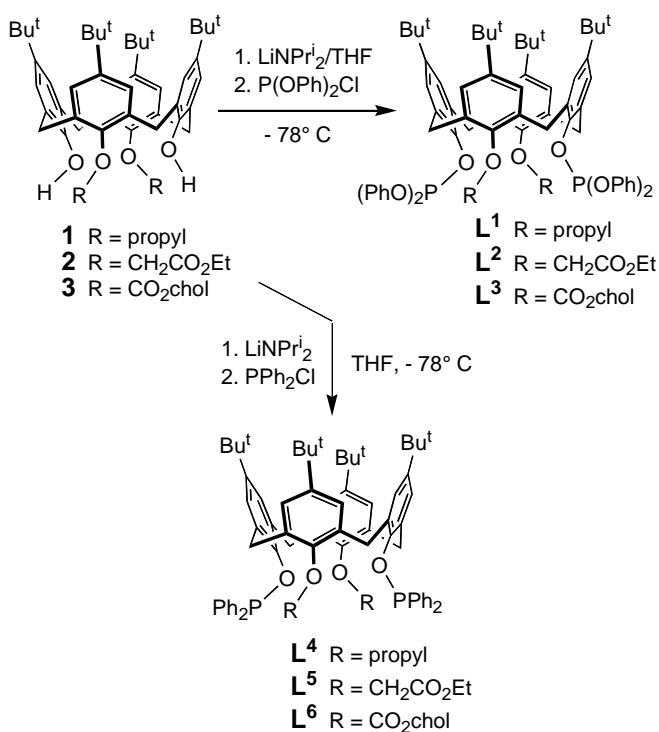


Fig. 1. NOESY spectrum (500 MHz, CDCl_3) of **3**.

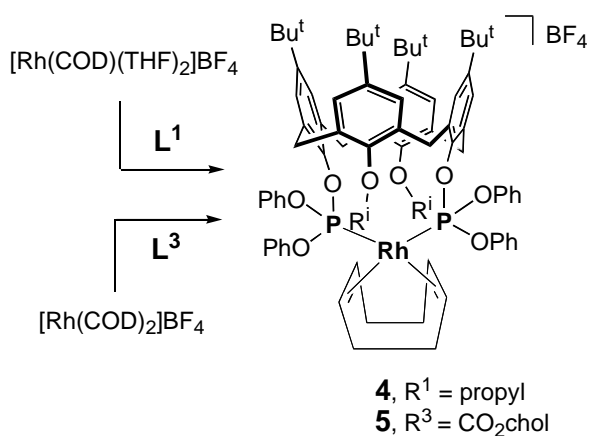
The three diphosphites **L¹-L³** were obtained by reacting the appropriate dihydroxy precursor with LiNPr_2^i and chlorodiphenylphosphite in THF. All three ligands are highly soluble in alkanes. Typically for triarylphosphites, each ^{31}P NMR spectrum displays a peak near 130 ppm.¹⁵ In the corresponding ^1H NMR spectra, the bridging ArCH_2Ar groups appear as AB patterns with AB separations larger than 1 ppm ($\Delta_{\text{AB}} = 1.48$ (**L¹**), 1.71 (**L²**), 1.34/1.36 (**L³**)), hence allowing unambiguous assignment of a cone conformation to all three calixarenes.¹⁶ This geometry was further confirmed by the ^{13}C NMR spectra that display ArCH_2Ar signals in the range expected for syn-oriented phenolic neighbours (≈ 29 -33 ppm).¹⁷ It is interesting to note that despite the dynamic

behaviour of **3**, anchoring of two "P(OPh)₂" units to this precursor selectively resulted in the formation of a conical species rather than a 1,3-alternate or a partial cone conformer. For the catalytic study (*vide infra*), the related phosphinites **L⁴-L⁶** were also prepared. These were obtained in a similar fashion using the same precursors, but with Ph₂PCl as reagent and like the related phosphites, all three adopt a cone conformation. They are characterized by phosphinite signals near 122 ppm in the corresponding ³¹P NMR spectra. As already observed for **L^{1-L³}**, the three phosphinites display high solubility in alkanes.



Our earlier studies have shown that certain 1,3-diphosphinito-calix[4]arenes are suitable for chelation, provided that the complexation reaction is carried out with a labile, cationic species that allows fast complexation.¹⁸ In the present study, the chelating ability of the phosphites **L^{1-L³}** was assessed by their reactions with square planar Rh(I) or Pd(II) precursors. Thus, reaction of **L¹** with one equiv. of [Rh(COD)(THF)₂]BF₄ (COD = 1,5-cyclooctadiene) afforded complex **4** in high yield, while reaction of **L³** with [Rh(COD)₂]BF₄ readily gave the related complex **5**. The ³¹P NMR spectra of these complexes are characterised by a doublet with a *J*(PRh) coupling constant of *ca.* 250 Hz (**4**: 101.0 ppm, *J*(PRh) = 252 Hz; **5**: 99.7 ppm, *J*(PRh) = 254

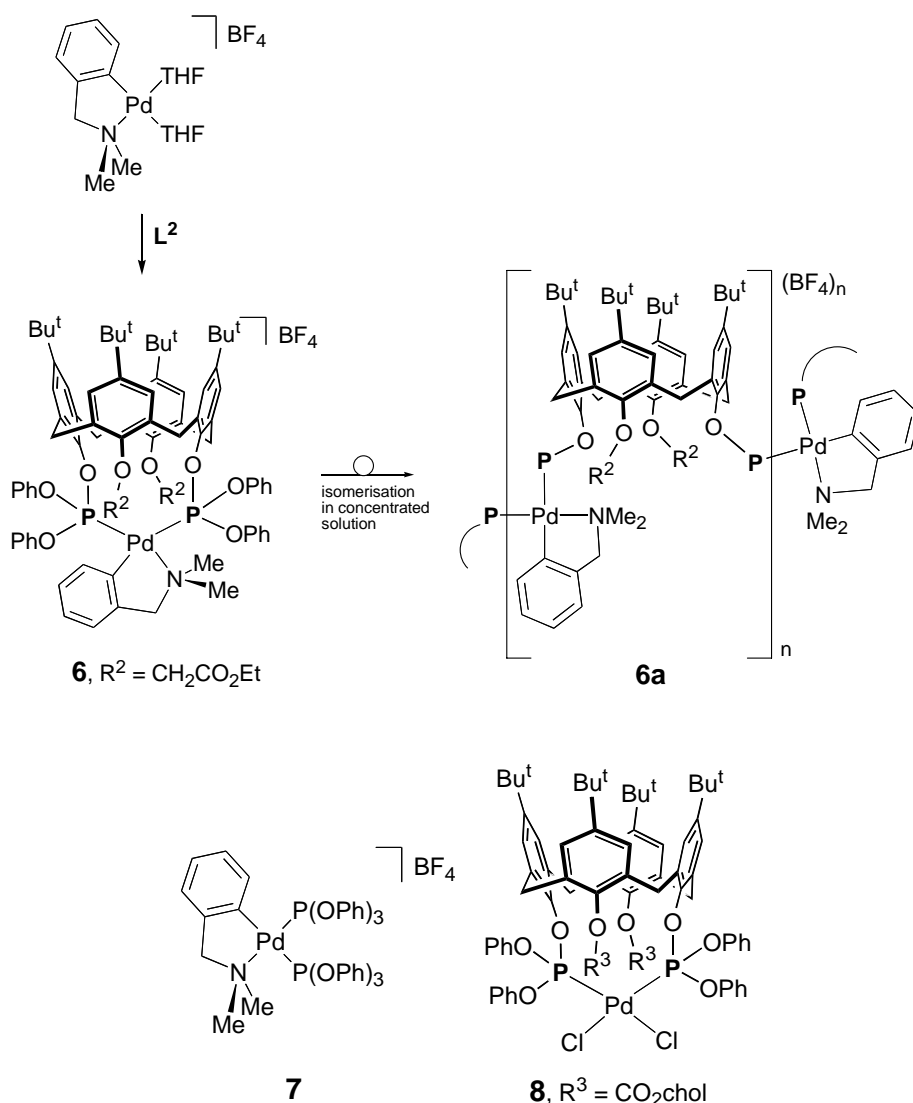
Hz). Chelate formation was inferred from the corresponding FAB MS spectra, which both show the expected $(M\text{-BF}_4)^+$ peak.



Reaction at high dilution of **L**² with the cyclometallated complex $[\text{Pd}(o\text{-C}_6\text{H}_4\text{CH}_2\text{NMe}_2)(\text{THF})_2]\text{BF}_4$ afforded in high yield the chelate complex **6**. Its MS spectrum (electrospray) shows an intense peak at m/e 1492 corresponding to the $[M\text{-BF}_4]^+$ ion. The ^{31}P NMR spectrum of **6** is characterized by an AB system with $\delta_A = 141.6$ and $\delta_B = 115.2$ ppm. The observed $J(\text{PP}')$ coupling constant, 54 Hz, is not unusual for cis-disposed phosphites (such coupling constants can reach values as high as 150 Hz)^{19,20} and hence, no conclusion about the ligand's bite angle in **6** can be drawn from this value. Upon standing complex **6** slowly converts irreversibly into another species, **6a**, characterized by an AB spectrum as well, with $J(\text{PP}') = 86$ Hz, but in this case the AB separation is only 9 ppm. It is likely that **6a**, which was not isolated, has an oligomeric structure in which the diphosphite behaves as a bridging unit. Its formation is probably favoured by the strong trans influence of the metallated carbon atom which by labilising the trans-positioned P atom results in formation of a less strained structure.

We devised that due to the strain release resulting from chelate opening, the PPdP' angles of **6a** would come closer to 90° . The ^{31}P NMR spectrum of **6a** was therefore compared to that of the bis-triphenylphosphite complex $[\text{Pd}(o\text{-C}_6\text{H}_4\text{CH}_2\text{NMe}_2)\{\text{P}(\text{OPh})_3\}_2]\text{BF}_4$ **7**, which was prepared in situ. The shape and position of the corresponding AB pattern is indeed very close to that of **6a** (AB separation: 11 ppm; $J(\text{PP}') = 89$ Hz). Finally, we note that the ^1H NMR spectrum of **6** reveals that the molecule has a C_1 -symmetrical structure (reflected, e.g. in inequivalence of the Bu^t

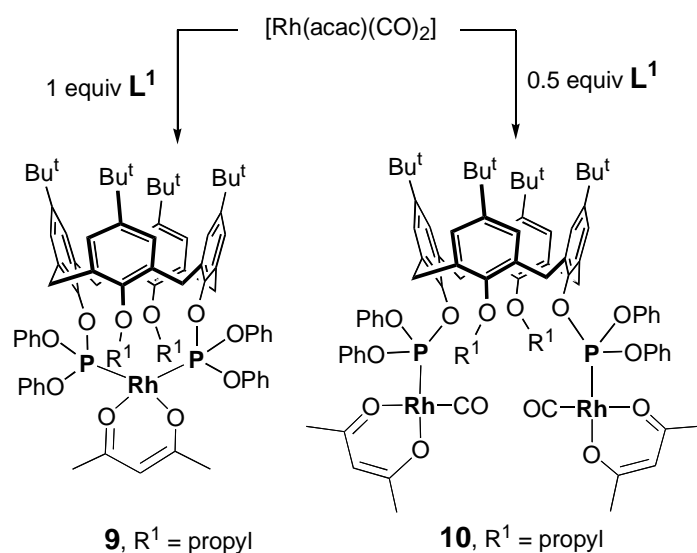
groups), an observation which suggests that the coordination plane of this chelate complex is inclined with respect to the calixarene axis.



Neutral chelate complexes of the phosphites could also be synthesised. Thus for example, reaction of [PdCl₂(COD)] with L³ afforded complex **8** in high yield, but this reaction needed to be carried out at medium to high dilution conditions in order to avoid oligomer formation. The formation of a chelate was established by an osmometric molecular weight determination (see experimental section).

The mononuclear complex **9** was formed by reacting one equiv. of diphosphine L¹ with [Rh(acac)(CO)₂]. As a result of fast CO displacement, this reaction did not need to be carried out at high dilution. When the reaction was repeated with only 0.5 equiv.

of **L¹**, the binuclear complex **10** was formed quantitatively. As shown by an NMR study, **10** is an intermediate in the synthesis of the chelate **9**.



2.2 Catalytic studies

The beneficial role of P(III)-ligands in rhodium-catalysed hydroformylation is well established and many sophisticated P-ligands have been designed over the last 40 years which have illustrated how the performance of rhodium-P(III) complexes depends on both the electronic and steric factors of the ligand. In the early 1990s, it became apparent that diphosphines having a natural bite angle larger than 90° may lead to high l:b ratios in the hydroformylation of alkenes.²¹ This behaviour was attributed to the greater stabilisation of reaction intermediates when the diphosphine can chelate in a diequatorial rather than equatorial-axial mode, the former favouring the formation of the linear aldehyde. However, recently van Leeuwen *et al.*²² and others²³ convincingly demonstrated that bis-equatorial coordination is not a prerequisite for high linearity. In view of these recent results, it appears that predicting the outcome of catalytic hydroformylation reactions still remains a difficult task, many parameters contributing to the formation of a major compound. One aspect of ligand design that certainly deserves more attention concerns the use of ligand systems able to generate about the metal centre pockets the walls of which may sterically interact with the coordinated olefin or the corresponding Rh-alkyl derivative.

The bulky phosphite and phosphinite ligands described above were tested in the rhodium-catalysed hydroformylation of 1-octene and styrene. All runs were carried out at 80 °C under a CO/H₂ pressure of 20 bar. Unless otherwise specified, the catalyst precursors were prepared *in situ*, in toluene at 80 °C, from [Rh(acac)(CO)₂] and the appropriate ligand under CO/H₂. The metal:olefin ratio applied during catalysis was 1:2500 in all cases. The ligand:metal ratio was between 1:1 and 4:1.

2.2.1 Hydroformylation of octene

The phosphites **L¹-L³** were investigated first. All three ligands, when mixed with [Rh(acac)CO]₂, effectively catalyse the hydroformylation of octene. It turned out that long activation periods (15 h) resulted in activities significantly better than those observed when the activation was stopped after 2 h (Table 1). However, we found that the 2 h activations could be made more efficient by adding NEt₃ to the [Rh(acac)(CO)₂] solution. The highest TOF, 1204 mol.(mol Rh)⁻¹.h⁻¹, was observed with the dipropyl derivative **L¹** and by using a L:Rh ratio of 1:1 (Table 1). For all three diphosphites, the activity dropped, as expected, on increasing the L:Rh ratio, while the selectivity for nonanal increased (*vide infra*). The observed activities are not unusual and fall in the range reported for other diphosphites.¹² As found with other diphosphites, olefin isomerisation occurred during catalysis, but in the present runs the amounts of internal olefins did not exceed 12 %. The l:b ratios (Table 1) observed with **L¹-L³**, when present in excess, were higher than those obtained with the moderately bulky diphosphites **E** and **F**, although the activities of the latter were higher. The most striking results are the rather high l:b ratios, ca. 10, observed with ligands **L²** and **L³**, both bearing side groups that incorporate a carbonyl function (*cf.* l:b = 5 for the dipropylated calixarene **L¹**, l:b = 2.2 for **E**, l:b = 1.2 for **F**, and l:b = 2.8 for P(OPh)₃).

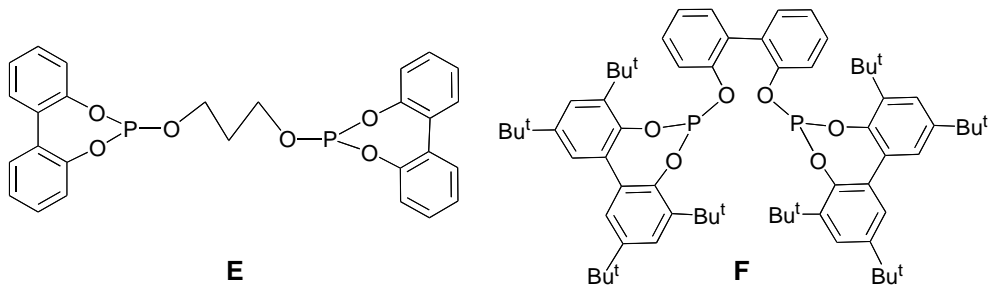


Table 1. 1-Octene hydroformylation with phosphites **L¹-L³**.

Ligand	L/Rh	Activation period	TOF ^b	l:b ^c	Isomerisation ^d (%)
P(OPh) ₃	20		-	2.8	-
L¹	1	2 h	632	2.59	6.97
L¹	1	15 h	1204	2.35	9.15
L¹	1	2 h (+ 30 NEt ₃)	816	2.61	8.41
L¹	2	2 h	120	5.02	5.15
L¹	2	15 h	156	4.99	4.29
L¹	2	2 h (+ 30 NEt ₃)	129	5.33	5.50
L¹	4	2 h	124	5.33	1.85
L²	1	2 h	416	2.82	4.34
L²	1	15 h	629	3.17	8.03
L²	1	2 h (+ 30 NEt ₃)	707	2.85	12.00
L²	2	2 h	60	9.57	6.98
L²	2	15 h	247	9.56	3.09
L²	2	2 h (+ 30 NEt ₃)	211	8.99	6.66
L²	4	2 h	62	9.66	6.78
L³	1	2 h	328	2.86	5.50
L³	1	15 h	1045	2.70	11.64
L³	1	2 h (+ 30 NEt ₃)	580	2.71	12.28
L³	2	2 h	39	10.61	8.57
L³	2	15 h	65	10.65	4.86
L³	2	2 h (+ 30 NEt ₃)	55	10.70	8.00
L³	4	2 h	38	9.23	6.32

^a 1-octene/Rh = 2500. Initial pressure (at 80 °C) P = 20 bar CO/H₂ (1/1), T = 80 °C, toluene/n-decane (20 cm³/0.5 cm³). ^b Determined at ca. 30% conversion. ^c The l:b ratio takes into account branched aldehydes when observed. ^d isomerised 1-octene/all octenes.

The origin of the higher aldehyde selectivity of **L¹-L³**, when compared to that of **E**, could of course arise from a bite angle significantly larger than 90°, hence favouring equatorial-equatorial binding of the diphosphite and accordingly driving the catalysis preferentially towards the linear aldehyde. Molecular mechanics calculations carried out with SPARTAN²⁴ indicate that this angle is close to 113° in the square planar complex **8**. Note that in a silver complex obtained from a related diphosphite, a bite angle as high as 134° was found in the solid state, thus illustrating the high flexibility of such diphosphites.¹⁸ A possible explanation for the significantly higher l:b ratios obtained with **L²** and **L³** compared to **L¹** is the marked confinement of the metal inside the pocket constituted by the four OPh groups and the two auxiliary substituents of these calixarenes, a confinement which for steric reasons would favour the formation of a "Rh(*n*-alkyl)" intermediate over that of an "Rh(*iso*-alkyl)" one, whenever the reaction is under thermodynamic control. Note that olefin insertion into the Rh-H bond was shown to occur reversibly with rhodium phosphite complexes. The presence of C=O functions in **L²** and **L³** that may coordinate in a hemilabile fashion is another factor that may regulate the form of the pocket. Thus, the outcome of the reaction is possibly controlled by the shape of the pocket. Molecular mechanics calculations show that in the corresponding phosphinites **L⁴-L⁶**, like in the Börner/Schmutzler systems **A** and **B**, the pocket about the metal is considerably more open, the auxiliary ORⁱ substituents here being pushed outwards by the PPh₂ groups (this is mainly due to the larger cone angles of the individual phosphinite units) (Fig. 2). In keeping with these geometrical features, **L⁴-L⁶** lead to lower selectivities for linear aldehyde (Table 2). It is worth mentioning that these latter selectivities compare with those reported for the 1,3-diphosphonito-2,4-dimethoxy-calixarene **A**.

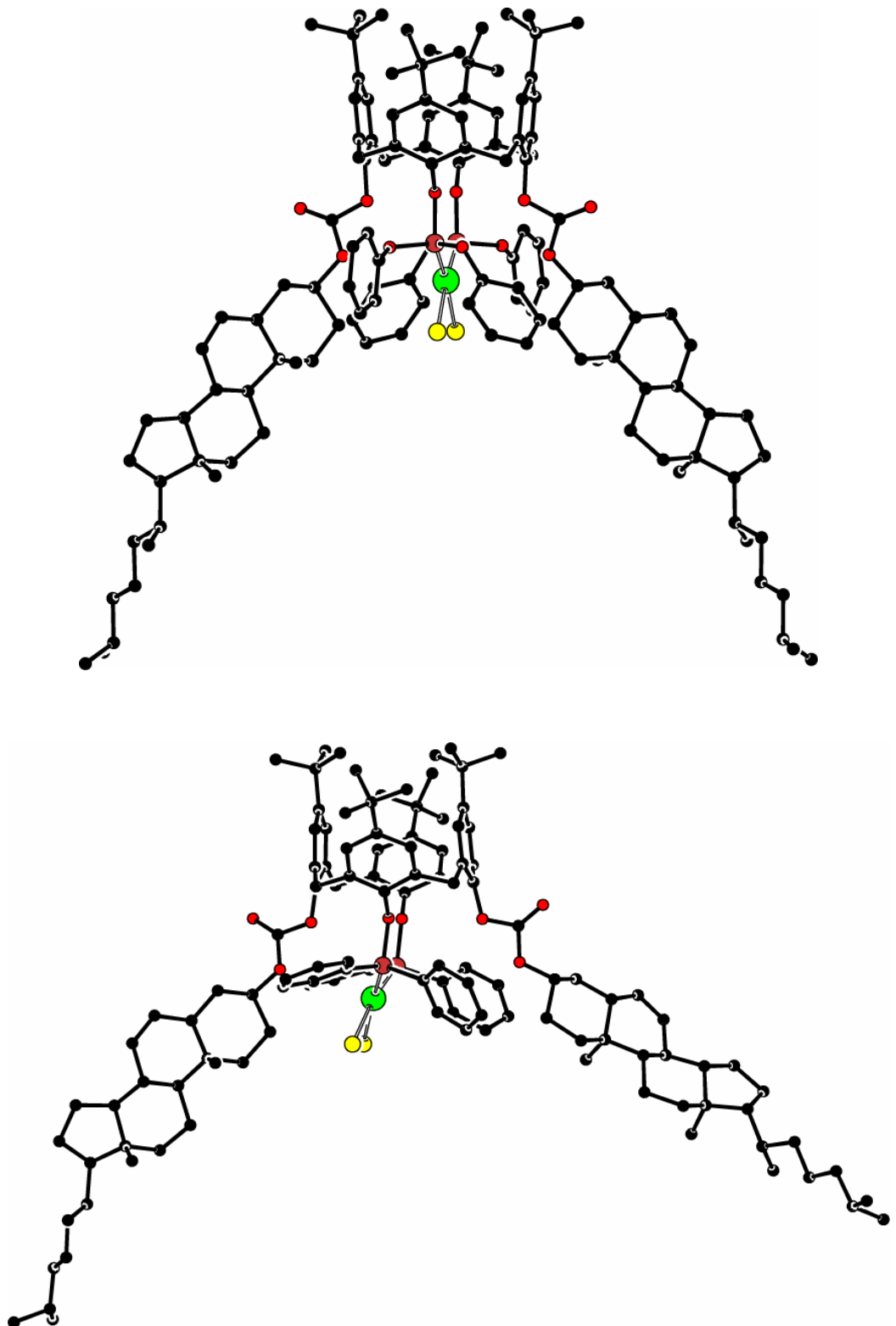


Fig. 2. Molecular modelling structures of $[PdCl_2 \bullet L^3]$ (**8**) (top) and $[PdCl_2 \bullet L^6]$ (bottom) showing the pockets about the metal centre.

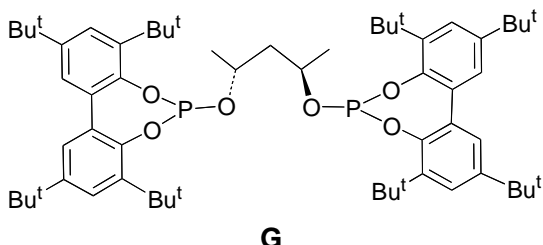
Table 2. 1-Octene hydroformylation with phosphinites **L⁴-L⁶**.

Ligand	L/Rh	TOF ^b	l:b ^c	Isomerisation ^d (%)
L₄	1	2625	1.59	5.84
L₄	2	1660	1.61	2.90
L₅	1	1032	2.49	10.18
L₅	2	110	3.08	5.74
L₆	1	1219	2.19	1.22
L₆	2	1087	2.00	1.60

^a 1-octene/Rh = 2500, initial pressure (at 80 °C) P = 20 bar CO/H₂ (1/1), T = 80 °C, toluene/n-decane (20 cm³/0.5 cm³), incubation overnight. ^b Determined at ca. 30% conversion. ^c The l:b ratio takes into account branched aldehydes when observed. ^d isomerized 1-octene/all octenes.

2.2.2 Hydroformylation of styrene

Hydroformylation of styrene with P-ligands, phosphites and phosphines as well, usually gives high amounts of branched aldehyde. Typically, diphosphite **G** results in a 2-phenylpropanal:3-phenylpropanal ratio of 96:4. For all ligands **L^{1-L⁶}**, the proportion of the linear aldehyde considerably increases (Table 3) in comparison with **G**, be the ligand a phosphite or a phosphinite. For example, with the diester-diphosphite **L²**, b:l = 66/34 while for the diester-diphosphinite **L⁵**, b:l = 64/36. The increased linear aldehyde selectivity corroborates the trend that was found in the hydroformylation of octene. Styrene being sterically more demanding than octene, the substrate sensitivity to the presence of a pocket is possibly enhanced in this case. Finally, we wish to mention that styrene hydroformylation using the preformed cationic complex [Rh(norbornadiene)**L⁴**]SbF₆²⁵ resulted in b:l ratios similar to those obtained with a [Rh(acac)(CO)₂]/**L⁴** 1:1 mixture, hence showing that it is not mandatory to use a pre-formed complex.

**Table 3.** Styrene hydroformylation with **L¹-L⁶**.

Ligand	L/Rh	TOF ^b	b:l	Ligand	L/Rh	TOF ^b	b:l
L₁	1	2033	67/33	L₄	1	854	66/34
L₁	2	1975	63/37	L₄	2	240	74/26
L₂	1	140	66/34	L₅	1	891	64/36
L₂	2	28	88/12	L₅	2	86	64/36
L₃	1	789	73/27	L₆	1	210	59/41
L₃	2	587	75/25	L₆	2	22	67/33

^a styrene/Rh = 2500, initial pressure (at 80 °C) P = 20 bar CO/H₂ (1/1), T = 80 °C, toluene/n-decane (20 cm³/0.5 cm³) , incubation overnight. ^b Determined at ca. 30% conversion.

3 Conclusion

We have shown that the calix[4]arene-derived phosphites and phosphinites used in the present study are suitable for the formation of 14-membered chelate rings and effectively catalyse the hydroformylation of olefins. The unexpected linear selectivities observed in the hydroformylation of octene and styrene are likely to arise from a combination of a bite angle larger than 90° and the existence of a pocket at the metal centre which favours the formation of "Rh-n-alkyl" intermediates, although we have not proved that the reaction is under thermodynamic control (however, this is usually the case with phosphites).¹² The relevance of pocket formation about the metal centre in the outcome of hydroformylation reactions has emerged recently and was formulated on the basis of studies exploiting the particular properties of other diphosphites.²⁶ In these systems, the pockets are generated by large P-substituents, contrasting with the present

where the pockets arise mainly from the presence of appropriate side groups supported by the macrocyclic platform. Variation of these auxiliary groups should result in the formation of optimised pockets.

4 References

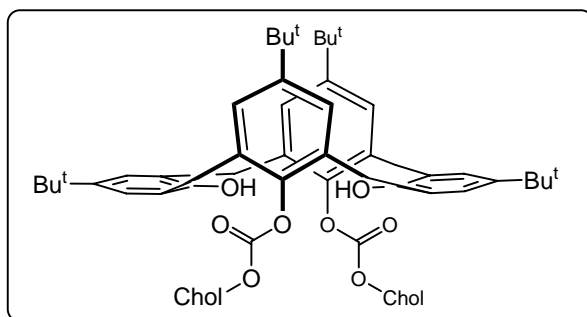
1. C. D. Gutsche, in *Calixarenes Revisited, Monographs in Supramolecular Chemistry*, ed. J. F. Stoddart, The Royal Society of Chemistry, Cambridge, **1998**.
2. S. Steyer, C. Jeunesse, D. Armspach, D. Matt and J. Harrowfield, in *Calixarenes 2001*, Asfari Z., Böhmer V., Harrowfield J., Vicens J. (eds.), Kluwer, Dordrecht, **2001**, pp 513-535.
3. P. D. Harvey, *Coord. Chem. Rev.*, 2002, **233-234**, 289.
4. C. Wieser-Jeunesse, D. Matt, M. R. Yaftian, M. Burgard and J. Harrowfield, *C. R. Acad. Sci. Paris, Ser. IIc*, 1998, **1998**, 479.
5. I. Neda, T. Kaukorat and R. Schmutzler, *Main Group Chemistry News*, 1998, **6**, 4.
6. I. S. Antipin, E. K. Kazakova, W. D. Habicher and A. I. Konovalov, *Russ. Chem. Rev.*, 1998, **67**, 905.
7. R. Paciello, L. Siggel and M. Röper, *Angew. Chem. Int. Ed.*, 1999, **38**, 1920.
8. F. J. Parlevliet, C. Kiener, J. Fraanje, K. Goubitz, M. Lutz, A. L. Spek, P. C. J. Kamer and P. W. N. M. van Leeuwen, *J. Chem. Soc., Dalton Trans.*, 2000, 1113.
9. C. J. Cobley, D. D. Ellis, A. G. Orpen and P. G. Pringle, *J. C. S. , Dalton Trans.*, 2000, 1109.
10. C. Kunze, D. Selent, I. Neda, R. Schmutzler, A. Spannenberg and A. Börner, *Heteroatom Chem.*, 2001, **12**, 577.
11. C. Kunze, D. Selent, I. Neda, M. Freytag, P. G. Jones, R. Schmutzler, W. Baumann and A. Börner, *Z. Anorg. Allg. Chem.*, 2002, **628**, 779.
12. P. C. J. Kamer, J. N. H. Reek and P. W. N. M. Van Leeuwen, in *Rhodium Catalyzed Hydroformylation*, Van Leeuwen, P. W. N. M. and Claver C. (eds.), Kluwer, Dordrecht, **2000**, pp. 35-62.
13. C. Kunze, I. Neda, M. Freytag, P. G. Jones and R. Schmutzler, *Z. Anorg. Allg. Chem.*, 2002, **628**, 545.
14. S. Steyer, C. Jeunesse, D. Matt, R. Welter and M. Wesolek, *J. C. S. , Dalton Trans.*, 2002, 4264.
15. *Handbook of Phosphorus-31 Nuclear Magnetic Resonance Data*, ed. J. C. Tebby, CRC Press, Boca Raton, Florida, **1991**.

16. C. D. Gutsche, in *Calixarenes, Monographs in Supramolecular Chemistry*, ed. J. F. Stoddart, ch. 4, Royal Society of Chemistry, Cambridge, **1989**.
17. C. Jaime, J. de Mendoza, P. Prados, P. M. Nieto and C. Sánchez, *J. Org. Chem.*, 1991, **56**, 3372.
18. C. Jeunesse, C. Dieleman, S. Steyer and D. Matt, *J. Chem. Soc., Dalton Trans.*, 2001, 881.
19. M. F. Garbauskas, J. S. Kasper and L. N. Lewis, *J. Organometal. Chem.*, 1984, **276**, 241.
20. A. M. Trzeciak, W. Wojtków, Z. Ciunik and J. J. Ziolkowski, *Catal. Lett.*, 2001, **77**, 245.
21. C. P. Casey, G. Whiteker, M. G. Melville, L. M. Petrovich, J. A. Gavnev and D. R. Powell, *J. Am. Chem. Soc.*, 1992, **114**, 5535.
22. C. Dieleman, P. C. J. Kamer, J. N. H. Reek and P. W. N. M. van Leeuwen, *Helv. Chim. Acta*, 2001, **84**, 3269.
23. W. Ahlers, M. Roeper, P. Hofmann, D. C. Warth and R. Paciello, (*BASF-AG*) WO 2001058589, 2001.
24. MACSPARTAN, version 1.1.8, Wavefunction, Inc., Irvine, CA, USA, 1998.
25. J. Gagnon, C. Loeber, D. Matt and P. D. Harvey, *Inorg. Chim. Acta*, 1996, **242**, 137.
26. R. Paciello, L. Siggel, H.-J. Kneuper, N. Walker and M. Röper, *J. mol. Catal. A: Chemical*, 1999, **143**, 85.
27. J. Suffert, *J. Org. Chem.*, 1989, **54**, 509.
28. C. D. Gutsche and M. Iqbal, *Org. Synth.*, 1989, **68**, 234.
29. K. Iwamoto, A. Yanagi, K. Araki and S. Shinkai, *Chem. Lett.*, 1991, **3**, 473.
30. E. Collins, A. McKervey and S. J. Harris, *J. Chem. Soc., Perkin Trans. 1*, 1989, 372.
31. C. Loeber, D. Matt, P. Briard and D. Grandjean, *J. C. S., Dalton Trans.*, 1996, 513.
32. J. P. Forsman and D. Lipkin, *J. Am. Chem. Soc.*, 1953, **75**, 3145.
33. W. Hewertson, B. C. Smith and R. A. Shaw, *Inorg. Syntheses*, 1966, **8**, 68.
34. D. Drew and J. R. Doyle, in *Inorg. Syntheses*, Ed. R. J. Angelici, Wiley, New York, **1990**, Vol. 28, 346-349.
35. A. C. Cope and E. C. Friedrich, *J. Am. Chem. Soc.*, 1968, **90**, 909.

5 Experimental

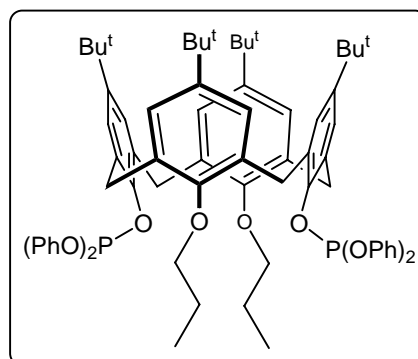
All manipulations involving phosphites and phosphinites were performed in Schlenk-type flasks under dry nitrogen. Solvents were dried by conventional methods and distilled immediately prior to use. CDCl_3 was passed down a 5cm-thick alumina column and stored under nitrogen over molecular sieves (4 Å). Routine ^1H , $^{13}\text{C}\{^1\text{H}\}$ and $^{31}\text{P}\{^1\text{H}\}$ spectra were recorded with Bruker FT instruments (AC-200, AC-300, ARX-500). ^1H NMR spectra were referenced to residual protonated solvents (7.26 ppm for CDCl_3 and 5.32 for CD_2Cl_2), ^{13}C chemical shifts are reported relative to deuterated solvents (77.0 ppm for CDCl_3 and 53.8 ppm for CD_2Cl_2), and the ^{31}P NMR data are given relative to external H_3PO_4 . Mass spectra were recorded either on a ZAB HF VG analytical spectrometer using *m*-nitrobenzyl alcohol as matrix or on a MicroTOF Bruker Daltonic spectrometer (MALDI) using CH_2Cl_2 or CH_3CN as solvant. *n*-BuLi/hexane solutions were titrated according to a conventional method.²⁷ 5,11,17,23-tetra-*tert*-butyl-25,26,27,28-tetrahydroxycalix[4]arene (abbreviated *p*-Bu^t-calix[4]-(OH)₄),²⁸ 5,11,17,23-tetra-*tert*-butyl-25,27-dihydroxy-26,28-dipropoxycalix[4]arene (1),²⁹ 5,11,17,23-tetra-*tert*-butyl-25,27-di(ethoxycarbonylmethoxy)-26,28-dihydroxycalix[4]arene (2),³⁰ 5,11,17,23-tetra-*tert*-butyl-25,27-dipropoxy-26,28-bis(diphenylphosphanyloxy)calix[4]arene (**L**⁴),³¹ 5,11,17,23-tetra-*tert*-butyl-25,27-bis(ethoxycarbonylmethoxy)-26,28-bis(diphenylphosphanyloxy)calix[4]arene (**L**⁵),³¹ $(\text{PhO})_2\text{PCl}$,^{32,33} $[\text{PdCl}_2(\text{COD})]$,³⁴ $[\text{Pd}(o\text{-C}_6\text{H}_4\text{NMe}_2)\text{Cl}]_2$,³⁵ were prepared using literature procedures. The abbreviation dmiba stands for *N,N*-dimethylbenzylamine.

5,11,17,23-Tetra-*tert*-butyl-25,27-bis(cholesteryloxycarbonyloxy)-26,28-dihydroxy-calix[4]arene (3).



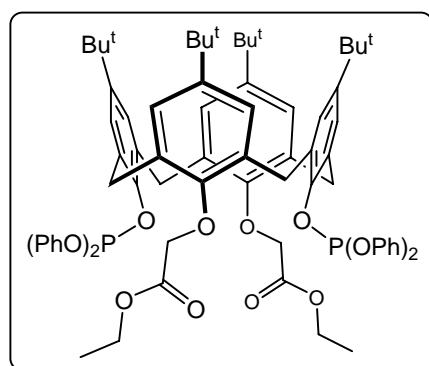
A mixture of *p*-Bu^t-calix[4]-OH₄ (3.245 g, 5.00 mmol), cholesteryl chloroformate (5.614 g, 12.50 mmol) and NEt₃ (5 cm³) in CH₂Cl₂ (100 cm³) was stirred for 12 h at room temperature. The solution was then treated with 50 cm³ HCl (1 M) and water (2 x 50 cm³). The organic layer was dried over MgSO₄ then filtered and evaporated to dryness. The residue was purified by flash chromatography using AcOEt-hexane (25:75, v/v) as eluent. Some unidentified cholesteryl derivatives eluted first followed by **3** (SiO₂, *R*_f = 0.25, AcOEt-hexane, 25:75, v/v). After evaporation, the residue was taken up in CH₂Cl₂. Addition of methanol afforded the product as a white microcrystalline powder. Yield: 6.047 g, 4.10 mmol, 82 %; m.p.: 170-177 °C. IR (KBr, cm⁻¹): ν(C=O) = 1763. ¹H NMR (300 MHz, CDCl₃): δ 7.08 (s, 4H, *m*-ArH), 6.82 (s, 4H, *m*-ArH), 5.42 (d, 2H, H-6, ³J = 4 Hz), 4.70 (s, 2H, OH, exchange with D₂O), 4.60 (m, 2H, H-3), 3.87 and 3.45 (AB spin system, 8H, ArCH₂Ar, ²J = 14 Hz), 2.58-0.69 (86H, 2 x cholesteryl), 1.35 (s, 18H, C(CH₃)₃), 0.97 (s, 18H, C(CH₃)₃). ¹³C{¹H} NMR (50 MHz, CDCl₃): δ 153.31-142.28 (aryl C), 139.38 (C-5 tentative assignment), 131.87-125.90 (aryl C), 123.16 (s, C-6), 79.22 (s, C-3), 56.79 (s, C-14), 56.25 (s, C-17), 50.09 (s, C-9), 42.41 (s, C-13), 39.83 (s, C-12), 39.61 (s, C-1 tentative assignment), 38.03 (s, CH₂), 36.99 (s, CH₂), 36.68 (s, C-10), 36.29 (s, CH₂), 35.88 (s, CH), 34.01 (s, C(CH₃)₃), 33.2 (s, ArCH₂Ar), 31.98 (s, C-7), 31.78 and 31.12 (2s, C(CH₃)₃), 28.32 (s, C-16), 28.09 (s, CH), 27.71 (s, CH₂), 24.38 (s, CH₂), 23.93 (s, CH₂), 22.91 (s, CH₃), 22.66 (s, CH₃), 21.16 (s, C-11), 19.36 (s, CH₃), 18.82 (s, CH₃), 11.96 (s, CH₃). Found: 81.52, H 9.80 %. Calc. for C₁₀₀H₁₄₄O₈ (*M*_r = 1474.21): C 81.47, H 9.84 %.

5,11,17,23-Tetra-*tert*-butyl-25,27-dipropoxy-26,28-bis(diphenoxypyrophosphoryloxy)calix[4]arene (L**¹).**



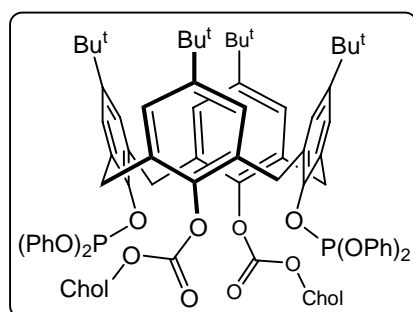
The reaction was carried out at -78 °C. To a solution of **1** (1.990 g, 2.70 mmol) in THF (150 cm³) was added a 1.3 M solution of *n*-BuLi/hexane (4.3 cm³, 5.60 mmol). After 0.5 h, (PhO)₂PCl (1.440 g, 5.70 mmol, *ca.* 1.2 cm³) was added. The resulting mixture was stirred for 2 h and then warmed up to room temperature (30 min). After evaporation to dryness, the residue was taken with toluene (50 cm³). The lithium salt was removed by filtration through a bed of Celite and washed with toluene (2 x 10 cm³). The filtered solution was evaporated to dryness upon which the residue was redissolved in CH₂Cl₂. Addition of pentane and cooling at -78 °C afforded **L**¹ as a white powder. Yield: 1.521 g, 1.31 mmol, 48 %; m.p. 210-211 °C. ¹H NMR (300 MHz, CDCl₃): δ 7.27-7.22 and 7.08-6.97 (m, 24H, *m*-ArH and P(OPh)₂), 6.66 (s, 4H, *m*-ArH), 4.64 and 3.16 (AB spin system, 8H, ArCH₂Ar, ²J = 12.9 Hz), 3.92 (t, 4H, OCH₂, *J* = 8.2 Hz), 2.08 (m, 4H, CH₂CH₃), 1.25 (s, 18H, C(CH₃)₃), 0.96 (s, 18H, C(CH₃)₃), 0.78 (t, 6H, CH₂CH₃, ³J = 7.4 Hz). ¹³C{¹H} NMR (75 MHz, CDCl₃): δ 154.34-133.97 (C_{quat}), 129.52-120.10 (aryl C), 76.86 (s, OCH₂), 33.98 (s, C(CH₃)₃), 33.77 (s, C(CH₃)₃), 32.31 (s, ArCH₂Ar), 31.62 (s, C(CH₃)₃), 31.43 (s, C(CH₃)₃), 22.96 (s, CH₂CH₃), 9.94 (s, CH₂CH₃). ³¹P{¹H} NMR (121 MHz, CDCl₃): δ 135.26 (s, P(OPh)₂). Found: C 73.79, H 7.58 %. Calc. for C₇₄H₈₆O₈P₂•0.5 CH₂Cl₂ (*M*_r = 1165.45 + 42.47): C, 74.08; H, 7.26%.

5,11,17,23-Tetra-*tert*-butyl-25,27-bis(ethoxycarbonylmethoxy)-26,28-bis(diphenoxypyrophosphanyloxy)calix[4]arene (L**²).**



To a solution of diisopropylamine (0.63 cm³, 4.80 mmol) in THF (20 cm³) was added, at -78 °C, a 1.6 M solution of *n*-BuLi/hexane (3.0 cm³, 4.80 mmol). After stirring for 0.5 h, the solution was transferred via canula to a solution of **2** (1.935 g, 2.36 mmol) in THF (100 cm³). After stirring for 1 h, (PhO)₂PCl (1.192 g, 4.72 mmol, *ca.* 1.0 cm³) was added and the resulting mixture stirred for a further hour at -78 °C. The mixture was then allowed to reach room temperature. The solvent was evaporated and the residue taken up with toluene (50 cm³). The insoluble lithium salt was filtered off using Celite and washed with toluene (2 x 10 cm³). The filtrate and washing solutions were evaporated under vacuum to afford **L**² as a white powder. Yield: 2.325 g, 1.85 mmol, 78 %; m.p. 39-40 °C, IR (KBr, cm⁻¹): ν(C=O) = 1761. ¹H NMR (300 MHz, CDCl₃): δ 7.26-7.21 and 7.07-6.99 (m, 24H, *m*-ArH and P(OPh)₂), 6.63 (s, 4H, *m*-ArH), 4.95 and 3.24 (AB spin system, 8H, ArCH₂Ar, ²J = 13.4 Hz), 4.95 (s, 4H, OCH₂CO₂), 3.99 (q, 4H, CH₂CH₃, ³J = 7.1 Hz), 1.26 (s, 18H, C(CH₃)₃), 1.12 (t, 6H, CH₂CH₃, ³J = 7.1 Hz), 0.95 (s, 18H, C(CH₃)₃). ¹³C{¹H} NMR (75 MHz, CDCl₃): δ 170.51 (s, CO₂), 153.40-129.70 (C_{quat}), 129.52-120.43 (aryl C), 70.52 (s, OCH₂CO₂), 60.27 (s, CH₂CH₃), 34.03 (s, C(CH₃)₃), 33.79 (s, C(CH₃)₃), 33.02 (s, ArCH₂Ar), 31.61 (s, C(CH₃)₃), 31.18 (s, C(CH₃)₃), 14.05 (s, CH₂CH₃). ³¹P{¹H} NMR (121 MHz, CDCl₃): δ 130.54 (s, P(OPh)₂). Found: C 72.18, H 6.96 %. Calc. for C₇₆H₈₆O₁₂P₂ (*M*_r = 1253.44): C 72.82, H 6.92 %.

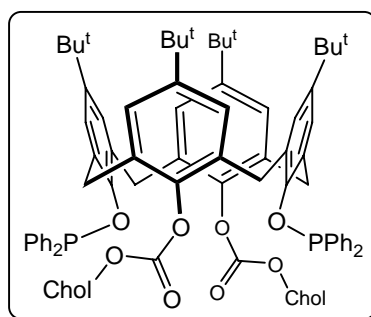
5,11,17,23-Tetra-*tert*-butyl-25,27-bis(cholesteryloxycarbonyloxy)-26,28-bis(diphenoxypyrophosphanyloxy)calix[4]arene (\mathbf{L}^3).



To a solution of diisopropylamine (0.63 cm³, 4.80 mmol) in THF (20 cm³) was added, at -78 °C, a 1.6 M solution of *n*-BuLi/hexane (3.0 cm³, 4.80 mmol). After stirring for 0.5 h, the solution was transferred via canula to a solution of **3** (3.538 g, 2.40 mmol) in THF (100 cm³). After stirring for 1 h, (PhO)₂PCl (1.213 g, 4.80 mmol, *ca.* 1.0 cm³) was added and the resulting mixture stirred for an additional hour. The mixture was allowed to reach room temperature (2 h). The solvent was removed in vacuo and the residue was taken up with toluene (50 cm³). The insoluble lithium salt was filtered off using Celite and washed with toluene (2 x 10 cm³). The filtrate and washing solutions were evaporated to dryness to afford **L**³ as a white powder. Yield: 3.853 g, 2.02 mmol, 84 %; m.p. 93-95 °C, IR (KBr, cm⁻¹): ν(C=O) = 1756 s, 1727 sh. ¹H NMR (300 MHz, CDCl₃): δ 7.24-7.11 and 7.01-6.89 (m, 24H, *m*-ArH and P(OPh)₂), 6.60 (s, 4H, *m*-ArH), 5.20 (d, 2H, H-6 of cholestryl, ³J = 4.9 Hz), 4.58 and 3.24 (AB spin system, 4H, ArCH₂Ar, ²J = 13.1 Hz), 4.60 and 3.24 (AB spin system, ²J = 13.2 Hz, 4H, ArCH₂Ar), 4.23 (m, 2H, H-3 of cholestryl), 2.36-0.67 (86H, cholestryl), 1.36 (s, 18H, C(CH₃)₃), 0.90 (s, 18H, C(CH₃)₃). ¹³C{¹H} NMR (75 MHz, CDCl₃): δ 154.69-143.77 (aryl C_{quat}), 139.88 (s, C-5 or aryl C), 135.25-125.05 (aryl C_{quat}), 123.04 (C-6 tentative assignment), 122.36-120.83 (aryl C), 78.59 (s, C-3), 56.69 (s, C-14), 56.15 (s, C-17), 49.92 (s, C-9), 42.33 (s, C-13), 39.75 (s, C-12), 39.54 (s, C-1, tentative assignment), 37.43 (s, CH₂), 37.00 (s, CH₂), 36.53 (s, C-10), 36.20 (s, CH₂), 35.82 (s, CH), 34.21 (s, C(CH₃)₃), 33.84 (s, C(CH₃)₃), 32.30 (s, ArCH₂Ar), 31.85 (s, ArCH₂Ar), 31.69 (s, C(CH₃)₃), 31.11 (s, C(CH₃)₃), 28.25 (s, C-16), 28.04 (s, CH), 27.08 (s, CH₂), 24.31 (s, CH₂), 23.86 (s, CH₂), 22.85 (s, CH₃), 22.58 (s, CH₃), 21.04 (s, C-11), 19.53 (s, CH₃), 18.74 (s, CH₃), 11.87 (s, CH₃); ³¹P{¹H} NMR (121 MHz, CDCl₃): δ 127.62 (s,

P(OPh)_2). Found: C 78.47 H 8.31 %. Calc. for $\text{C}_{124}\text{H}_{162}\text{O}_{12}\text{P}_2$ ($M_r = 1906.55$): C 78.12, H 8.56 %.

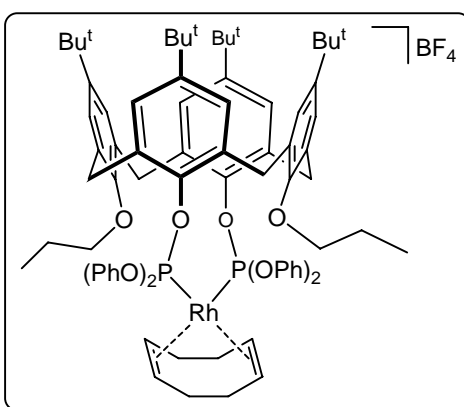
5,11,17,23-Tetra-*tert*-butyl-25,27-bis(cholesteryloxycarbonyloxy)-26,28-bis(diphenylphosphanyloxy)calix[4]arene (L^6).



To a solution of diisopropylamine (0.73 cm^3 , 5.57 mmol) in THF (20 cm^3) was added a 1.6 M solution of *n*-BuLi/hexane (3.5 cm^3 , 5.60 mmol). After stirring for 30 minutes, this solution was transferred via canula to a solution of **3** (4.080 g, 2.77 mmol) in THF (100 cm^3). After stirring for 1 h, Ph_2PCl (1.222 g, 5.54 mmol, ca. 1.0 cm^3) was added and the resulting mixture stirred for an additional hour. The mixture was warmed up to room temperature (2 h). The solvent was evaporated and the residue was redissolved in toluene (50 cm^3). The lithium salt filtrated off using a bed of Celite and washed with toluene ($2 \times 10 \text{ cm}^3$). The filtrate and washing solutions were evaporated under vacuum to afford L^6 as a white powder. Yield: 4.08 g, 2.22 mmol, 80 %; m.p. 138-140 °C, IR (KBr, cm^{-1}): $\nu(\text{C=O}) = 1771$ and 1742 . ^1H NMR (300 MHz, CDCl_3): δ 7.79-7.74 and 7.41-7.17 (m, 20H, PPh_2), 7.01 (s, 4H, *m*-ArH), 6.44 (s, 4H, *m*-ArH), 5.26 (d, 2H, H-6, $^3J = 4.5 \text{ Hz}$), 4.55 (m, 2H, H-3), 3.95 and 2.81 (AB spin system, 4H, Ar CH_2 Ar, $^2J = 13.3 \text{ Hz}$), 3.92 and 2.81 (AB spin system, 4H, Ar CH_2 Ar, $^2J = 13.3 \text{ Hz}$), 2.37-0.70 (86H, 2 x cholesteryl), 1.29 (s, 18H, $\text{C}(\text{CH}_3)_3$), 0.84 (s, 18H, $\text{C}(\text{CH}_3)_3$). $^{13}\text{C}\{\text{H}\}$ NMR (75 MHz, CDCl_3): δ 152.24-140.63 (quaternary aryl C), 140.25 (s, C-5 or aryl C), 134.90-125.05 (aryl C), 122.28 (s, C-6 tentative assignment), 78.07 (s, C-3), 56.83 (s, C-14), 56.23 (s, C-17), 50.07 (s, C-9), 42.39 (s, C-13), 39.85 (s, C-12), 39.56 (s, C-1 tentative assignment), 37.88 (s, CH₂), 37.18 (s, CH₂), 36.61 (s, C-10), 36.24 (s, CH₂), 35.85 (s, CH), 34.17 (s, $\text{C}(\text{CH}_3)_3$), 33.68 (s, $\text{C}(\text{CH}_3)_3$), 32.04 (s, ArCH₂Ar), 31.94 (s, ArCH₂Ar), 31.62 (s, $\text{C}(\text{CH}_3)_3$), 31.17 (s, $\text{C}(\text{CH}_3)_3$), 30.98 (s, C_{quat}), 30.77 (s, C_{quat}), 28.30

(s, C-16), 28.06 (s, CH), 27.55 (s, CH₂), 24.37 (s, CH₂), 23.89 (s, CH₂), 22.87 (s, CH₃), 22.61 (s, CH₃), 21.50 (s, C-11), 19.54 (s, CH₃), 18.78 (s, CH₃), 11.92 (s, CH₃). $^{31}\text{P}\{\text{H}\}$ NMR (121 MHz, CDCl₃): δ 122.47 (s, PPh₂). Found: C 80.09, H 8.86 %. Calc. for C₁₂₄H₁₆₂O₈P₂ (M_r = 1842.56): C 80.83, H 8.86 %.

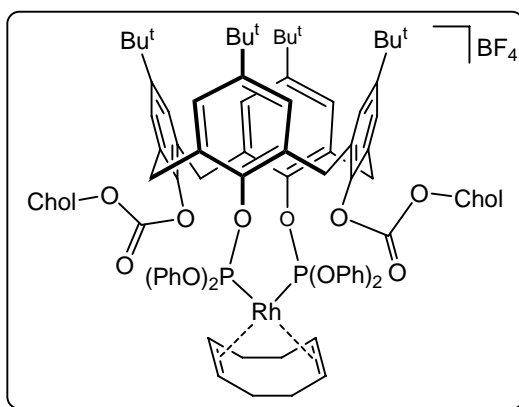
cis-P,P'-{[5,11,17,23-tetra-tert-butyl-25,27-dipropoxy-26,28-bis(diphenoxypyrophosphoryloxy)calix[4]arene]-1,5-cyclooctadiene} rhodium (I) tetrafluoroborate (4).



A solution of AgBF₄ (0.052 g, 0.266 mmol) in THF (1 cm³) was added to a solution of [{Rh(cyclooctadiene)Cl}₂] (0.066 g, 0.133 mmol) in CH₂Cl₂ (10 cm³). Stirring was stopped after 5 min and the solution was decanted to eliminate AgCl. The supernatant was filtered through Celite and added to a solution of L¹ (0.155 g, 0.133 mmol) in CH₂Cl₂ (50 cm³). After 1 h the solution was concentrated to *ca.* 5 cm³ and addition of hexane afforded **4** as an orange precipitate. Yield: 0.105 g, 0.15 mmol, 79 %; m.p. 123 °C (decomp.). ^1H NMR (300 MHz, CDCl₃): δ 7.26-7.17 (20H, P(OPh)₂), 7.13 (s, 4H, *m*-ArH), 6.78 and 6.77 (2s, 8H, *m*-ArH), 6.40 (s, 4H, *m*-ArH), 5.39 (broad signal, 4H, HC=CH of COD), 4.86 and 3.23 (AB spin system, 8H, ArCH₂Ar, 2J = 13.2 Hz,), 3.98 (t, 4H, OCH₂, 3J = 7.9 Hz), 2.27 (m, 2H, CH₂ of COD), 1.61 (m, 4H, OCH₂CH₂), 1.35 (s, 18H, C(CH₃)₃), 0.83 (s, 18H, C(CH₃)₃), 0.75 (t, 6H, CH₂CH₃, 3J = 7.5 Hz). $^{13}\text{C}\{\text{H}\}$ NMR (75 MHz, CDCl₃): δ 151.47-130.08 (quaternary aryl C), 129.88-119.58 (aryl C), 101.96 (s, CH of COD), 78.01 (s, OCH₂), 34.24 (s, C(CH₃)₃), 33.67 (s, C(CH₃)₃), 32.83 (s, ArCH₂Ar), 31.45 (s, C(CH₃)₃), 30.98 (s, C(CH₃)₃), 30.20 (s, CH₂ of COD), 21.77 (s, CH₂CH₃), 9.79 (s, CH₂CH₃). $^{31}\text{P}\{\text{H}\}$ NMR (121 MHz, CDCl₃): δ

101.0 (d, $J(P\text{-Rh}) = 252$ Hz, P(OPh)₂). FAB mass spectrum: m/z (%) 1375.5 (25) [($M\text{-BF}_4$)⁺, expected isotopic profile], 1267.4 [($(M\text{-BF}_4\text{-COD})^+$, expected isotopic profile)]. Found: C 67.58, H 6.56 %. Calc for C₈₂H₉₈BF₄O₈P₂Rh ($M_r = 1463.35$): C 67.31, H 6.75 %.

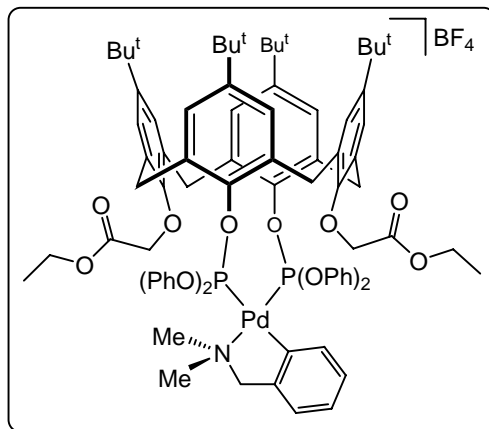
cis-P,P'-{[5,11,17,23-tetra-*tert*-butyl-25,27-bis(cholesteryloxycarbonyloxy)-26,28-bis(diphenoxypyrophosphoryloxy)calix[4]arene]-1,5-cyclooctadiene}rhodium(I) tetrafluoro borate (5).



A solution of **L**³ (0.235 g, 0.123 mmol) in THF (100 cm³) was dropwise added to a cold (-78 °C) solution of [Rh(COD)₂]BF₄ (0.050 g, 0.123 mmol) in THF (100 cm³). After 3h the solution was allowed to reach room temperature and stirred for another 12 h. The solvent was removed in vacuo and the residue was redissolved in CH₂Cl₂. Addition of pentane and cooling at -78 °C afforded **5** as a yellow powder. Yield: 0.234 g, 0.11 mmol, 86%; m.p. 109-111 °C, IR (KBr, cm⁻¹): ν(CO) = 1756. ¹H NMR (300 MHz, CDCl₃): δ 7.23-7.19 and 6.84-6.77 (m, 24H, *m*-ArH and P(OPh)₂), 6.47 (s, 4H, *m*-ArH), 5.58 (m, 4H, CH of COD), 5.37 (d, 2H, H-6, ³J = 4.9 Hz), 4.64 (m, 2H, H-3), 4.55 and 3.19 (AB spin system, ²J = 13.6 Hz, 4H, ArCH₂Ar), 4.52 and 3.20 (AB spin system, ²J = 13.5 Hz, 4H, ArCH₂Ar), 2.49-0.67 (86H, cholesteryl), 2.37 (m, 2H, CH₂ of COD), 1.39 (s, 18H, C(CH₃)₃), 0.86 (s, 18H, C(CH₃)₃). ¹³C{¹H} NMR (75 MHz, CDCl₃): δ 152.94-143.78 and 135.98 (quaternary aryl C), 138.62 (s, C-5 or aryl C), 130.11-123.64 (s, aryl C), 121.05 (s, C-6 tentative assignment), 119.96 (s, aryl C), 115.37 (s, CH of COD), 79.70 (s, C-3), 56.60 (s, C-14), 56.07 (s, C-17), 49.89 (s, C-9), 42.27 (s, C-13), 39.60 (s, C-12), 39.46 (s, C-1 tentative assignment), 37.86 (s, CH₂),

36.69 (s, C-10), 36.14 (s, CH₂), 35.73 (s, CH), 34.31 (s, C(CH₃)₃), 33.83 (s, C(CH₃)₃), 32.78 (s, ArCH₂Ar), 32.30 (s, CH₂ of COD), 31.85 (s, ArCH₂Ar), 31.75 (s, CH), 31.43 (s, C(CH₃)₃), 30.85 (s, C(CH₃)₃), 28.17 (s, C-16), 27.96 (s, CH), 27.56 (s, CH₂), 24.22 (s, CH₂), 23.77 (s, CH₂), 22.78 (s, CH₃), 22.52 (s, CH₃), 20.99 (s, C-11), 19.31 (s, CH₃), 18.67 (s, CH₃), 11.81 (s, CH₃). ³¹P{¹H} NMR (121 MHz, CDCl₃): δ 99.7 (d, *J*(P-Rh) = 254 Hz, P(OPh)₂). ESI TOF mass spectrum *m/z* 2117.1 ([*M* - BF₄]⁺, expected isotopic profile). Found: C 65.11, H 7.20 %. Calc. for C₁₃₂H₁₇₄BF₄O₁₂P₂Rh•3 CH₂Cl₂ (*M*_r = 2204.5 + 3 x 84.93): C 65.93, H 7.38 %.

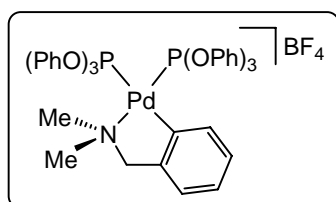
cis-P,P'-(*o*-dimethylaminomethylphenyl-C,N)-{5,11,17,23-tetra-*tert*-butyl-25,27-bis(ethoxycarbonylmethoxy)-26,28-bis(diphenoxypyrophosphoryloxy)calix[4]arene} palladium(II) tetrafluoroborate (6).



A solution of AgBF₄ (0.032 g, 0.165 mmol) in THF (1 cm³) was added to a solution of [Pd(o-C₆H₄NMe₂)Cl]₂ (0.046 g, 0.083 mmol) in CH₂Cl₂ (20 cm³). Stirring was stopped after 5 min and the solution was decanted to eliminate AgCl. The supernatant was filtered through Celite and added to a solution of L² (0.209 g, 0.167 mmol) in CH₂Cl₂ (50 cm³). The solution was stirred overnight and concentrated to *ca* 5 cm³. Addition of pentane afforded a pale yellow solid **6**. Yield: 0.227 g, 0.140 mmol, 84 %; m.p. 118-119 °C, IR (KBr, cm⁻¹): ν (CO) = 1758. ¹H NMR (300 MHz, CDCl₃) (assignment using COSY): δ 8.10-8.04 and 7.35-6.43 (m, 32H, C₆H₄ of dmba, *m*-ArH and P(OPh)₂), 5.33 and 3.42 (AB spin system, 2H, ArCH₂Ar, ²J = 13.4 Hz), 5.21 and 3.38 (AB spin system, ²J = 12.5 Hz, 2x2H, ArCH₂Ar), 5.04 and 3.47 (AB spin system, ²J = 14.2 Hz, 2H, ArCH₂Ar), 4.50 and 4.30 (AB spin system, ²J = 16.9 Hz, 4H,

OCH_2CO_2), 3.96 (q, $^3J = 7.0$ Hz, 2H, CH_2CH_3), 3.81 (q, $^3J = 7.1$ Hz, 2H, CH_2CH_3), 3.34 and 3.08 (ABX (with X = P), $^2J(HH) = 13.1$ Hz, $^4J(PH) = 3.1$ Hz, $^4J(PH) = 4.5$ Hz, 2H, NCH_2), 2.45 (d, $^4J(PH) = 4.3$ Hz, 3H, $N(CH_3)_3$), 2.36 (d, $^4J(PH) = 4.5$ Hz, 3H, $N(CH_3)_3$), 1.44 (s, 9H, $C(CH_3)_3$), 1.38 (s, 9H, $C(CH_3)_3$), 1.10 (t, $^3J = 7.0$ Hz, 3H, CH_2CH_3), 0.99 (t, $^3J = 7.1$ Hz, 3H, CH_2CH_3), 0.88 (s, 9H, $C(CH_3)_3$), 0.84 (s, 9H, $C(CH_3)_3$); $^{13}C\{^1H\}$ NMR (75 MHz, $CDCl_3$): δ 169.73 (s, CO_2), 169.49 (s, CO_2), 153.11-120.01 (aryl C), 73.04 (s, OCH_2CO_2), 71.09 (s, OCH_2CO_2), 65.22 (d, $^3J(PC) = 3$ Hz, NCH_2), 60.63 (s, CH_2CH_3), 60.45 (s, CH_2CH_3), 43.56 (s, $N(CH_3)_2$), 43.11 (s, $N(CH_3)_2$), 34.38 (s, $C(CH_3)_3$), 34.29 (s, $C(CH_3)_3$), 33.79 (s, $C(CH_3)_3$), 33.75 (s, $C(CH_3)_3$), 32.87 (s, $ArCH_2Ar$), 32.63 (s, $ArCH_2Ar$), 31.61 (s, $C(CH_3)_3$), 31.06 (s, $C(CH_3)_3$), 14.18 (s, CH_2CH_3), 13.98 (s, CH_2CH_3); $^{31}P\{^1H\}$ NMR (121 MHz, $CDCl_3$): δ 141.6 and 115.2 (AB system, $J(PP') = 54$ Hz). ES mass spectrum (CH_2Cl_2): m/z 1492.5 ($[M - BF_4]^+$, 100 %). Found: C 63.95, H 6.41, N 0.62 %. Calc for $C_{85}H_{98}BF_4NO_{12}P_2Pd \bullet 0.25 CH_2Cl_2$ ($M_r = 1580.86 + 21.23$): C 63.91, H 6.20, N 0.87 %. The isomerisation product **6a** was obtained quantitatively after 24 h from a concentrated (ca. 2×10^{-3} mmol.cm $^{-3}$) solution of **6**. $^{31}P\{^1H\}$ NMR (121 MHz, $CDCl_3$): δ 105.3 and 96.4 (AB system, $J(PP') = 86$ Hz). As observed for **6**, the 1H NMR spectrum of **6a** reveals a C_1 -symmetrical structure.

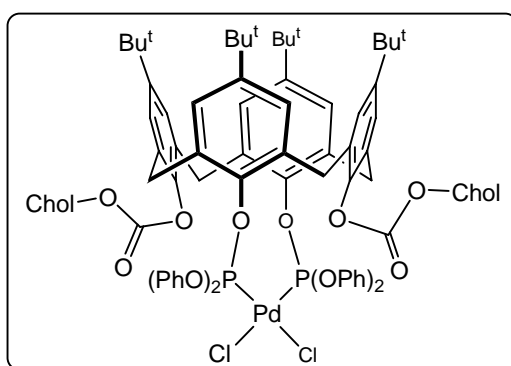
In situ preparation of $\{[o\text{-}(dimethylaminomethyl)phenyl-C,N]\text{-bis(triphenylphosphite)}\}$ palladium(II) tetrafluoroborate (7).



A solution of $AgBF_4$ (0.035 g, 0.180 mmol) in THF (1 cm 3) was added to a solution of $[Pd(o\text{-}C_6H_4CH_2NMe_2)Cl]_2$ (0.050 g, 0.091 mmol) in CH_2Cl_2 (20 cm 3). Stirring was stopped after 5 min and the solution was decanted to eliminate $AgCl$. The supernatant was filtered through Celite and added to a solution of $P(OPh)_3$ (70 μL , 0.083 g, 0.282 mmol) in CH_2Cl_2 (50 cm 3). The solution was stirred overnight and the

volatiles removed. $^{31}\text{P}\{\text{H}\}$ NMR (121 MHz, CDCl_3): δ 112.2 and 101.4 (AB spin system, $J(\text{P-P}) = 89$ Hz, $(\text{P}(\text{OAr})_3)_2$).

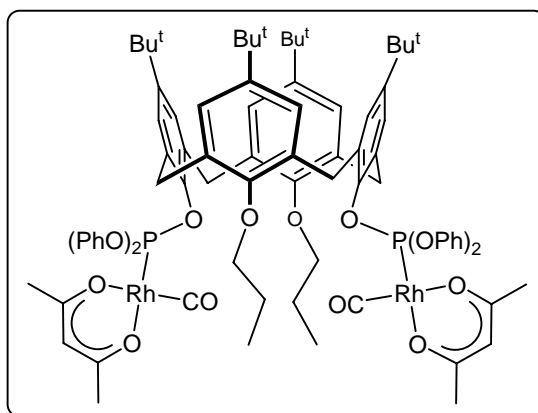
cis-P,P'-Dichloro{5,11,17,23-tetra-*tert*-butyl-25,27-bis(cholesteryloxycarbonyloxy)-26,28-bis(diphenoxypyrophosphanyloxy)calix[4]arene}palladium (II) (8**).**



A solution of **L**³ (0.200 g, 0.105 mmol) in THF (75 cm³) was added dropwise to a cold (-78 °C) solution of [PdCl₂(COD)] (0.030 g, 0.105 mmol) in THF (75 cm³). After 3 h the solution was allowed to reach room temperature and stirred for a further 12h. Solvent evaporation afforded **8** as a pale yellow powder. The complex was then recrystallised in a CH_2Cl_2 -pentane mixture at -78 °C. Yield: 0.199 g, 0.095 mmol, 90 %; m.p. 168-169 °C, IR (KBr, cm⁻¹): $\nu(\text{CO}) = 1758$. ^1H NMR (300 MHz, CDCl_3): δ 7.32-7.07 and 6.79-6.78 (m, 24H, *m*-ArH and P(OPh)₂), 6.47 (s, 4H, *m*-ArH), 5.30 (d, 2H, H-6, $^3J = 4.7$ Hz), 4.74 and 3.34 (AB spin system, 4H, ArCH₂Ar, $^2J = 13.8$ Hz), 4.74 and 3.32 (AB spin system, 4H, ArCH₂Ar, $^2J = 13.8$ Hz), 4.60 (m, 2H, H-3), 2.72 (broad t, 2 x 1H, H-cholest not assigned), 2.38-0.68 (86H, cholesteryl), 1.44 (s, 18H, C(CH₃)₃), 0.88 (s, 18H, C(CH₃)₃). $^{13}\text{C}\{\text{H}\}$ NMR (75 MHz, CDCl_3): δ 154.35-143.98 (quaternary aryl C), 139.95 (s, C-5 or aryl C), 136.65-124.82 (aryl C), 122.33 (s, C-6 tentative assignment), 80.29 (s, C-3), 56.73 (s, C-14), 56.12 (s, C-17), 49.93 (s, C-9), 42.29 (s, C-13), 39.73 (s, C-12), 39.49 (s, C-1 tentative assignment), 37.84 (s, CH₂), 37.07 (s, CH₂), 36.66 (s, C-10), 36.16 (s, CH₂), 35.76 (s, CH), 34.33 (s, C(CH₃)₃), 33.83 (s, C(CH₃)₃), 32.79 (s, ArCH₂Ar), 31.92 (s, ArCH₂Ar), 31.80 (s, CH), 31.50 (s, C(CH₃)₃), 30.98 (s, C(CH₃)₃), 28.21 (s, C-16), 27.98 (s, CH), 27.42 (s, CH₂), 24.25 (s, CH₂), 23.80 (s, CH₂), 22.80 (s, CH₃), 22.54 (s, CH₃), 21.02 (s, C-11), 19.43 (s, CH₃), 18.69 (s, CH₃), 11.82 (s, CH₃). $^{31}\text{P}\{\text{H}\}$ NMR (121 MHz, CDCl_3): δ 75.91 (s, P(OPh)₂).

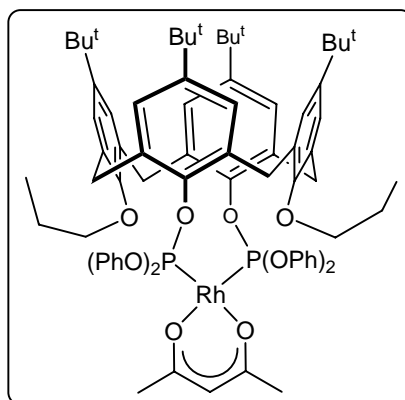
MALDI TOF mass spectrum: m/z 2010.1 ($[M - 2 \text{ Cl}]^+$, 100 %). Molecular weight determination by osmometry (CH_2Cl_2): 1990 ± 100 , corresponding to a monomer. Found: C 70.25, H 7.71 %. Calc. for $\text{C}_{124}\text{H}_{162}\text{Cl}_2\text{O}_{12}\text{P}_2\text{Pd} \bullet 0.5 \text{ CH}_2\text{Cl}_2$ ($M_r = 2083.88 + 42.46$): C 70.33, H 7.73 %.

Acetylacetonato-{5,11,17,23-tetra-*tert*-butyl-25,27-dipropoxy-26,28-bis(diphenoxypyrophosphanyloxy)calix[4]arene} rhodium (I) (9).



L¹ (0.136 g, 0.117 mmol) was added to a solution of $[\text{Rh}(\text{acac})(\text{CO})_2]$ (acac = MeCOCHCOMe) (0.030 g, 0.116 mmol) in CH_2Cl_2 (50 cm³). The solution turned from green to yellow within a few minutes. After 12h, the solvent was evaporated to dryness to afford **9** as a yellow solid which was washed quickly with small amounts of cold (-78°C) pentane. Yield: 0.132 g, 0.096 mmol, 83 %; m.p. > 173-175 °C (decomp.), IR (KBr, cm⁻¹): $\nu = 1593\text{s}$, 1580sh, 1518s (acac). ¹H NMR (300 MHz, CDCl_3): δ 7.34-7.21 and 7.11-6.94 (24H, *m*-ArH and P(OPh)₂), 6.44 (s, 4H, *m*-ArH), 5.13 and 3.18 (AB spin system, 8H, ArCH₂Ar, ²J = 13.1 Hz,), 4.94 (s, 1H, CH-acac), 3.86 (t, 4H, OCH₂, ³J = 7.8 Hz), 1.93 (m, 4H, OCH₂CH₂), 1.44 (s, 18H, C(CH₃)₃), 1.19 (s, 6H, CH₃-acac), 0.88 (s, 18H, C(CH₃)₃), 0.80 (t, 6H, CH₂CH₃, ³J = 7.4 Hz). ¹³C{¹H} NMR (75 MHz, CDCl_3): δ 184.52 (s, CO), 153.33-129.78 (quaternary aryl C), 127.90-120.07 (aryl C), 99.30 (s, CH-acac), 77.67 (s, OCH₂), 34.18 (s, C(CH₃)₃), 33.65 (s, C(CH₃)₃), 33.16 (s, ArCH₂Ar), 31.69 (s, C(CH₃)₃), 31.22 (s, C(CH₃)₃), 25.40 (s, CH₃-acac), 22.34 (s, CH₂CH₃), 10.42 (s, CH₂CH₃). ³¹P{¹H} NMR (121 MHz, CDCl_3): δ 115.4 (d, *J*(P-Rh) = 325 Hz, P(OPh)₂). MALDI TOF mass spectrum: m/z 1366.00 ($[M]^+$, 100 %). Found: C 69.55, H 6.93 %. Calc for $\text{C}_{79}\text{H}_{93}\text{O}_{10}\text{P}_2\text{Rh}$ ($M_r = 1367.43$): C 69.39, H 6.86 %.

Bis(acetylacetonato)biscarbonyl[5,11,17,23-tetra-*tert*-butyl-25,27-dipropoxy-26,28-bis(diphenoxypyrophosphanyloxy)calix[4]arene]dirhodium (I**) (**10**).**



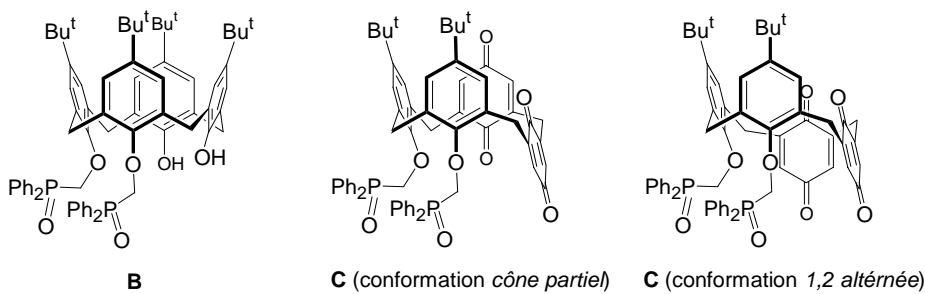
L¹ (0.124 g, 0.106 mmol) was added to a solution of [Rh(CO)₂acac] (acac = MeCOCHCOMe) (0.055 g, 0.213 mmol) in CH₂Cl₂ (50 cm³). After stirring for one night at room temperature, the solvent was evaporated affording **10** as a green microcrystalline powder which was dried under vacuum. The complex was washed quickly with small amounts of cold pentane. Yield: 0.151 g, 0.093 mmol, 88 %; m.p. 98.5-100 °C, IR (KBr, cm⁻¹): ν = 1591s, 1581sh, 1521s (acac). ¹H NMR (300 MHz, CDCl₃): δ 7.37-7.13 and 7.07-7.02 (m, 24H, *m*-ArH and P(OPh)₂), 6.54 (s, 4H, *m*-ArH), 5.36 (s, 2H, CH-acac), 4.83 and 3.34 (AB spin system, 8H, ArCH₂Ar, ²J = 13.1 Hz), 4.19 (t, 4H, OCH₂, ²J = 8.4 Hz), 2.45 (m, 4H, OCH₂CH₂), 2.01 (s, 6H, CH₃-acac), 1.70 (s, 6H, CH₃-acac), 1.38 (s, 18H, C(CH₃)₃), 0.87 (s, 18H, C(CH₃)₃), 0.81 (t, 6H, CH₃, ³J = 7.5 Hz). ¹³C{¹H} NMR (75 MHz, CDCl₃): δ 187.14 (s, CO), 185.38 (s, CO), 154.97-132.45 (quaternary aryl C), 132.40-121.08 (aryl C), 100.62 (s, CH-acac), 76.90 (s, OCH₂), 34.17 (s, C(CH₃)₃), 33.76 (s, C(CH₃)₃), 33.01 (s, ArCH₂Ar), 31.82 (s, C(CH₃)₃), 31.08 (s, C(CH₃)₃), 27.43 (d, CH₃-acac, J = 8.6 Hz), 26.49 (s, CH₃-acac), 23.68 (s, CH₂CH₃), 9.83 (s, CH₂CH₃). ³¹P{¹H} NMR (121 MHz, CDCl₃): δ 123.79 (d, J(P-Rh) = 288 Hz, P(OPh)₂). Found: C 63.27, H 6.31 %. Calc. for C₈₆H₁₀₀O₁₄P₂Rh₂ (M_r = 1625.46): C 63.55, H 6.20 %.

CONFORMATIONAL INSTABILITY OF A PROXIMALLY-DIFUNCTIONALIZED CALIX[4]-DIQUINONE.

Résumé	2
1 Introduction	2
2 Experimental	4
2.1 General	4
2.2 Alternative preparation of C	4
2.3 Important spectroscopic data for C	5
2.4 X-ray analysis	5
3 NMR and X-ray studies	7
4 Conclusion	11
5 References	12

Résumé

La troisième partie de cette thèse traite du produit d'oxydation du *p*-*tert*-butyl-5,11-bis(diphénylphosphinoxyloxymethyl)calix[4]arène **B** par Tl^{III}(CF₃SO₃)₃. La réaction conduit au macrocycle (**C**) comportant deux quinones adjacentes. Les spectres de RMN (¹H et ¹³C), à température ambiante, ne permettent pas de trancher quant à la conformation du calixarène formé. C'est la raison pour laquelle une étude par diffraction des rayons X a été entreprise. Cette étude montre qu'à l'état solide le composé est dans la conformation cône partiel, une des quinones ayant une orientation *anti*. Des expériences de ROESY mettent clairement en évidence une oscillation rapide de chacune des unités quinoniques autour de l'axe passant par les deux atomes de carbone CH₂ bordant les cycles. Cependant ces expériences ne permettent de démontrer ni l'existence d'un conformère 1,2-alterné ni celle d'un conformère cône. De cette étude, on retiendra surtout que les règles empiriques basées sur les déplacements chimiques ¹³C des ponts CH₂ qui permettent d'attribuer une conformation particulière à un calixarène ne sont pas applicables dans le cas des calix-quinones, et ce en raison de la mobilité de ces dernières.

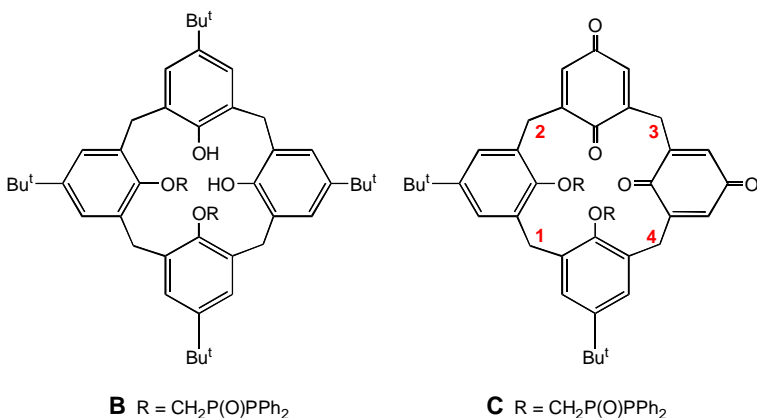


1 Introduction

Calixquinones constitute a particular class of calixarene derivatives in which at least one phenolic moiety has been converted into a quinonic unit.¹ They may be obtained straightforwardly through chemical reactions using oxidising agents such as K₂CrO₄/FeCl₃ or Tl(NO₃)₃²⁻⁴ or by electrochemical oxidation of calixarenes comprising

non-substituted hydroxy (phenolic) groups.^{5,6} One current application of the calixquinones is their use as sensors for the detection of various metal cations; the efficiency of the metal recognition process relying on several factors, notably the ability of the oxygen atom(s) of the quinone to bind the metal ion in combination with other donors linked to the calixarene skeleton as well as on the ligand's flexibility.⁷⁻¹⁴ While the structural chemistry of conventional calixarenes has been investigated in detail, relatively few studies about the conformational behaviour of the calixarene-quinones have been undertaken.¹⁵⁻¹⁷ For example, it may be anticipated that due to their relatively small size, the quinone rings may flip reversibly through the calixarene annulus, hence resulting in conformational instability of the whole calixarene structure. Unlike calix[4]arenes which contain only ArCH₂Ar units, the calix[4]quinones contain ArCH₂-quinone fragments, and accordingly, the NMR rules which allow conformational assignment of the conventional calixarenes and which are based on the ArCH₂Ar NMR signals, do not necessarily apply to the calixquinones.¹⁸⁻²⁰ Therefore, collecting NMR data of calixarene-quinones deserves interest.

We recently reported on the electrochemical synthesis of diquinone C, starting from the conical precursor 5,11,17,23-tetra-*tert*-butyl-25,26-bis(diphenylphosphinoymethoxy)-27,28-dihydroxycalix[4]arene **B**.⁵ In the present study, we describe the solid-state structure of this compound which contrasts with the apparent *C*_s-symmetrical structure found in solution. The present study also provides NMR data that complement our preliminary report. In the following, the CH₂ groups of the calixarene core will be referred to as bridging methylene groups, whatever the nature of the bridged rings, aryl or quinone. It should be mentioned here that while the solution conformation of distal calixarenes has been studied in detail, little is known about proximal calixdiquinones.^{1,20}



2 Experimental

2.1 General

Compound **C** was prepared according to the previously reported electrochemical method, then purified by flash chromatography using a dichloromethane–acetone mixture (80:20, v/v).⁵ An alternative preparation is also given below. The infrared spectrum of **C** (KBr pellet) was measured using a Perkin Elmer 1605 spectrometer. ¹H, ¹³C and ³¹P NMR data were recorded with FT Bruker AV-400 or AV-500 spectrometers. ¹H NMR spectra were referenced to residual protonated solvent (7.26 ppm for CDCl₃), ¹³C chemical shifts are reported relative to deuterated solvent (77.0 ppm for CDCl₃) and the ³¹P data are given relative to external H₃PO₄.

2.2 Alternative preparation of **C**

5,11,17,23-Tetra-*tert*-butyl-25,26-bis(diphenylphosphinoylmethoxy)-27,28-dihydroxy calix[4]arene (1.000 g, 0.93 mmol) was reacted with Tl(CF₃CO₂)₃ (3.000 g, 5.52 mmol) in CF₃CO₂H (TFA, 5 cm³). The reaction mixture was stirred for 24 h in the dark. After full evaporation of TFA, water (20 cm³) was poured into the flask and the mixture was stirred for 5 min upon which CH₂Cl₂ (50 cm³) was added. The organic phase was separated, washed three times with water (3x20 cm³), then dried over MgSO₄. The solution was then evaporated to dryness and the resulting residue purified by flash chromatography using AcOEt–hexane (80:20, v/v) as eluent. The compound was

obtained as an analytically pure yellow powder (SiO_2 , $R_f = 0.45$, AcOEt/hexane, 80:20, v:v).

2.3 Important spectroscopic data for C

IR (KBr) $\nu_{\max}/\text{cm}^{-1}$: 1652 s (C=O), 1195 ms (P=O). ^1H NMR (500 MHz, CD_2Cl_2 , 277 K): δ 7.75 (m, 4H, H of PPh), 7.65 (m, 4H, H_{PPh}), 7.52 (m, 4H, H_{PPh}), 7.43-7.38 (m, 8H, H_{PPh}), 6.76 and 6.49 (AB q, $^4J = 2$ Hz, 4H, *m*-ArH of ArBu^t), 6.46 and 5.76 (AB q, $^4J = 2$ Hz, 4H, $\text{H}_{\text{quinone}}$), 4.78 and 4.68 (AB q, $^2J = 14$ Hz, 4H, PCH₂), 4.57 and 3.07 (AB q, $^2J = 14$ Hz, 2H, ArCH₂Ar), 4.12 and 2.99 (AB q, $^2J = 13$ Hz, 4H, ArCH₂-quinone), 3.49 and 3.17 (AB q, $^2J = 13$ Hz, 2H, quinone-CH₂-quinone), 1.03 (s, 18 H, C(CH₃)₃). When the ^1H NMR spectrum of **C** was run in CDCl_3 (400 MHz, 293 K), the PCH₂ groups appear as an ABX spin system with $^2J(\text{PH}_A) = 0$ Hz and $^2J(\text{PH}_B) = 4$ Hz. ^{13}C NMR (100.63 MHz, CDCl_3 , 298K): δ 187.52 (s, C=O), 185.70 (s, C=O), 153.44-125.73 (aryl C and C=C of quinone), 70.87 (d, $J(\text{PC}) = 76$ Hz, P(O)CH₂), 33.96 (s, C(CH₃)₃), 32.41, 32.21, and 29.71 (3s, bridging CH₂), 31.29 (s, C(CH₃)₃). $^{31}\text{P}\{\text{H}\}$ NMR (161.99 MHz, CDCl_3 , 298K): δ 25.2 (s, P(O)Ph₂).

2.4 X-ray analysis

Single crystals suitable for X-ray study were grown by slow evaporation of a solution of **C** in an acetonitrile–ether mixture. Crystals of the compound under investigation were stuck with glue on glass fibber and mounted on a Nonius KappaCCD. The X-ray measurements were carried out with a graphite monochromator and ω, ψ scan mode. Data collection was carried out using the Nonius collect suite.²¹ The structures were solved by using direct methods with the program SIR92.²² Least square refinement was carried out using the program CRYSTALS.²³ Experimental details of the structure determination of **C** are compiled in Table 1 and important bond lengths and angles are given in Table 2.

Table 1. Crystallographic data

Molecular Formula	C ₆₂ H ₅₈ O ₈ P ₂
Molecular weight	993.09
Crystal size/mm	0.10*0.16*0.36
Crystal system	Monoclinic
Space group	P 2 ₁ /c
<i>a</i> /Å	10.3507(12)
<i>b</i> /Å	25.219(4)
<i>c</i> /Å	20.2315(14)
β /deg	101.166(8)
<i>V</i> /Å ³	5181.1(10)
<i>Z</i>	4
Color	colorless
<i>D</i> _{calc} /g cm ⁻³	1.273
<i>F</i> (000)	2096
μ /mm ⁻¹	0.141
Trans. min and max	0.98/0.99
Temperature/K	173
Wavelength /Å	0.71073
Radiation	MoK α graphite monochromated
Diffractometer	Nonius Kappa CCD
Scan mode	ω , $\pi\sigma\iota$
hkl limits	-13,13/-32,32/-25,26
θ limits/deg	3-27
Number of data meas.	119999
Number of data with $I > 2 \sigma(I)$	6524
Refinement method	Full matrix least squares on <i>F</i>
Weighting scheme	Chebichev polynomial with 4 parameters
Number of variables	649
Final <i>R</i> factor	0.043
<i>wR</i>	0.046
GOF	1.13
Largest peak in final difference (eÅ ⁻³)	0.35/-0.28

Table 2. Selected geometric parameters (\AA , deg)

P1—O1	1.4757 (17)	P2—O2	1.4718 (17)
P1—C37	1.819 (2)	P1—C38	1.805 (2)
P1—C44	1.800 (2)	P2—C50	1.813 (2)
P2—C51	1.794 (2)	P2—C57	1.788 (2)
O1—P1—C37	113.88 (10)	O1—P1—C38	112.51 (10)
C37—P1—C38	100.24 (10)	O1—P1—C44	111.58 (10)
C37—P1—C44	107.45 (10)	C38—P1—C44	110.56 (11)
O2—P2—C50	112.53 (10)	O2—P2—C51	113.07 (11)
C50—P2—C51	106.32 (11)	O2—P2—C57	113.18 (11)
C50—P2—C57	104.25 (10)	C51—P2—C57	106.82 (10)

3 NMR and X-ray studies

The room temperature ^1H NMR spectrum of **C** displays a single Bu^t signal (18H), an ABX system for the PCH_2 protons, an AB system (dd) for the protons of the quinonic rings and an AB system for the protons of the phenolic rings. These observations, together with the observation of a singlet at 25.2 ppm in the ^{31}P NMR spectrum are fully consistent with a C_s -symmetrical structure in solution. In keeping with this conclusion, the region of the bridging CH_2 units (Figure 1) shows three AB systems of relative intensity 1:2:1. The corresponding assignments could be made unambiguously *by* means of COSY and ROESY experiments. It is interesting to note that two of the bridging CH_2 groups give rise to a large AB separation, $\Delta = 1.50$ and 1.13 ppm, corresponding to the CH_2 bridges 1 and 2/4 respectively (see numbering in formula 1). In contrast, the methylene group linking the two quinone moieties results in an AB separation of only $\Delta = 0.32$ ppm. In conventional calix[4]arenes, AB separations higher than $\Delta = 0.7$ ppm are indicative of *syn*-oriented aryl rings, *anti*-oriented ones being usually smaller than $\Delta = 0.4$ ppm.²⁰ Obviously, applying this rule to compound **C** does not allow unambiguous conformational assignment. This is why an X-ray diffraction study was undertaken (*vide infra*). The ^{13}C NMR spectrum is again consistent with a C_s -symmetrical structure. The three signals of the four bridging methylene carbon atoms appear at δ 32.41, 32.21 and 29.71 ppm. Compared to

conventional calix[4]arenes, these values are typically those found in conical derivatives, *i.e.* with all rings in a *syn*-relationship. It should be remembered here that for *anti*-oriented rings the bridging methylene signals usually appear above $\Delta = 37$ ppm, while those linking *syn*-oriented aryl rings lie in the range 29-33 ppm.^{18,19}

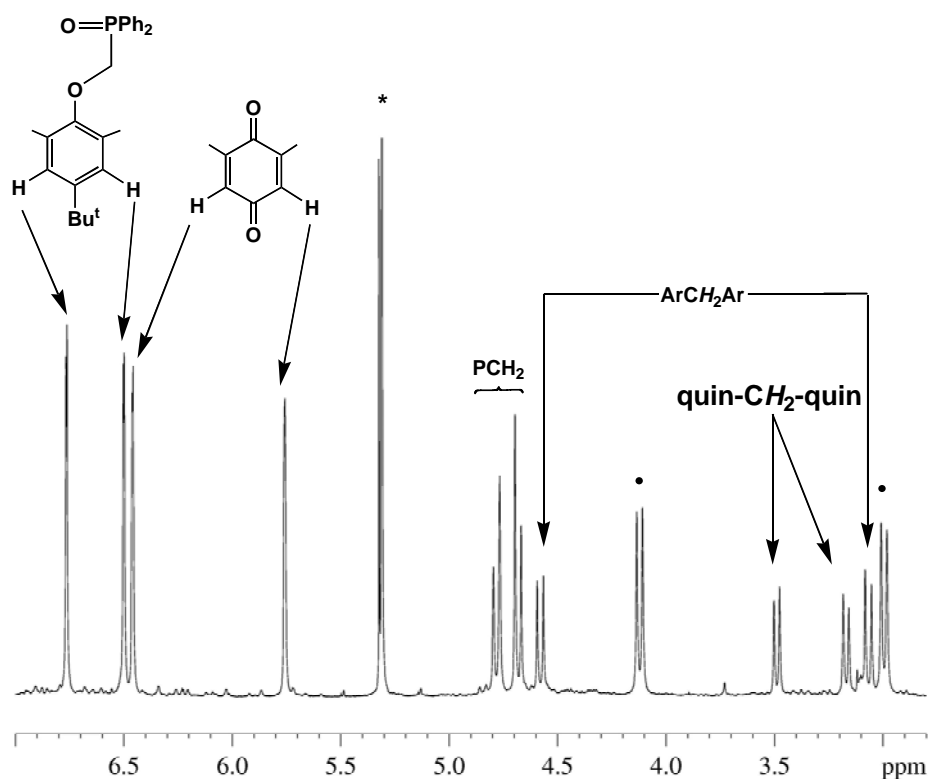
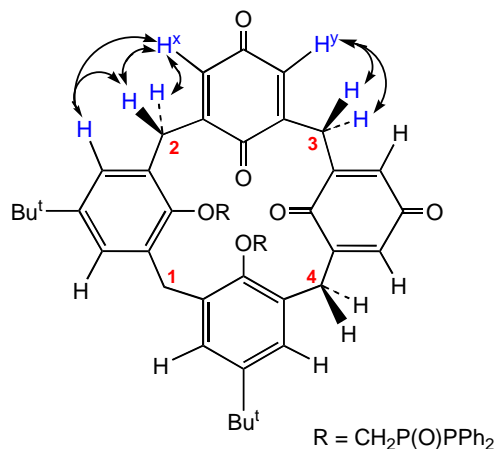


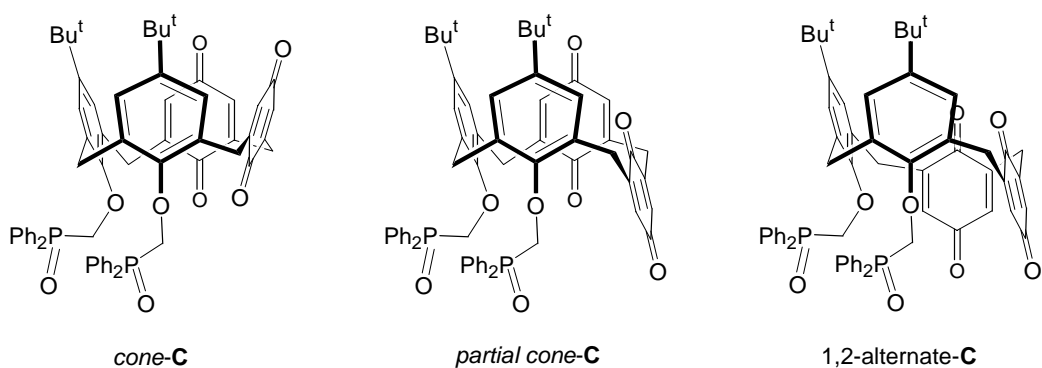
Figure 1. ^1H NMR (CD_2Cl_2) spectrum of **C**. Partial view showing the methylene signals and the H signals of the quinone and ArCH_2 rings. The dots correspond to the AB system of the ArCH_2 -quinone bridges.

As shown by a variable temperature study, the signals of the ^1H NMR spectrum (500 MHz) gradually broaden on cooling before collapsing near -60 °C. This observation is a clear indication that compound **C** is dynamic in solution. Note, we were not able to freeze out the motion on lowering the temperature. Furthermore, a 2D ROESY experiment revealed that both protons of methylene group 2 (which is equivalent to methylene group 4) correlate with the same ArH proton (H^x) of the neighbouring quinone ring (Scheme 1).



Scheme 1. Some correlations observed within **C**, as inferred from ROESY experiments. The molecule having an apparent C_s symmetry, only one half of the molecule has been considered.

This proximity is consistent with a fast flipping of the quinone rings about the axis defined by the two adjacent meta carbon atoms. However, the observed correlations do not allow establishing the type of conformers which equilibrate during the dynamics. The 2D spectrum also shows that the two protons of methylene group 3 correlate with the H^y protons of the adjacent quinones (Figure 2). This latter observation also does not allow discrimination between the possible conformers in exchange, which could be any of the three shown in Scheme 2. In view of the large size of the CH₂PPh₂(O) arms, we assume that the corresponding aryl rings cannot rotate through the calixarene annulus. (Scheme 1).



Scheme 2. Three possible conformers of **C**.

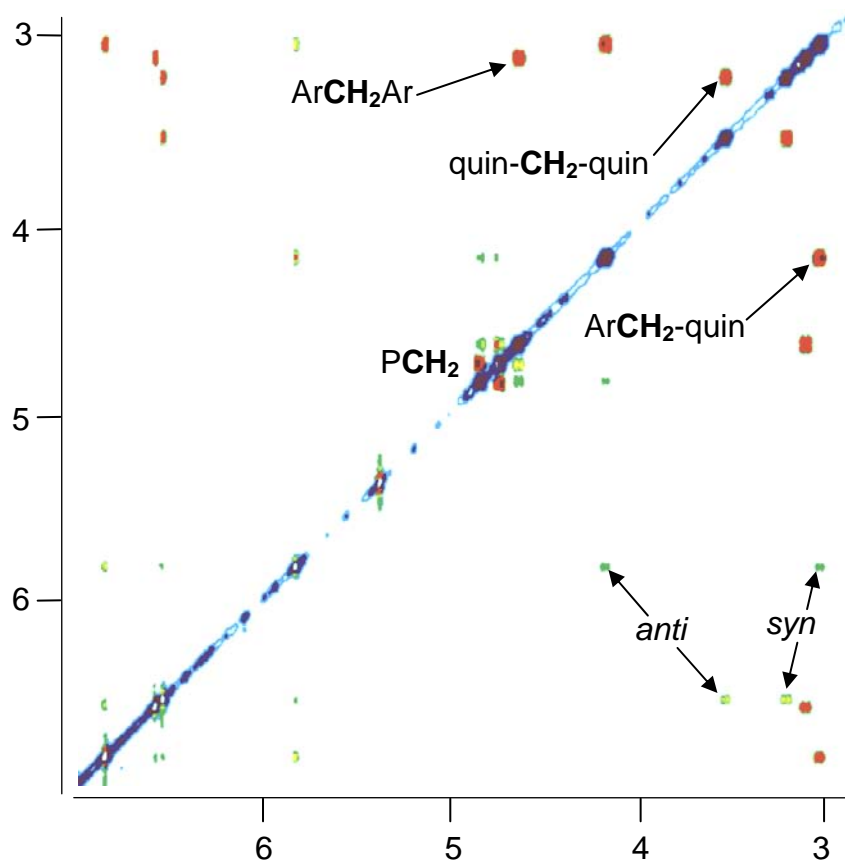


Figure 2. ROESY spectrum of compound **C** (CD_2Cl_2).

Single crystals of **C** were obtained from a solution of the compound in acetonitrile–ether. The solid-state structure is shown in Figure 3. The calixarene displays a partial cone conformation in which one quinone ring is anti-oriented (*down* orientation) with respect to the other three rings. Thus, this study establishes that in the solid state **C** possesses C_1 symmetry and, as expected, the unit cell contains both enantiomers. The quinone ring which has an "*up*" orientation and the opposite aryl ring are almost parallel (interplane angle *ca.* 9°). Three of the four rings constituting the calixarene core (namely those linked to O13, O20 and O27, respectively) are roughly perpendicular to the calixarene reference plane (defined as the best plane passing through the methylene bridges), while the fourth, being linked to the phosphoryl unit P=O(1), is strongly inclined to this plane (interplane angle 147°). There is no rational explanation for the latter observation, but we note that one methylenic proton of C37 approaches the phosphoryl oxygen O2 (separation: *ca.* 2.7 Å).

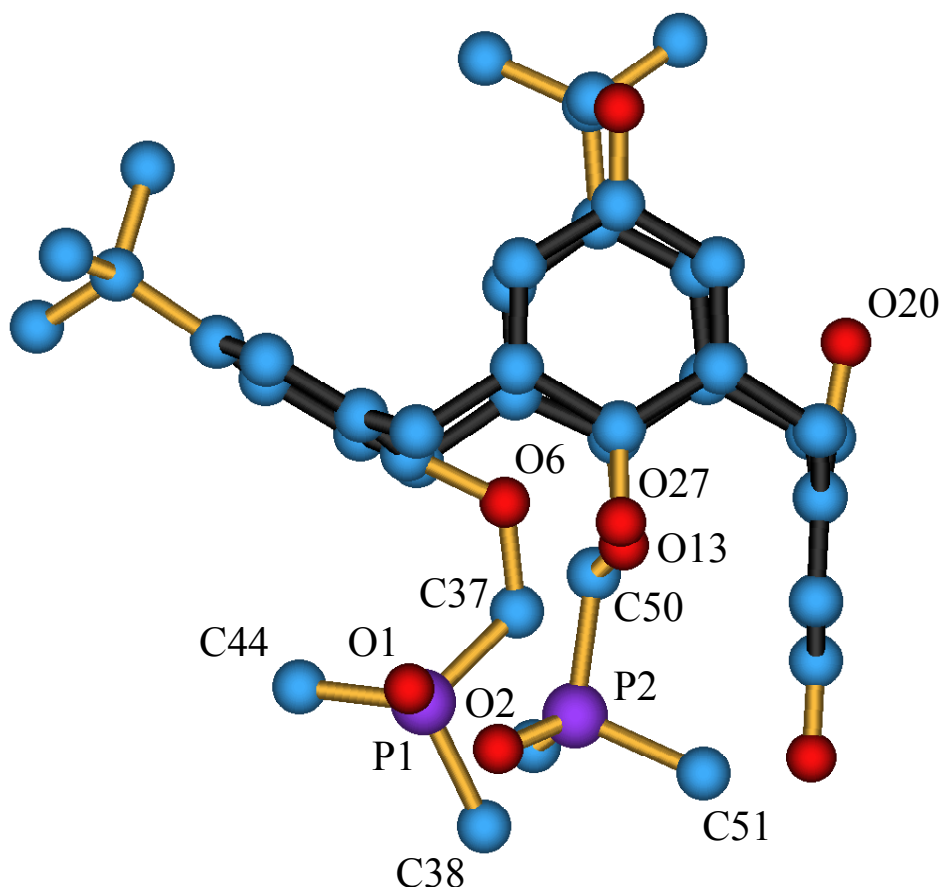


Figure 3. Molecular structure of **C**. For clarity, only the ipso carbon atoms of the phenyl rings were shown.

4 Conclusion

Overall, this study establishes the dynamic behaviour of calixquinone **C** in solution, which arises from a rapid oscillation of each quinone unit about the CC axis passing through the adjacent methylene carbons. In the solid state **C** was shown to adopt a *partial-cone* conformation. Although such a conformer is very likely to give rise in solution to an exchange with a *1,2-alternate* conformer and/or a *cone* conformer, these latter conformers could not be identified formally. Finally, it is noteworthy that the conventional NMR rules (based on ^1H and ^{13}C NMR chemical shifts of bridging methylene groups) used for conformational assignment of calix[4]arenes do not apply to conformationally mobile systems, in particular to calixquinones.

5 References

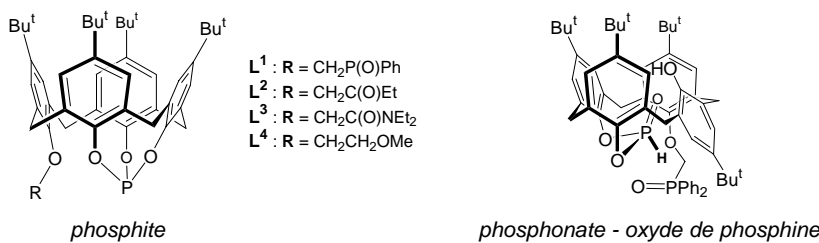
1. S. E. Biali, in *Calixarenes 2001*, Z. Asfari, V. Böhmer, J. Harrowfield, J. Vicens (eds.), Kluwer, Dordrecht, **2001**, pp 266-279.
2. A. Casnati, E. Comelli, M. Fabbi, V. Bocchi, G. Mori, F. Uguzzoli, A. Lanfredi M. M., A. Pochini and R. Ungaro, *Rec. Trav. Chim.-J. Roy. Neth. Chem.*, 1993, **112**, 384-392.
3. P. A. Reddy, C. D. Gutsche, *J. Org. Chem.*, 1993, **58**, 3245-3251.
4. D. Bethell, G. Dougherty and D. C. Cupertino, *J. Chem. Soc. Chem. Commun.*, 1995, 675-676.
5. R. Vataj, H. Ridaoui, A. Louati, V. Gabelica, S. Steyer, D. Matt, *J. Electroanal. Chem.*, 2002, **519**, 123-129.
6. R. Vataj, A. Louati, C. Jeunesse, D. Matt, *J. Electroanal. Chem.*, 2004, **565**, 295-299.
7. K. M. OConnor, D. W. M. Arrigan, G. Svehla, *Electroanal.*, 1995, **7**, 205-215.
8. T. D. Chung, D. Choi, S. K. Kang, S. K. Lee, S.-K. Chang, H. Kim, *J. Electroanal. Chem.*, 1995, 431-439.
9. M. Gomezkaifer, P. A. Reddy, C. D. Gutsche and L. Echegoyen, *J. Amer. Chem. Soc.*, 1997, **119**, 5222-5229.
10. D. Bethell, G. Dougherty and D. C. Cupertino, *Acta Chem. Scand.*, 1998, **52**, 407-416.
11. H. Cano-Yelo Bettega, J.-C. Moutet, G. Ulrich, R. Ziessel, *J. Electroanal. Chem.*, 1996, **406**, 247-250.
12. T. D. Chung, S. K. Kang, J. Kim, H.-S. Kim, H. Kim, *J. Electroanal. Chem.*, 1997, 438, 71-78.
13. T. D. Chung, J. Park, J. Kim, H. Lim, M.-J. Choi, J. R. Kim, S.-K. Chang, H. Kim, *Anal. Chem.*, 2001, **73**, 3975-3980.
14. J. Park, S. K. Kang, T. D. Chung, S.-K. Chang, H. Kim, *Microchem. J.*, 2001, **68**, 109-113.
15. J. Blixt, C. Detellier, *J. Amer. Chem. Soc.*, 1995, **117**, 8536-8540.
16. C. D. Gutsche, in *Calixarenes Revisited, Monographs in Supramolecular Chemistry*, J. F. Stoddart (ed.), The Royal Society of Chemistry, Cambridge, **1998**.

17. *Calixarenes in Action*, L. Mandolini, R. Ungaro (eds.), Imperial College Press, London, **2000**.
18. C. Jaime, J. de Mendoza, P. Prados, P. M. Nieto, C. Sanchez, *J. Org. Chem.*, 1991, **56**, 3372-3376.
19. C. Dieleman, S. Steyer, C. Jeunesse, D. Matt, *J. Chem. Soc. Dalton Trans.*, 2001, 2508-2517.
20. C. D. Gutsche in *Calixarenes, Monographs in Supramolecular Chemistry*, J. F. Stoddart (ed.), The Royal Society of Chemistry, Cambridge, **1989**, pp 110-111.
21. COLLECT Software, Nonius BV, 1997-2001.
22. A. Altomare, G. Cascarano, G. Giacovazzo, A. Guagliardi, M. C. Burla, G. Polidori, M. Camalli, *J. Appl. Crystallogr.*, 1994, **27**, 435.
23. a) D. J. Watkin, C . K. Prout, J. R. Carruthers, P. W. Betteridge, R. I. Cooper, CRYSTALS, **2001**, Issue 11, Chemical Crystallography Laboratory, Oxford (UK); b) J. R. Carruthers, D. J. Watkin, *Acta Crystallogr. Sect. A*, 1979, **35**, 698-699.

CONCLUSION.

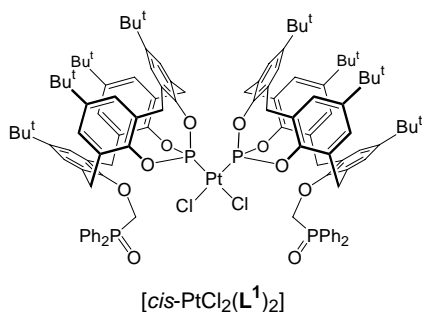
Ce mémoire décrit la synthèse ainsi que les propriétés complexes et catalytiques de divers phosphites et phosphinites construits sur le bord inférieur de *p*-*tert*-butyl-calix[4]arènes régiosélectivement préfonctionnalisés.

La première partie de cette thèse étudie la possibilité d'accéder à des phosphites encombrés par pontage de trois groupes hydroxy d'un calixarène monofonctionnalisé du type *cône*-calix[4]arène-(OH)₃-(OR) par un atome de phosphore. Les calixphosphites **L¹-L⁴** ont été obtenus par réaction du mélange PCl₃/NEt₃ avec les calixarènes monofonctionnalisés suivants: *p*-*tert*-butyl-calix[4]arène-(OH)₃-OR (R = -CH₂P(O)Ph₂ (**L¹**), -CH₂CO₂Et (**L²**), -CH₂CONEt₂ (**L³**), -CH₂CH₂OMe (**L⁴**)). Ces phosphites adoptent tous la conformation "cône". En raison de la présence d'une fonctionnalité oxygénée dans le quatrième substituant phénolique, ils constituent potentiellement des ligands *P,O*-chélatants. Le phosphite **L¹** est relativement robuste puisque stable en présence de soude; en revanche, au contact d'une solution acide il est immédiatement converti en phosphonate. L'oxydation lente de **L¹** par l'air conduit à un composé hybride phosphate-oxyde de phosphine.

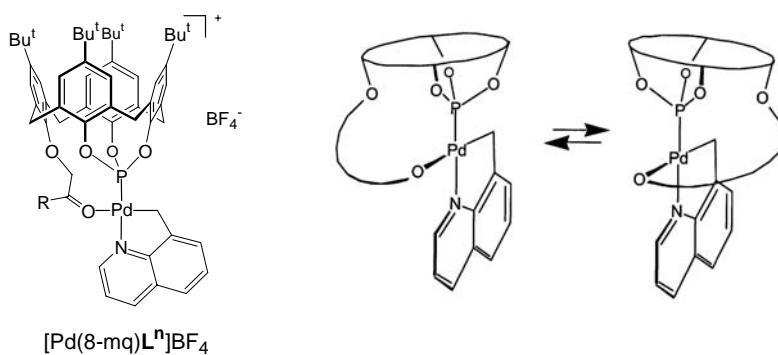


Dans les complexes suivants, [RuCl₂(*p*-cymène)**L¹**], [*cis*-PtCl₂(**L¹**)₂], [*trans*-PdCl₂(**L¹**)₂], [Pd(8-mq)Cl(**Lⁿ**)] (8-mqH = 8-methylquinoléine, n = 1-3), [Pd(dmba)Cl(**L¹**)] (dmbaH = *N,N*-dimethylbenzylamine), [Pd(η^3 -C₄H₇)Cl(**L²**)], [Rh(acac)(CO)**Lⁿ**] (n = 1-3) et [RhCl(CO)(**L¹**)₂], les ligands phosphites ont un comportement κ^1P (coordination monodentate). L'encombrement marqué de **L¹** est manifeste dans le complexe bis-phosphite [*cis*-PtCl₂(**L¹**)₂] pour lequel on observe un

empêchement de la rotation des deux ligands autour des axes Pt–P. Une étude structurale par diffraction des rayons X non seulement établit que le phosphite possède un angle de cône supérieur à 180°, mais fait également apparaître la forte déformation subie par la matrice calix[4]arène par suite du P-pontage.



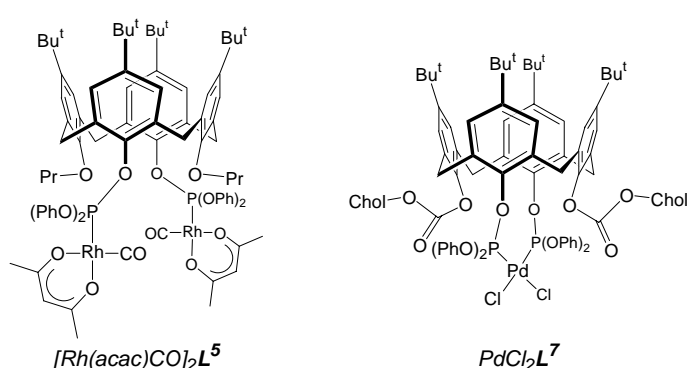
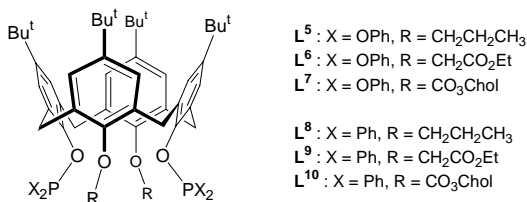
La bonne préorganisation de ces ligands permet d'obtenir des complexes chélates impliquant l'atome de phosphore et l'atome d'oxygène de la fonction auxiliaire. Une telle situation est notamment rencontrée dans les complexes $[Pd(8\text{-mq})L^n]BF_4$ ($n = 1\text{-}3$), (8-mqH = 8-méthylquinoléine). Une étude par diffraction des rayons X montre que dans le complexe $[Pd(8\text{-mq})L^2]BF_4$ la boucle P,O (incorporant la matrice calixarène) est située en dehors du plan métallique. En solution, la molécule présente un comportement dynamique, la boucle P,O basculant en alternance de part et d'autre du plan de coordination. Ce mouvement est facilité par la grande flexibilité du cœur calixarénique.



Les quatre phosphites $L^1\text{-}L^4$, associés à du rhodium, ont été testés en hydroformylation d'octène. Ces systèmes sont rapides (ex. TOF = 4400 mol(octène).mol(Rh) $^{-1}\cdot h^{-1}$ pour L^4) et les activités correspondent à celles attendues pour des phosphites d'encombrement moyen. Une diminution de l'activité est observée lorsque le caractère donneur de la fonction auxiliaire augmente: $L^4 > L^1 > L^2 > L^3$. Ceci

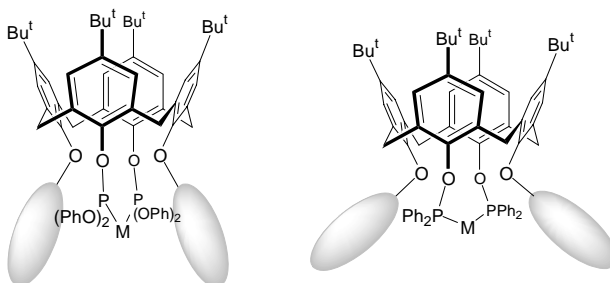
suggère une coordination (transitoire) de cette dernière durant le processus catalytique, entraînant des modifications de la géométrie du calixarène et par voie de conséquence des propriétés électroniques et stériques du phosphite. La nature du groupement auxiliaire a également un impact sur la sélectivité en aldéhyde linéaire, la proportion de ce dernier augmentant sensiblement avec le caractère donneur du groupe auxiliaire (ex. L/B = 3.6 avec **L²** et L/B = 1.4 avec **L⁴**). Il est raisonnable de considérer que la coordination de la fonction latérale, lorsqu'elle se produit, modifie les interactions stériques entre le ligand et le substrat coordonné.

La seconde partie de ce mémoire décrit des calixarènes porteurs de deux groupes PX₂ (X = OPh ou Ph) greffés sur des atomes d'oxygène occupant des positions distales de la matrice. Ces ligands (**L⁵-L¹⁰**) ont été obtenus par introduction de deux fragments PX₂ (X = OPh ou Ph) sur des calixarènes 1,3-dialkylés (propoxy, ester, carbonate de cholestéryle). Les ligands formés adoptent tous la conformation "cône". Les diphosphites **L⁵-L⁷** peuvent se comporter soit comme ligands *bis*-monodentates κ^1P , κ^1P' (ex. {[Rh(acac)CO]₂**L⁵**}), soit en ligand chélatant (ex . [PdCl₂**L⁷**]).



Associés à du rhodium, tous les ligands synthétisés se sont avérés actifs en hydroformylation d'oléfines. Dans le cas de l'octène, les phosphinites présentent une

activité supérieure aux phosphites (ex. TOF = 2600 mol(octène).mol(Rh)⁻¹.h⁻¹ avec Rh(acac)(CO)₂/**L**⁸). En revanche, les phosphites sont plus sélectifs que les phosphinites correspondants. Ainsi, alors qu'avec les phosphinites les rapports L/B sont généralement proches de 2, ce rapport est toujours supérieur à 5 avec les phosphites et peut dépasser 10 lorsqu'on emploie des diphosphites porteurs de fonctions auxiliaires carbonylées. La comparaison avec le rapport L/B = 2.8, obtenu avec P(OPh)₃, suggère qu'avec les phosphites une coordination transitoire de la fonction latérale se produit lors de la réaction catalytique. Ce phénomène accentue vraisemblablement la formation d'une poche autour du métal favorisant alors la formation d'un intermédiaire "Rh(*n*-alkyle)" par rapport à un intermédiaire "Rh(*iso*-alkyle)". A signaler que les modèles moléculaires montrent qu'avec les diphosphites, les fonctions auxiliaires sont plus proches du métal qu'avec les phosphinites. Ce rapprochement est facilité par l'encombrement plus faible des groupes P(OPh)₂ par rapport aux groupes PPh₂.



Ces ligands ont également été testés en hydroformylation du styrène. Dans tous les cas, le rapport L/B est supérieur à ce qu'on observe avec PPh₃ (L/B = 5/95). C'est avec les ligands porteurs de groupements carbonyle que cet effet est le plus marqué (ex L/B = 40/60 avec **L**¹⁰). La quantité anormalement élevée d'aldéhyde linéaire semble confirmer les conclusions déduites de l'étude d'hydroformylation de l'octène. On peut mentionner qu'aucune induction asymétrique n'est observée avec les ligands chiraux **L**⁷ et **L**¹⁰, probablement parce que les centres stéréogènes sont trop éloignés du centre catalytique.

La troisième partie de cette thèse traite du produit d'oxydation du *p*-*tert*-butyl-5,11-bis(diphénylphosphinoxyloxymethyl)calix[4]arène **B** par Tl^{III}(CF₃SO₃)₃. La réaction conduit au macrocycle (**C**) comportant deux quinones adjacentes. Les spectres de RMN (¹H et ¹³C), à température ambiante, ne permettent pas de trancher quant à la

conformation du calixarène formé. C'est la raison pour laquelle une étude par diffraction des rayons X a été entreprise. Cette étude montre qu'à l'état solide le composé est dans la conformation cône partiel, une des quinones ayant une orientation *anti*. Des expériences de ROESY mettent clairement en évidence une oscillation rapide de chacune des unités quinoniques autour de l'axe passant par les deux atomes de carbone CH₂ bordant les cycles. Cependant ces expériences ne permettent ni de démontrer l'existence d'un conformère 1,2-alterné ni celle d'un conformère cône. De cette étude, on retiendra surtout que les règles empiriques basées sur les déplacements chimiques ¹³C des ponts CH₂ qui permettent d'attribuer une conformation particulière à un calixarène ne sont pas applicables dans le cas des calix-quinones, et ce en raison de la mobilité de ces dernières.

